4. ELECTRODIALYSIS IN PRACTICE

Electrodialysis technology has progressed significantly during the past 40 years since the introduction of synthetic ion-exchange membranes in 1949[53]. The first two decades of this period saw the development of classical or unidirectional standard electrodialysis. However, during the past decade, the main feature has been the development of the polarity reversal process - the so-called electrodialysis reversal (EDR)[84]. This form of electrodialysis desalination has virtually displaced unidirectional ED for most brackish water applications and is slowly gaining a significant share of this market.

EDR is at present mainly used for the desalination of brackish waters to produce fresh potable and industrial water. Unidirectional ED is used on a large scale in Japan for concentrating seawater to produce brine for salt production[85] and is also used on a small scale for seawater desalination[86] and for brackish water desalination[87].

Outside the water desalination field, ED is also being used on a large and increasing scale in North America and Europe to de-ash cheese whey to produce a nutritious high quality protein food supplement[53]. It is also finding application in the treatment of industrial waste waters for water recovery, reuse and effluent volume reduction[61, 88].

4.1 Electrodialysis Processes and Stacks

Different types of ED processes and stacks are used commercially for ED applications[6]. The filter-press- and the unit-cell stacks are the most familiar.

4.1.1 Filter-Press Stacks

The filter press stack configuration[6, 8] in which alternate cation- and anion-exchange membranes are arranged between compartment frames in a plate-and-frame filter press assembly is shown in Figure 4.1.

Salt solution flows between the alternately placed cation and anion permeable membranes in the ED stack. Direct current (DC) provides the motive force for ion migration through the ion-exchange membranes and the ions are removed or concentrated in the alternate water passage by means of permselective ion-exchange membranes. This process is called the standard ED process.

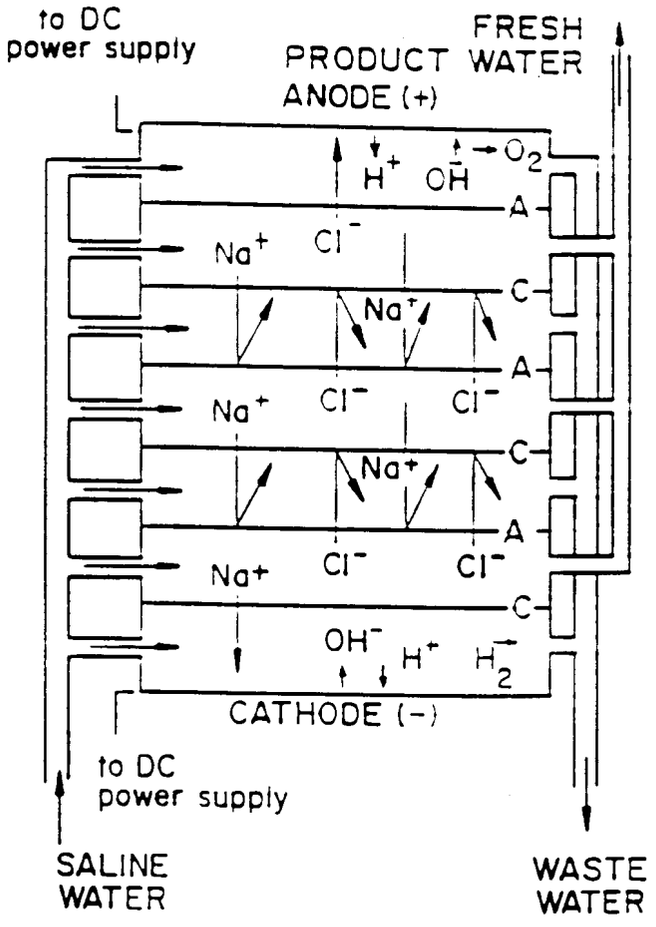

Figure 4.1: **Plate-and-frame type EDR membrane stack.**
C = cation membrane. A = anion membrane.

The standard ED process often requires the addition of acid and/or polyphosphate to the brine stream to inhibit the precipitation of sparsely soluble salts (such as $CaCO_3$ and $CaSO_4$) in the stack. To maintain performance, the membrane stack needs to be cleaned periodically to remove scale and other surface fouling matter. This can be done in two ways[8] by cleaning in-place (CIP); and stack disassembly.

Special cleaning solutions (dilute acids or alkaline brine) are circulated through the membrane stacks for in-place cleaning, but at regular intervals the stacks need to be disassembled and mechanically cleaned to remove scale and other surface-fouling matter. Regular stack disassembly is a time-consuming operation and is a disadvantage of the standard ED process.

The electrodialysis reversal process (EDR) operates on the same basic principles as the standard ED process. In the EDR process, the polarity of the electrodes is automatically reversed periodically (about three to four times per hour) and, by means of motor operated valves, the 'fresh product water' and 'waste water' outlets from the membrane stack are interchanged. The ions are thus transferred in opposite directions across the membranes. This aids in breaking up and flushing out scale, slime and other deposits from the cells. The product water emerging from the previous brine cells is usually discharged to waste for a period of one to two minutes until the desired water quality is restored.

The automatic cleaning action of the EDR process usually eliminates the need to dose acid and/or polyphosphate, and scale formation in the electrode compartments is minimized due to the continuous change from basic to acidic conditions. Essentially, therefore, three methods of removing scale and other surface fouling matter are used in the EDR process[8], viz., cleaning in place, stack disassembly as used in the standard ED process; and reversal of flow and polarity in the stacks. The polarity reversal system greatly extends the intervals between the rather time-consuming task of stack disassembly and reassembly, with an overall reduction in maintenance time.

The capability of EDR to control scale precipitation more effectively than standard ED is a major advantage of this process, especially for applications requiring high water recoveries. However, the more complicated operation and maintenance requirements of EDR equipment necessitate more labour and a greater skill level and may be a disadvantage of the process.

4.1.2 Unit-Cell Stack

A unit cell stack is shown in Figure 4.2. In this case the cation- and anion exchange membranes are sealed together at the edges to form a concentrating cell which has the shape of an envelope-like bag[6]. Many of these concentrating cells can be placed between electrodes in an ED stack.

The concentrating cells are separated by screen-like spacers. The feed flows between these concentrating cells and the direction of current through the stack is such as to cause ionic flow into the bags. Water flow into the cells is due to electro-osmosis (water is drawn along with the ions), and osmosis (water flows from the feed solution to the more concentrated brine). Small tubes are attached to each unit cell to allow

overflow of the brine. Because brine is pumped out of the cells mainly by the inflow of electro-osmotic water flow, this variant of ED is called electro-osmotic pumping ED.

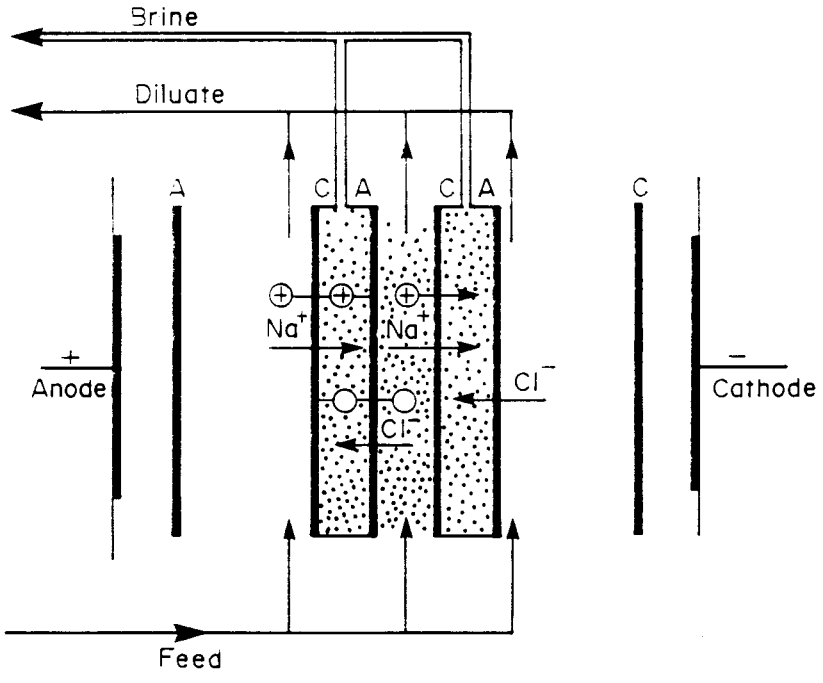

Figure 4.2: Schematic diagram of an ED unit cell stack. C = cation membrane. A = anion membrane.

4.2 Ion-Exchange Membranes

Ion-exchange membranes are ion-exchangers in film form. There are two types: anion-exchange and cation-exchange membranes. Anion-exchange membranes contain cationic groups fixed to the resin matrix. The fixed cations are in electroneutrality with mobile anions in the interstices of the resin. When such a membrane is immersed in a solution of an electrolyte, the anions in solution can intrude into the resin matrix and replace the anions initially present, but the cations are prevented from entering the matrix by the repulsion of the cations affixed to the resin.

Cation-exchange membranes are similar. They contain fixed anionic groups that permit intrusion and exchange of cations from an external source, but exclude anions. This type of exclusion is called Donnan exclusion.

Details of methods for making ion-exchange membranes are presented in the literature[89 - 91] Heterogeneous membranes have been made by incorporating ion-exchange particles into film-forming resins (a) by dry molding or calendering mixtures of the ion-exchange and film-forming materials; (b) by dispersing the ion-exchange material in a solution of the film-forming polymer, then casting films from the solution and evaporating the solvent; and (c) by dispersing the ion-exchange material in a partially polymerized film-forming polymer, casting films, and completing the polymerization.

Heterogeneous membranes with usefully low electrical resistances contain more than 65% by weight of the cross-linked ion-exchange particles. Since these ion-exchange particles swell when immersed in water, it has been difficult to achieve adequate mechanical strength and freedom from distortion combined with low electrical resistance.

To overcome these and other difficulties with heterogeneous membranes, homogeneous membranes were developed in which the ion-exchange component forms a continuous phase throughout the resin matrix. The general methods of preparing homogeneous membranes are as follows[6]:

- Polymerization of mixtures of reactants (e.g., phenol, phenolsulfonic acid, and formaldehyde) that can undergo condensation polymerization. At least one of the reactants must contain a moiety that either is, or can be made, anionic or cationic.
- Polymerization of mixtures of reactants (e.g., styrene, vinylpyridine, and divinylbenzene) that can polymerize by additional polymerization. At least one of the reactants must contain an anionic or cationic moiety, or one that can be made so. Also, one of the reactants is usually a cross-linking agent to provide control of the solubility of the films in water.
- Introduction of anionic or cationic moieties into preformed films by techniques such as imbibing styrene into polyethylene films, polymerizing the imbibed monomer, and then sulfonating the styrene. A small amount of cross-linking agent (e.g., divinylbenzene) may be added to control leaching of the ion-exchange component. Other similar techniques, such as graft polymerization of imbibed monomers, have been used to attach ionized groups onto the molecular chains of preformed films.
- Casting films from a solution of a mixture of a linear film-forming polymer and

a linear polyelectrolyte, and then evaporating the solvent.

Membranes made by any of the above methods may be cast or formed around scrims or other reinforcing materials to improve their strength and dimensional stability.

The properties of some representative commercially available ion-exchange membranes as reported by the manufacturers are shown in Table 4.1[6].

Table 4.1: Reported Properties of Ion-Exchange Membranes*

Manufacturer and Designation	Type of Membrane	Area Resistance (ohm-cm²)	Transference Number of Counterion[a]	Strength	Approximate Thickness (mm)	Dimensional Changes on Wetting and Drying (%)	Size available
AMF[b]		(0,6 *N* KCl)		Mullen burst (kPa)			
C-60	Cat-exch	5 ± 2	0,80 (0,5/1,0 *N* KCl)	310	0,30		
C-100	Cat-exch	7 ± 2	0,90 (0,5/1,0 *N* KCl)	414	0,22	10 - 13	1,1 m wide rolls
A-60	An-exch	6 ± 2	0,80 (0,5/1,0 *N* KCl)	310	0,30		
A-100	An-exch	8 ± 2	0,90 (0,5/1,0 *N* KCl)	379	0,23	12 - 15	1,1 m wide rolls
ACI[c]		(0,5 *N* NaCl)		Tenstile strength (kg/mm²)			
CK-1	Cat-exch	1,4	0,85 (0,25/0,5 *N* NaCl)		0,23		
DK-1	Cat-exch	1,8	0,85 (0,25/0,5 *N* NaCl)	2 to 2,4	0,23	15 - 23	1,1 x 1,1 m
CA-1	An-exch	2,1	0,92 (0,25/0,5 *N* NaCl)		0,23		
DA-1	An-exch	3,5	0,92 (0,25/0,5 *N* NaCl)	2 to 2,3	0,23	12 - 18	1,1 x 1,1 m
AGC[d]		(0,5 *N* NaCl)		Mullen burst (kPa)			
CMV	Cat-exch	3	0,93 (0,5/1,0 *N* NaCl)	1 241	0,15		
CSV	Cat-exch	10	0,92 (0,5/1,0 *N* NaCl)	1 241	0,30		
AMV	An-exch	4	0,95 (0,5/1,0 *N* NaCl)	1 531	0,15	< 2	1,1 m wide rolls
ASV	An-exch	5	0,95 (0,5/1,0 *N* NaCl)	1 531	0,15		
IC[f]		(0,1 *N* NaCl)		Mullen burst (kPa)			
MC-3142	Cat-exch	12	0,94 (0,/51,0 *N* NaCl)	1 379	0,20		
MC-3235	Cat-exch	18	0,95 (0,/10,2 *N* NaCl)	1 137	0,30	< 3[g]	1 x 3 m
MC-3470	Cat-exch	35	0,96 (0,/10,2 *N* NaCl)	1 379	0,20		
MA-3148	An-exch	20	0,90 (0,5/1,0 *N* NaCl)	1 379	0,20		
MA-3236	An-exch	120	0,93 (0,5/1,0 *N* NaCl)	1 137	0,30	< 3[g]	1 x 3 m
IM-12	An-exch[h]	12	0,96 (0,1/0,2 *N* NaCl)[g]	999	0,15[g]	Not given	
MA-3475R	An-exch	11	0,99 (0,5/1,0 *N* NaCl)	1 379	0,36	Not given	
II[i]				Mullen burst (kPa)			
CR-61	Cat-exch	11	0,93 (0,2 *N* NaCl)[b]	793	0,58	Cracks on drying	0,5 x 1 m
AR-111A	An-exch	11	0,93 (0,1/0,2 *N* NaCl) (by electrophoretic method in 0,5 *N* NaCl)	862	0,61		
TSC[j]				Mullen burst (kPa)			
CL-2,5T	Cat-exch	3	0,98	551	0,15		
CLS-25T	Cat-exch[k]	3	0,98	551	0,15	Not given	1 x 1,3 m
AV-4T	An-exch	4	0,98	1 034	0,18		
AVS-4T	An-exch[k]	5	0,98	965	0,18	Not given	1 x 1,3 m

* Properties are those reported by manufacturer, except for those membranes designated with footnote g.
a Calculated from concentration potentials measured between solutions of the two normalities listed.
b American Machine and Foundry Co., Stamford, Connecticut.
c Asahi Chemical Industry, Ltd. Tokyo, Japan.
d Asahi Glass Co., Ltd., Tokyo, Japan.
e Membranes that are selective for univalent (over multivalent) ions.
f Ionac Chemical Co., Birmingham, New Jersey.
g Measured at Southern Research Institute.
h Special anion-exchange membrane that is highly diffusive to acids.
i Ionics, Inc., Cambridge, Massachusetts.
j Tokluyama Soda Co., Ltd., Tolkyo, Japan.
k Univalent selective membranes.

4.3 Fouling

Fouling of ED membranes by dissolved organic and inorganic compounds may be a serious problem in practical electrodialysis[6, 92, 93] unless the necessary precautions (pretreatment) are taken. Organic fouling is caused by the precipitation of large negatively charged anions on the anion-permeable membranes in the dialysate compartments.

Organic fouling of anion permeable membranes takes place in a number of ways[92]:

a) The anion is small enough to pass through the membrane by electromigration but causes only a small increase in electrical resistance and a decrease in permselectivity of the membrane;

b) The anion is small enough to penetrate the membrane, but its electromobility in the membrane is so low that its hold-up in the membrane causes a sharp increase in the electrical resistance and a decrease in the permselectivity of the membrane;

c) The anion is too big to penetrate the membrane and accumulates on the surface (to some extent determined by the hydrodynamic conditions and also by a phase change which may be brought about by the surface pH). The decrease in electrical resistance and permselectivity of the membrane is slight. The accumulation can be removed by cleaning.

In case (c) the electrodialysis process will operate without serious internal membrane fouling and only mechanical (or chemical) cleaning will be necessary. Case (b) would make it almost impossible to operate the electrodialysis process. In case (a), the electrodialysis process can be used if the concentration of large anions in solution is low or if the product has a high enough value to cover the high electrical energy costs.

Inorganic fouling is caused by the precipitation (scaling) of slightly soluble inorganic compounds (such as $CaSO_4$ and $CaCO_3$) in the brine compartments and the fixation of multivalent cations (such as Fe and Mn) on the cation-permeable membranes. Organic anions or multivalent cations can neutralize or even reverse the fixed charge of the membranes, with a significant reduction in efficiency. Fouling also causes an increase in membrane stack resistance which, in turn, increases electrical consumption and adversely effects the economics of the process.

The following constituents are, to a greater of lesser extent, responsible for membrane fouling[94]:

- Traces of heavy metals such as Fe, Mn and Cu.
- Dissolved gases such as O_2, CO_2 and H_2S.
- Silica in diverse polymeric and chemical forms.
- Organic and inorganic colloids.
- Fine particulates of a wide range of sizes and composition.
- Alkaline earths such as Ca, Ba and Sr.
- Dissolved organic materials of both natural and man-made origin in a wide variety of molecular weights and compositions[92].
- Biological materials - viruses, fungi, algae, bacteria - all in varying stages of reproduction and life cycles.

Many of these foulants may be controlled by pretreatment steps which usually stabilize the ED process. However, according to Katz[94], the development of the EDR process has helped to solve the pretreatment problem more readily in that it provides self-cleaning of the vital membrane surfaces as an integral part of the desalting process.

4.4 Pretreatment

Pretreatment techniques for ED are similar to those used for RO[8]. Suspended solids are removed by sand and cartridge filters ahead of the membranes. Suspended solids, however, must be reduced to a much lower level for RO than for ED. The precipitation of slightly soluble salts in the standard ED process may be minimized by ion-exchange softening and/or reducing the pH of the brine through acid addition and/or the addition of an ihibiting agent.

Organics are removed by carbon filters, and hydrogen sulphide by oxidation and filtration. Biological growths are prevented by a chlorination-dechlorination step. The dechlorination step is necessary to protect the membranes from oxidation. Iron and manganese are removed by green sand filters, aeration, or other standard water treatment methods. It has been suggested that multivalent metal and organic ions, and hydrogen sulphide, however, must be reduced to a lower level for EDR than for RO[95].

The overall requirements for pretreatment in ED, may be somewhat less rigorous than for RO due to the nature of the salt separation and the larger passages provided[8].

In ED, the ions (impurities) move through the membranes, while in RO the water moves under a high pressure through the membranes while the salts are rejected. Salts with a low solubility can, therefore, more readily precipitate on spiral and hollow fine fibre RO membranes to cause fouling and to block the small water passages. Suspended solids can also more readily form a deposit. However, this might not be the case with tubular RO membranes. With the EDR process, precipitated salts in the brine compartments can be more readily dissolved and flushed out of the system using polarity reversal without the need for chemical pretreatment.

However, high removals of suspended solids, iron, manganese, organics and hydrogen sulphide are still critical to avoid fouling and suppliers of EDR equipment recommend pretreatment of the feed water[8], if it contains the following ions: Fe > 0,3 mg/ℓ; Mn > 0,1 mg/ℓ; H_2S > 0,3 mg/ℓ; free chlorine and turbidity > 2 NTU. In every case, of course, a careful examination of the prospective water would be necessary to determine suitability and pretreatment.

A certain degree of fouling is, however, unavoidable. Membranes should, therefore, be washed regularly with dilute acid and alkali solutions to restore performance.

4.5 Post-treatment

The EDR product water is usually less aggressive than the RO product because acid is usually not added in EDR for scale control[95]. Post-pH adjustment may, therefore, not be required as with RO. Non-ionic matter in the feed such as silica, particulates, bacteria, viruses, pyrogens and organics will not be removed by the ED process and must, if necessary, be dealt with during post-treatment.

4.6 Seawater Desalination

There is limited application of ED for seawater desalination because of high costs[8]. A small batch system (120 m^3/d) has been in operation in Japan since 1974 to produce water of potable quality at a power consumption of 16,2 kWh/m^3 product water[96]. A 200 m^3/d seawater EDR unit was evaluated in China[97]. This unit operated at 31°C; its performance was stable; total electric power consumption was 18,1 kWh/m^3 product water and the product water quality of 500 mg/ℓ TDS met all the requirements for potable water. When the stacks were disassembled for inspection, there were no signs of scale formation.

With the commercial ED units currently available, the energy usage for seawater desalination is relatively high compared with that of RO. However, work under the Office of Water Research and Technology (OWRT) programmes has indicated that high-temperature ED may possibly be competitive with RO[98]. Results have shown that the power consumption can be reduced to the levels required for seawater RO (8 kWh/m^3) and that a 50% water recovery can probably be attained.

4.7 Brackish Water Desalination for Drinking-Water Purposes

A considerable number of standard ED plants for the production of potable water from brackish water are in operation[8, 87]. These plants are operating successfully. However, after the introduction of the reversal process in the early 1970's, Ionics Incorporated shifted almost all their production to this process[94].

The major application of the EDR process is for the desalination of brackish water. The power consumption and, to some degree, the cost of equipment required is directly proportional to the TDS to be removed from the feed water[8]. Thus, as the feedwater TDS increases, the desalination costs also increase. In the case of the RO process, a cost: TDS removal relationship also exists, but it is not as pronounced. Often the variation in the scaling potential of the feed water and its effect on the percentage of product water recovery can be more important than the cost: TDS relationship.

Thus, for applications requiring low TDS removals, ED is often the most energy-efficient method, whereas with highly saline feed waters RO may be expected to use less energy and is preferred. The economic crossover point between ED and RO based on operating costs is, however, difficult to define precisely and needs to be determined on a site-specific basis. Apart from local power costs, other factors must also be considered in determining the overall economics. Among these, to the advantage of ED, are the high recoveries possible (up to 90%), the elimination of chemical dosing (with EDR), and the reliability of performance that is characteristic of the ED process.

4.8 Energy Consumption

The energy consumption of a typical EDR plant is as follows[8]:

Pump	:	0,5 to 1,1 kWh/m^3 product water
Membrane stack	:	0,7 kWh/m^3 product water/1 000 mg of TDS removed
Power losses	:	5% of total energy usage

The major energy requirement, therefore, is for pumping the water through the ED unit and for the transport of the ions through the membranes.

4.9 Treatment of a High Scaling, High TDS Water with EDR

The successful performance of EDR on high calcium sulphate waters has been reported[84]. Brown[99] has described the performance of and EDR plant treating 300 m^3/d of a high calcium sulphate water with a TDS of 9 700 mg/ℓ. The only pretreatment applied was iron removal on green sand. The quality of the feed, product and brine is shown in Table 4.2

The water recovery and energy consumption were 40% and 7,7 kWh/m^3 of product water, respectively. No attempt was made to optimize water recovery. The stack resistance increased by only 3% after one year of operation, which clearly indicates the successful operation of the EDR unit in spite of the super saturated condition of the brine with respect to calcium sulphate. Membrane life times are estimated to be 10 years.

The main developments in EDR during the past few years have been the following:

- **EDR has achieved $CaSO_4$** saturation in the brine stream of up to 440% without performance decline on tests of several hundred hours' duration[99].
- EDR has desalted a hard (Ca^{2+} approx. 150 mg/ℓ) brackish water of 4 000 mg/ℓ TDS at water recoveries of up to 93% without cumbersome and expensive pre-softening[94].
- An EDR test unit has achieved 95% or greater recovery of a limited 4 000 mg/ℓ TDS brackish water resource by substituting a more abundant 14 000 mg/ℓ saline water in the brine stream[100]. The substitution of seawater in the brine stream would be freely available in coastal or island locations with limited high quality brackish water resources.
- The development, extensive field testing and subsequent large-scale commercial usage of a new family of thick (0,5 mm), rugged anti-fouling anion-permeable membranes in the USA with much higher current efficiencies and chlorine resistance than those formerly available[100].

Table 4.2: Water Quality Before and After EDR Treatment

Constituent	Feed (mg/ℓ)	Product (mg/ℓ)	Brine (mg/ℓ)
Na^+	2 090	79	3 694
Ca^{++}	652	4	1 390
Mg^{++}	464	4	964
Cl^-	3 687	111	7 084
HCO_3^-	134	25	175
$SO_4^=$	2 672	19	5 000
TDS	9 727	242	18 307
pH	7,0	6,8	7,2

4.10 Brackish Water Desalination for Industrial Purposes

In the past most ED plants treated brackish waters of 1 000 to 10 000 mg/ℓ TDS and produced general purpose industrial product water of 200 to 500 mg/ℓ TDS. However, ED capital and construction costs have declined during recent years to the point where it is already feasible to treat water containing 200 to 1 000 mg/ℓ TDS and produce product water containing as little as 3 to 5 mg/ℓ TDS[101]. These low TDS levels are achieved by multistaging. The systems, which often employ ion-exchange (IX) units as 'polishers', are usually referred to as ED/IX systems.

4.11 ED/IX System

New and existing ion-exchange facilities can be converted to ED/IX systems by addition of ED units upstream of the ion-exchange units. The ED unit reduces chemical consumption, waste, service interruptions and resin replacement of the ion-exchanger in proportion to the degree of prior mineral removal achieved[101]. For small capacity systems (2 to 200 m^3/d) the optimum ED demineralization will usually be 90% or greater; for larger installations, and particularly those where adequate ion-exchange capacity is already provided, the optimum demineralization via ED is more likely to be in the 60 to 80% range.

It must, however, be stressed that RO may also be used for the abovementioned application. RO may function better than ED because it removes silica and organic material better than ED. However, the choice of the treatment method (ED or RO) would be determined by the specific requirements and costs for a particular situation.

Honeywell in the USA, which manufactures printed circuit boards and does zinc plating and anodizing, used IX for the treatment of their process waters before they changed

over to an ED/IX system[102]. ED was chosen instead of RO because of lower membrane replacement costs. Process waters of varying degrees of purity are required, dissolved solids being the primary concern. Water with a TDS of about 50 mg/ℓ is suitable for zinc plating and anodizing and water with a TDS with a minimum specific resistance of 100 000 ohms is satisfactory for circuit board fabrication operations[102]. The purity of the treated water (raw water TDS - 250 to 500 mg/ℓ) after treatment with the ED/IX system was better than expected. Service runs have been up to ten times longer than before.

4.12 Industrial Wastewater Desalination for Water Reuse, Chemical Recovery and Effluent Volume Reduction

Large volumes of water containing varying amounts of salt, which are generated by washing and regenerating processes, blowdown from cooling towers, disposal of dilute chemical effluents, to name a few, present significant problems, particularly when zero effluent discharge is required. The problem is one of too much water carrying comparatively little salt, but still having a TDS content too great for acceptance to a receiving stream. Many industries face this problem today and have to consider the application of processes for concentrating salts or desalting water. The ED system for water recovery and brine concentration may be one of the best suited to alleviate the problem.

Some typical examples are given to illustrate this principle:

4.12.1 Electrodialysis of nickel plating solutions

During many plating operations, a substantial amount of bath solution adheres to plated work pieces as they leave the plating tank. In this manner valuable materials are lost as 'drag-out' into the subsequent rinse tank. This contaminated rinse solution can be passed through an ED system where these valuable materials can be recovered and returned to the plating tank.

One such opportunity of significant industrial importance is provided by nickel electroplating operations[103]. Earlier work by Trivedi and Prober[104] demonstrated the successful application of ED to nickel solutions. Later, Eisenmann[105] and Itoi[103] reported the use of ED to recover nickel from electroplating rinse waters.

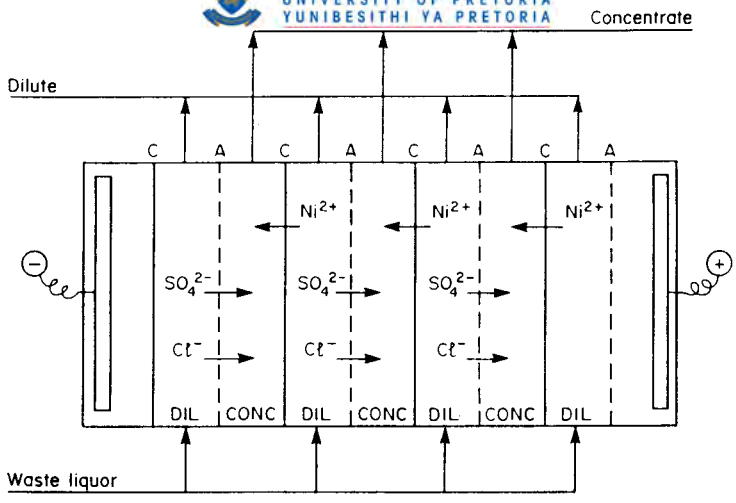

Figure 4.3: Electrodialysis of the washwater from a nickel galvanizing operation.

The wash water from a nickel galvanizing line is treated by ED as shown in Figure 4.3.

The results achieved in an existing facility are given in Table 4.3. The concentration ratio of the concentrated solution to the dilute solution is greater than 100. The concentrated solution is reused in the plating bath while the dilute solution is reused as wash water. The recovery of nickel discharged from the wash tank is approximately 90% or greater.

If organic electrolytes are present in the additives used in the galvanization bath, they must be removed prior to ED treatment to prevent organic fouling of the ED membranes.

Table 4.3: Electrodialysis of a Nickel Galvanization Effluent

Constituent	Effluent (g/ℓ)	Concentrate (g/ℓ)	Diluent (g/ℓ)
$NiSO_4$	12,47	133,4	1,27
$NiCl_2$	1,81	29,1	0,039

4.12.2 Treatment of cooling tower blowdown for water recovery and effluent volume reduction

The range of TDS levels encountered in cooling tower blowdown waters usually varies from about 1 500 to 4 000- mg/ℓ and higher levels at about 4 000 to 12 000- mg/ℓ

have also been reported[106]. The disposal of large volumes of this saline effluent can be a serious problem. The application of ED for the treatment of blowdown streams to recover good quality water for reuse and produce a small volume of concentrate promises to be the best prospective system available[107,108].

Blowdown waters from cooling towers can be concentrated tenfold or more using ED, while recovering and recycling the desalted water to the cooling tower at one-half its original concentration[88]. To accomplish this, blowdown is pretreated, filtered and passed through the ED system. By recirculation of the brine, it is possible to concentrate the salts into a small stream, while allowing for recovery of about 90% of the water.

The concentration of cooling blowdown waters in an EDR pilot plant at one of Eskom's power stations was evaluated[81]. Pretreatment of the blowdown water with lime softening, clarification, pH reduction, filtration and chlorination was found to be a basic precondition for successful operation. The operating experience on the EDR pilot plant was sufficiently positive to warrant full-scale application.

Detailed design studies and cost estimates for ED and several other alternative blowdown recovery/concentration systems have been reported[88]. The side stream process design which utilizes ED results in the lowest capital costs for the conditions specified. According to Wirth and Westbrook[88], it is expected that if the cost comparison were made on overall annual operating costs, the same results would occur.

4.13 Other Possible Industrial Applications

4.13.1 Concentration of sodium sulphate and its conversion into caustic soda and sulphuric acid

A pilot study has demonstrated the feasibility of the concentration of a sodium sulphate solution with ED in a first stage and the subsequent conversion into caustic soda and sulphuric acid in a second stage[109]. The sodium sulphate solution (20 to 40 g/ℓ) was treated in a multi-compartment electrodialyzer to yield a brine (260 - 320 g/ℓ, 10% of feed volume) and a product (2 g/ℓ, 90% of feed volume) which could be used as reclaimed water.

The brine was treated further in a three-compartment electrodialyzer to produce caustic soda and sulphuric acid at a concentration of 17 to 19% by mass and a power consumption of approximately 3,1 to 3,3 kWh/kg sodium sulphate decomposed. The sodium sulphate content of both products was about 1%.

4.13.2 Recovery of acid and caustic soda from ion-exchange regeneration wastes

Laboratory results of an electrodialytic process for acid and caustic recovery from ion-exchange regenerant wastes have been described[110]. The object of the study was to minimize the discharge of dissolved salts from a water treatment plant producing boiler feed water while recovering some of the pollution abatement process costs from the savings in regenerant chemical costs.

It was shown that the electrodialytic process for recovery of sulphuric acid and sodium hydroxide from ion-exchange regenerant wastes, and substantially reducing the amount of salt discharged to drain, is technically feasible. The nett costs for acid and caustic waste treatment was estimated at US \$4,20 and \$3,00/m^3 waste treated, respectively.

4.13.3 Concentration of dilute chemical effluents

Laboratory investigations have shown that dilute (approximately 2%) solutions of NH_4NO_3, Na_2SO_4, $NaNO_3$ and NaCl can be concentrated to approximately 20% by ED at an energy consumption of about 1 kWh/kg salt[111]. The brine volumes were less than 10% of the original volume.

4.14 Polarisation

The current which is passed through an ED stack is carried almost exclusively by ions of the same sign. In the solution, all types of ions carry this current. The rate at which the current can pass through the solution is limited by the diffusion rate of ions to the membrane surface since there will inevitably be changes in the concentration of the solution close to the membrane surface. It is apparent that as the current density is increased, it becomes more difficult for the ions in the solution to carry the required current. This effect is know as concentration polarization[11]. The greater the current density used the greater are these polarization effects. Polarization also becomes a problem the more dilute the solution becomes.

The main effects of polarization are[6]:

i) the differences in concentration result in increased membrane potentials and so the power required per unit charge passed is increased.

ii) The current efficiency can also be reduced which means that the current required per unit of output is also increased.

iii) When it is attempted to carry current in excess of the ions available to be transported through the membrane, the water "splits" into hydroxide and hydrogen ions. At the anion membrane the current is carried by hydroxide ions through the membrane and hydrogen ions are rejected to the solution. At the cation membrane the opposite effect occurs: hydroxide ions are transported to the membrane and are rejected to the solution. This effect is to be avoided since, firstly, both the current and the voltage efficiency are reduced (some of the current serves to split the water instead of desalting it and there is an increased voltage requirement) and secondly, when the water splits the pH in the boundary layer on the membrane surface can change increasing the likelihood of scale formation.

4.15 Cell Stack

It has already been shown that the basic unit in an ED plant is the cell pair where cation and anion permeable membranes are alternately arranged so as to produce adjacent diluate and concentrate streams. A number of cell pairs are located between a pair of electrodes to form what is known as a cell stack. The number of cell pairs varies depending on the manufacturer but is usually about 300.

In any cell pair the membranes are separated by a spacer. The hydrodynamic design of the flow between the membranes is of extreme importance[6]. It is essential that as far as it is practicable turbulent flow exists in individual cell pairs. Streamline flow produces a relatively stagnant or slow moving layer on the membrane surface. Since the current carrying ions have to diffuse through this film at low solution concentration, polarization becomes more likely. There are a number of requirements a spacer must meet. The fluid should flow at the same rate across the whole active membrane area and should be turbulent within the limits of pressure drop. The manifold must supply each spacer equally. The spacer should support the membrane, this being particularly

important in the region between the manifolds. The spacer material should be inert, should possess physical properties so as to permit a hydraulic seal when pressurised and be dimensionally stable.

The spacers are usually perforated PVC nets and, depending on the design, are 0,5 mm to 1 mm thick[6]. The size of the spacer depends on the size of the membrane used. In general, large components tend to cost less per unit of effective membrane area. However, practical considerations such as the ease of handling and mechanical strength must be taken into account. Components which are thin result in lower operating costs but there are difficulties in providing good flow distribution. It is apparent that the presence of the spacer reduces the active membrane area since it also serves to support the membrane. There is an advantage in utilising as much of the membrane surface area as possible but this results in difficulties in supporting and sealing the membranes. A membrane of about 1,5 m^2 is probably the maximum practicable, usually the area is 0,5 m^2 to 1 m^2. The effective membrane area is about 85 % of the total membrane area.

Stack sealing is of importance to stack operation. The spacer should seal easily since the lower compression force required to seal the stack, the less likely will be the chance of damaging components. This aspect of design becomes most complex in the region of manifolds. This area should be as small as possible but should not cause a high pressure drop. Also, since a seal must be made round this area the support in this region must be able to withstand the compressive scaling forces of the stack.

The stack itself should be easy to maintain. It often occurs that only a few cell pairs in the stack require maintenance. In a large stack it is desirable to be able to open the stack at any section and remove a cell pair without disturbing any of the other cell pairs.

The electrodes must be made of a material which is corrosion resistant, since at the cathode the flow becomes alkaline while at the anode gaseous chlorine and oxygen are formed. It is normal to have separate feeds to the anode and cathode, the anode rinse going to a drain while the cathode rinse is treated with acid and then recirculated. The maximum voltage across a stack is 3 volts per cell pair and so a normal stack voltage will be about 900 volts.

4.16 Process Design

Since the amount of desalting depends directly on the current level it is a straight-forward exercise to calculate the performance of a given stack at a particular current density. In order to achieve a given level of desalination the plant can either be run in a batch process or in a once-through process[6].

In a batch process, the water to be desalinated is stored in a tank and then partially desalted by passing it through the stack to a second tank having been further desalted. After each pass the concentration is checked and the process is repeated until the required level of demineralization is achieved. This method is often used when the feed water is subject to changes in composition. For example, in a lot of cases brackish well water is liable to increase in salinity at high pumping rates.

In a once-through system, the required desalting is achieved by passing the diluate stream through successive stacks arranged hydraulically in series. This process tends to be used in the higher capacity plants and requires less control systems. Where possible (i.e. where the feed water salinity can be guaranteed) a continuous type of plant is always to be preferred. Since plant operation is simpler, the likelihood of breakdown is reduced and the capital cost is reduced.

In both systems the concentrate streams are recycled to minimize blow-down and possible use of chemicals. The flow of the concentrate stream is normally 25% or less than that of the diluate stream. To minimize the electrical resistance of the stack it is desirable to have the concentrate stream at the maximum concentration possible (this also minimizes the blow-down to waste). The normal limiting factor for the degree of concentration is the solubility of calcium sulphate.

In both systems the limiting current density controls the amount of desalination possible. The onset of polarization manifests itself in the change of chemical conditions in the plant and also in an increase in the voltage requirements maintaining the current. The lower the salt content in the water, the lower will be the limiting current density. Electrodialysis, therefore, is not applicable in the production of high purity waters.

5. EXPERIMENTAL

5.1 Membranes

The membrane and membrane types shown in Table 5.1 were selected for the EOP study of sodium chloride-, hydrochloric acid- and caustic soda solutions.

Table 5.1 Membrane and membrane types selected for EOP of Sodium Chloride-, Hydrochloric Acid- and Caustic Soda Solutions

Membranes	Anionic (A) Cationic (C)	Type	Salt	Acid	Base
Selemion AMV	A	Homogeneous	✓	✓	✓
Selemion CMV	C	Homogeneous	✓	✓	✓
Ionac MA 3470	A	Heterogeneous	✓	✓	✓
Ionac MC 3475	C	Heterogeneous	✓	✓	✓
Raipore R 4030	A	Homogeneous	✓		
Raipore R 4010	C	Homogeneous	✓		
Ionics A 204 UZL 386	A	Homogeneous	✓		
Ionics C 61 CZL 386	C	Homogeneous	✓		
WTPSA-1	A	Heterogeneous	✓		
WTPSC-1	C	Heterogeneous	✓		
WTPVCA-2	A	Heterogeneous	✓		
WTPVCC-2	C	Heterogeneous	✓		
WTPSTA-3	A	Heterogeneous	✓		
WTPSTC-3	C	Heterogeneous	✓		
Selemion AAV	A	Homogeneous		✓	
Selemion CHV	C	Homogeneous		✓	
ABM-1	A	Homogeneous		✓	
Selemion CHV	C	Homogeneous		✓	
ABM-2	A	Heterogeneous		✓	
Selemion CHV	C	Homogeneous		✓	
ABM-3	A	Heterogeneous		✓	
Selemion CHV	C	Homogeneous		✓	
Selemion AMP	A	Homogeneous			✓
Selemion CMV	C	Homogeneous			✓

5.2 Membrane Preparation

The WTA (WATERTEK anion) and WTC (WATERTEK cation) ion-exchange membranes were prepared as follows:

Resin (strong acid and strong base) with a particle size of less than 70 μm was suspended in appropriate swelling, base and casting solutions and the membranes were cast on polypropylene support material. The membranes were dried for approximately 1 hour in a convection oven at temperatures from 65 to 80°C before use. Polysulphone (for WTPSA-1; WTPSC-1 membranes), polyvinyl chloride (for

WTPVCA-2, WTPVCC-2 membranes) and polystyrene (for WTPSTA-3, WTPSTC-3 membranes) were used as base materials. N- methyl-2 pyrolidone (NMP) was used as casting solution for the polysulphone (PS) based membranes while cyclohexanone was used as casting solution for the polyvinyl chloride and polystyrene based (PST) membranes.

The ABM membranes for acid EOP studies were supplied by the membrane research group of the Weizmann Institute of Science in Israel. The membranes used in the sealed-cell ED tests were also developed by the membrane research group of the Weizmann Institute of Science in Israel. The membranes were made from microbeads of styrene-divinylbenzene copolymer which were modified to cation- and anion-exchange particles. The cation-exchange particles were formed by chlorosulphonation with chlorosulphonic acid followed by hydrolysis to yield the sulphonated product. The anion-exchange particles were formed by chloromethylation followed by amination with triethylamine to yield the anion-exchange particles.

The ion-exchange membranes were formed by casting a suspension of the particles on a fabric. The suspension was evaporated to dryness to yield the dry membrane. The cation- and anion-exchange membranes were then heat-sealed to give the membrane bags.

5.3 Unit-Cell Construction

A unit cell can be constructed in the following number of ways : -

a) glueing the membrane edges together with a suitable glue;
b) glueing the membrane edges to either side of an injection moulded nylon ring (Figure 5.1) which has a brine exit within it[1]; and
c) mounting of the membranes between gaskets as in the filter press stack design.

For experiment, the volume, however, of the brine compartment must be kept to a minimum in order to minimize time for achieving the steady state and for beginning to measure water flow. An injection moulded nylon ring (Figure 5.1) was used in the EOP experiments as the unit cell.

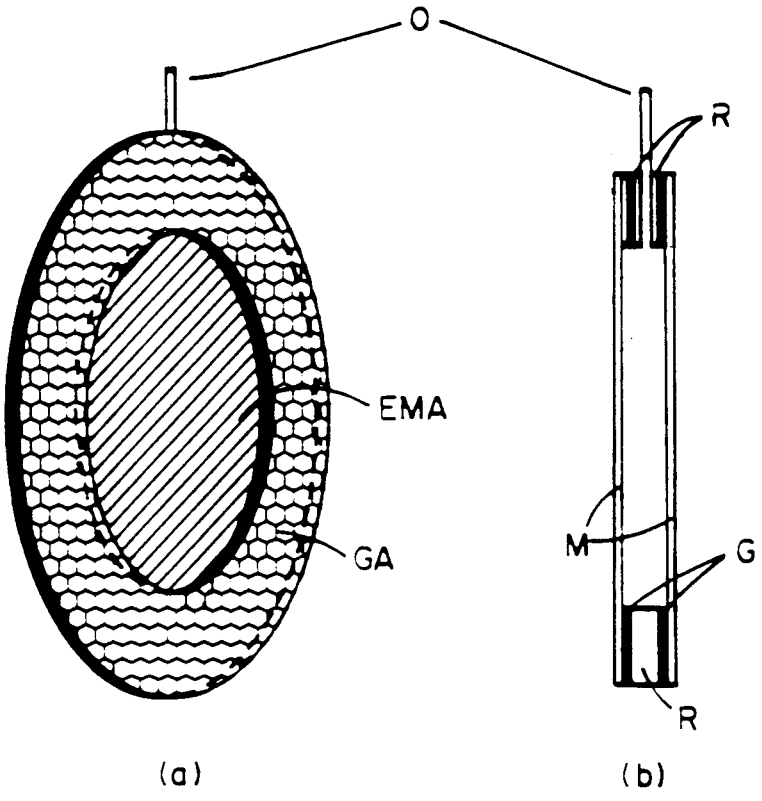

Figure 5.1: **Schematic of injection moulded nylon ring that was used for construction of the membrane bag. The membranes are glued to both sides of the ring.**

a : Front view **b : Lateral view**
O : brine outlet **EMA : Effective membrane area**
GA: Glueing area **M : Membrane**
G : Glue **R : Nylon ring.**

5.4 Determination of Brine Concentration, Current Efficiency and Water Flow as a Function of Feed Concentration and Current Density

The EOP cell used in the experiments was described by Oren and Litan[112] and is shown in Figure 5.2. It consists of two symmetric units, each of which contains a separate electrode. A carbon slurry was circulated through the electrode compartments and was used as electrode rinse solution. The membranes were attached to the nylon ring with silicon sealant and the nylon ring (membrane bag) was placed between the two circulation cells and rubber rings were used to secure sealing. Approximately 40 litres of solution containing salt, acid or base was circulated through the cell renewing its content approximately 60 times per minute. In this way an approximately constant feed concentration was maintained during the experiments.

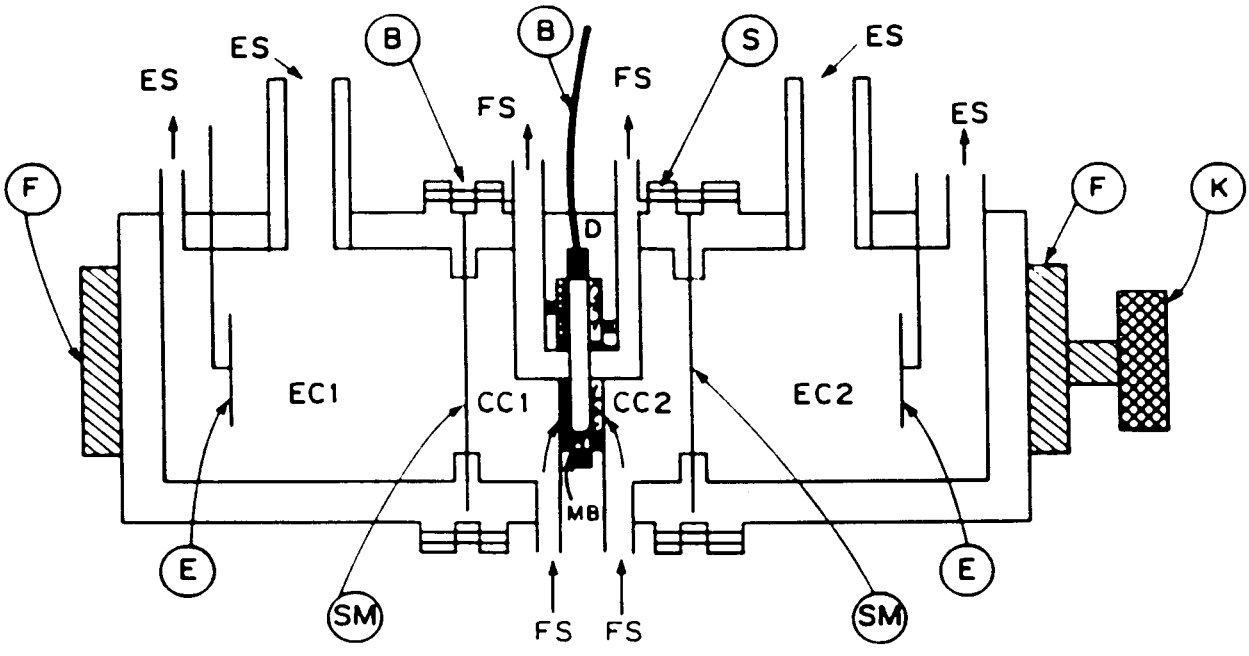

Figure 5.2: **Schematic diagram of the apparatus used for the EOP experiments. EC1 and EC2: Electrode cells; CC1 and CC2: Circulation cells for the feed solution (FS); B: Brine outlet; MB: Membrane bag; SM: Membrane separating the electrode compartments from the feed solution; E: Electrodes; D: Perforated porous polypropylene disks; S: Stainless Steel Screws; F: Clamping frame; K: Tightening knob.**

Efficient stirring and streaming of the solution in the cell were effected by the Meares and Sutton's method of forcing the solution onto the membrane surface through perforated polypropylene discs[112]. This has been shown to be a very efficient way of stirring. Constant current was supplied to the cell by a Hewlett Packard constant current source. Current was measured with a Hewlett Packard digital multimeter. Brine samples were collected at certain intervals and their volume and concentration determined. Each point on the plots of c_b versus I, and of J versus I_{eff} was the average of 3 to 5 measurements after the system had reached the stationary state. Concentration changes in the feed solution during the time of the experiments were found to be negligible.

Current efficiency, ϵ_p, was calculated as follows[1]:

$$\epsilon_p = \frac{2Jc_b}{I/F} = \frac{c_b(V/t)}{I/F} \equiv \Delta\bar{t} \qquad \text{(see eq. 3.10.37)}$$

where c_b represents the brine concentration, V the volume of the solution that enters the bag per unit area (7,55 cm^2) in t seconds (V/t = 2J), I the applied current density (mA/cm^2) and F is Faraday's constant.

The maximum brine concentration, c_b^{max}, was determined from the following relation

$$c_b^{max} = \frac{I}{2\beta F} \qquad \text{(see eq. 3.10.28)}$$

where 2ß is the electro-osmotic coefficient determined from the slope of the J versus I_{eff} plots and F is Faraday's constant.

5.5 Determination of Membrane Characteristics

5.5.1 Membrane potential

The difference between the counter- and co-ion transport number, Δt, which is called the apparent transport number or membrane permselectivity, was measured as follows:

The potential ($\Delta\Psi_m$) of a membrane is usually measured between 0,1/0,2 mol/ℓ or 0,5/1,0 mol/ℓ sodium chloride solutions in a specially designed cell with calomel electrodes. The theoretical potential, $\Delta\Psi_i$, is calculated from the activities of the two solutions. Membrane permselectivity, Δt, can then be calculated from these values where $\Delta\Psi_m$ is the measured potential and a_s^{11}/a_s^{1} is the ratio of salt activities on both sides of the membrane.

$$\Delta t = \frac{\Delta\Psi_m}{\Delta\Psi_i} \qquad \text{(see eq. 3.11.11)}$$

where $\Delta t = 2t_1 - 1$ and

$$\Delta\Psi_i = \frac{RT}{F} \ln \frac{a_s^{11}}{a_s^{1}} \qquad \text{(see eq. 3.11.10)}$$

5.5.2 Ion-Exchange Capacity

Membrane capacity was determined as follows[113]:

Approximately 3 g dried membrane sample (weighed accurately) was equilibrated with 150 ml 1 mol/ℓ hydrochloric acid for 16 hours at room temperature. The membrane

sample was rinsed free of chloride. The sample was then treated with 200 mℓ 4% sodium carbonate solution for 2 hours, neutralized to below pH 8,3 with 0,1 mol/ℓ sulphuric acid, potassium chromate (2 mℓ) added and the sample titrated with standardized 0,1 mol/ℓ silver nitrate and the total anion membrane exchange capacity calculated.

5.5.3 Gel Water Content

The gel water content of the membranes was determined as follows[113]:

Membrane samples (pretreated to their reference form[113]) were blotted dry with filter paper and mass recorded. The membrane sample was then dried at 105°C for 16 hours and the dried mass recorded. The gel water content (%) was calculated from the mass loss.

5.5.4 Membrane Resistance

Membrane resistance was measured between platinum electrodes coated with platinum black in a specially designed membrane resistance measurement cell with a resistance meter. Salt concentrations of 0,1 and 0,5 mol/ℓ sodium chloride were used. Membrane resistance was expressed in ohm.cm^2.

5.6 Determination of Salt and Acid Diffusion Rate through Membranes

Salt and acid diffusion rate through *Selemion* AMV and AAV membranes was determined in the cell shown in Figure 5.3. The cell consists of two half-cells containing stirrers with a volume of approximately 200 mℓ per half-cell. A membrane with an exposed area of 2,55 cm^2 was clamped between the two half-cells and salt or acid solution with a concentration difference of 0,05/2 mol/ℓ and 0,05/4 mol/ℓ was placed in the two half-cells. Diffusion was allowed to take place and the rate of concentration change in the two cells was determined.

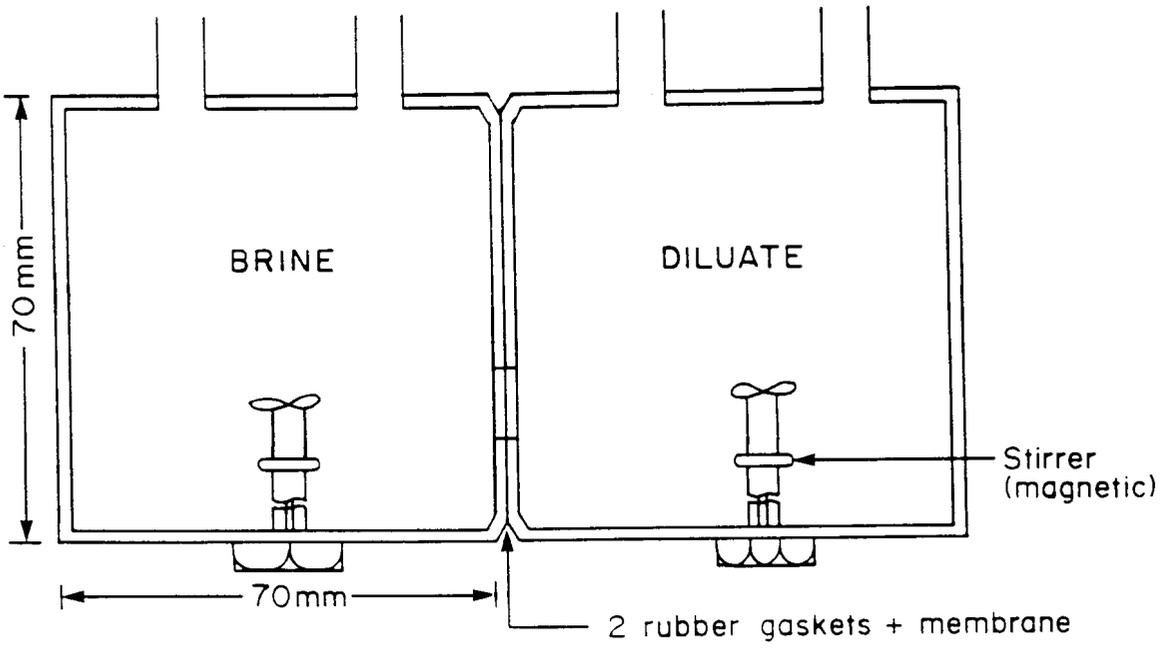

Figure 5.3: Diagram of cell used for determination of diffusion of hydrochloric acid and sodium chloride through membranes (membrane area = 2,55 cm²).

5.7 Bench-Scale EOP-ED Stack

A bench-scale EOP-ED stack has been designed and constructed from materials available in South Africa. A simplified diagram of the membrane configuration in the stack is shown in Figure 5.4. The stack is similar to a conventional filter-press type ED stack. The only difference is that brine is not circulated through the brine compartments as is the case in conventional ED. Water enters the brine compartments by means of electro-osmosis and runs out of these compartments in a groove in the spacer at the top of each brine cell. The stack contained 10 cell pairs with an effective membrane area of 169 cm².

The end plates were made from PVC. A diagram of the end plates is shown in Figure 5.5. Water flow through the stack into the diluating and brine compartments was directed by the manifold shown in Figure 5.5. Gaskets made from polycarbonate (2 mm) and teflon (2 mm) were used in the stack to separate the membranes from each other. A diagramme of a gasket is shown in Figure 5.6. PVC spacers (0,3 mm) were used to separate the membranes from each other. Platinized titanium or graphite electrodes were used in the stack.

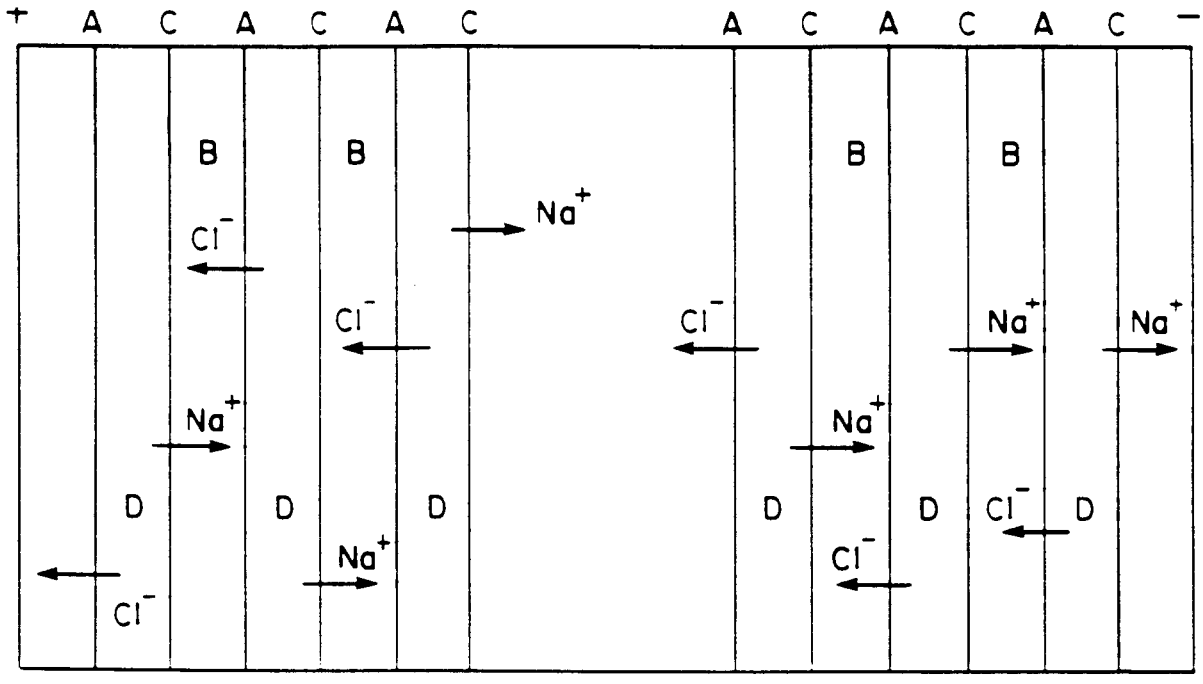

Figure 5.4: **Simplified diagram of membrane configuration in EOP-ED stack. B = brine compartment; D = diluating compartment.**

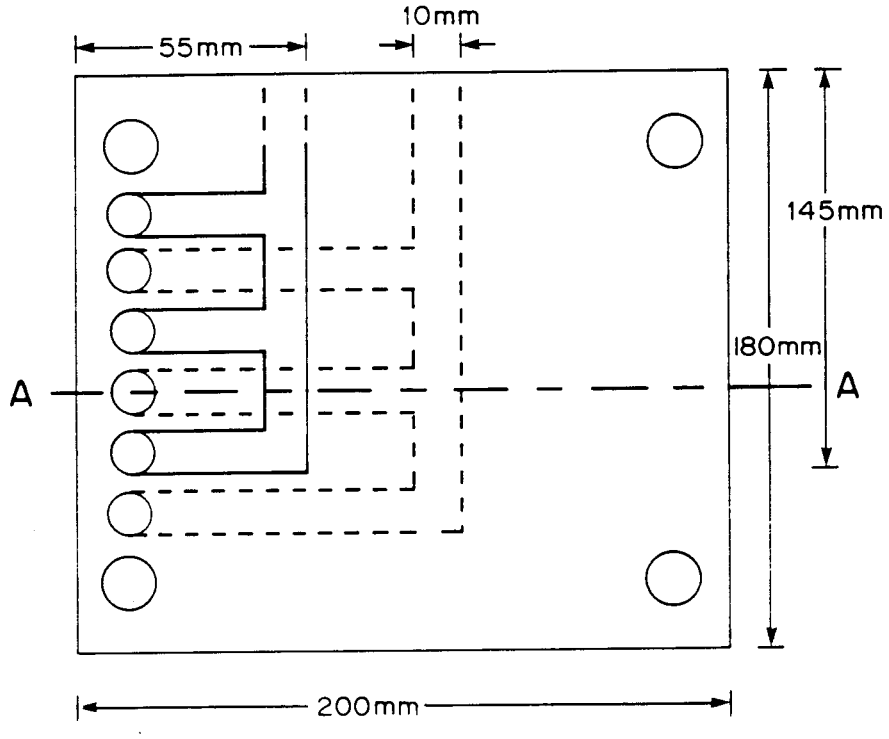

Figure 5.5: **End plates of EOP-ED stack.**

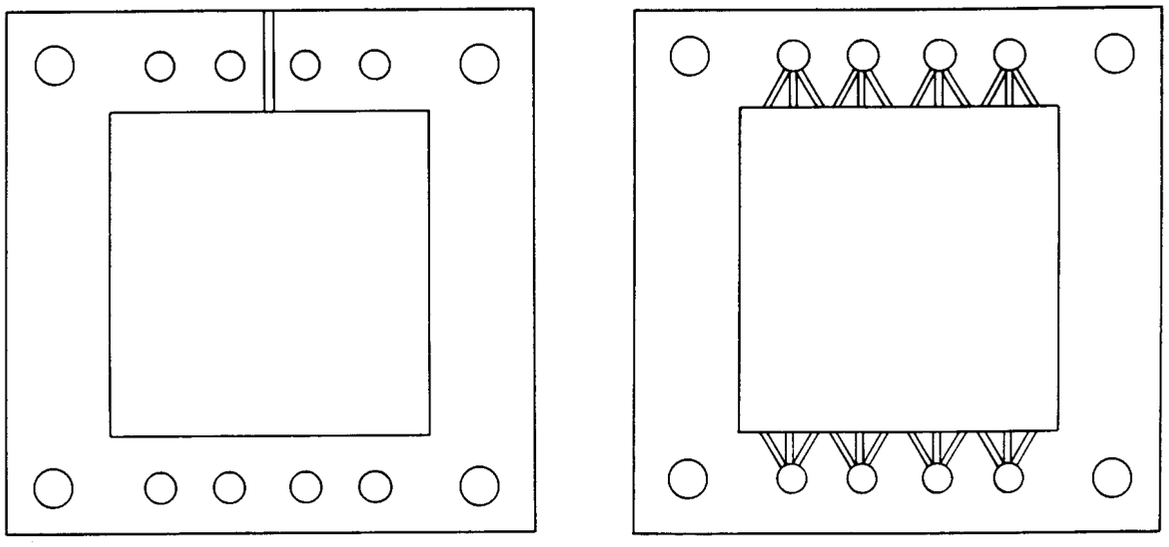

a) Brine gasket **b) Diluating gasket**

Figure 5.6: Gaskets used in EOP-ED stack.

Ionac MA-3475 and MC-3470 membranes were used for concentration/desalination of sodium chloride solutions while *Selemion* AAV and CHV and *Selemion* AMV and CMV membranes were used for hydrochloric acid and caustic soda concentration/desalination, respectively.

Solutions of sodium chloride, hydrochloric acid and caustic soda in deionized water of different initial concentrations were concentrated/desalinated at different cell pair voltages in the stack. The experimental set-up is shown in Figure 5.7. Feed (c_f), product (c_p) and brine (c_b) concentrations were determined from conductivity measurements.

A typical ED experiment was conducted as follows:

Feed solution (12 ℓ) was circulated at a linear flow velocity of 1 cm/s through the dialysate compartments. The electrode solution consisted of 2 litre of a 2% carbon slurry in 1 mol/ℓ sodium chloride solution. The pH of this solution was adjusted to approximately 5 and circulated through the electrode compartments.

Direct current voltage of 0,5; 1,0; 1,5; 2,0; 3 and 4 volt was applied across a cell pair. Voltage between the cells was measured with platinum wire connected to a voltmeter. Platinum wire was inserted between the first and last brine cell. Current was recorded at 15 minute intervals and the concentration potential (V_n) was determined by interrupting the current for a few seconds. The final brine volume and the concentration of the desalinated feed (product water) and brine were determined at the end of the runs.

Current efficiency (CE), water recovery (WR), brine volume (BV), electrical energy consumption (EEC), concentration factor (CF), output (OP) (water yield), d_{eff} and R_{cp} were determined from the experimental data. Graphs were compiled of reduction in feed water concentration as a function of time and of cell pair resistance (V_{cp}) as a function of specific resistance (p) of the dialysate. An example of the calculations is shown in Appendix C.

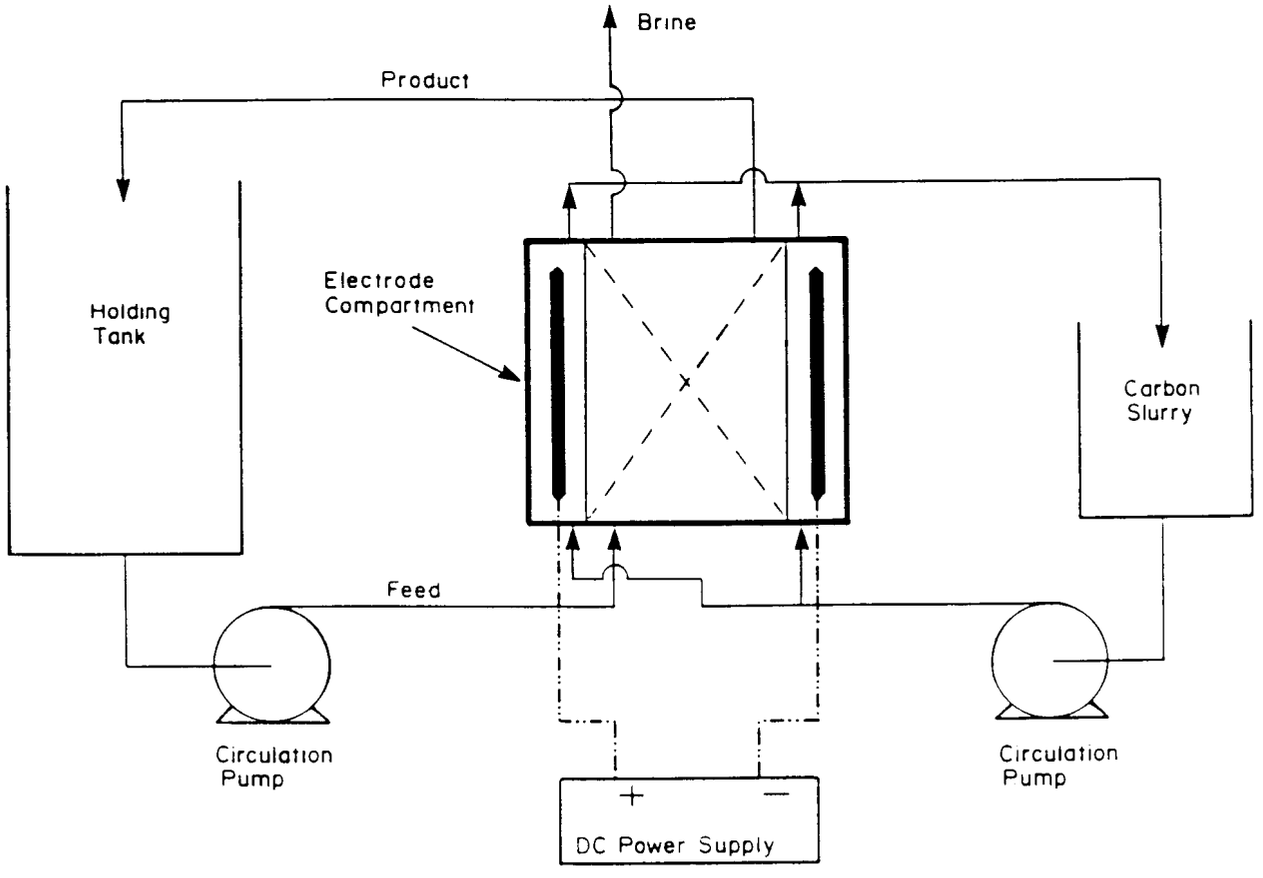

Figure 5.7: Experimental set-up for EOP-ED of sodium chloride, hydrochloric acid and caustic soda solutions.

5.8 Sealed-Cell ED Stack

A simplified diagram of the sealed-cell (SCED) membrane stack is shown in Figure 5.8. The brine sealed cells with outlets are arrayed in an open vessel, separated by spacers (0,3 mm). The dialysate enters through a suitable port at the bottom of the vessel and runs out through an overflow. Direct current is applied through carbon suspension electrodes[4]. The external dimensions of the sealed brine cells are 60 x 80 mm, giving an effective membrane area of 100 cm^2 per cell pair (cp).

Solutions of sodium chloride, ammonium nitrate, sodium sulphate, sodium nitrate and calcium chloride in deionized water of different initial concentrations were concentrated/desalinated at different cell pair voltages in the SCED unit. Feed (c_f), product (c_p) and brine (c_b) concentrations were determined from conductivity measurements. Various industrial effluents were also treated with SCED.

Feed solution (15 ℓ) was circulated at a linear flow velocity of 15 cm/s through the dialysate compartments. The electrode solution consisted of 2 ℓ of a 2 % carbon slurry in 1 mol/ℓ sodium chloride solution. The pH of the solution was adjusted to approximately 5 and circulated through the electrode compartments.

Electrodialysis was started by applying a DC voltage of approximately 0,5 Volt per cell pair across 17 membrane bags. Voltage between the membrane bags was measured with calomel electrodes connected to a salt bridge. Current was recorded at 10 or 20 minute intervals during ED and V_n was determined during interruption of the current for a short period. The final brine volume, concentration of the desalinated feed (product water) and brine were determined at the end of the runs.

Current efficiency (CE), water recovery (WR), brine volume (BV), electrical energy consumption (EEC), concentration factor (CF), output (OP) (water yield), effective thickness of dialysate compartment (d_{eff}), and membrane resistance (R_{cp}) were determined from the experimental data. Graphs were plotted of feed water concentration, brine concentration, current efficiency and electrical energy consumption as a function of time, and of cell pair voltage as a function of the specific resistance (p) of the dialysate.

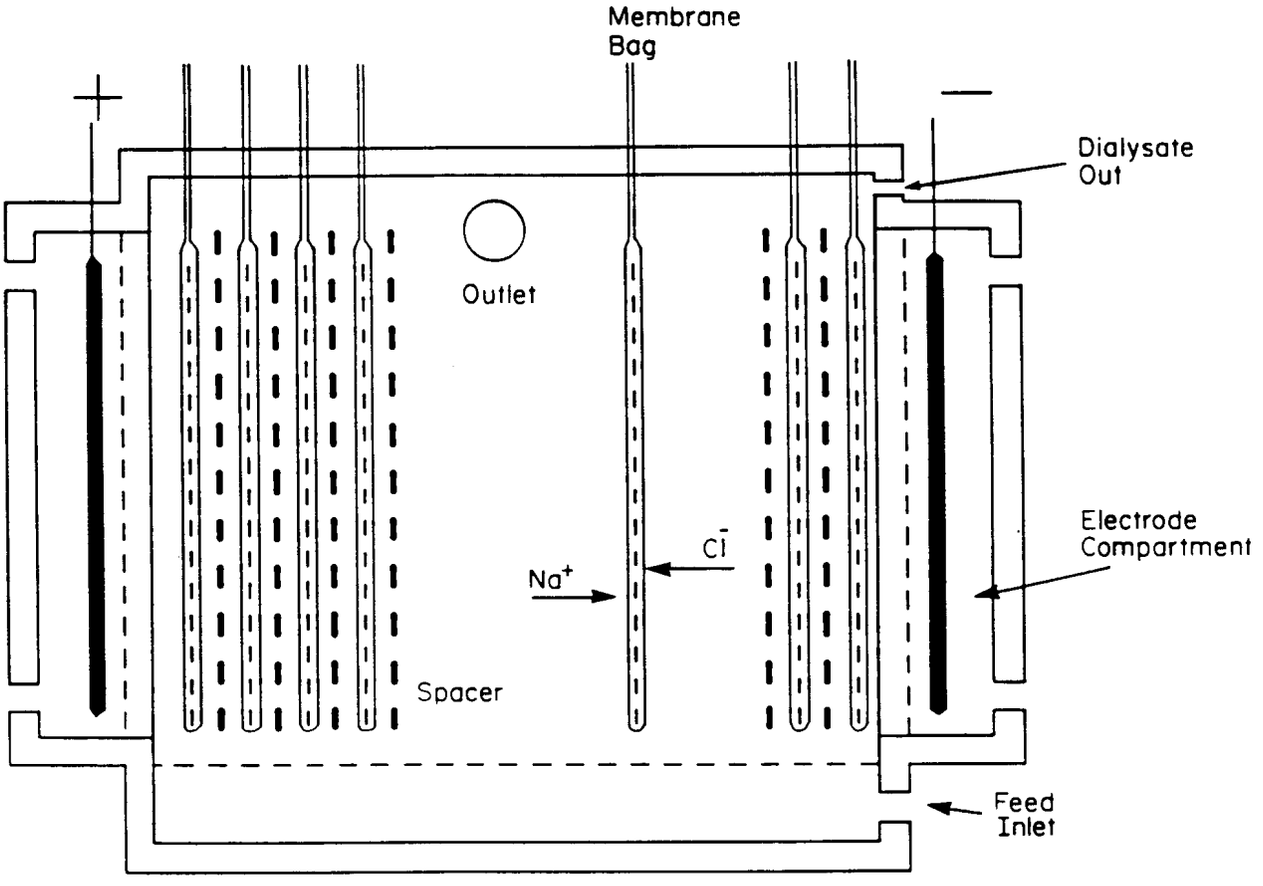

Figure 5.8: Simplified diagram of SCED membrane stack.

6. ELECTRO-OSMOTIC PUMPING OF SODIUM CHLORIDE SOLUTIONS WITH DIFFERENT ION-EXCHANGE MEMBRANES

Brine concentrations, water flows and current efficiencies were determined at different current densities for different sodium chloride feed water concentrations. Membrane permselectivities (apparent transport numbers - Δt's) were measured at the same concentration differences as encountered during EOP experiments when brine concentration had reached the steady state. The EOP results are summarized in Tables 6.1 to 6.28 for the different membranes.

6.1 Brine Concentration

Brine concentration (c_b) as a function of current density (I) is shown in Figures 6.1 to 6.7. Initially brine concentration increases rapidly and then levels off at higher current densities. Brine concentration increases with increasing current density and increasing feed water concentration. Highest brine concentrations were obtained with *Selemion* and *Ionac* membranes (Table 6.29). Brine concentrations of 25,1 and 23,4% were obtained at high current density (0,1 mol/ℓ feed) with *Selemion* and *Ionac* membranes, respectively. Lower brine concentrations were obtained with the *Ionics* and WTPS membranes (19,0 and 20,9%, respectively) while the lowest concentrations were obtained with the *Raipore*, WTPVC and WTPST membranes (14,4, 15,1 and 15,4%, respectively). The concentration performance of the WTPS membranes compares favourably with that of the commercially available membranes.

It appears that the brine concentration will reach a maximum value, c_b^{max}. This was predicted from the flow equations[1]. Maximum brine concentration was nearly reached in the case of the *Raipore*- (Fig. 6.3), WTPVC- (Fig. 6.6) and WTPST- (Fig. 6.7) membranes at 0,05 mol/ℓ feed concentration at high current density. Maximum brine concentration was also nearly reached in the case of the *Selemion*- (Fig. 6.1), *Ionac*- (Fig. 6.2), *Raipore*- (Fig. 6.3), *Ionics*- (Fig. 6.4), WTPS- (Fig 6.5), WTPVC- (Fig. 6.6) and WTPST- (Fig. 6.7) membranes in the 0,1 to 1,0 mol/ℓ feed concentration range at high current densities.

Maximum brine concentration, c_b^{max}, was calculated from the following two relationships, viz.

$$c_b^{max} = \frac{1}{2\beta F} \qquad \text{(see eq. 3.10.28)}$$

Table 6.1 : Electro-osmotic pumping experimental conditions and results for 0,05 mol/ℓ sodium chloride (Selemion AMV and CMV)

Current Density	Brine concentration c_b, mol/l		Water flow	Current Efficiency	Effective Current Density	Transport Numbers				
i, mA/cm²	$c_{b\,exp.}$	$c_{b\,calc.}$	J, cm/h	e_p, %	i_{eff}, mA/cm²	Δt^c	Δt^a	$\bar{\Delta}t$	$\bar{t}_1^c$	$\bar{t}_2^a$
5	1,62	1,59	0,102	62,37	3,12	0,91	0,82	0,87	0,96	0,91
10	2,15	2,76	0,115	66,22	6,62	0,88	0,82	0,85	0,94	0,91
15	2,65	3,35	0,137	64,79	9,72	0,85	0,78	0,82	0,93	0,89
20	2,81	3,54	0,170	64,93	12,99	0,86	0,75	0,81	0,93	0,88
30	3,31	4,05	0,217	64,15	19,25	0,84	0,73	0,79	0,92	0,86

Electro-osmotic coefficient (2ß) = 0,219 ℓ/F (slope = 0,008194 mℓ/mAh)
J_{osm} = y-intercept = 0,06023 cm/h
c_c^{max} = 4,55 mol/l
$\Delta t^c = t_1^c - t_2^c$

$\Delta t^a = t_2^a - t_1^a$
$\bar{\Delta}t$ = Average transport number of membrane pair
$\bar{t}_1^c$ = Transport number of cation through cation membrane
$\bar{t}_2^a$ = Transport number of anion through anion membrane.

Table 6.2 : Electro-osmotic pumping experimental conditions and results for 0,1 mol/ℓ sodium chloride (Selemion AMV and CMV)

Current Density	Brine concentration c_b, mol/l		Water flow	Current Efficiency	Effective Current Density	Transport Numbers				
i, mA/cm²	$c_{b\,exp.}$	$c_{b\,calc.}$	J, cm/h	e_p, %	i_{eff}, mA/cm²	Δt^c	Δt^a	$\bar{\Delta}t$	$\bar{t}_1^c$	$\bar{t}_2^a$
5	1,79	2,1	0,076	73,0	3,65	0,94	0,81	0,87	0,97	0,90
10	2,37	2,64	0,118	74,4	7,47	0,89	0,78	0,84	0,94	0,89
15	2,83	3,02	0,152	76,7	11,51	0,89	0,75	0,82	0,94	0,88
20	3,02	3,21	0,188	76,1	15,23	0,88	0,73	0,81	0,94	0,87
30	3,58	3,74	0,238	76,2	22,86	0,85	0,74	0,80	0,93	0,87
40	3,91	4,09	0,286	75,0	30,01	0,89	0,68	0,78	0,94	0,84
50	4,29	4,33	0,330	75,9	37,95	0,82	0,71	0,77	0,91	0,85

Electro-osmotic coefficient (2ß) = 0,198 ℓ/F (slope = 0,00739 mℓ/mAh)
J_{osm} = y-intercept 0,067696 cm/h
c_c^{max} = 5,05 mol/l
$\Delta t^c = t_1^c - t_2^c$

$\Delta t^a = t_2^a - t_1^a$
$\bar{\Delta}t$ = Average transport number of membrane pair
$\bar{t}_1^c$ = Transport number of cation through cation membrane
$\bar{t}_2^a$ = Transport number of anion through anion membrane.

Table 6.3 : Electro-osmotic pumping experimental conditions and results for 0,5 mol/ℓ sodium chloride (Selemion AMV and CMV)

Current Density	Brine concentration c_b, mol/l		Water flow	Current Efficiency	Effective Current Density	Transport Numbers				
i, mA/cm²	$c_{b\,exp.}$	$c_{b\,calc.}$	J, cm/h	e_p, %	i_{eff}, mA/cm²	Δt^c	Δt^a	$\bar{\Delta}t$	$\bar{t}_1^c$	$\bar{t}_2^a$
5	1,72	1,71	0,0895	82,5	4,13	0,92	0,71	0,82	0,96	0,86
10	2,74	2,33	0,122	89,66	8,96	0,86	0,67	0,76	0,93	0,83
20	3,54	2,82	0,190	91,72	18,34	0,81	0,63	0,72	0,91	0,81
30	3,94	3,27	0,248	87,35	26,21	0,86	0,59	0,72	0,93	0,80
40	4,20	3,26	0,323	90,89	36,36	0,81	0,60	0,71	0,90	0,80
50	4,50	3,51	0,378	91,23	45,62	0,84	0,58	0,71	0,92	0,79
60	4,66	3,62	0,440	91,46	54,88	0,85	0,57	0,71	0,93	0,79

Electro-osmotic coefficient (2ß) = 0,187 ℓ/F (slope = 0,006959 mℓ/mAh)
J_{osm} = y-intercept = 0,062409 cm/h
c_c^{max} = 5,36 mol/l
$\Delta t^c = t_1^c - t_2^c$

$\Delta t^a = t_2^a - t_1^a$
$\bar{\Delta}t$ = Average transport number of membrane pair
$\bar{t}_1^c$ = Transport number of cation through cation membrane
$\bar{t}_2^a$ = Transport number of anion through anion membrane.

Table 6.4: Electro-osmotic pumping experimental conditions and results for 1,0 mol/ℓ sodium chloride (Selemion AMV and CMV)

Current Density	Brine concentration c_b, mol/l		Water flow	Current Efficiency	Effective Current Density	Transport Numbers				
I, mA/cm²	$c_{b\,exp.}$	$c_{b\,calc.}$	J, cm/h	e_p, %	I_{eff}, mA/cm²	Δt^c	Δt^a	$\bar{\Delta}t$	$\bar{t}_1^c$	$\bar{t}_2^a$
10	2,95	2,41	0,113	89,00	8,90	0,84	0,62	0,73	0,92	0,81
20	3,73	2,90	0,174	87,14	17,43	0,82	0,55	0,68	0,91	0,77
30	4,12	3,16	0,236	86,95	26,09	0,79	0,55	0,67	0,90	0,78
40	4,55	3,51	0,279	85,21	34,08	0,80	0,51	0,66	0,90	0,76
50	5,07	3,70	0,328	89,28	44,64	0,79	0,52	0,65	0,89	0,76
60	5,10	3,79	0,384	87,52	52,51	0,80	0,50	0,65	0,90	0,75

Electro-osmotic coefficient (2ß) = 0,154 ℓ/F (slope = 0,005757 mℓ/mAh)
J_{osm} = y-intercept = 0,078991 cm/h
c_b^{max} = 6,48 mol/l
$\Delta t^c = t_1^c - t_2^c$

$\Delta t^a = t_2^a - t_1^a$
$\bar{\Delta}t$ = Average transport number of membrane pair
$\bar{t}_1^c$ = Transport number of cation through cation membrane
$\bar{t}_2^a$ = Transport number of anion through anion membrane.

Table 6.5 : Electro-osmotic pumping experimental conditions and results for 0,05 mol/ℓ sodium chloride (Ionac MA-3475 and MC-3470)

Current Density	Brine concentration c_b, mol/l		Water flow	Current Efficiency	Effective Current Density	Transport Numbers				
I, mA/cm²	$c_{b\,exp.}$	$c_{b\,calc}$	J, cm/h	e_p, %	I_{eff}, mA/cm²	Δt^c	Δt^a	$\bar{\Delta}t$	$\bar{t}_1^c$	$\bar{t}_2^a$
5	1,50	1,82	0,0883	71,01	3,55	0,93	0,80	0,86	0,96	0,90
10	2,16	2,80	0,1112	64,41	6,44	0,91	0,76	0,83	0,95	0,88
15	2,60	3,45	0,1324	61,54	9,23	0,90	0,73	0,82	0,95	0,87
20	2,87	4,05	0,1456	56,04	11,21	0,83	0,74	0,79	0,92	0,87
25	3,25	4,60	0,1589	55,39	13,85	0,86	0,71	0,78	0,93	0,85

Electro-osmotic coefficient (2ß) = 0,186 ℓ/F (slope = 0,0069464 mℓ/mAh)
J_{osm} = y-intercept = 0,0657676 cm/h
c_b^{max} = 5,37 mol/l
$\Delta t^c = t_1^c - t_2^c$

$\Delta t^a = t_2^a - t_1 a$
$\bar{\Delta}t$ = Average transport number of membrane pair
$\bar{t}_1^c$ = Transport number of cation through cation membrane
$\bar{t}_2^a$ = Transport number of anion through anion membrane.

Table 6.6 : Electro-osmotic pumping experimental conditions and results for 0,1 mol/ℓ sodium chloride (Ionac MA-3475 and MC-3470)

Current Density	Brine concentration c_b, mol/l		Water flow	Current Efficiency	Effective Current Density	Transport Numbers				
I, mA/cm²	$c_{b\,exp.}$	$c_{b\,calc}$	J, cm/h	ep, %	I_{eff}, mA/cm²	Δt^c	Δt^a	$\bar{\Delta}t$	$\bar{t}_1^c$	$\bar{t}_2^a$
5	1,92	2,29	0,0662	68,17	3,41	0,89	0,73	0,81	0,95	0,87
10	2,49	2,94	0,0997	64,19	6,42	0,88	0,70	0,79	0,94	0,85
15	2,89	3,65	0,1186	61,70	9,25	0,86	0,68	0,77	0,93	0,84
20	3,18	3,84	0,14834	63,23	12,65	0,86	0,67	0,76	0,93	0,83
30	3,4	4,27	0,1977	60,09	18,03	0,84	0,67	0,75	0,92	0,83
40	3,81	4,89	0,2295	58,62	23,45	0,84	0,66	0,75	0,92	0,83
50	4,00	5,32	0,2649	56,81	28,40	0,85	0,66	0,76	0,93	0,83

Electro-osmotic coefficient (2ß) = 0,206 ℓ/F (slope = 0,0076844 mℓ/mAh)
J_{osm} = y-intercept = 0,0503481 cm/h
c_c^{max} = 4,85 mol/l
$\Delta t^c = t_1^c - t_2^c$

$\Delta t^a = t_2^a - t_1^a$
$\bar{\Delta}t$ = Average transport number of membrane pair
$\bar{t}_1^c$ = Transport number of cation through cation membrane
$\bar{t}_2^a$ = Transport number of anion through anion membrane.

Table 6.7 : Electro-osmotic pumping experimental conditions and results for 0,5 mol/ℓ sodium chloride (Ionac MA-3475 and MC-3470)

Current Density	Brine concentration c_b, mol/l		Water flow	Current Efficiency	Effective Current Density	Transport Numbers				
I, mA/cm²	$c_{b\,exp.}$	$c_{b\,calc.}$	J, cm/h	e_p, %	I_{eff}, mA/cm²	Δt^c	Δt^a	$\bar{\Delta}t$	$\bar{t}_1^c$	$\bar{t}_2^a$
5	2,37	1,69	0,07568	96,17	4,81	0,80	0,57	0,69	0,90	0,79
10	2,95	2,57	0,097	76,81	7,68	0,80	0,54	0,67	0,90	0,77
20	3,69	3,03	0,1589	78,61	15,72	0,78	0,52	0,65	0,89	0,76
30	3,99		0,205	73,19	21,95					
40	4,05	3,84	0,2472	67,10	26,84	0,77	0,50	0,64	0,88	0,75
50	4,37	4,42	0,26136	61,23	30,62	0,75	0,49	0,62	0,87	0,75
60	4,51	4,91	0,2825	56,93	34,16	0,73	0,51	0,62	0,87	0,75
70	4,59	5,05	0,3178	55,87	39,11	0,73	0,50	0,61	0,86	0,75

Electro-osmotic coefficient (2ß) = 0,190 ℓ/F (slope = 0,0070843 mℓ/mAh)
J_{osm} = y-intercept = 0,0454963 cm/h
c_b^{max} = 5,26 mol/l
$\Delta t^c = t_1^c - t_2^c$

$\Delta t^a = t_2^a - t_1^a$
$\bar{\Delta}t$ = Average transport number of membrane pair
$\bar{t}_1^c$ = Transport number of cation through cation membrane
$\bar{t}_2^a$ = Transport number of anion through anion membrane.

Table 6.8: Electro-osmotic pumping experimental conditions and results for 1,0 mol/ℓ sodium chloride (Ionac MA-3475 and MC-3470)

Current Density	Brine concentration c_b, mol/l		Water flow	Current Efficiency	Effective Current Density	Transport Numbers				
I, mA/cm²	$c_{b\,exp.}$	$c_{b\,calc.}$	J, cm/h	e_p, %	I_{eff}, mA/cm²	Δt^c	Δt^a	$\bar{\Delta}t$	$\bar{t}_1^c$	$\bar{t}_2^a$
20	3,96	2,76	0,1766	93,73	18,75	0,76	0,54	0,65	0,88	0,77
40	4,47	3,36	0,286	85,70	34,28	0,75	0,54	0,64	0,88	0,77
60	4,56	3,62	0,411	83,648	50,19	0,78	0,55	0,67	0,89	0,78
80	4,91	3,68	0,5033	82,804	66,24	0,73	0,51	0,62	0,87	0,76

Electro-osmotic coefficient (2ß) = 0,187 ℓ/F (Slope 0,0069749 mℓ/mAh)
J_{osm} = y-intercept = 0,0487359 cm/h
c_b^{max} = 5,35 mol/l
$\Delta t^c = t_1^c - t_2^c$

$\Delta t^a = t_2^a - t_1^a$
$\bar{\Delta}t$ = Average transport number of membrane pair
$\bar{t}_1^c$ = Transport number of cation through cation membrane
$\bar{t}_2^a$ = Transport number of anion through anion membrane.

Table 6.9 : Electro-osmotic pumping experimental conditions and results for 0,05 mol/ℓ sodium chloride (Raipore R4030 anion and R4010 cation)

Current Density	Brine concentration c_b, mol/l		Water flow	Current Efficiency	Effective Current Density	Transport Numbers				
I, mA/cm²	$c_{b\,exp.}$	$c_{b\,calc.}$	J, cm/h	e_p, %	I_{eff}, mA/cm²	Δt^c	Δt^a	$\bar{\Delta}t$	$\bar{t}_1^c$	$\bar{t}_2^a$
5	0,86	1,44	0,1059	48,85	2,44	0,79	0,84	0,82	0,90	0,92
10	1,19	1,84	0,1589	50,70	5,07	0,74	0,82	0,78	0,87	0,91
15	1,47	2,32	0,1827	48,02	7,20	0,71	0,81	0,76	0,85	0,90
20	1,55	2,50	0,2225	46,23	9,25	0,70	0,80	0,75	0,85	0,90
30	1,62	2,57	0,317	46,01	13,80	0,67	0,79	0,73	0,83	0,90

Electro-osmotic coefficient (2ß) = 0,547 ℓ/F (slope = 0,0204201 mℓ/mAh)
J_{osm} = y-intercept = 0,0348506
c_b^{max} = 1,83 mol/l
$\Delta t^c = t_1^c - t_2^c$

$\Delta t^a = t_2^a - t_1^a$
$\bar{\Delta}t$ = Average transport number of membrane pair
$\bar{t}_1^c$ = Transport number of cation through cation membrane
$\bar{t}_2^a$ = Transport number of anion through anion membrane.

Table 6.10: Electro-osmotic pumping experimental conditions and results for 0,1 mol/ℓ sodium chloride (Ralpore R4030 anion and R4010 cation)

Current Density	Brine concentration c_b, mol/l		Water flow	Current Efficiency,	Effective Current Density	Transport Numbers				
I, mA/cm²	$c_{b\,exp.}$	$c_{b\,calc.}$	J, cm/h	ϵ_p, %	I_{eff}, mA/cm²	Δt^c	Δt^a	$\bar{\Delta}t$	$\bar{t}_1^c$	$\bar{t}_2^a$
5	0,99	1,35	0,1148	60,62	3,03	0,83	0,83	0,83	0,92	0,92
10	1,37	1,72	0,172	63,23	6,32	0,78	0,80	0,79	0,89	0,90
20	1,86	2,28	0,251	62,74	12,55	0,75	0,77	0,76	0,88	0,89
30	2,16	2,57	0,3192	61,61	18,48	0,71	0,75	0,73	0,86	0,88
40	2,33	2,68	0,3973	62,04	24,82	0,71	0,72	0,71	0,85	0,86
50	2,47	2,86	0,467	61,97	30,99	0,70	0,73	0,72	0,85	0,86

Electro-osmotic coefficient (2ß) = 0,320 ℓ/F (slope = 0,0119546 mℓ/mAh)
J_{osm} = y-intercept = 0,0985769 cm/h
c_b^{max} = 3,13 mol/l
$\Delta t^c = t_1^c - t_2^c$

$\Delta t^a = t_2^a - t_1^a$
$\bar{\Delta}t$ = Average transport number of membrane pair
$\bar{t}_1^c$ = Transport number of cation through cation membrane
$\bar{t}_2^a$ = Transport number of anion through anion membrane.

Table 6.11 : Electro-osmotic pumping experimental conditions and results for 0,5 mol/ℓ sodium chloride (Ralpore R4030 anion and R4010 cation)

Current Density	Brine concentration c_b, mol/l		Water flow	Current Efficiency	Effective Current Density	Transport Numbers				
I, mA/cm²	$c_{b\,exp.}$	$c_{b\,calc.}$	J, cm/h	ϵ_p, %	I_{eff}, mA/cm²	Δt^c	Δt^a	$\bar{\Delta}t$	$\bar{t}_1^c$	$\bar{t}_2^a$
5	1,28	1,89	0,0894	61,11	3,05	0,98	0,83	0,90	0,99	0,91
10	1,65	2,21	0,1456	64,36	6,44	0,92	0,80	0,86	0,96	0,90
20	2,07	2,51	0,2384	66,14	13,23	0,86	0,75	0,80	0,93	0,87
30	2,38	2,67	0,3178	67,59	20,27	0,81	0,71	0,76	0,91	0,85
40	2,62	2,76	0,3947	69,30	27,72	0,78	0,68	0,73	0,89	0,84
50	2,92	2,96	0,4450	69,66	34,83	0,77	0,64	0,71	0,89	0,82
60	3,08	3,22	0,4760	65,61	39,36	0,74	0,64	0,69	0,87	0,82
70	3,32	3,10	0,5615	71,35	49,95	0,71	0,62	0,67	0,86	0,81
90	3,46	3,24	0,6880	70,97	63,87	0,72	0,61	0,66	0,86	0,81

Electro-osmotic coefficient (2ß) = 0,251 ℓ/F (slope 0,0093668 mℓ/mAh)
J_{osm} = y-intercept = 0,1117984 cm/h
c_b^{max} = 3,98 mol/l
$\Delta t^c = t_1^c - t_2^c$

$\Delta t^a = t_2^a - t_1^a$
$\bar{\Delta}t$ = Average transport number of membrane pair
$\bar{t}_1^c$ = Transport number of cation through cation membrane
$\bar{t}_2^a$ = Transport number of anion through anion membrane.

Table 6.12: Electro-osmotic pumping experimental conditions and results for 1,0 mol/ℓ sodium chloride (Rlapore R4030 anion and R4010 cation)

Current Density	Brine concentration c_b, mol/l		Water flow	Current Efficiency	Effective Current Density	Transport Numbers				
I, mA/cm²	$c_{b\,exp.}$	$c_{b\,calc.}$	J, cm/h	ϵ_p, %	I_{eff}, mA/cm²	Δt^c	Δt^a	$\bar{\Delta}t$	$\bar{t}_1^c$	$\bar{t}_2^a$
30	2.6	2.08	0.339	78.77	23.63	0.67	0.59	0.63	0.83	0.80
50	3.14	2.473	0.461	77.59	38.80	0.65	0.57	0.61	0.83	0.79
70	3.34	2.62	0.5934	75.89	53.13	0.64	0.56	0.60	0.82	0.78
90	3.48	2.96	0.7205	74.68	67.21	0.72	0.55	0.63	0.86	0.78

Electro-osmotic coefficient (2ß) = 0,236 ℓ/F (Slope = 0.0087973 mℓ/mAh)
J_{osm} = y-intercept = 0,1265161 cm/h
c_b^{max} = 4,24 mol/l
$\Delta t^c = t_1^c - t_2^c$

$\Delta t^a = t_2^a - t_1^a$
$\bar{\Delta}t$ = Average transport number of membrane pair
$\bar{t}_1^c$ = Transport number of cation through cation membrane
$\bar{t}_2^a$ = Transport number of anion through anion membrane.

Table 6.13: Electro-osmotic pumping experimental conditions and results for 0,05 mol/ℓ sodium chloride (Ionics A-204-UZL-386 and C-61-CZL-386)

Current Density	Brine concentration c_b, mol/l		Water flow	Current Efficiency	Effective Current Density	Transport Numbers				
I, mA/cm²	$c_{b\,exp.}$	$c_{b\,calc.}$	J, cm/h	ϵ_p, %	I_{eff}, mA/cm²	Δt^c	Δt^a	$\bar{\Delta}t$	$\bar{t}_1^c$	$\bar{t}_2^a$
5	1,51	2,26	0,0662	53,61	2,68	0,78	0,82	0,80	0,89	0,91
10	1,87	2,69	0,1059	53,11	5,31	0,74	0,79	0,76	0,87	0,89
15	2,19	3,13	0,1324	51,84	7,78	0,72	0,76	0,74	0,86	0,88
20	2,52	3,72	0,1456	48,92	9,78	0,70	0,75	0,73	0,85	0,88
30	2,80	4,53	0,1766	44,18	13,25	0,69	0,74	0,71	0,85	0,87

Electro-osmotic coefficient (2ß) = 0,234 ℓ/F (slope = 0,0087337 mℓ/mAh)
J_{osm} = y-intercept = 0,0612608 cm/h
c_b^{max} = 4,27 mol/l
$\Delta t^c = t_1^c - t_2^c$

$\Delta t^a = t_2^a - t_1^a$
$\bar{\Delta}t$ = Average transport number of membrane pair
$\bar{t}_1^c$ = Transport number of cation through cation membrane
$\bar{t}_2^a$ = Transport number of anion through anion membrane.

Table 6.14: Electro-osmotic pumping experimental conditions and results for 0,1 mol/ℓ sodium chloride (Ionics A-204-UZL-386 and C-61-CZL-386)

Current Density	Brine concentration c_b, mol/l		Water flow	Current Efficiency	Effective Current Density	Transport Numbers				
I, mA/cm²	$c_{b\,exp.}$	$c_{b\,calc.}$	J, cm/h	ϵ_p, %	I_{eff}, mA/cm²	Δt^c	Δt^a	$\bar{\Delta}t$	$\bar{t}_1^c$	$\bar{t}_2^a$
5	1,55	1,97	0,0728	60,53	3,03	0,76	0,78	0,77	0,88	0,89
10	1,87	2,41	0,1165	58,43	5,84	0,74	0,76	0,75	0,87	0,88
15	2,24	2,81	0,1457	58,32	8,75	0,72	0,74	0,73	0,86	0,87
20	2,61	3,32	0,1589	55,60	11,11	0,70	0,72	0,71	0,85	0,86
30	3,00	3,95	0,1942	52,07	15,62	0,67	0,70	0,69	0,84	0,85
40	3,25	4,60	0,2207	48,07	19,23	0,66	0,70	0,68	0,83	0,85

Electro-osmotic coefficient (2ß) = 0,204 ℓ/F (slope = 0.0076266 mℓ/mAh)
J_{osm} = y-intercept = 0,0748388 cm/h
c_b^{max} = 4,89 mol/l
$\Delta t^c = t_1^c - t_2^c$

$\Delta t^a = t_2^a - t_1^a$
$\bar{\Delta}t$ = Average transport number of membrane pair
$\bar{t}_1^c$ = Transport number of cation through cation membrane
$\bar{t}_2^a$ = Transport number of anion through anion membrane.

Table 6.15: Electro-osmotic pumping experimental conditions and results for 0,5 mol/ℓ sodium chloride (Ionics A-204-UZL-386 and C-61-CZL-386)

Current Density	Brine concentration c_b, mol/l		Water flow	Current Efficiency	Effective Current Density	Transport Numbers				
I, mA/cm²	$c_{b\,exp.}$	$c_{b\,calc.}$	J, cm/h	ϵ_p, %	I_{eff}, mA/cm²	Δt^c	Δt^a	$\bar{\Delta}t$	$\bar{t}_1^c$	$\bar{t}_2^a$
10	2,42	2,20	0,1059	68,74	6,87	0,61	0,63	0,62	0,81	0,82
20	2,75	2,60	0,1766	65,09	13,02	0,61	0,62	0,62	0,81	0,81
30	3,08	2,97	0,2260	62,21	18,67	0,60	0,60	0,60	0,79	0,80
40	3,28	3,20	0,2754	60,56	24,22	0,59	0,59	0,60	0,79	0,80
50	3,48	3,43	0,3178	59,31	29,65	0,58	0,59	0,58	0,79	0,79
60	3,77	3,44	0,3443	58,00	34,80	0,56	0,57	0,57	0,78	0,79
70	3,8	3,70	0,3973	57,82	40,47	0,56	0,57	0,56	0,78	0,78
80	3,91	3,94	0,4291	56,22	44,98	0,56	0,57	0,57	0,78	0,79
90	3,94	4,00	0,4768	55,95	50,36	0,56	0,57	0,57	0,78	0,79
100	3,98	4,20	0,5033	53,70	53,70	0,56	0,57	0,57	0,78	0,79

Electro-osmotic coefficient (2ß) = 0.211 ℓ/F (slope = 0.0078875 mℓ/mAh)
J_{osm} = y-intercept = 0,0780686 cm/h
c_b^{max} = 4,73 mol/l
$\Delta t^c = t_1^c - t_2^c$

$\Delta t^a = t_2^a - t_1^a$
$\bar{\Delta}t$ = Average transport number of membrane pair
$\bar{t}_1^c$ = Transport number of cation through cation membrane
$\bar{t}_2^a$ = Transport number of anion through anion membrane.

Table 6.16: Electro-osmotic pumping experimental conditions and results for 1,0 mol/ℓ sodium chloride (Ionics A-204-UZL-386 and C-61-CZL-386)

Current Density	Brine concentration c_b, mol/l		Water flow	Current Efficiency	Effective Current Density	Transport Numbers				
I, mA/cm²	$c_{b\,exp.}$	$c_{b\,calc.}$	J, cm/h	e_p, %	I_{eff}, mA/cm²	Δt^c	Δt^a	$\bar{\Delta}t$	$\bar{t}_1^c$	$\bar{t}_2^a$
30	3,48	2,49	0,2472	76,88	23,06	0,58	0,52	0,55	0,79	0,76
50	3,72	2,72	0,3708	73,96	36,98	0,57	0,51	0,54	0,79	0,75
70	3,94	3,13	0,4450	67,15	47,00	0,57	0,50	0,53	0,78	0,75
90	4,08	3,46	0,5298	64,38	57,94	0,59	0,50	0,54	0,79	0,75

Electro-osmotic coefficient (2ß) = 0,216 ℓ/F (slope = 0,0080659 mℓ/mAh)
J_{osm} = y-intercept = 0,0655084 cm/h
c_b^{max} = 4,63 mol/l
$\Delta t^c = t_1^c - t_2^c$

$\Delta t^a = t_2^a - t_1^a$
$\bar{\Delta}t$ = Average transport number of membrane pair
$\bar{t}_1^c$ = Transport number of cation through cation membrane
$\bar{t}_2^a$ = Transport number of anion through anion membrane.

Table 6.17: Electro-osmotic pumping experimental conditions and results for 0,05 mol/ℓ sodium chloride (WTPSA-1, WTPSC-1)

Current Density	Brine concentration c_b, mol/l		Water flow	Current Efficiency	Effective Current Density	Transport Numbers				
I, mA/cm²	$c_{b\,exp.}$	$c_{b\,calc.}$	J, cm/h	e_p, %	I_{eff}, mA/cm²	Δt^c	Δt^a	$\bar{\Delta}t$	$\Delta\bar{t}_1^c$	$\bar{t}_2^a$
5	1,66	2,20	0,0695	61,88	3,09	0,82	0,83	0,82	0,91	0,91
10	1,99	2,36	0,1280	60,78	6,08	0,81	0,81	0,81	0,90	0,90
15	2,4	3,16	0,1390	59,64	8,95	0,78	0,79	0,79	0,89	0,89
20	2,85	3,85	0,1456	55,65	11,13	0,72	0,77	0,75	0,86	0,88
25	3,32	4,45	0,1523	54,22	13,55	0,70	0,75	0,73	0,85	0,86

Electro-osmotic coefficient (2ß) = 0,087 ℓ/F (slope = 0,0032427 mℓ/mAh)
J_{osm} = y-intercept = 0,1090328 cm/h
c_b^{max} = 11,50 mol/l
$\Delta t^c = t_1^c - t_2^c$

$\Delta t^a = t_2^a - t_1^a$
$\bar{\Delta}t$ = Average transport number of membrane pair
$\bar{t}_1^c$ = Transport number of cation through cation membrane
$\bar{t}_2^a$ = Transport number of anion through anion membrane.

Table 6.18: Electro-osmotic pumping experimental conditions and results for 0,1 mol/ℓ sodium chloride (WTPSA-1, WTPSC-1)

Current Density	Brine concentration c_b, mol/l		Water flow	Current Efficiency	Effective Current Density	Transport Numbers				
I, mA/cm²	$c_{b\,exp.}$	$c_{b\,calc.}$	J, cm/h	e_p, %	I_{eff}, mA/cm²	Δt^c	Δt^a	$\bar{\Delta}t$	$\bar{t}_1^c$	$\bar{t}_2^a$
5	1,68	2,06	0,0728	65,61	3,28	0,81	0,79	0,80	0,90	0,90
10	2,10	2,52	0,1165	65,46	6,55	0,79	0,78	0,79	0,89	0,89
15	2,53	3,07	0,1390	62,87	9,43	0,76	0,76	0,76	0,88	0,88
20	2,91	3,81	0,1456	56,82	11,36	0,74	0,74	0,74	0,87	0,87
30	3,42		0,1655	50,59	15,17					
40	3,58	5,74	0,1854	44,48	17,79	0,711	0,72	0,71	0,86	0,86

Electro-osmotic coefficient (2ß) = 0,156 ℓ/F (slope = 0,0058244 mℓ/mAh)
J_{osm} = y-intercept = 0,0801568 cm/h
c_b^{max} = 6,41 mol/l
$\Delta t^c = t_1^c - t_2^c$

$\Delta t^a = t_2^a - t_1^a$
$\bar{\Delta}t$ = Average transport number of membrane pair
$\bar{t}_1^c$ = Transport number of cation through cation membrane
$\bar{t}_2^a$ = Transport number of anion through anion membrane.

Table 6.19: Electro-osmotic pumping experimental conditions and results for 0,5 mol/ℓ sodium chloride (WTPSA-1, WTPSC-1)

Current Density	Brine concentration c_b, mol/l		Water flow	Current Efficiency	Effective Current Density	Transport Numbers				
I, mA/cm²	$c_{b\,exp.}$	$c_{b\,calc.}$	J, cm/h	ϵ_p, %	I_{eff}, mA/cm²	Δt^c	Δt^a	$\bar{\Delta}t$	$\bar{t}_1^c$	$\bar{t}_2^a$
10	2,22	2,12	0,1218	72,51	7,25	0,72	0,66	0,69	0,86	0,83
20	3,17	3,034	0,1589	67,53	13,51	0,68	0,61	0,64	0,84	0,81
30	3,68	3,95	0,1766	58,06	17,42	0,65	0,60	0,62	0,82	0,80
40	3,77		0,2030	51,58	20,63					
50	3,90		0,2207	46,16	23,07					
60	4,01		0,2295	41,13	24,68					
80	4,1	6,951	0,2560	35,18	28,42	0,62	0,57	0,60	0,81	0,78
100	4,24	7,937	0,2825	32,11	32,11	0,63	0,57	0,60	0,81	0,78

Electro-osmotic coefficient (2ß) = 0,175 ℓ/F (slope = 0,0065332 mℓ/mAh)
J_{osm} = y-intercept = 0,0699265 cm/h
c_b^{max} = 5,71 mol/l
$\Delta t^c = t_1^c - t_2^c$

$\Delta t^a = t_2^a - t_1^a$
$\bar{\Delta}t$ = Average transport number of membrane pair
$\bar{t}_1^c$ = Transport number of cation through cation membrane
$\bar{t}_2^a$ = Transport number of anion through anion membrane.

Table 6.20: Electro-osmotic pumping experimental conditions and results for 1,0 mol/ℓ sodium chloride (WTPSA-1, WTPSC-1)

Current Density	Brine concentration c_b, mol/l		Water flow	Current Efficiency	Effective Current Density	Transport Numbers				
I, mA/cm²	$c_{b\,exp.}$	$c_{b\,calc.}$	J, cm/h	ϵ_p, %	I_{eff}, mA/cm²	Δt^c	Δt^a	$\bar{\Delta}t$	$\bar{t}_1^c$	$\bar{t}_2^a$
30	3,77	2,63	0,2225	74,96	22,49	0,54	0,51	0,52	0,77	0,75
50	4,06	3,50	0,2667	58,04	29,02	0,51	0,49	0,50	0,76	0,74
70	4,17	4,82	0,2790	44,56	31,19	0,53	0,50	0,51	0,76	0,75
90	4,27	5,78	0,2914	37,06	33,35	0,51	0,49	0,50	0,76	0,75

Electro-osmotic coefficient (2ß) = 0,175 ℓ/F (slope = 0,0065210 mℓ/mAh)
J_{osm} = y-intercept = 0,0762254 cm/h
c_b^{max} = 5,72 mol/l
$\Delta t^c = t_1^c - t_2^c$

$\Delta t^a = t_2^a - t_1^a$
$\bar{\Delta}t$ = Average transport number of membrane pair
$\bar{t}_1^c$ = Transport number of cation through cation membrane
$\bar{t}_2^a$ = Transport number of anion through anion membrane.

Table 6.21: Electro-osmotic pumping experimental conditions and results for 0,05 mol/ℓ sodium chloride (WTPVCA-2, WTPVCC-2)

Current Density	Brine concentration c_b, mol/l		Water flow	Current Efficiency	Effective Current Density	Transport Numbers				
I, mA/cm²	$c_{b\,exp.}$	$c_{b\,calc.}$	J, cm/h	ϵ_p, %	I_{eff}, mA/cm²	Δt^c	Δt^a	$\bar{\Delta}t$	$\bar{t}_1^c$	$\bar{t}_2^a$
5	0.99	1,36	0,1077	56,24	2,81	0,79	0,77	0,79	0.90	0,89
10	1.3	1,77	0,1562	54,46	5.44	0,75	0,74	0,74	0.87	0,87
15	1.64	2,18	0,1788	52,40	7,86	0,75	0,64	0,70	0.87	0,82
20	1.74	2,07	0,2119	49,42	9,88	0,68	0,49	0,59	0.84	0,75
30	1.85	2,7	0,2913	48.17	14.45	0,75	0,66	0.70	0.87	0,83

Electro-osmotic coefficient (2ß) = 0,412 ℓ/F (slope = 0,0153695 mℓ/mAh)
J_{osm} = y-intercept = 0,0649212 cm/h
c_b^{max} = 2,43 mol/l
$\Delta t^c = t_1^c - t_2^c$

$\Delta t^a = t_2^a - t_1^a$
$\bar{\Delta}t$ = Average transport number of membrane pair
$\bar{t}_1^c$ = Transport number of cation through cation membrane
$\bar{t}_2^a$ = Transport number of anion through anion membrane.

Table 6.22: Electro-osmotic pumping experimental conditions and results for 0,1 mol/ℓ sodium chloride (WTPVCA-2, WTPVCC-2)

Current Density	Brine concentration c_b, mol/l		Water flow	Current Efficiency	Effective Current Density	Transport Numbers				
I, mA/cm²	$c_{b\,exp.}$	$c_{b\,calc.}$	J, cm/h	ϵ_p, %	I_{eff}, mA/cm²	Δt^c	Δt^a	$\bar{\Delta}t$	$\bar{t}_1^c$	$\bar{t}_2^a$
5	1,05	0,94	0,1509	59,65	2,98	0,79	0,74	0,76	0,89	0,87
10	1,47	1,80	0,1483	58,45	5,85	0,73	0,70	0,71	0,86	0,85
15	1,72	2,12	0,1854	56,99	8,55	0,72	0,68	0,70	0,86	0,84
20	1,92	2,17	0,2219	54,53	10,91	0,66	0,63	0,65	0,83	0,81
30	2,26	2,92	0,256	51,71	15,51	0,70	0,64	0,67	0,85	0,82
40	2,58	3,47	0,2825	48,853	19,54	0,68	0,64	0,66	0,84	0,82

Electro-osmotic coefficient (2ß) = 0,261 ℓ/F (slope = 0,0097235 mℓ/mAh)
J_{osm} = (y-intercept = 0,0994504 cm/h
c_b^{max} = 3,84 mol/l
$\Delta t^c = t_1^c - t_2^c$

$\Delta t^a = t_2^a - t_1^a$
$\bar{\Delta}t$ = Average transport number of membrane pair
$\bar{t}_1^c$ = Transport number of cation through cation membrane
$\bar{t}_2^a$ = Transport number of anion through anion membrane.

Table 6.23: Electro-osmotic pumping experimental conditions and results for 0,5 mol/ℓ sodium chloride (WTPVCA-2, WTPVCC-2)

Current Density	Brine concentration c_b, mol/l		Water flow	Current Efficiency	Effective Current Density	Transport Numbers				
I, mA/cm²	$c_{b\,exp.}$	$c_{b\,calc.}$	J, cm/h	ϵ_p, %	I_{eff}, mA/cm²	Δt^c	Δt^a	$\bar{\Delta}t$	$\bar{t}_1^c$	$\bar{t}_2^a$
5	1,43	1,23	0,0971	74,463	3,7231	0,6620	0,6148	0,6384	0,83	0,81
10	1,77		0,1562	74,153	7,4153					
15	2,08	1,70	0,1942	72,207	10,831	0,6128	0,5666	0,5897	0,81	0,78
20	2,26		0,2295	69,54	13,908					
30	2,58		0,2913	67,173	20,152					
40	2,81	2,33	0,3443	64,848	25,939	0,5696	0,5070	0,5383	0,78	0,75
60	3,02	2,581	0,429	57,9	34,74	0,5179	0,4715	0,4947	0,76	0,74

Electro-osmotic coefficient (2ß) = 0,267 ℓ/F (slope = 0,0099646 mℓ/mAh)
J_{osm} = y-intercept = 0,0869006 cm/h
c_b^{max} = 3,74 mol/l
$\Delta t^c = t_1^c - t_2^c$

$\Delta t^a = t_2^a - t_1^a$
$\bar{\Delta}t$ = Average transport number of membrane pair
$\bar{t}_1^c$ = Transport number of cation through cation membrane
$\bar{t}_2^a$ = Transport number of anion through anion membrane.

Table 6.24: Electro-osmotic pumping experimental conditions and results for 1,0 mol/ℓ sodium chloride (WTPVCA-2, WTPVCC-2)

Current Density	Brine concentration c_b, mol/l		Water flow	Current Efficiency	Effective Current Density	Transport Numbers				
I, mA/cm²	$c_{b\,exp.}$	$c_{b\,calc.}$	J, cm/h	ϵ_p, %	I_{eff}, mA/cm²	Δt^c	Δt^a	$\bar{\Delta}t$	$\bar{t}_1^c$	$\bar{t}_2^a$
10	2,0	1,25	0,20	81,66	8,17	0,55	0,47	0,51	0,78	0,73
20	2,4	1,37	0,25	80,67	16,13	0,47	0,44	0,46	0,74	0,72
40	3,14	1,68	0,37	78,04	31,22	0,43	0,40	0,42	0,72	0,70
60	3,26	1,88	0,48	70,22	42,13	0,41	0,40	0,41	0,70	0,70

Electro-osmotic coefficient (2ß) = 0,221 ℓ/F (slope = 0,0082250 mℓ/mAh)
J_{osm} = y-intercept = 0,125719 cm/h
c_t^{max} = 4,54 mol/l
$\Delta t^c = t_1^c - t_2^c$

$\Delta t^a = t_2^a - t_1^a$
$\bar{\Delta}t$ = Average transport number of membrane pair
$\bar{t}_1^c$ = Transport number of cation through cation membrane
$\bar{t}_2^a$ = Transport number of anion through anion membrane.

Table 6.25: Electro-osmotic pumping experimental conditions and results for 0,05 mol/ℓ sodium chloride (WTPSTA-3, WTPSTC-3)

Current Density	Brine concentration c_b, mol/l		Water flow	Current Efficiency	Effective Current Density	Transport Numbers				
I, mA/cm²	$c_{b\,exp.}$	$c_{b\,calc.}$	J, cm/h	ϵ_p, %	I_{eff}, mA/cm²	Δt^c	Δt^a	$\bar{\Delta}t$	$\bar{t}_1^c$	$\bar{t}_2^a$
10	1,65	2,29	0,1368	60,53	6,05	0,87	0,81	0,84	0,93	0,90
15	1,92	2,65	0,1721	59,08	8,86	0,82	0,81	0,81	0,91	0,90
20	2,08	3,01	0,1960	54,65	10,93	0,81	0,78	0,80	0,90	0,90
25	2,11	3,20	0,2295	51,69	12,92	0,78	0,80	0,79	0,89	0,89
30	2,16	3,32	0,2649	51,13	15,34	0,79	0,78	0,79	0,89	0,89

Electro-osmotic coefficient (2ß) = 0,371 ℓ/F (slope = 0,0138276 mℓ/mAh)
J_{osm} = y-intercept = 0,0502337 cm/h
c_b^{max} = 2,69 mol/l
$\Delta t^c = t_1^c - t_2^c$

$\Delta t^a = t_2^a - t_1^a$
$\bar{\Delta}t$ = Average transport number of membrane pair
$\bar{t}_1^c$ = Transport number of cation through cation membrane
$\bar{t}_2^a$ = Transport number of anion through anion membrane.

Table 6.26: Electro-osmotic pumping experimental conditions and results for 0,1 mol/ℓ sodium chloride (WTPSTA-3, WTPSTC-3)

Current Density	Brine concentration c_b, mol/l		Water flow	Current Efficiency	Effective Current Density	Transport Numbers				
I, mA/cm²	$c_{b\,exp.}$	$c_{b\,calc.}$	J, cm/h	ϵ_p, %	I_{eff}, mA/cm²	Δt^c	Δt^a	$\bar{\Delta}t$	$\bar{t}_1^c$	$\bar{t}_2^a$
10	1,76	2,14	0,1404	66,24	6,62	0,83	0,77	0,80	0,92	0,89
15	1,87	2,31	0,1920	64,18	9,63	0,83	0,76	0,79	0,91	0,88
20	2,19	2,71	0,2154	63,24	12,65	0,82	0,75	0,78	0,91	0,88
30	2,35	2,90	0,2914	61,19	18,36	0,78	0,74	0,76	0,88	0,87
40	2,55	3,23	0,3496	59,75	23,90	0,78	0,74	0,76	0,89	0,87
50	2,64	2,96	0,4186	59,24	29,62	0,63	0,69	0,66	0,82	0,85

Electro-osmotic coefficient (2ß) = 0,317 ℓ/F (slope = 0,011834 mℓ/mAh)
J_{osm} = y-intercept = 0,0691379 cm/h
c_b^{max} = 3,15 mol/l
$\Delta t^c = t_1^c - t_2^c$

$\Delta t^a = t_2^a - t_1^a$
$\bar{\Delta}t$ = Average transport number of membrane pair
$\bar{t}_1^c$ = Transport number of cation through cation membrane
$\bar{t}_2^a$ = Transport number of anion through anion membrane.

Table 6.27: Electro-osmotic pumping experimental conditions and results for 0,5 mol/ℓ sodium chloride (WTPSTA-3, WTPSTC-3)

Current Density	Brine concentration c_b, mol/l		Water flow	Current Efficiency	Effective Current Density	Transport Numbers				
I, mA/cm²	$c_{b\,exp.}$	$c_{b\,calc.}$	J, cm/h	ϵ_p, %	I_{eff}, mA/cm²	Δt^c	Δt^a	$\bar{\Delta}t$	$\bar{t}_1^c$	$\bar{t}_2^a$
10	2,02	1,87	0,1377	74,96	7,50	0,74	0,65	0,69	0,87	0,82
20	2,45	2,23	0,2225	73,07	14,61	0,72	0,61	0,66	0,86	0,81
30	2,85	2,56	0,2826	71,96	21,59	0,70	0,59	0,65	0,85	0,80
40	2,91	2,56	0,3576	69,74	27,90	0,65	0,58	0,61	0,82	0,79
50	3,11	2,88	0,4026	67,13	33,57	0,67	0,57	0,62	0,83	0,79
70	3,29	2,75	0,5033	63,41	44,39	0,53	0,53	0,53	0,76	0,76
90	3,37	3,45	0,6093	61,15	55,04	0,65	0,60	0,63	0,82	0,80
110	3,41	3,59	0,7152	59,43	65,38	0,65	0,60	0,62	0,82	0,80

Electro-osmotic coefficient (2ß) = 0,259 ℓ/F (slope = 0,0096672 mℓ/mAh)
J_{osm} = y-intercept = 0,0793991 cm/h
c_L^{max} = 3,86 mol/l
$\Delta t^c = t_1^c - t_2^c$

$\Delta t^a = t_2^a - t_1^a$
$\bar{\Delta}t$ = Average transport number of membrane pair
$\bar{t}_1^c$ = Transport number of cation through cation membrane
$\bar{t}_2^a$ = Transport number of anion through anion membrane.

Table 6.28: Electro-osmotic pumping experimental conditions and results for 1,0 mol/ℓ sodium chloride (WTPSTA-3, WTPTSC-3)

Current Density	Brine concentration c_b, mol/l		Water flow	Current Efficiency	Effective Current Density	Transport Numbers				
I, mA/cm²	$c_{b\,exp.}$	$c_{b\,calc.}$	J, cm/h	e_p, %	I_{eff}, mA/cm²	Δt^c	Δt^a	$\bar{\Delta}t$	$\bar{t}_1^c$	$\bar{t}_2^a$
30	2,94	2,02	0,3179	83,51	25,05	0,62	0,52	0,57	0,81	0,76
50	3,27	2,18	0,4715	82,67	41,33	0,61	0,49	0,55	0,81	0,75
70	3,41	2,45	0,5827	76,10	53,27	0,60	0,49	0,55	0,80	0,74
90	3,47	2,43	0,7159	73,92	66,53	0,54	0,49	0,52	0,77	0,75

Electro-osmotic coefficient (2β) = 0,257 ℓ/F (slope = 0,0095674 mℓ/mAh)
$J_{osm.}$ = y-intercept = 0,0766808 cm/h
c_b^{max} = 3,90 mol/l
$\Delta t^c = t_1^c - t_2^c$

$\Delta t^a = t_2^a - t_1^a$
$\bar{\Delta}t$ = Average transport number of membrane pair
$\bar{t}_1^c$ = Transport number of cation through cation membrane
$\bar{t}_2^a$ = Transport number of anion through anion membrane.

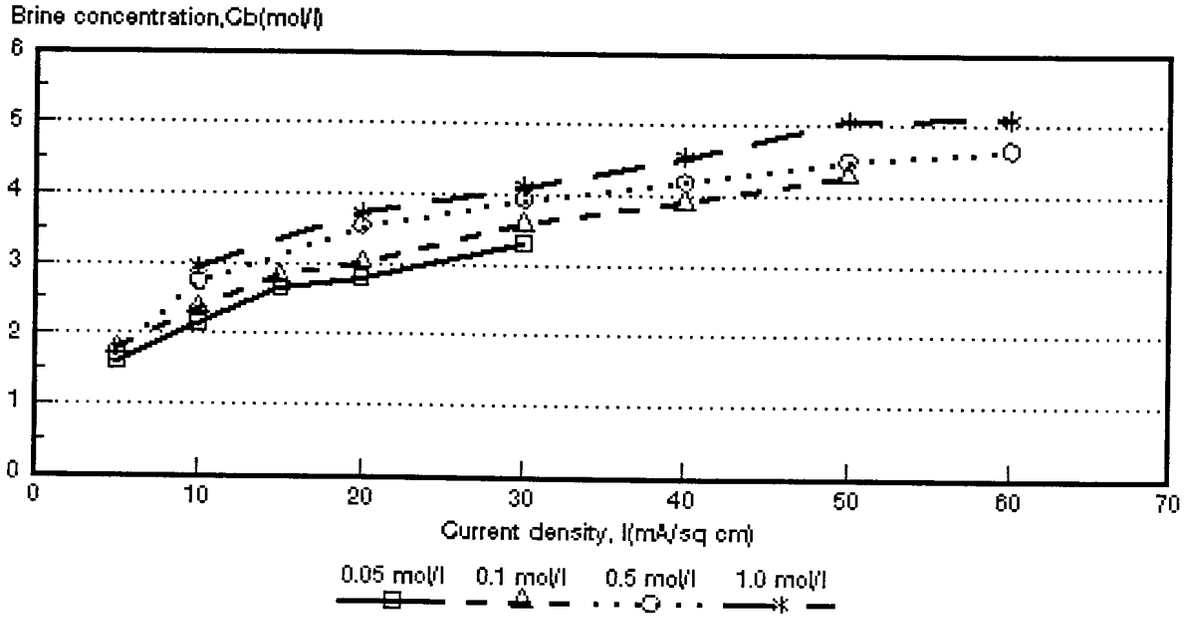

Figure 6.1: Brine concentration as a function of current density for 4 different NaCl feed concentrations. *Selemion* AMV and CMV membranes.

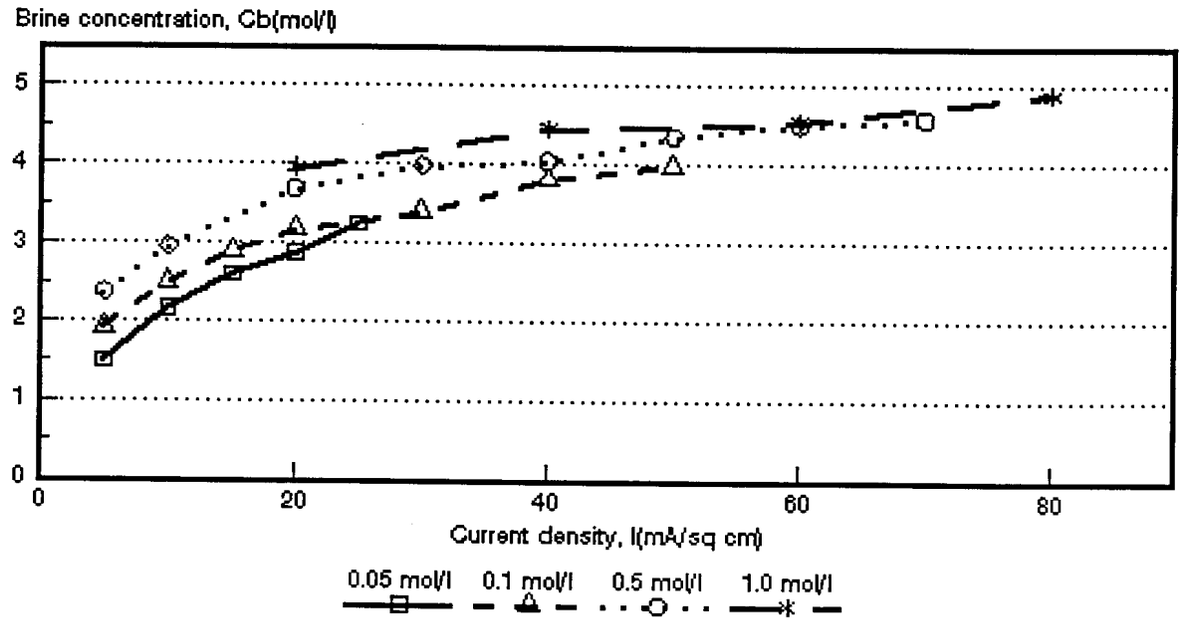

Figure 6.2: **Brine concentration as a function of current density for 4 different NaCl feed concentrations. *Ionac* MA-3475 and MC-3470 membranes.**

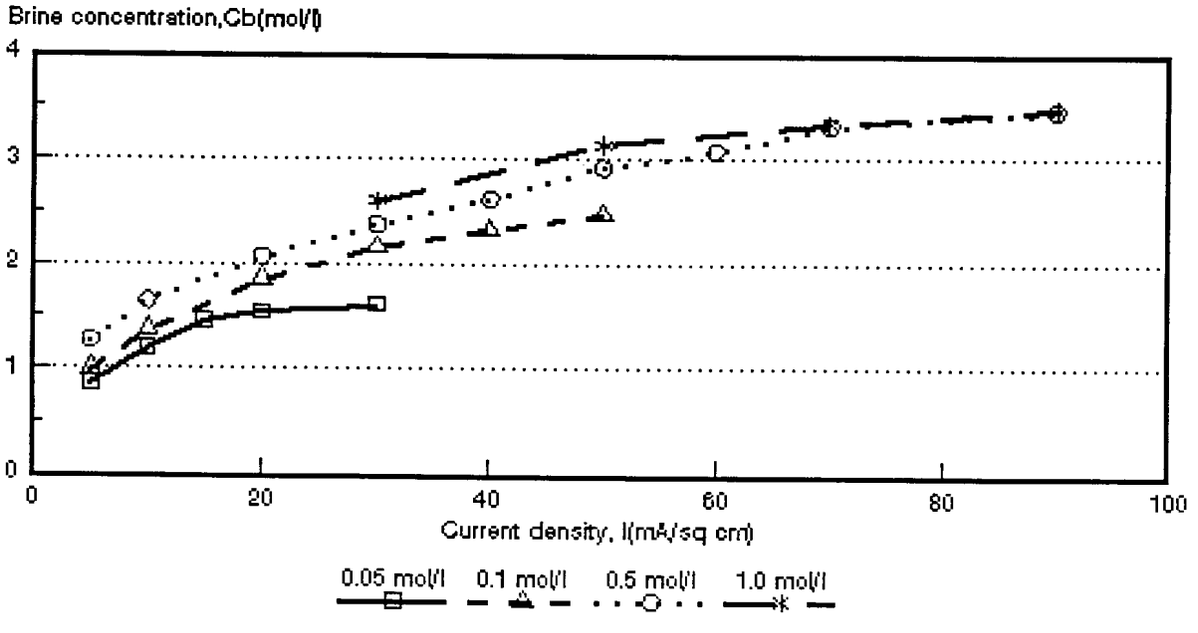

Figure 6.3: **Brine concentration as a function of current density for 4 different NaCl feed concentrations. *Raipore* R4030 and R4010 membranes.**

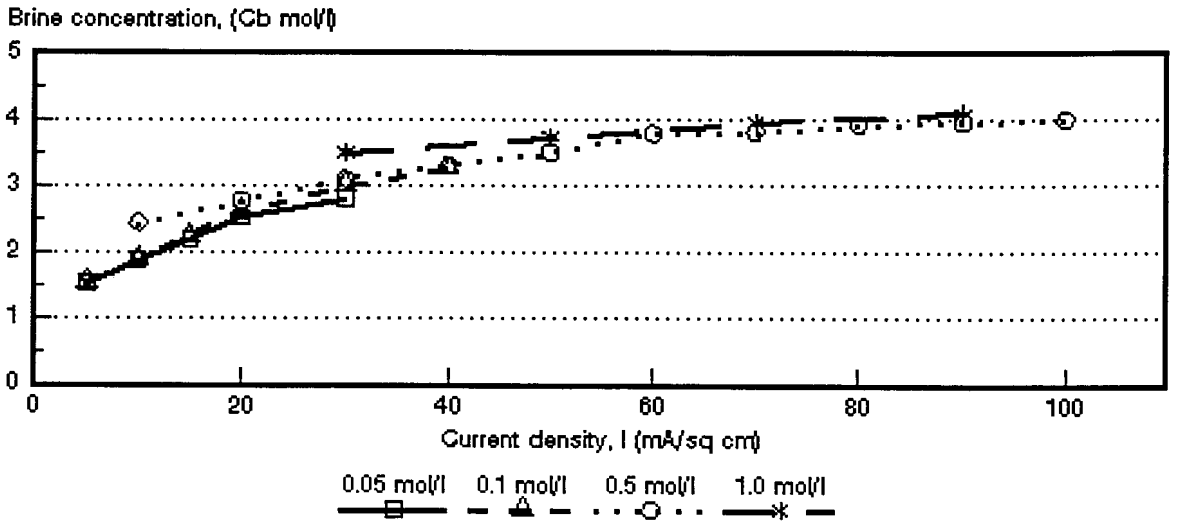

Figure 6.4: **Brine concentration as a function of current density for 4 different NaCl feed concentrations. *Ionics* A-204-UZL-386 and C-61-CZL-386 membranes.**

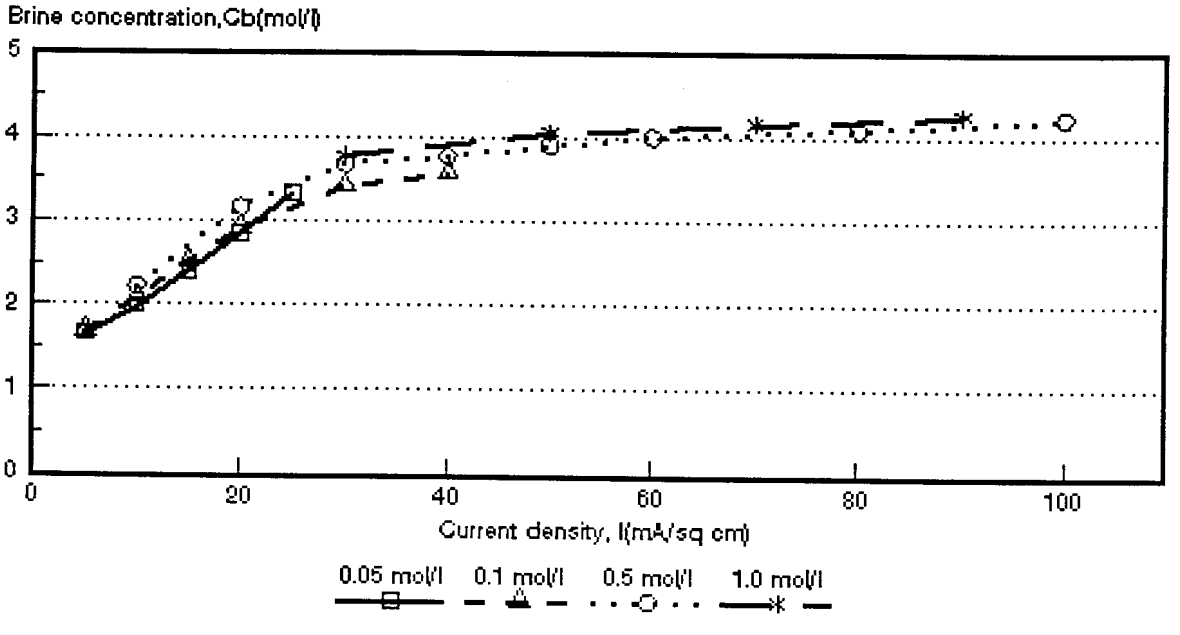

Figure 6.5: **Brine concentration as a function of current density for 4 different NaCl feed concentrations. WTPSA-1 and WTPSC-1 membranes.**

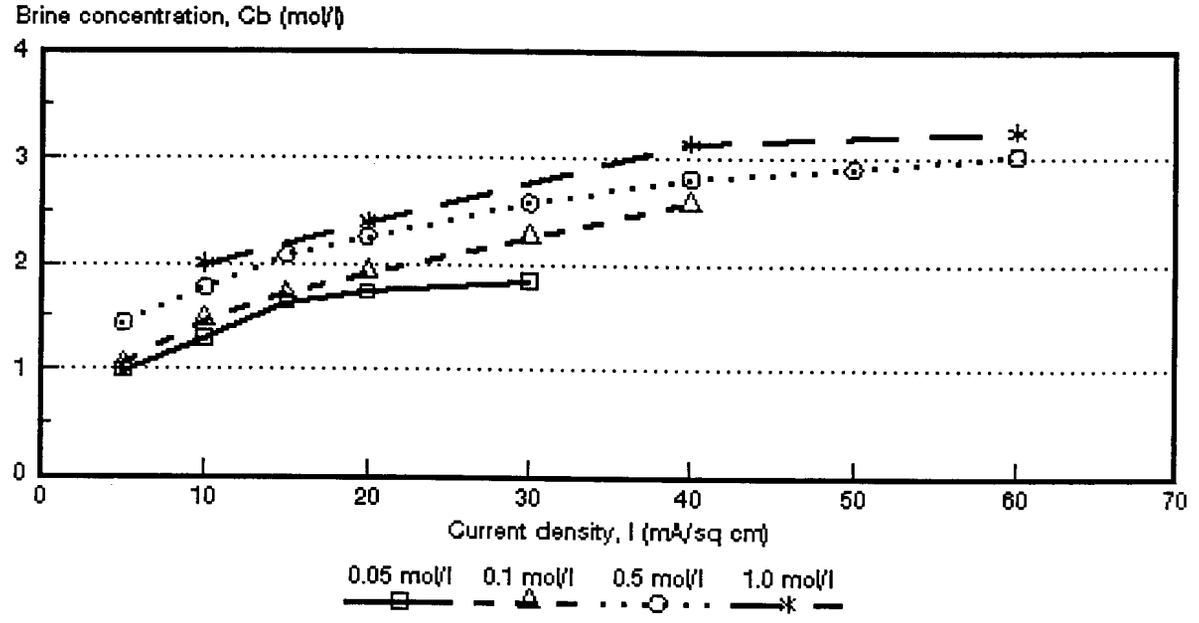

Figure 6.6: **Brine concentration as a function of current density for 4 different NaCl feed concentrations. WTPVCA-2 and WTPVCC-2 membranes.**

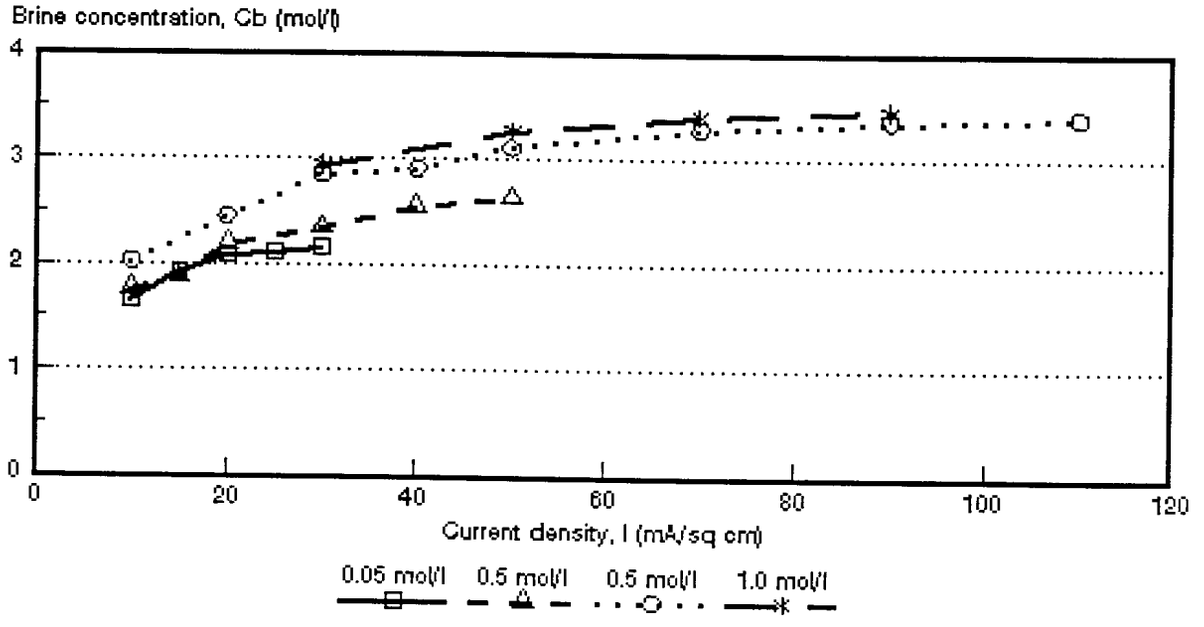

Figure 6.7: **Brine concentration as a function of current density for 4 different NaCl feed concentrations. WTPSTA-3 and WTPSTC-3 membranes.**

Table 6.29: Brine concentrations obtained at the highest current densities investigated for different sodium chloride feed concentrations

Feed Concentration mol/ℓ	Brine Concentration* (%)						
	Selemion	Ionac	Raipore	Ionics	WTPS	WTPVC	WTPST
0,05	19,3	19,0	9,5	16,4	19,4	10,8	12,6
0,10	25,1	23,4	14,4	19,0	20,9	15,1	15,4
0,50	27,2	26,8	20,2	23,3	24,8	17,7	19,9
1,0	29,8	28,7	20,3	23,8	25,0	19,1	20,3

* Brine concentrations obtained from data in Tables 6.1 to 6.28.

$$\text{and } c_b^{max} = c_b(1 + J_{osm}/J_{elosm}) \qquad \text{(see eq. 3.10.31)}$$

The results are shown in Tables 6.30 and Figures 6.8 to 6.14. Very good correlations were obtained with the above two relationships to determine c_b^{max}. Consequently, any one of these two methods can be used to determine c_b^{max}.

Maximum brine concentration seems to depend more on feed concentration in the case of the *Selemion*- (Fig. 6.8), *Raipore*- (Fig. 6.10), WTPS- (Fig. 6.12), WTPVC- (Fig. 6.13) and WTPST- (Fig. 6.14) membranes than has been experienced with the *Ionac*- (Fig. 6.9) and *Ionics*- (Fig. 6.11) membranes. This effect was especially pronounced for the *Selemion*-, *Raipore*- and WTPS membranes, and to a lesser extent for the WTPVC- and WTPST membranes. Much less change in maximum brine concentration as a function of feed concentration was experienced with the *Ionac*- (Fig. 6.9) and *Ionics* (Fig. 6.11) membranes. The *Ionac*- and *Ionics* membranes showed almost no dependence of maximum brine concentration on feed concentration in the feed concentration range of 0,05 to 1,0 mol/ℓ. It is interesting to note that the calculated maximum brine concentration has been very high at 0,05 mol/ℓ feed concentration in the case of the WTPS membranes (Fig. 6.12). The maximum brine concentration first declined very rapidly and then much slower to become almost independent of feed concentration in the 0,1 to 1,0 mol/ℓ feed concentration range. This opposite behaviour encountered with the more hydrophobic WTPS membranes can be ascribed to membrane swelling when the membranes come into contact with water[42].

Brine concentrations at different current densities were predicted from measured transport numbers and volume flows (J) with the relationship:

$$c_b = \frac{I\bar{\Delta}t}{2FJ} \qquad \text{(see eq. 3.10.17)}$$

The experimental and calculated brine concentrations are shown in Tables 6.1 to 6.28 and Figures 6.15 to 6.42. The calculated brine concentrations were determined from the average value of the apparent transport numbers (Δt's) of a membrane pair ($\bar{\Delta}t$) and from the water flows (J).

The correlation between the calculated and experimentally determined brine concentrations expressed as the ratio c_{bcalc}/c_{bexp} is shown in Table 6.31. The calculated brine concentrations were higher than the experimentally determined brine concentrations in the 0,05 to 0,1 mol/ℓ feed concentration range in the case of the *Selemion*-, *Ionac*-, *Ionics*-, WTPS-, WTPVC- and WTPST membranes (Figs. 6.15 to 6.42 and Table 6.31). The calculated brine concentration was still higher than the experimentally determined brine concentration at 0,5 mol/ℓ feed concentration for the *Raipore* membranes (Fig. 6.25). However, calculated brine concentrations became less than the experimentally determined brine concentrations in the 0,5 to 1,0 mol/ℓ feed concentration range in the case of the *Selemion*- (Fig's. 6.17 and 6.18), *Ionac*- (Fig's. 6.21 and 6.22), *Ionics*- (Fig's. 6.29 and 6.30), WTPVC- (Fig's. 6.37 and 6.38) and WTPST (Fig's. 6.41 and 6.42) membranes. Calculated brine concentration became less than the experimentally determined brine concentration at 1,0 mol/ℓ feed concentration for the *Raipore*- (Fig. 6.26) and WTPS- (Fig. 6.34) membranes.

Good correlations were obtained between the calculated and experimentally determined brine concentrations for all the membranes investigated depending on feed concentration and current density used (Table 6.31). For the *Selemion* membranes the ratio c_{bcalc}/c_{bexp} varied between 1,0 and 1,07 in the current density range from 15 to 50 mA/cm^2 (0,1 mol/ℓ feed). In the case of the *Ionac* membranes the ratio c_{bcalc}/c_{bexp} varied between 0,95 and 1,1 in the current density range from 40 to 70 mA/cm^2 (0,5 mol/ℓ feed). The c_{bcalc}/c_{bexp} ratio for the *Raipore* membranes varied between 0,93 and 1,05 in the 40 to 90 mA/cm^2 current density range (0,5 mol/ℓ feed). The correlation between c_{bcalc}/c_{bexp} for the *Ionics* membranes varied between 0,91 and 1,06 in the current density range from 10 to 100 mA/cm^2 (0,5 mol/ℓ feed). The WTPS membranes showed a very good correlation of 0,95 to 1,07 of c_{bcalc}/c_{bexp} in the current density range from 10 to 30 mA/cm^2 (0,5 mol/ℓ feed). However, a poor correlation was obtained at high current densities. The WTPVC membranes showed a correlation of c_{bcalc}/c_{bexp} of 0,82 to 0,86 in the 5 to 60 mA/cm^2 current density range (0,5 mol/ℓ

feed) while the WTPST membranes showed a correlation of 0,84 to 1,05 in the 10 to 110 mA/cm^2 current density range (0,5 mol/ℓ feed). Therefore, brine concentration should be reasonably accurately predicted from simple transport number and water flow determinations depending on feed water concentration and current density used.

Table 6.30: Maximum brine concentration calculated from $c_b^{max} = 1/2\ F\beta^*$ and $c_b^{max} = c_b\ (1 + J_{osm}/J_{elosm})^{**}$

Feed Concentration	Maximum Brine Concentration, c_b^{max} (mol/ℓ)													
	Selemion		Ionac		Raipore		Ionics		WTPS		WTPVC		WTPST	
mol/ℓ	1	2	1	2	1	2	1	2	1	2	1	2	1	2
0,05	4,55	4,54	5,37	5,31	1,83	1,83	4,27	4,29	11,5	11,38	2,43	2,44	2,69	2,71
0,10	5,05	5,06	4,85	4,80	3,13	3,12	4,89	4,83	6,41	6,42	3,84	3,71	3,15	3,11
0,50	5,36	5,31	5,26	5,29	3,98	4,02	4,73	4,74	5,71	5,76	3,74	3,77	3,86	3,85
1,00	6,48	6,49	5,35	5,44	4,24	4,22	4,63	4,63	5,72	5,74	4,54	4,66	3,90	3,89

1 : $c_b^{max} = 1/2\ F\beta$

2 : $c_b^{max} = c_b\ (1 + J_{osm} / J_{elosm})$

* : Calculated from electro-osmotic coefficients (Tables 6.1 to 6.28)

** : Calculated from $J_{elosm} = J - J_{osm}$ (y-intercept and the corresponding c_b values) (Tables 6.1 to 6.28).

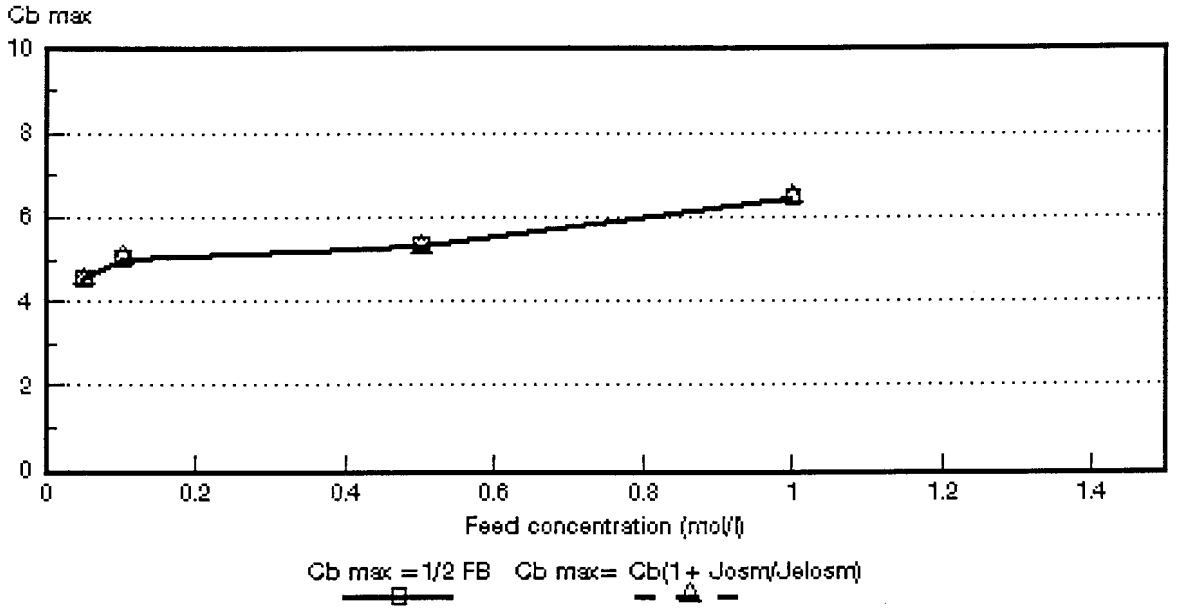

Figure 6.8: c_b^{max} **as a function of feed concentration for different NaCl feed concentrations.** ***Selemion*** **AMV and CMV membranes.**

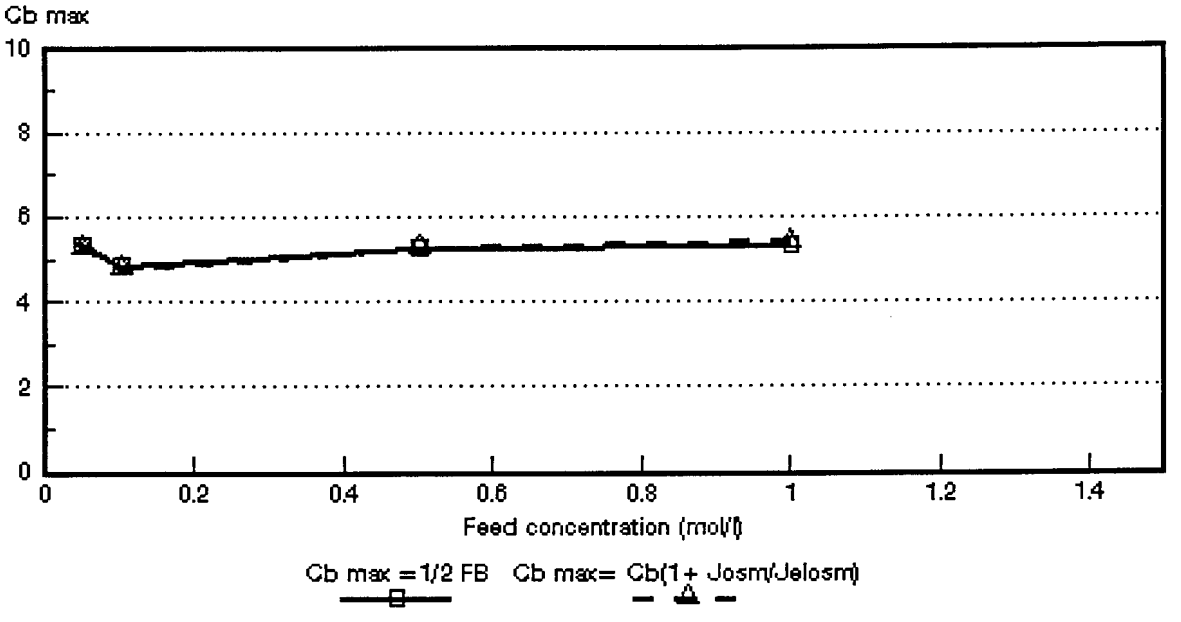

Figure 6.9: c_b^{max} **as a function of feed concentration for different NaCl feed concentrations.** ***Ionac*** **MA-3475 and MC-3470 membranes.**

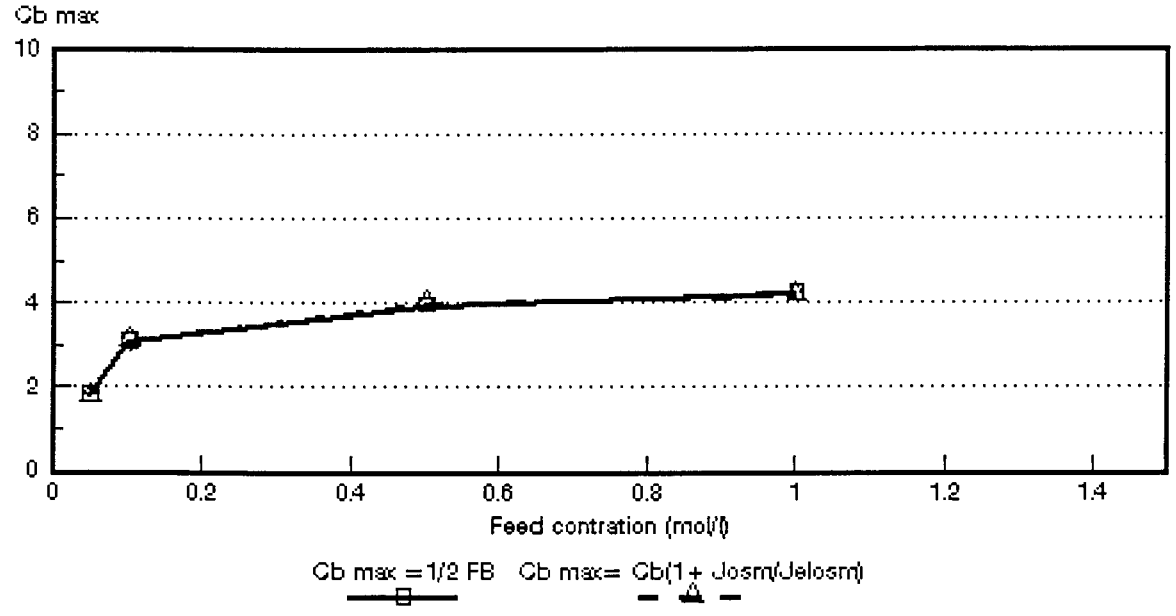

Figure 6.10: c_b^{max} **as a function of feed concentration for different NaCl feed concentrations.** ***Raipore*** **R4030 and R4010 membranes.**

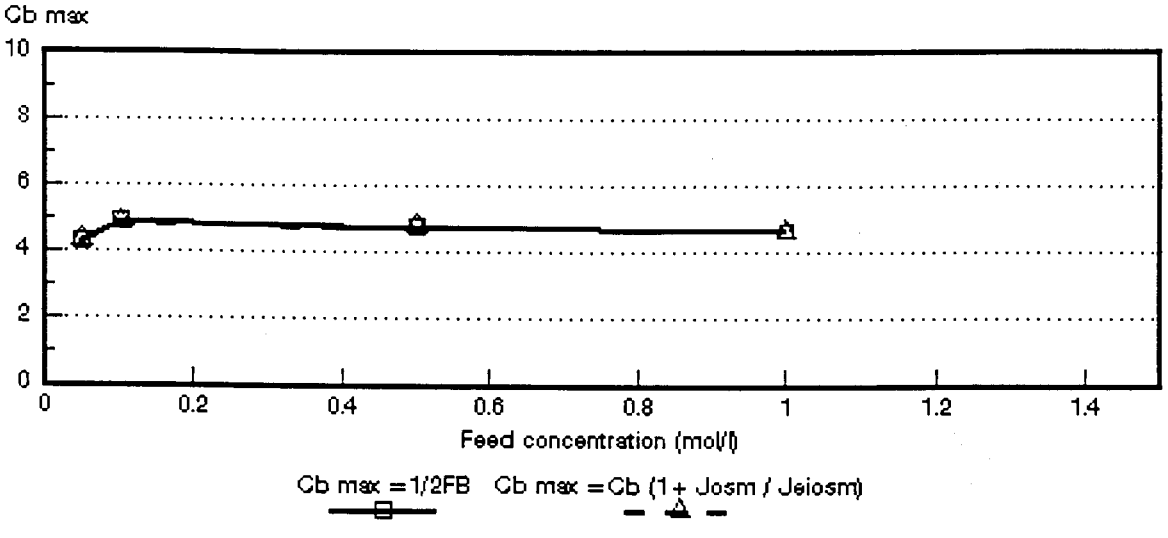

Figure 6.11: c_b^{max} **as a function of feed concentration for different NaCl feed concentrations.** ***Ionics*** **A-204-UZL-386 and C-61-CZL-386 membranes.**

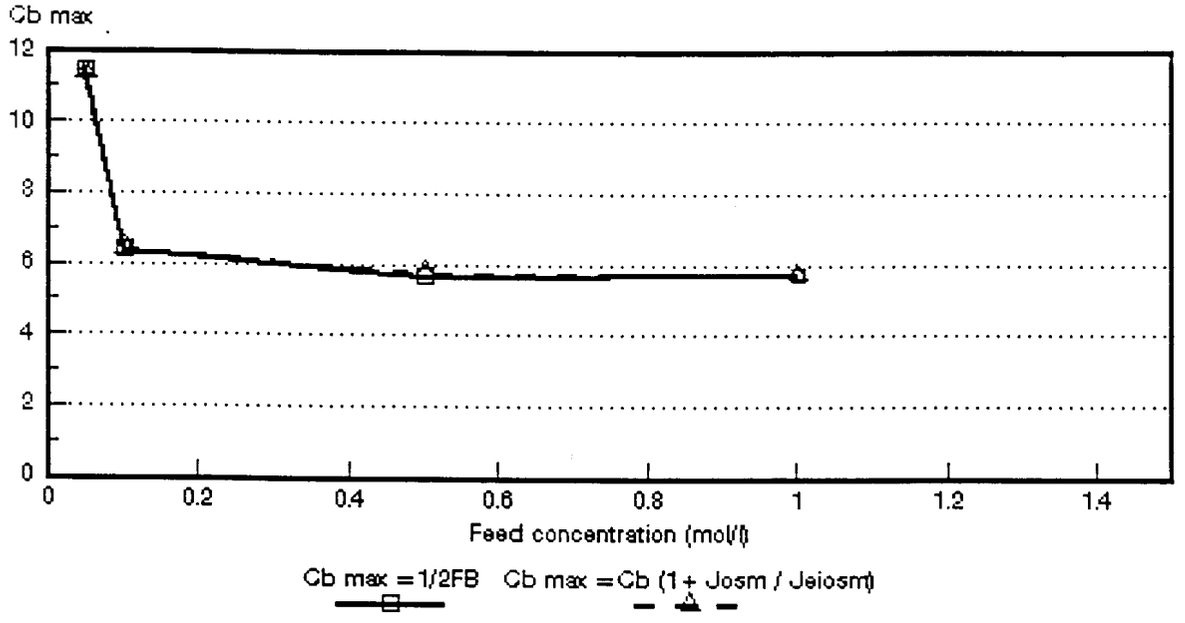

Figure 6.12: **c_b^{max} as a function of feed concentration for different NaCl feed concentrations. WTPSA-1 and WTPSC-1 membranes.**

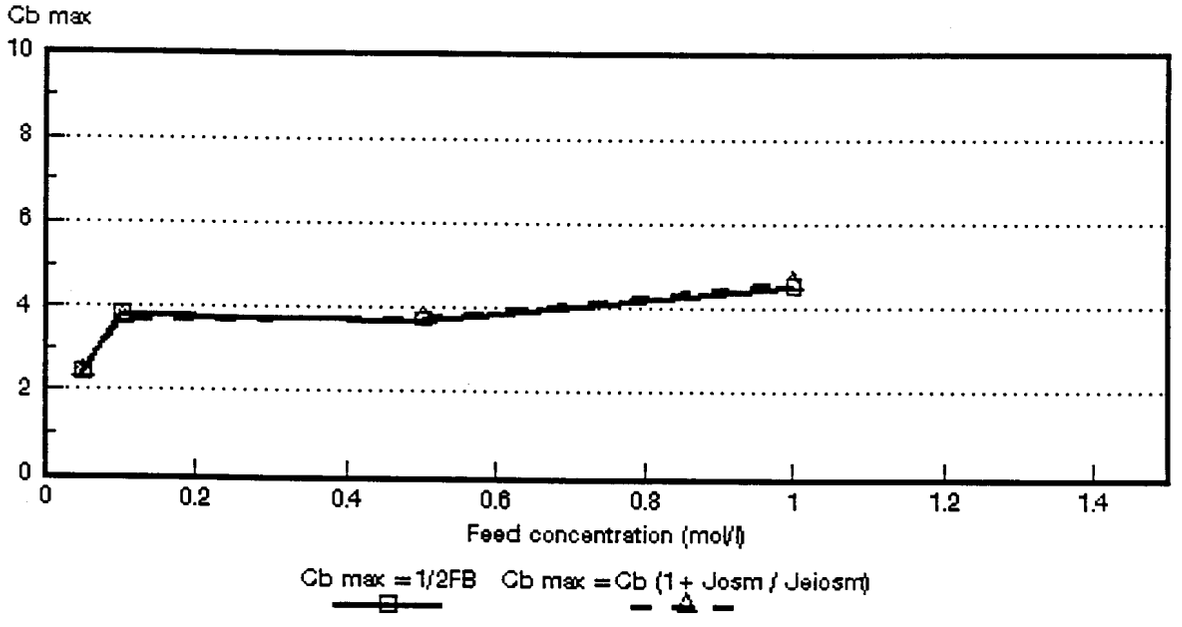

Figure 6.13: **c_b^{max} as a function of feed concentration for different NaCl feed concentrations. WTPVCA-2 and WTPVCC-2 membranes.**

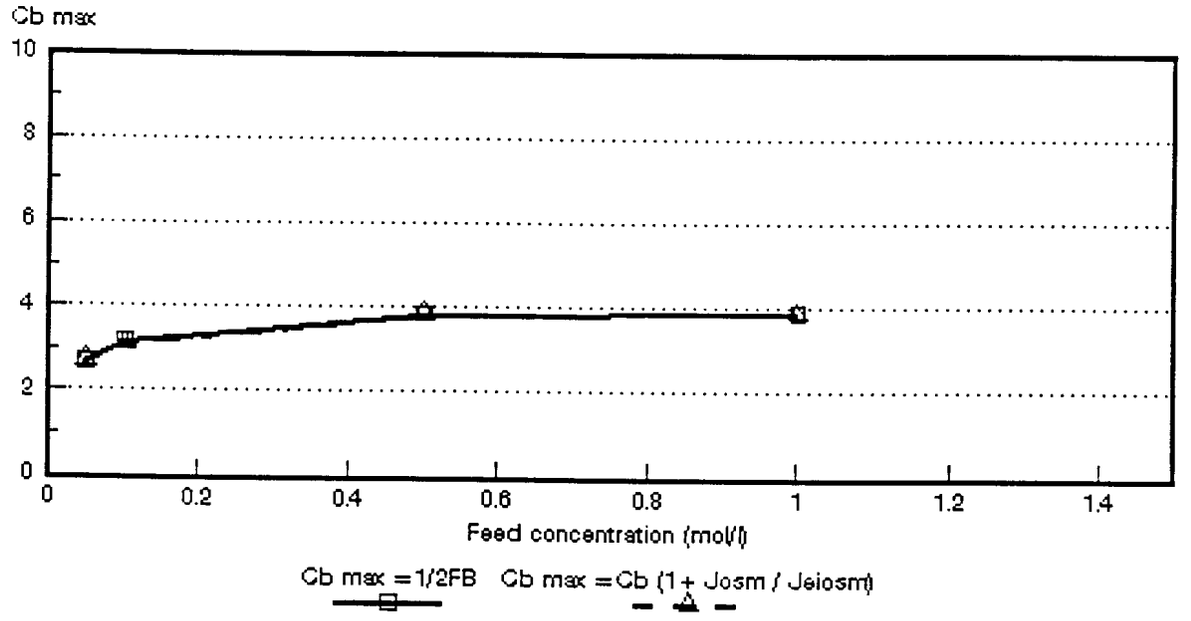

Figure 6.14: **c_b^{max} as a function of feed concentration for different NaCl feed concentrations. WTPSTA-3 and WTPSTC-3 membranes.**

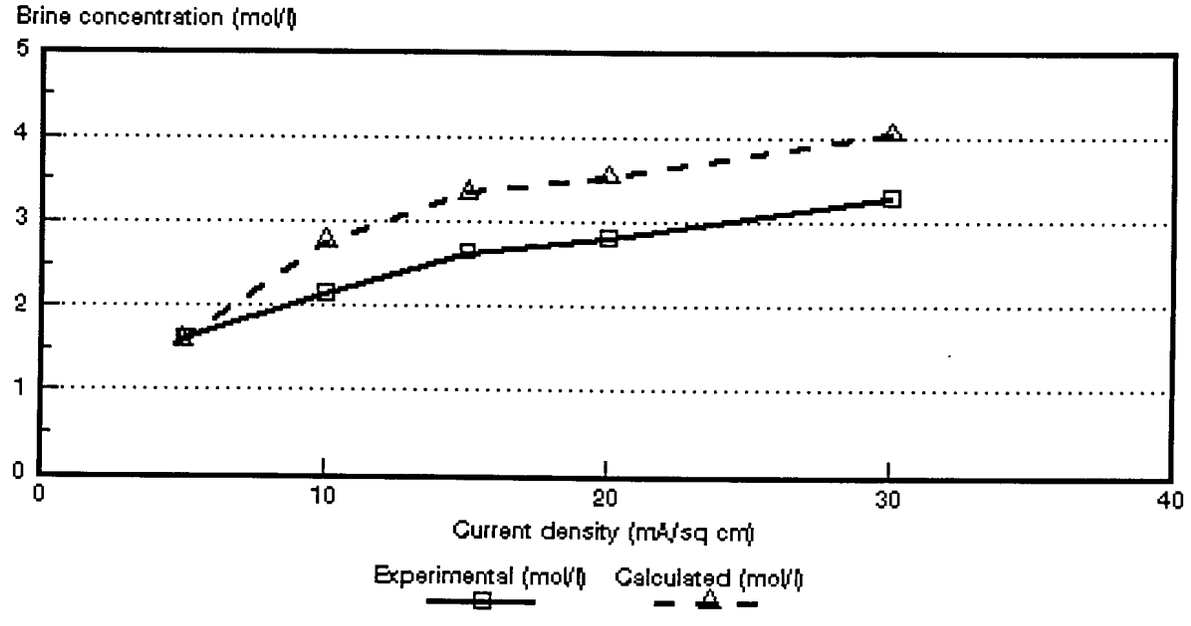

Figure 6.15: **Experimental and calculated brine concentrations as a function of current density for 0,05 mol/ℓ NaCl feed solution. *Selemion* AMV and CMV membranes.**

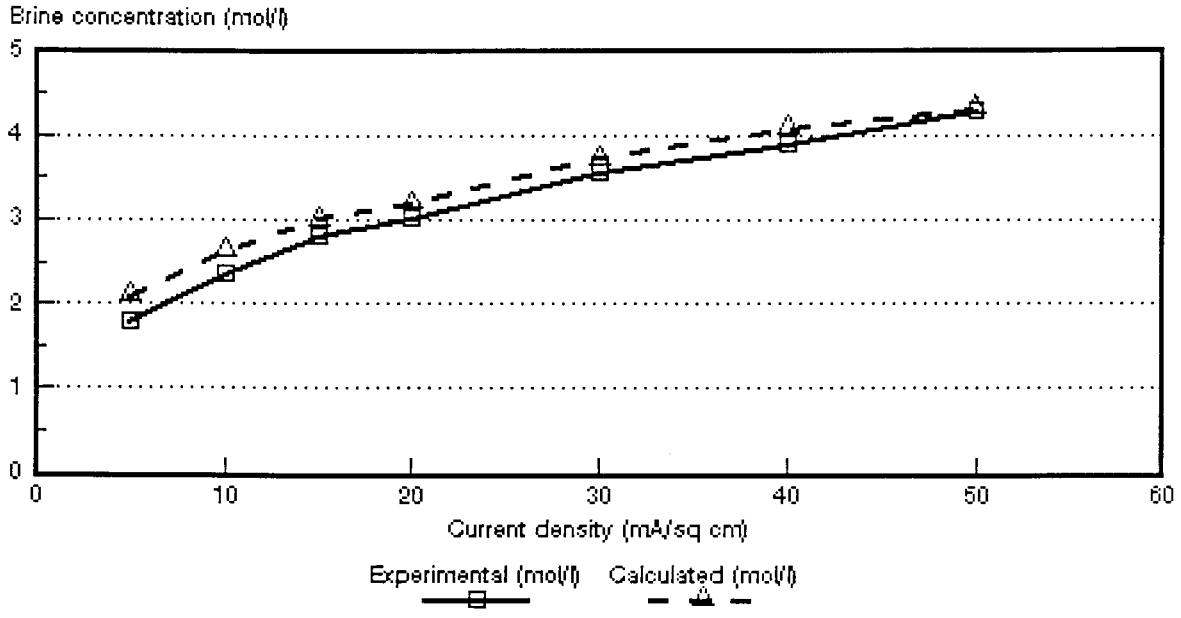

Figure 6.16: **Experimental and calculated brine concentrations as a function of current density for 0,1 mol/ℓ NaCl feed solution. *Selemion* AMV and CMV membranes.**

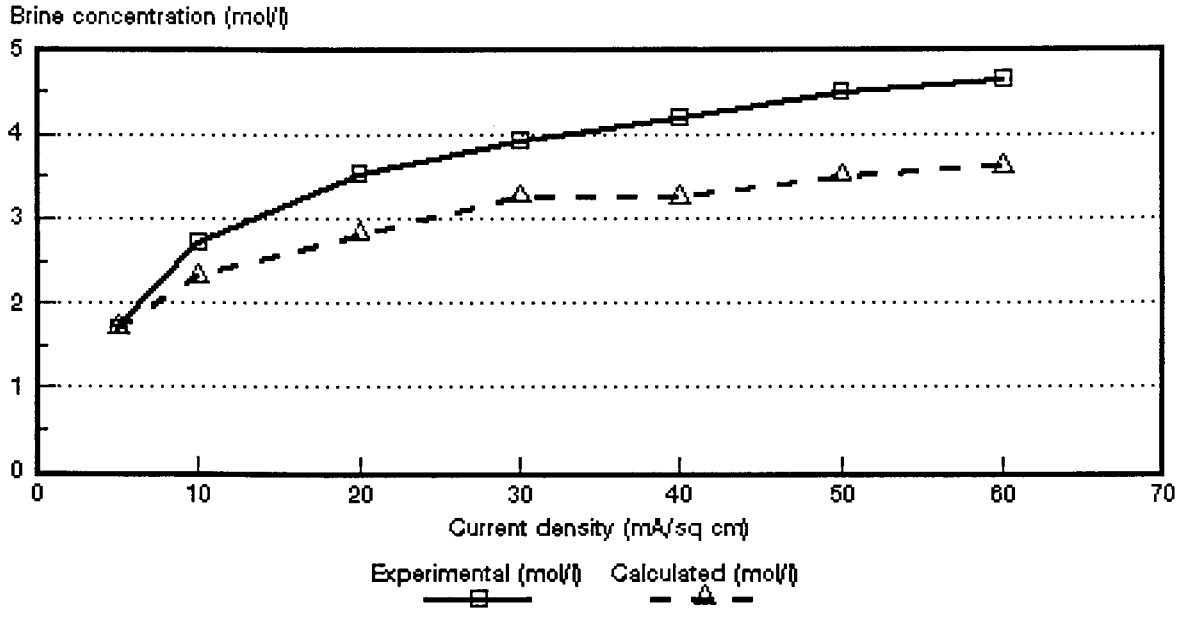

Figure 6.17: **Experimental and calculated brine concentrations as a function of current density for 0,5 mol/ℓ NaCl feed solution. *Selemion* AMV and CMV membranes.**

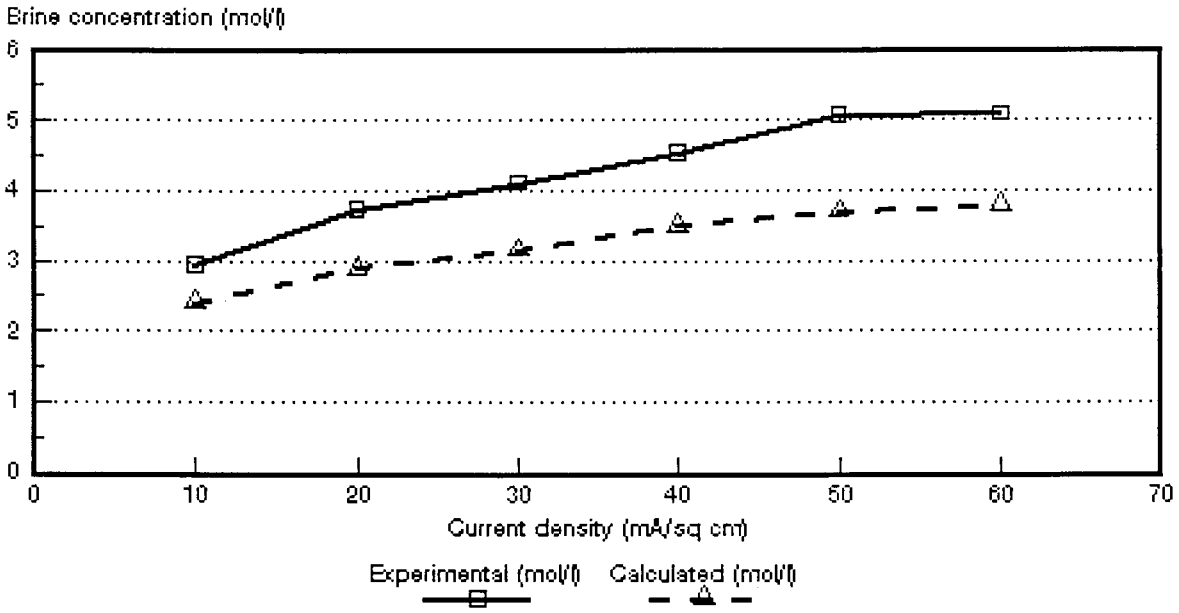

Figure 6.18: **Experimental and calculated brine concentrations as a function of current density for 1,0 mol/ℓ NaCl feed solution. *Selemion* AMV and CMV membranes.**

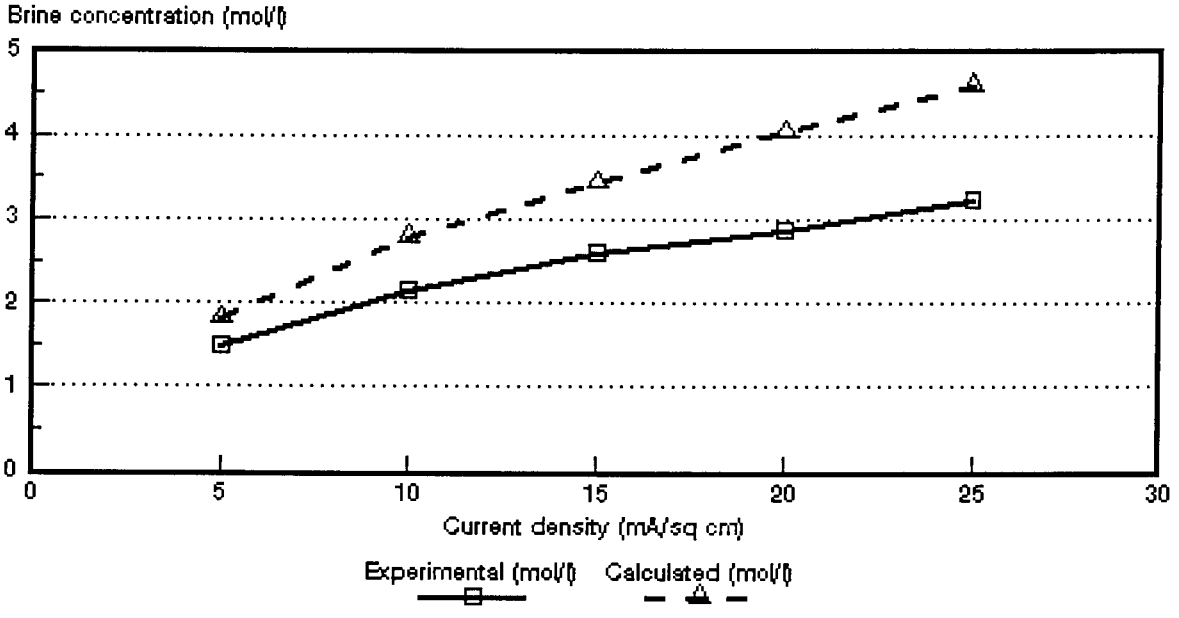

Figure 6.19: **Experimental and calculated brine concentrations as a function of current density for 0,05 mol/ℓ NaCl feed solution. *Ionac* MA-3475 and MC-3470 membranes.**

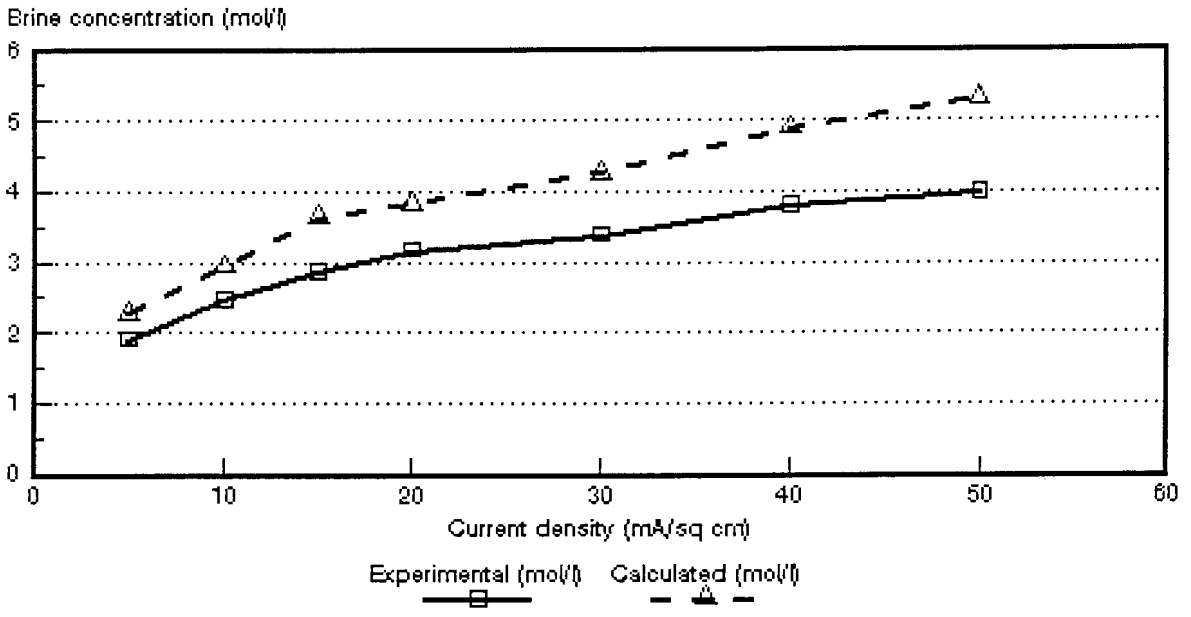

Figure 6.20: **Experimental and calculated brine concentrations as a function of current density for 0,1 mol/ℓ NaCl feed solution. *Ionac* MA-3475 and MC-3470 membranes.**

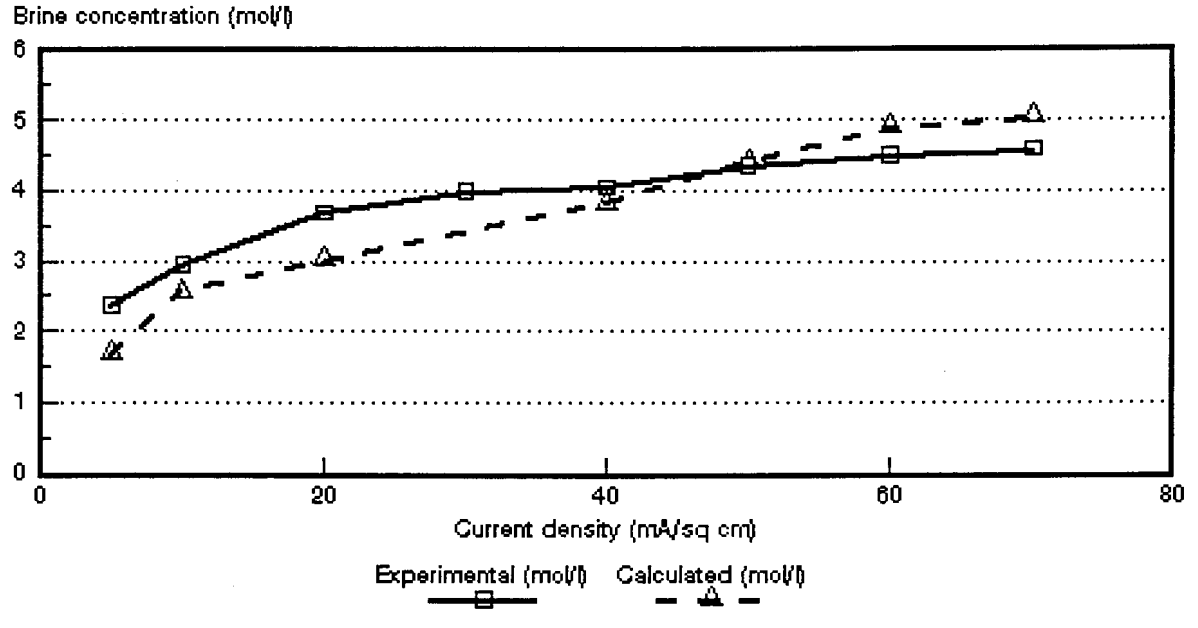

Figure 6.21: **Experimental and calculated brine concentrations as a function of current density for 0,5 mol/ℓ NaCl feed solution. *Ionac* MA-3475 and MC-3470 membranes.**

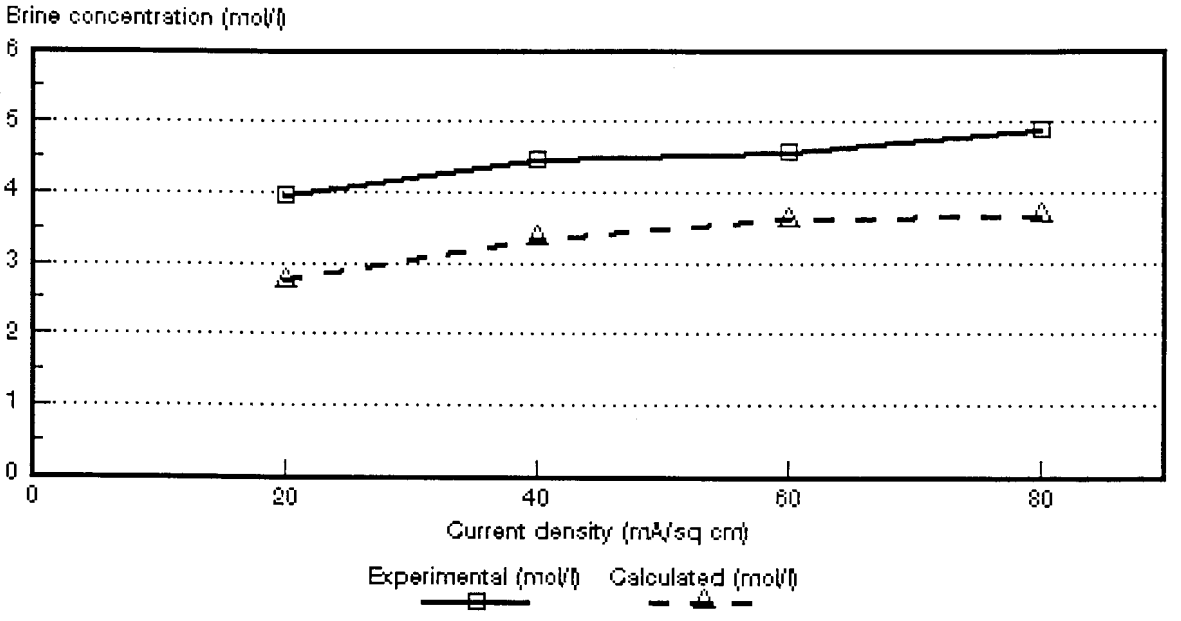

Figure 6.22: **Experimental and calculated brine concentrations as a function of current density for 1,0 mol/ℓ NaCl feed solution. *Ionac* MA-3475 and MC-3470 membranes.**

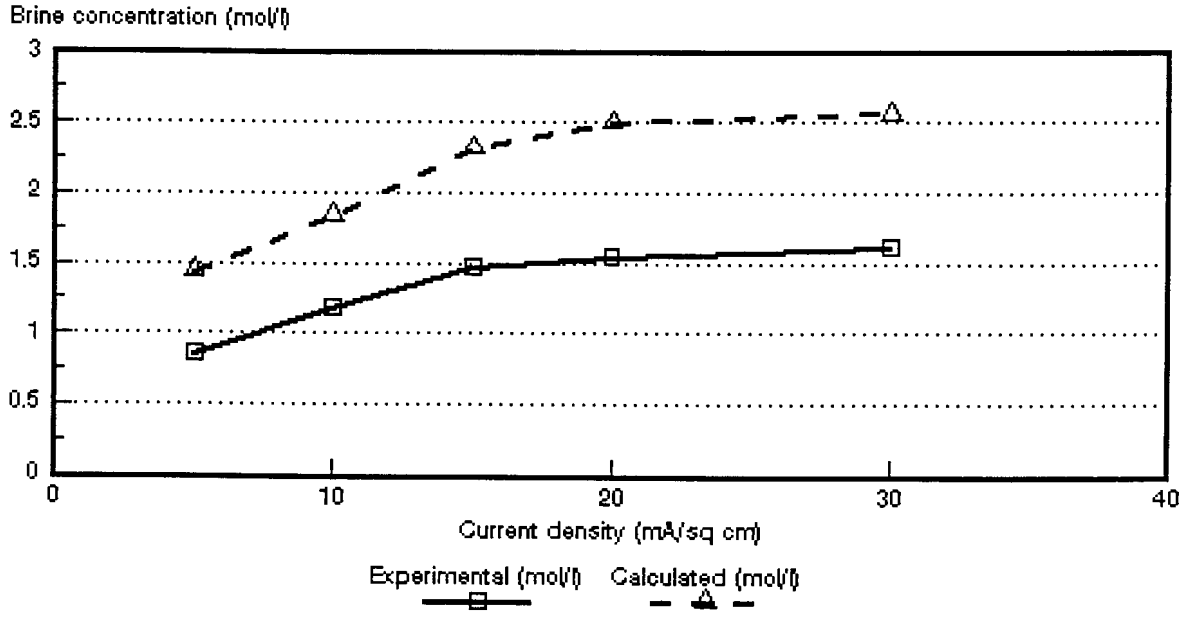

Figure 6.23: **Experimental and calculated brine concentrations as a function of current density for 0,05 mol/ℓ NaCl feed solution. *Ralpore* R4030 and R4010 membranes.**

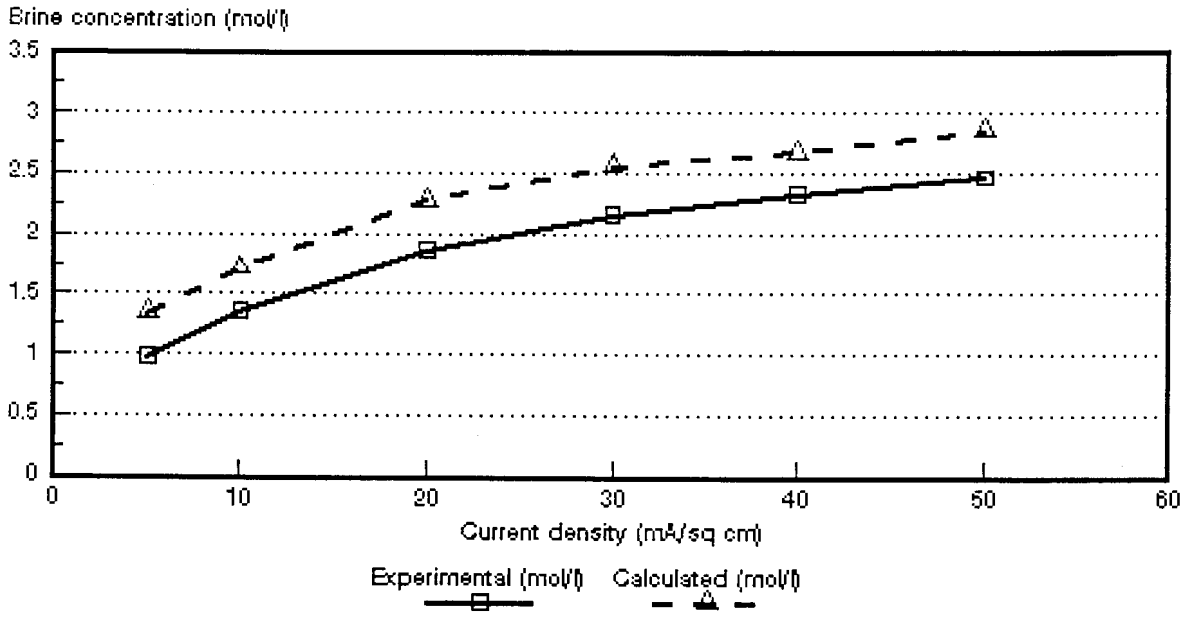

Figure 6.24: **Experimental and calculated brine concentrations as a function of current density for 0,1 mol/ℓ NaCl feed solution. *Raipore* R4030 and R4010 membranes.**

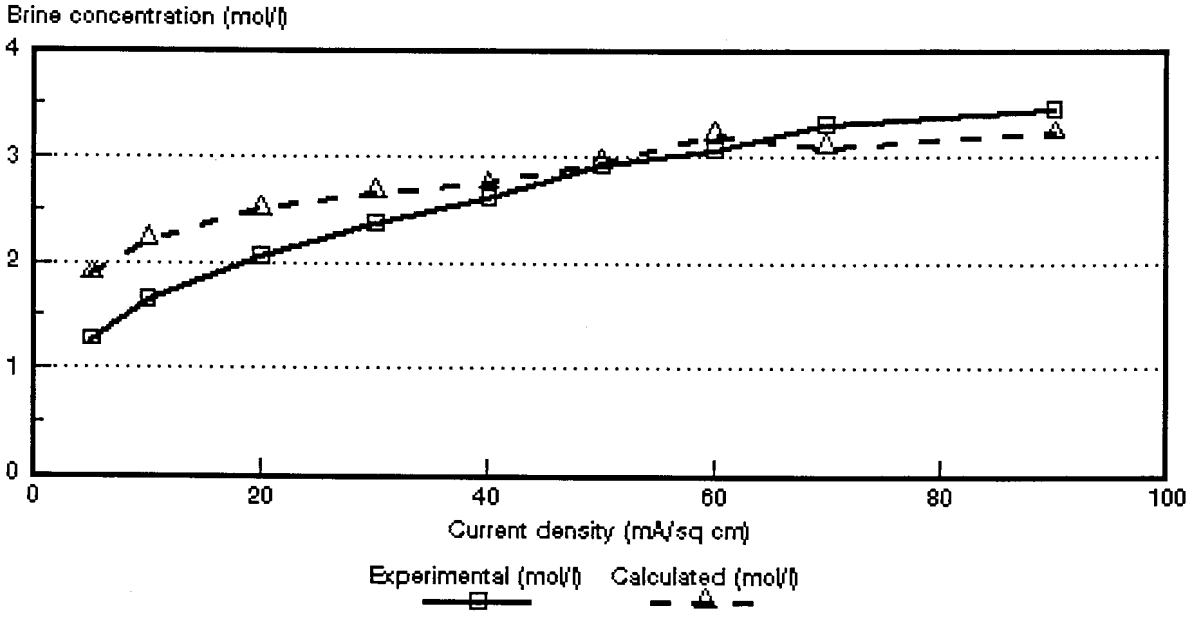

Figure 6.25: **Experimental and calculated brine concentrations as a function of current density for 0,5 mol/ℓ NaCl feed solution. *Raipore* R4030 and R4010 membranes.**

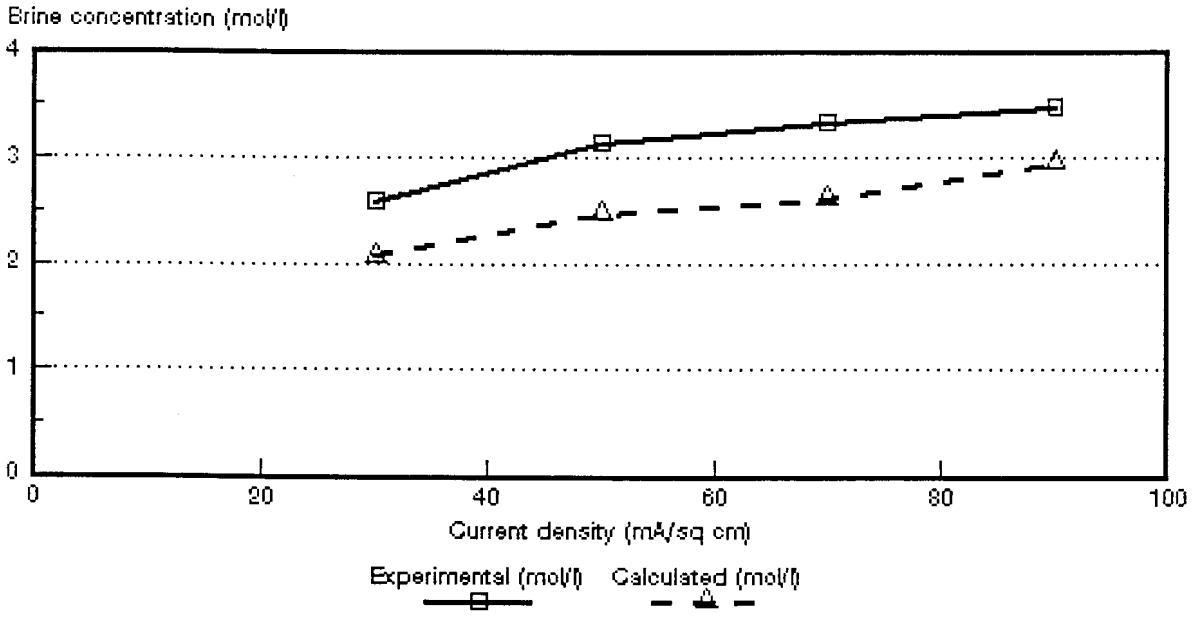

Figure 6.26: **Experimental and calculated brine concentrations as a function of current density for 1,0 mol/ℓ NaCl feed solution. *Raipore* R4030 and R4010 membranes.**

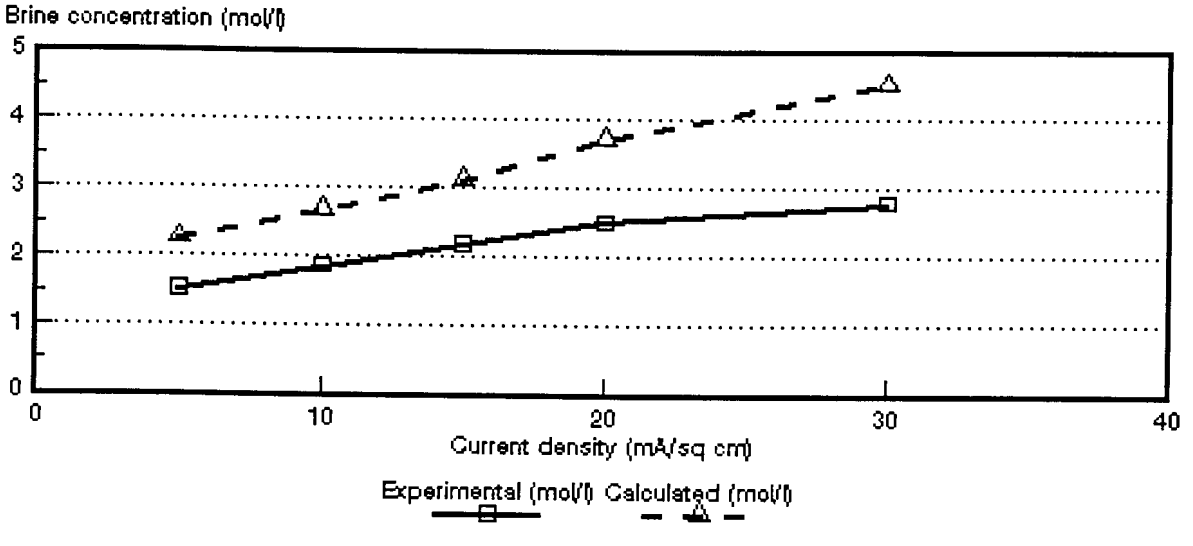

Figure 6.27: **Experimental and calculated brine concentrations as a function of current density for 0,05 mol/ℓ NaCl feed solution. *Ionics* A-204-UZL-386 and C-61-CZL-386 membranes.**

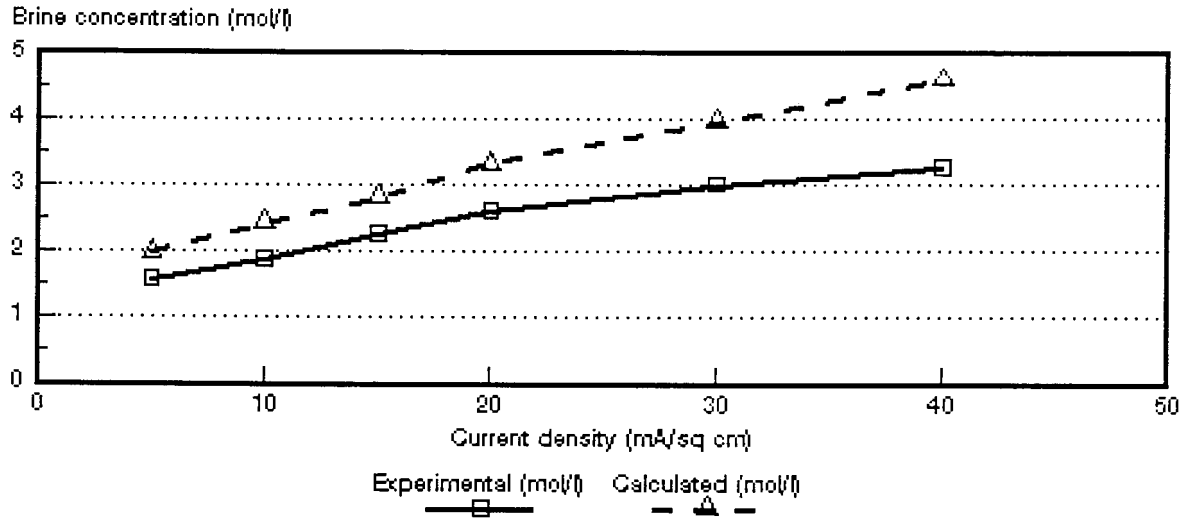

Figure 6.28: **Experimental and calculated brine concentrations as a function of current density for 0,1 mol/ℓ NaCl feed solution. *Ionics* A-204-UZL-386 and C-61-CZL-386 membranes.**

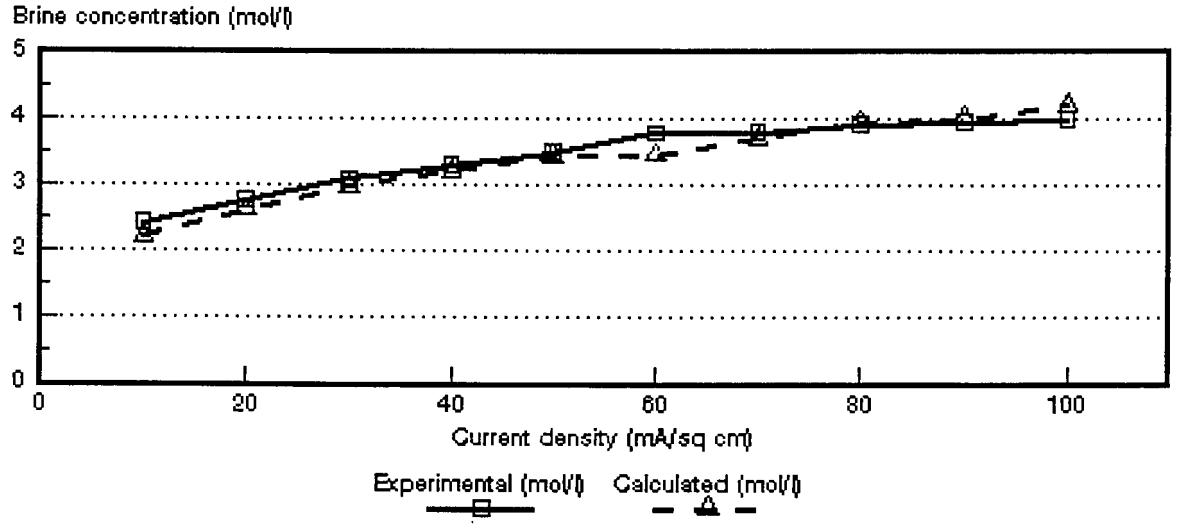

Figure 6.29: **Experimental and calculated brine concentrations as a function of current density for 0,5 mol/ℓ NaCl feed solution. *Ionics* A-204-UZL-386 and C-61-CZL-386 membranes.**

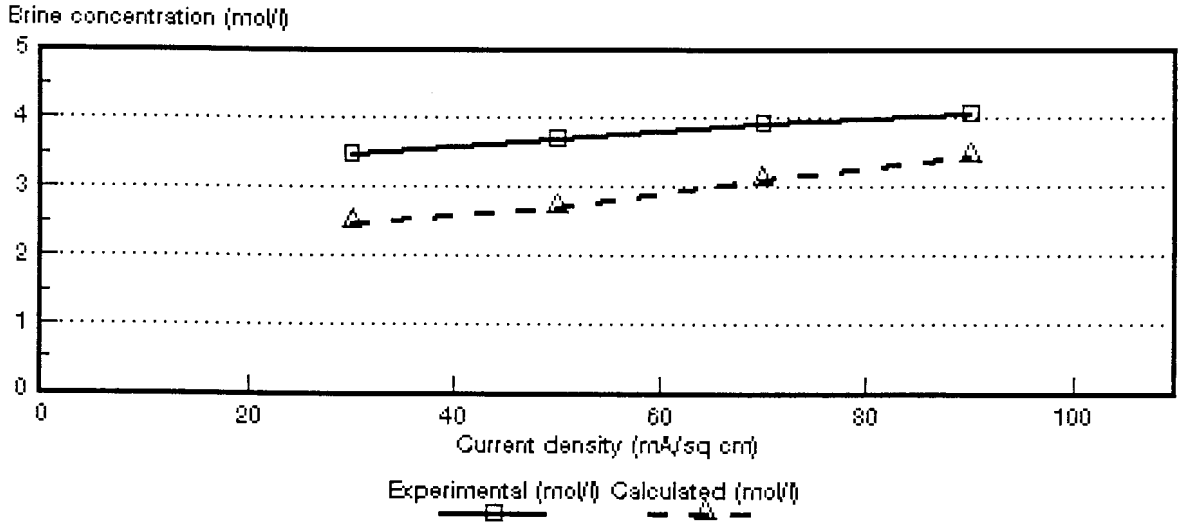

Figure 6.30: **Experimental and calculated brine concentrations as a function of current density for 1,0 mol/ℓ NaCl feed solution. *Ionics* A-204-UZL-386 and C-61-CZL-386 membranes.**

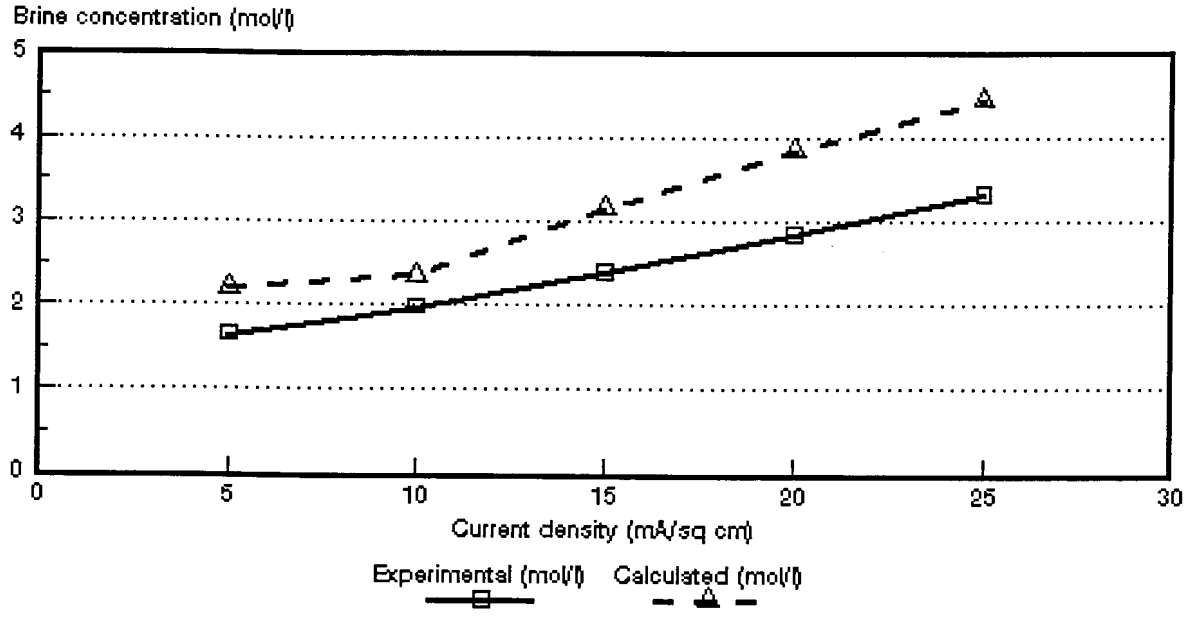

Figure 6.31: **Experimental and calculated brine concentrations as a function of current density for 0,05 mol/ℓ NaCl feed solution. WTPSA-1 and WTPSC-1 membranes.**

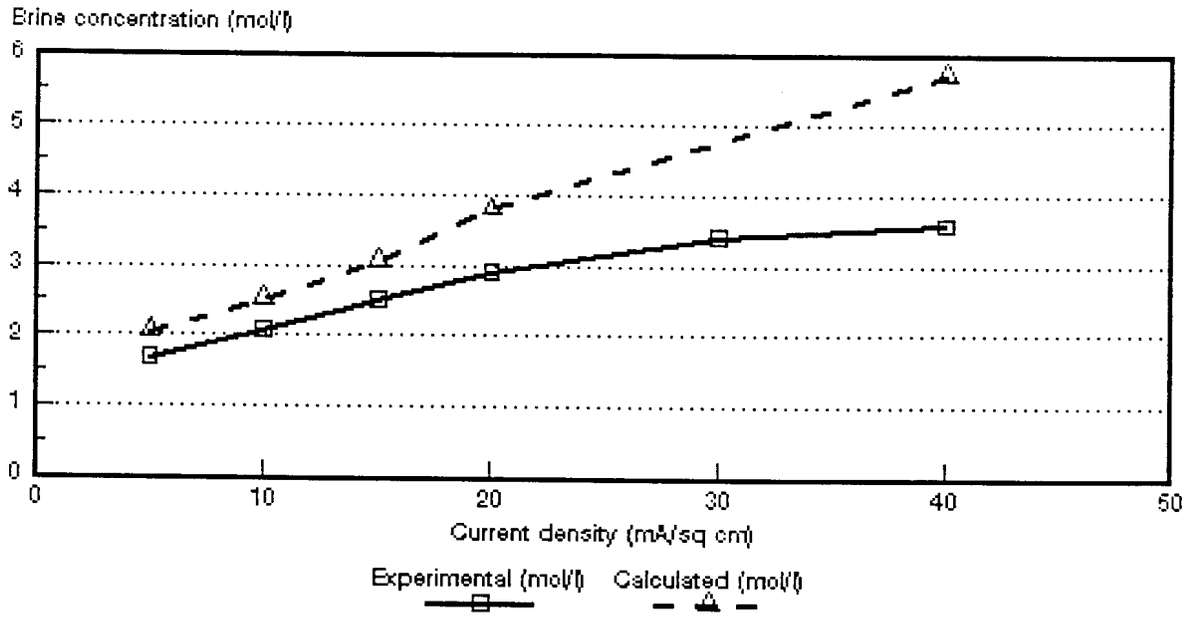

Figure 6.32: **Experimental and calculated brine concentrations as a function of current density for 0,1 mol/ℓ NaCl feed solution. WTPSA-1 and WTPSC-1 membranes.**

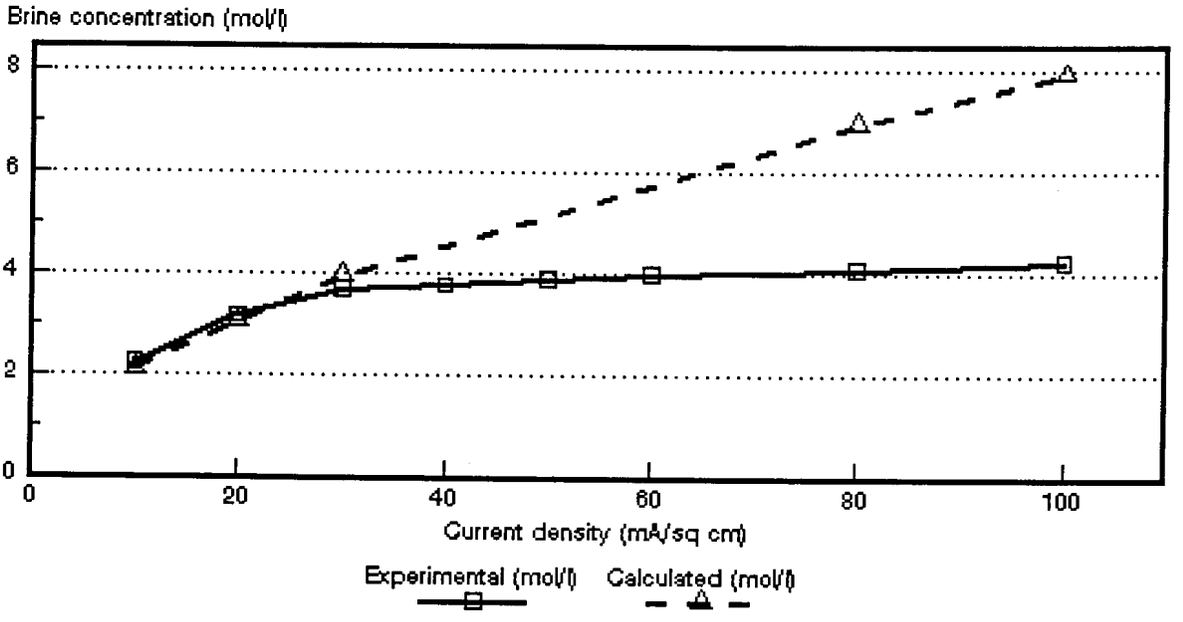

Figure 6.33: **Experimental and calculated brine concentrations as a function of current density for 0,5 mol/ℓ NaCl feed solution. WTPSA-1 and WTPSC-1 membranes.**

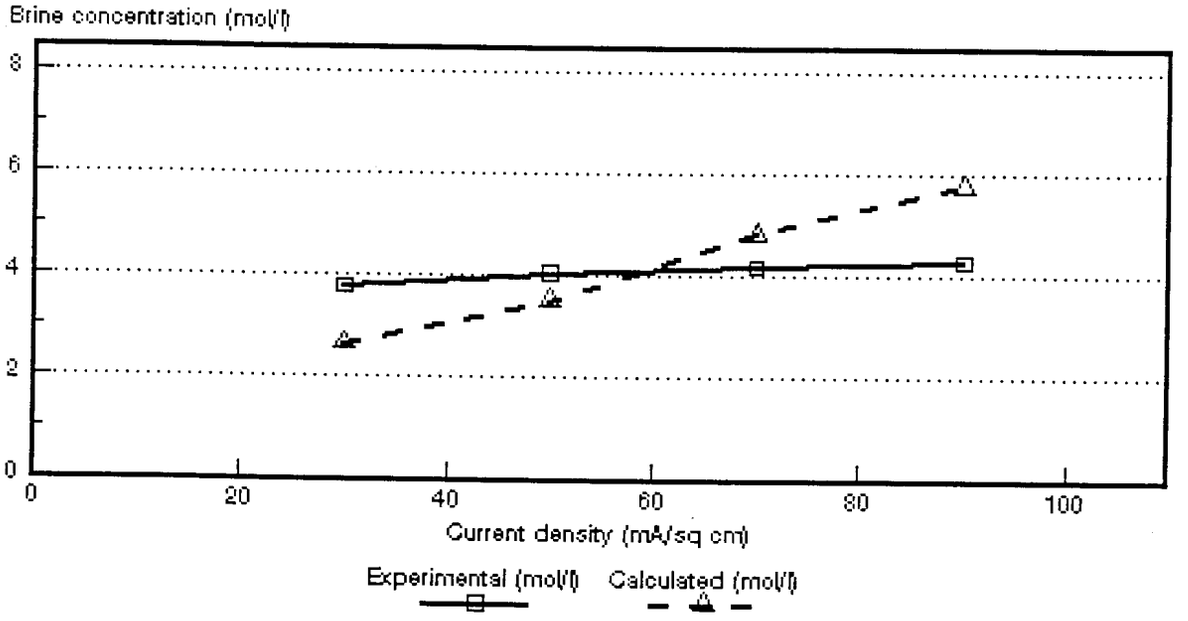

Figure 6.34: **Experimental and calculated brine concentrations as a function of current density for 1,0 mol/ℓ NaCl feed solution. WTPSA-1 and WTPSC-1**

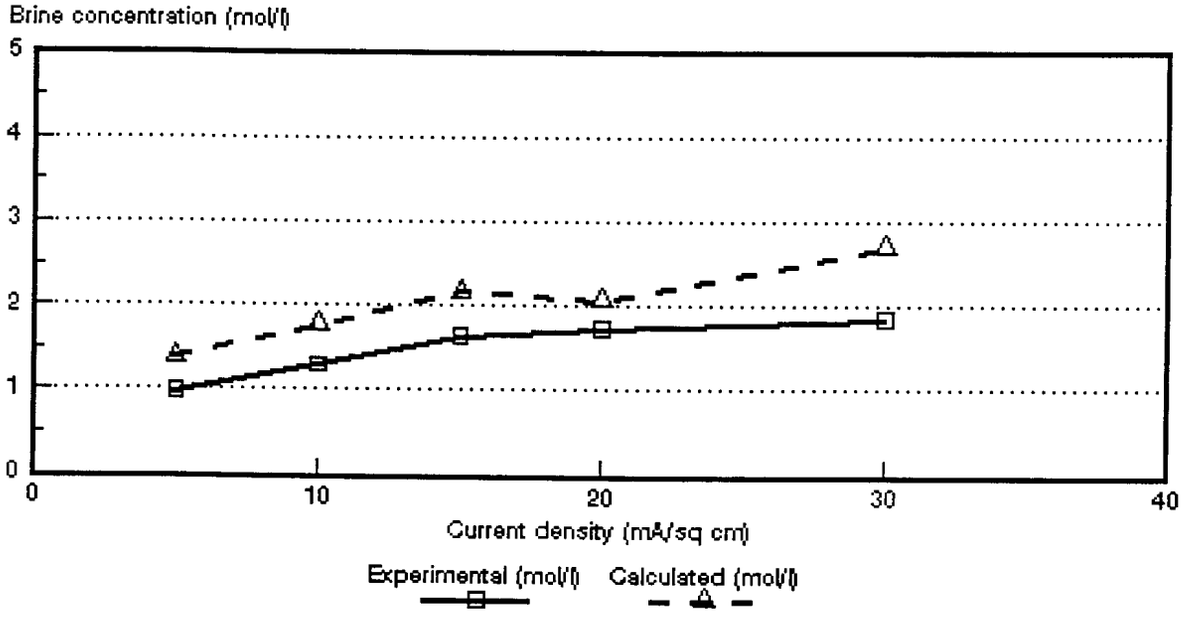

Figure 6.35: **Experimental and calculated brine concentrations as a function of current density for 0,05 mol/ℓ NaCl feed solution. WTPVCA-2 and WTPVCC-2 membranes.**

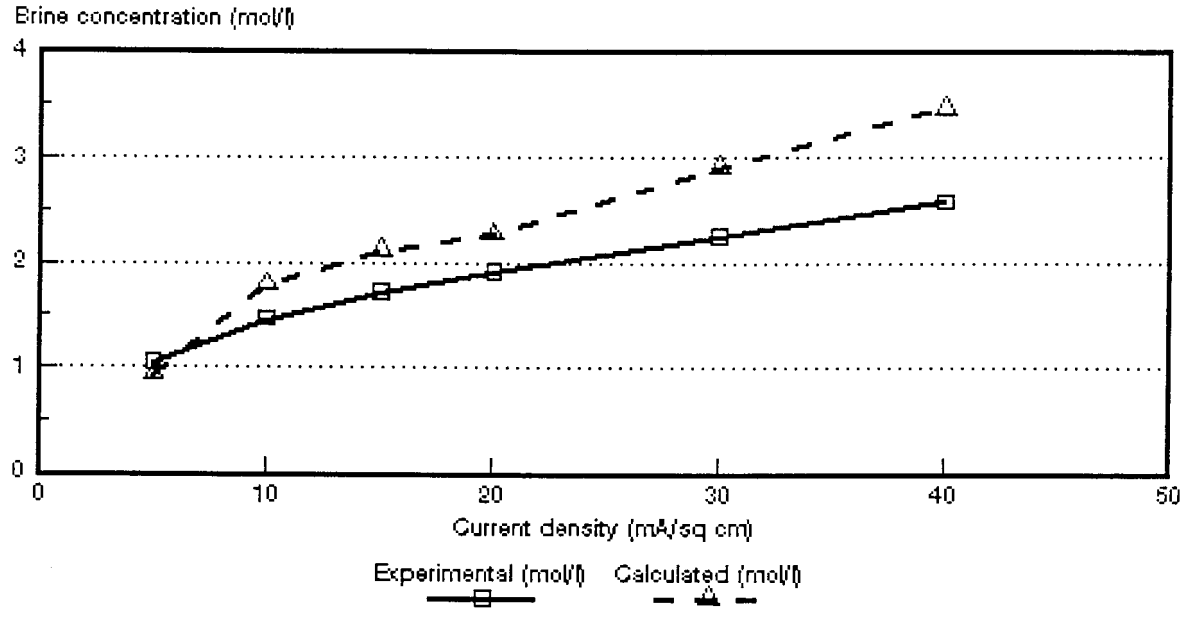

Figure 6.36: **Experimental and calculated brine concentrations as a function of current density for 0,1 mol/ℓ NaCl feed solution. WTPVCA-2 and WTPVCC-2 membranes.**

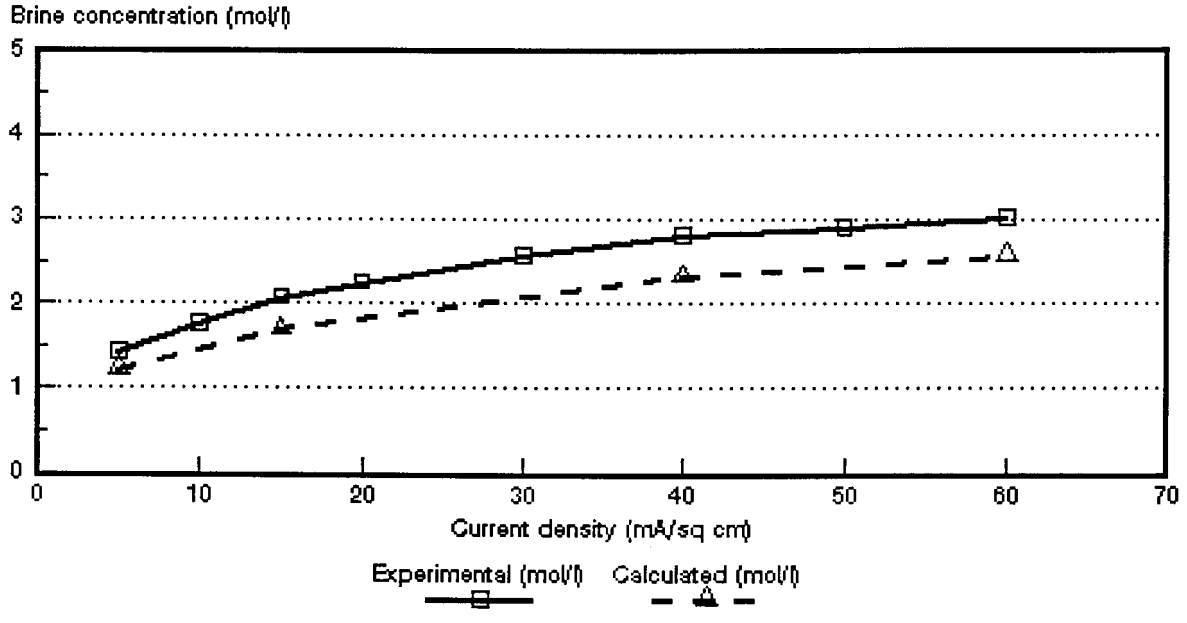

Figure 6.37: **Experimental and calculated brine concentrations as a function of current density for 0,5 mol/ℓ NaCl feed solution. WTPVCA-2 and WTPVCC-2 membranes.**

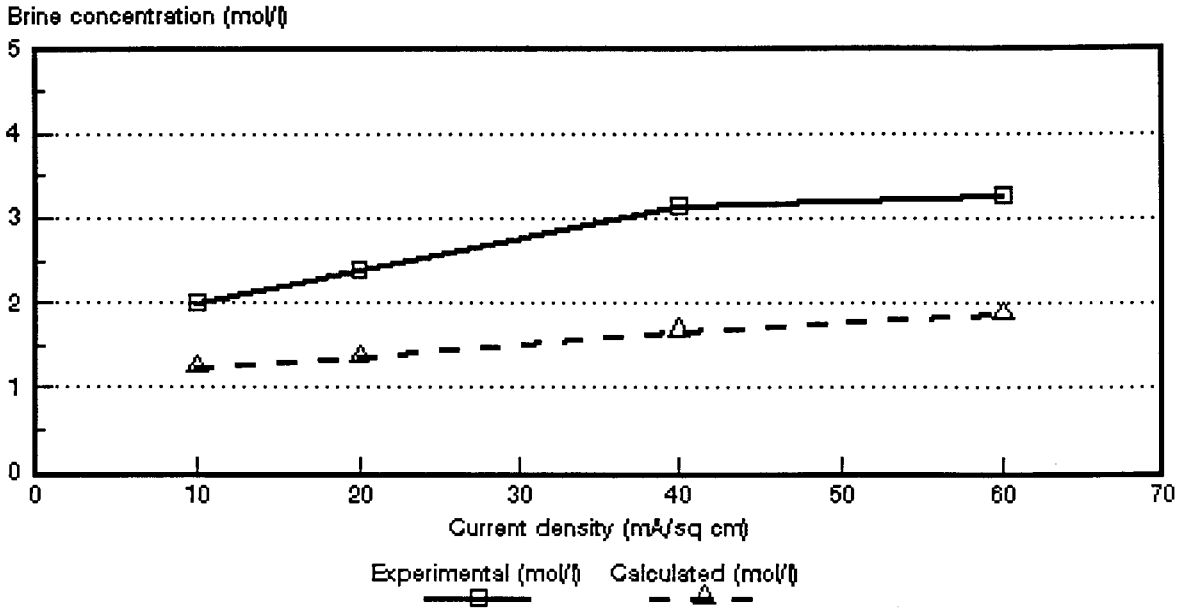

Figure 6.38: **Experimental and calculated brine concentrations as a function of current density for 1,0 mol/ℓ NaCl feed solution. WTPVCA-2 and WTPVCC-2 membranes.**

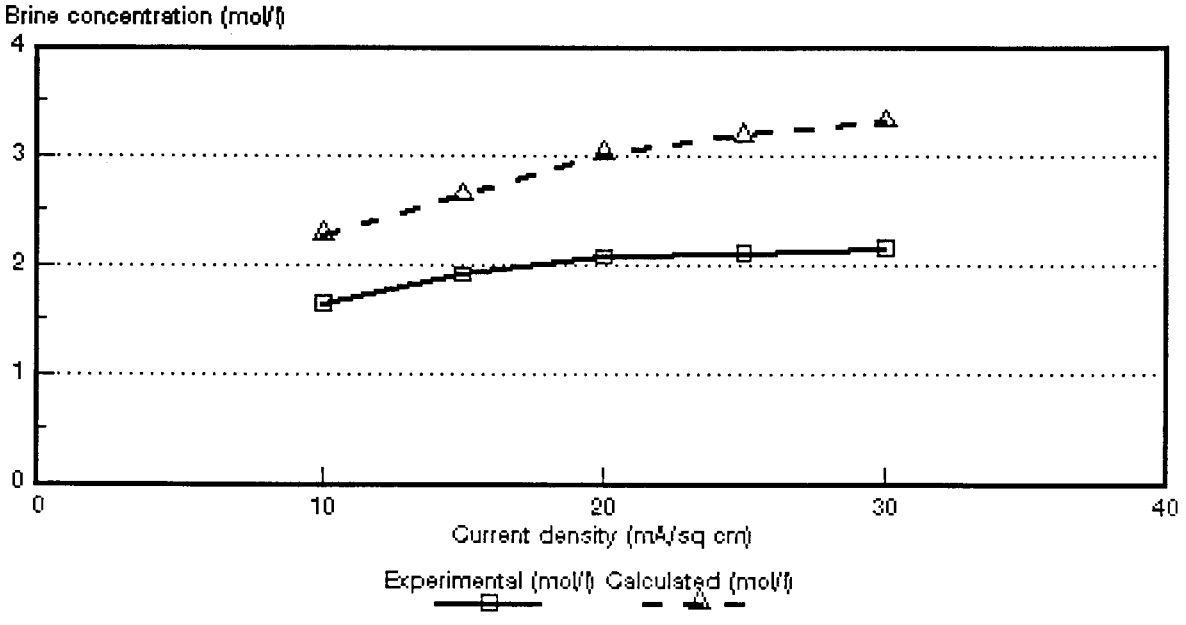

Figure 6.39: **Experimental and calculated brine concentrations as a function of current density for 0,05 mol/ℓ NaCl feed solution. WTPSTA-3 and WTPSTC-3 membranes.**

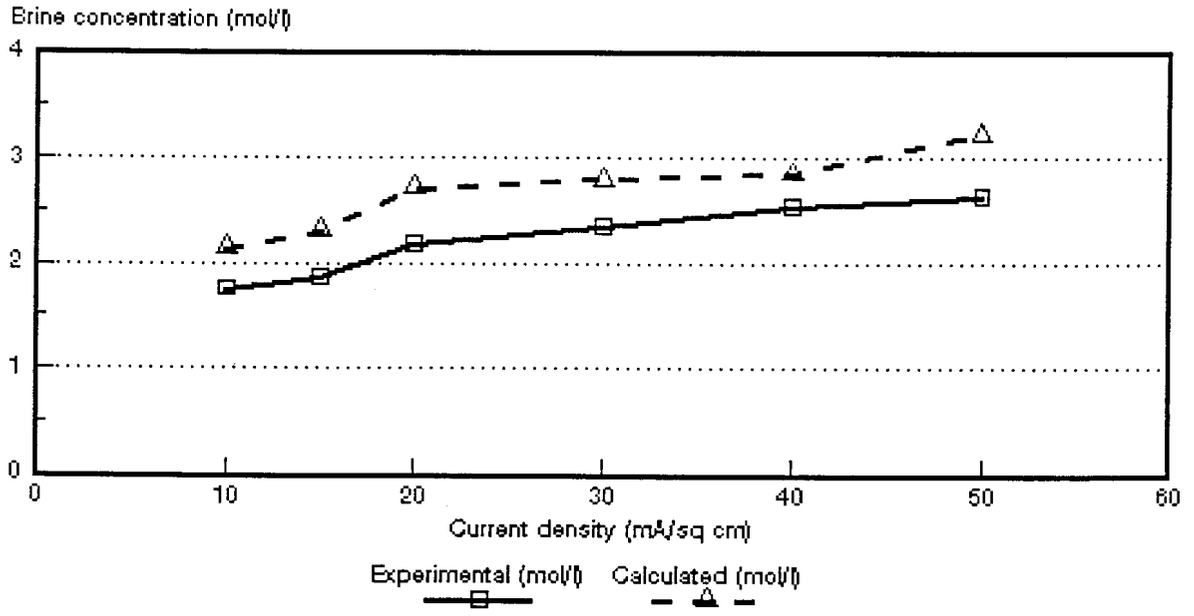

Figure 6.40: **Experimental and calculated brine concentrations as a function of current density for 0,1 mol/ℓ NaCl feed solution. WTPSTA-3 and WTPSTC-3 membranes.**

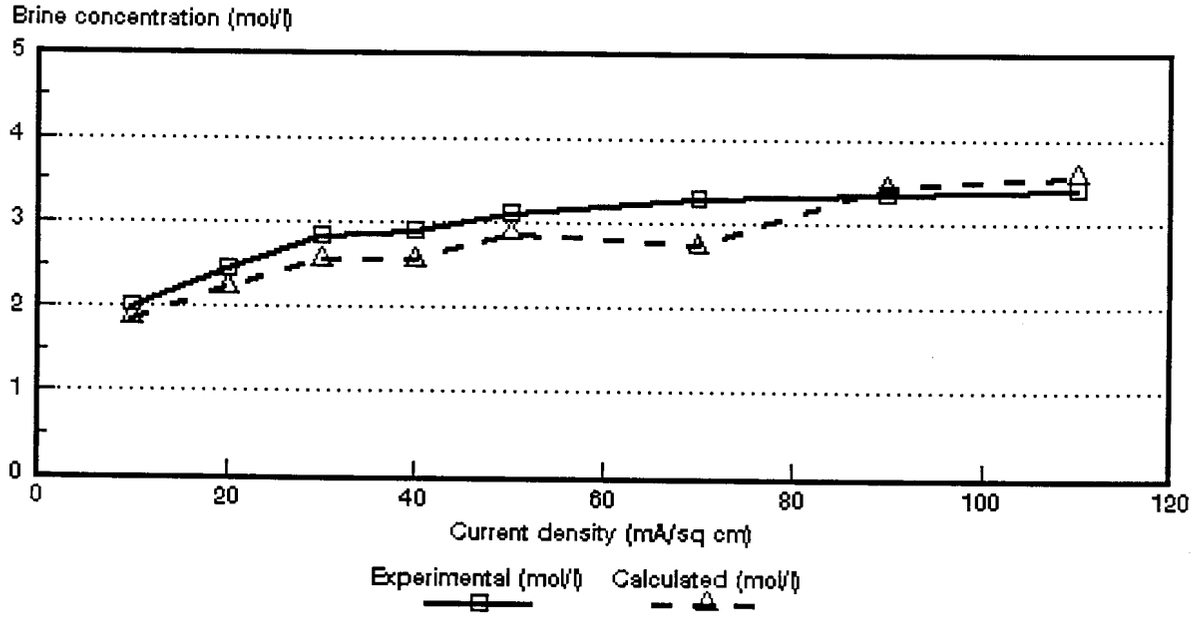

Figure 6.41: **Experimental and calculated brine concentrations as a function of current density for 0,5 mol/ℓ NaCl feed solution. WTPSTA-3 and WTPSTC-3 membranes.**

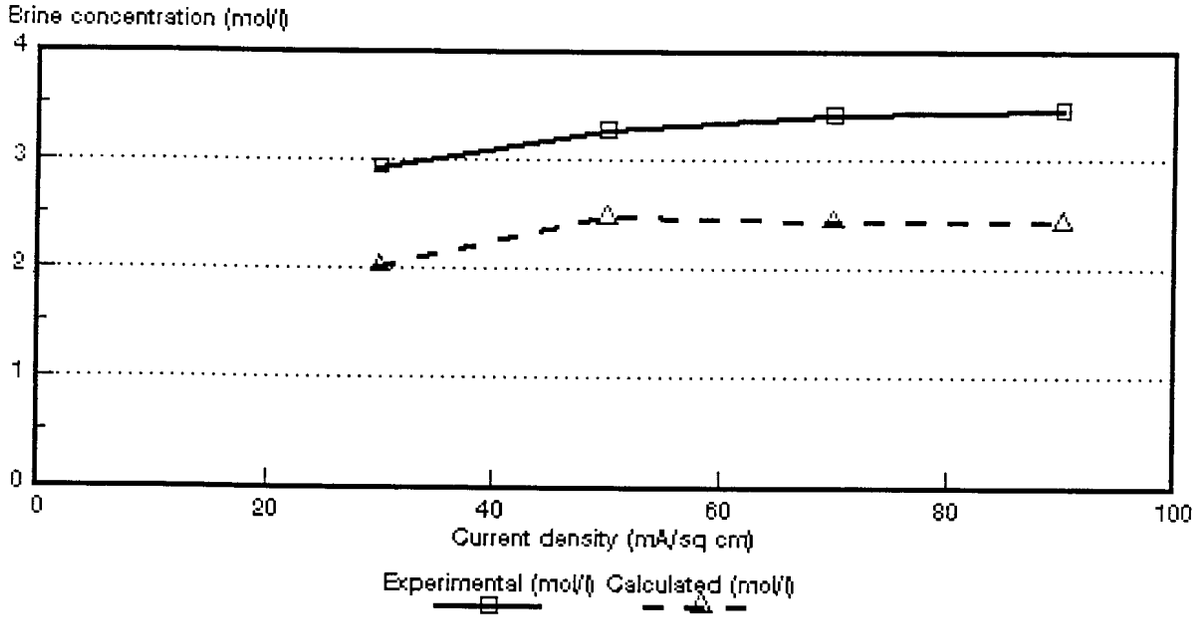

Figure 6.42: **Experimental and calculated brine concentrations as a function of current density for 1,0 mol/ℓ NaCl feed solution. WTPSTA-3 and WTPSTC-3 membranes.**

Table 6.31: Correlation between calculated ($c_{b\ calc}$) and experimentally ($c_{b\ exp}$) determined brine concentrations.

Current Density	$c_{b calc}/c_{b exp}$																											
	Selemion AMV & CMV Concentration, mol/ℓ				Ionac MA-3475 & MC-3470 Concentration, mol/ℓ				Raipore R4030 & R4010 Concentration, mol/ℓ				Ionics A-204-UZL & C-61-CZL Concentration, mol/ℓ				WTPS WTPSA & WTPSA Concentration, mol/ℓ				WTPVC WTPVCA & WTPVCC Concentration, mol/ℓ				WTPST WTPSTA & WTPSTC Concentration, mol/ℓ			
mA/cm²	0,05	0,1	0,5	1,0	0,05	0,1	0,5	1,0	0,05	0,1	0,5	1,0	0,05	0,1	0,5	1,0	0,05	0,1	0,5	1,0	0,05	0,1	0,5	1,0	0,05	0,1	0,5	1,0
5	0,98	1,17	0,99		1,21	1,19	0,71		1,67	1,36	1,48		1,50	1,27			1,33	1,22			1,37	0,90	0,86					
10	1,28	1,11	0,85	0,82	1,30	1,18	0,87		1,54	1,26	1,34		1,43	1,29	0,91		1,19	1,20	0,95		1,36	1,22		0,63	1,39	1,22	0,93	
15	1,26	1,07			1,33	1,26			1,57				1,43	1,25			1,32	1,21			1,33	1,23	0,82		1,38	1,23		
20	1,26	1,06	0,79	0,78	1,41	1,21	0,82	0,70	1,61	1,23	1,21		1,48	1,27	0,95		1,35	1,31	0,96		1,19	1,13		0,57	1,45	1,24	0,91	
25					1,42												1,34								1,52			
30	1,22	1,04	0,83	0,77		1,26			1,56	1,19	1,12	0,80	1,62	1,31	0,96	0,72			1,07	0,70	1,46	1,29			1,54	1,23	0,99	0,69
40		1,05	0,77	0,77		1,28	0,95	0,75		1,15	1,05			1,42	0,98			1,60				1,34	0,83	0,54		1,27	0,88	
50		1,00	0,78	0,73		1,33	1,01			1,16	1,01	0,79			0,99	0,73				0,86						1,12	0,93	0,66
60			0,77	0,74			1,09	0,79			1,05				0,91								0,85	0,57				
70							1,10				0,93	0,78			0,97	0,79				1,16							0,84	0,72
80								0,75							1,01				1,70									
90											0,94	0,85			1,02	0,85				1,35							1,02	0,70
100															1,06				1,87									
110																											1,05	

6.2 Current Efficiency

Current efficiency (ϵ_p) determined during the EOP experiments as a function of current density is shown in Figures 6.43 to 6.49 for the different membranes. Current efficiency increases with increasing feed water concentration in the concentration range from 0,05 to 1,0 mol/ℓ. However, current efficiency was slightly lower at the highest feed concentration in the case of the *Selemion* membranes (Fig 6.43). It is interesting to note that current efficiency has been significantly higher at the higher feed concentrations in the case of the *Ionac*- (Fig. 6.44), *Raipore*- (Fig. 6.45), *Ionics*- (Fig. 6.46), WTPS- (Fig. 6.47), WTPVC- (Fig. 6.48) and WTPST- (Fig 6.49) membranes.

No significant change in current efficiency was observed as a function of current density in the case of the *Selemion* membranes in the feed concentration range studied (Fig 6.43). This showed that the limiting current density was not reached in the range of current densities and feed water concentrations used for these membranes. However, changes in current efficiency, especially at the lower feed concentration levels (0,05 to 0,5 mol/ℓ), were experienced with the *Ionac*- (Fig. 6.44), *Raipore*- (Fig. 6.45, 0,05 mol/ℓ), *Ionics*- (Fig. 6.46, 0,05 to 1,0 mol/ℓ), WTPS- (Fig. 6.47, 0,05 to 1,0 mol/ℓ), WTPVC- (Fig. 6.48, 0,05 to 1,0 mol/ℓ) and WTPST- (Fig. 6.49, 0,05 to 1,0 mol/ℓ) membranes. This showed that the limiting current density was exceeded with increasing current density. A significant reduction in current efficiency was experienced in the case of the WTPS membranes at the higher feed concentrations at relatively low current densities (Fig. 6.47). This showed that the limiting current density was exceeded and that polarization was taking place.

The apparent transport numbers for a membrane pair ($\bar{\Delta}t$), for the anion- (Δt^a) and cation- (Δt^c) membranes, determined from membrane potential measurements for a concentration difference similar to that obtained in the EOP experiments at the different current densities and feed water concentrations used, are shown in Figures 6.50 to 6.77. The current efficiencies (ϵ_p) as determined by the EOP method and shown in Figures 6.43 to 6.49 are also shown in Figures 6.50 to 6.77. The correlation between the apparent transport numbers ($\bar{\Delta}t$, Δt^a and Δt^c) and the current efficiency (ϵ_p) is shown in Tables 6.32 to 6.34.

The apparent transport numbers ($\bar{\Delta}t$, Δt^a, Δt^c) were higher than the current efficiencies at the lower feed water concentrations (0,05 to 0,1 mol/ℓ) (Tables 6.32 to 6.34 and Figs. 6.50 to 6.77). However, the apparent transport numbers became smaller than the

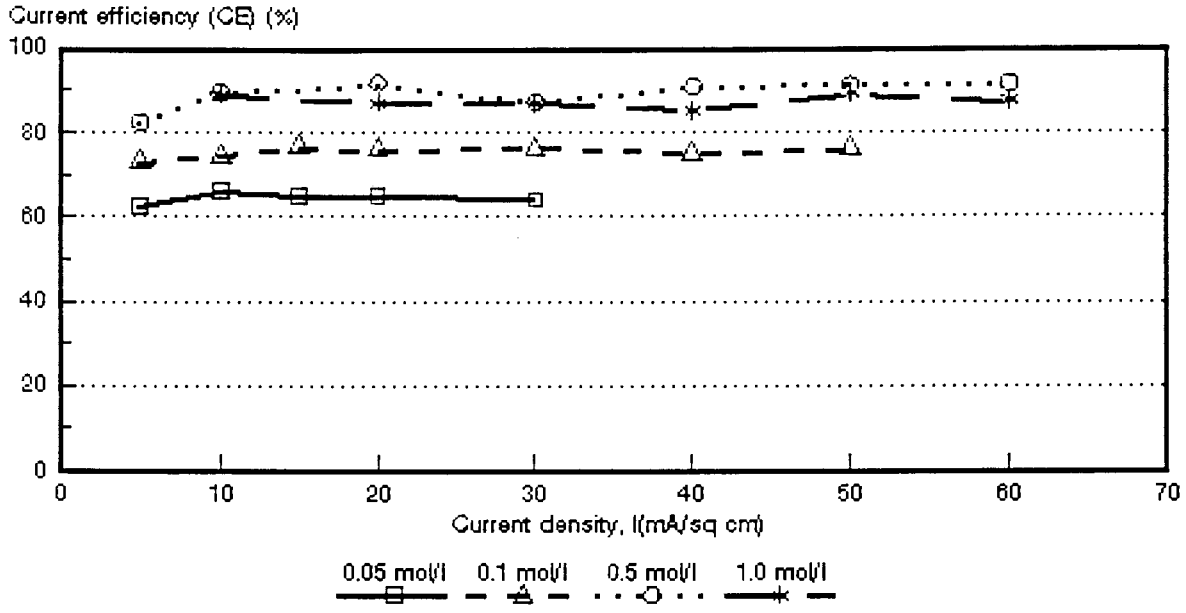

Figure 6.43: **Current efficiency (ϵ_p) as a function of current density for 4 different NaCl feed concentrations. *Selemion* AMV and CMV membranes.**

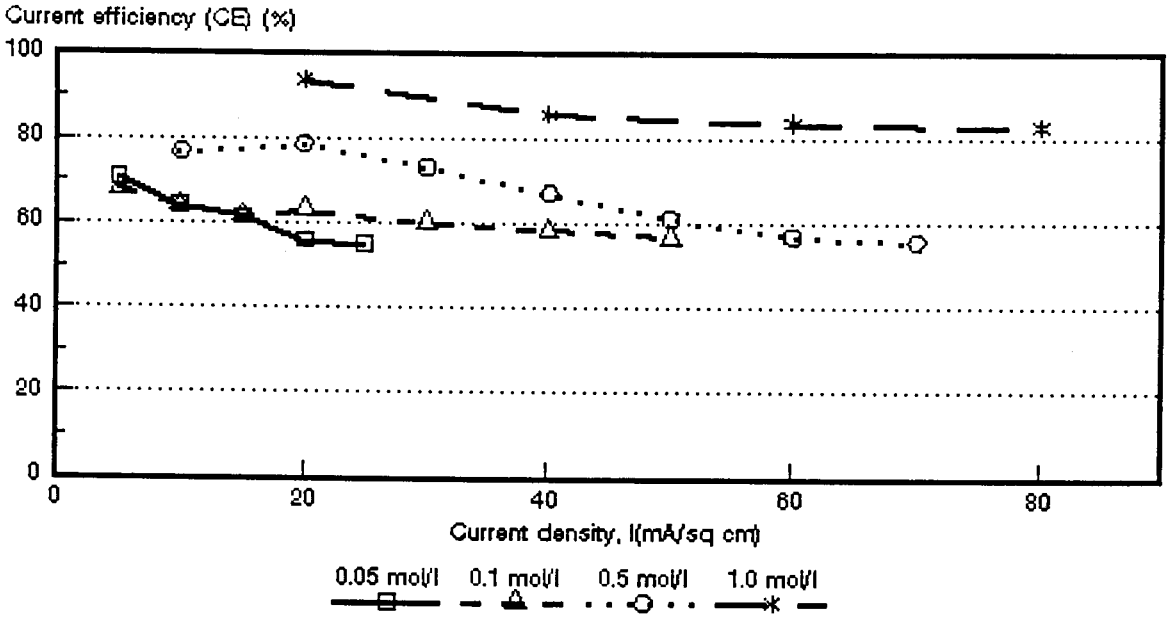

Figure 6.44: **Current efficiency (ϵ_p) as a function of current density for 4 different NaCl feed concentrations. Ionac MA-3475 and MC-3470 membranes.**

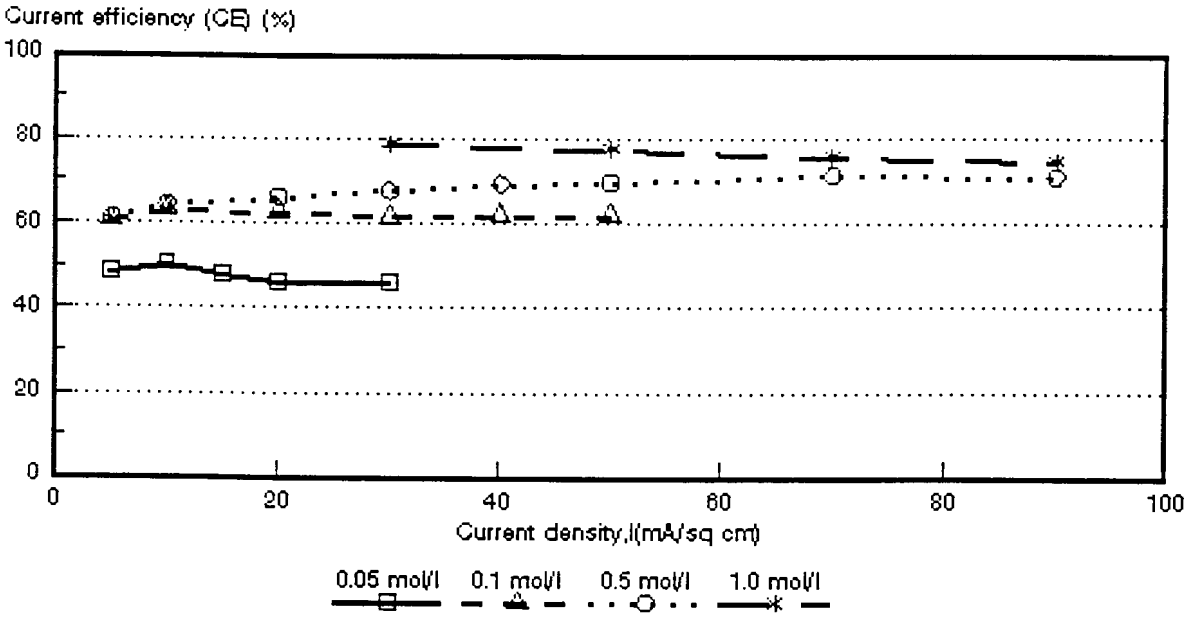

Figure 6.45: **Current efficiency (e_p) as a function of current density for 4 different NaCl feed concentrations. *Raipore* R4030 and R4010 membranes.**

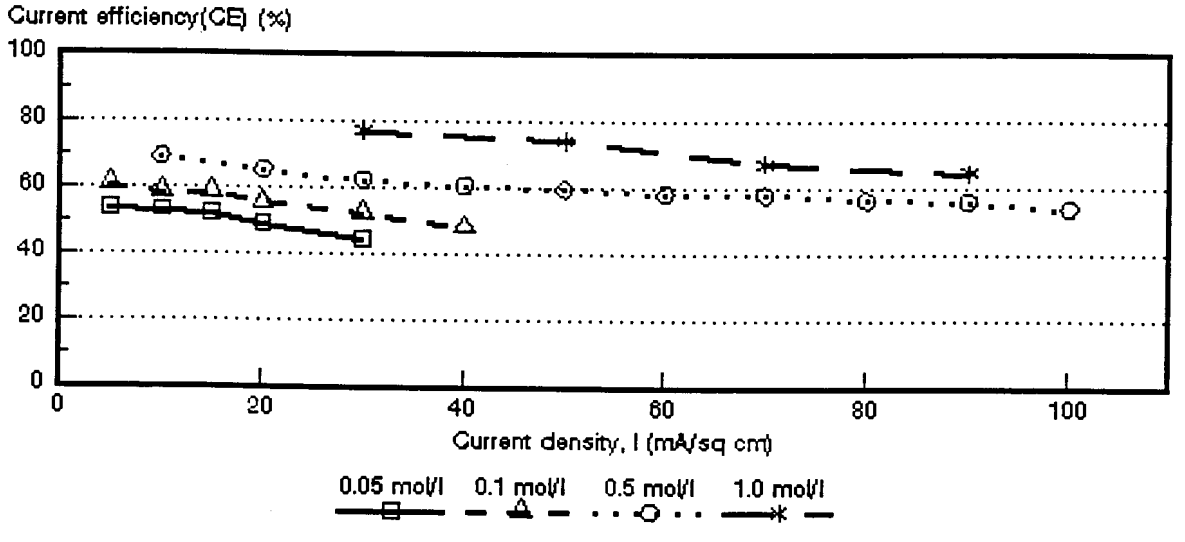

Figure 6.46: **Current efficiency (e_p) as a function of current density for 4 different NaCl feed concentrations. *Ionics* A-204-UZL-386 and C-61-CZL-386 membranes.**

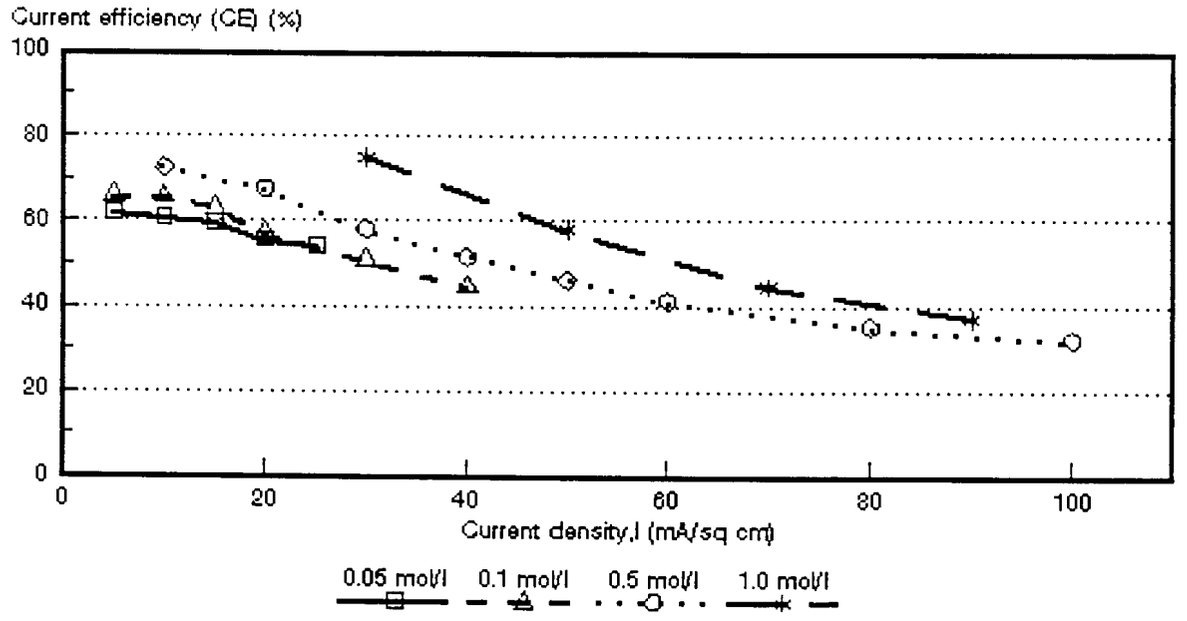

Figure 6.47: **Current efficiency (ϵ_p) as a function of current density for 4 different NaCl feed concentrations. WTPSA-1 and WTPSC-1 membranes**

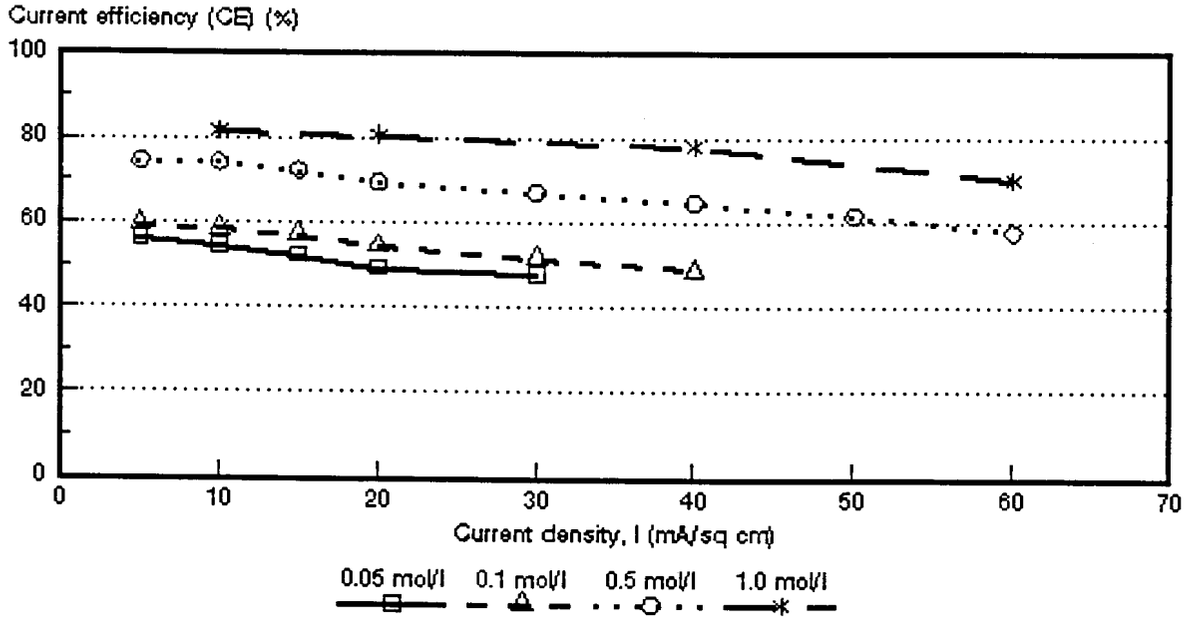

Figure 6.48: **Current efficiency (ϵ_p) as a function of current density for 4 different NaCl feed concentrations. WTPVCA-2 and WTPVCC-2 membranes.**

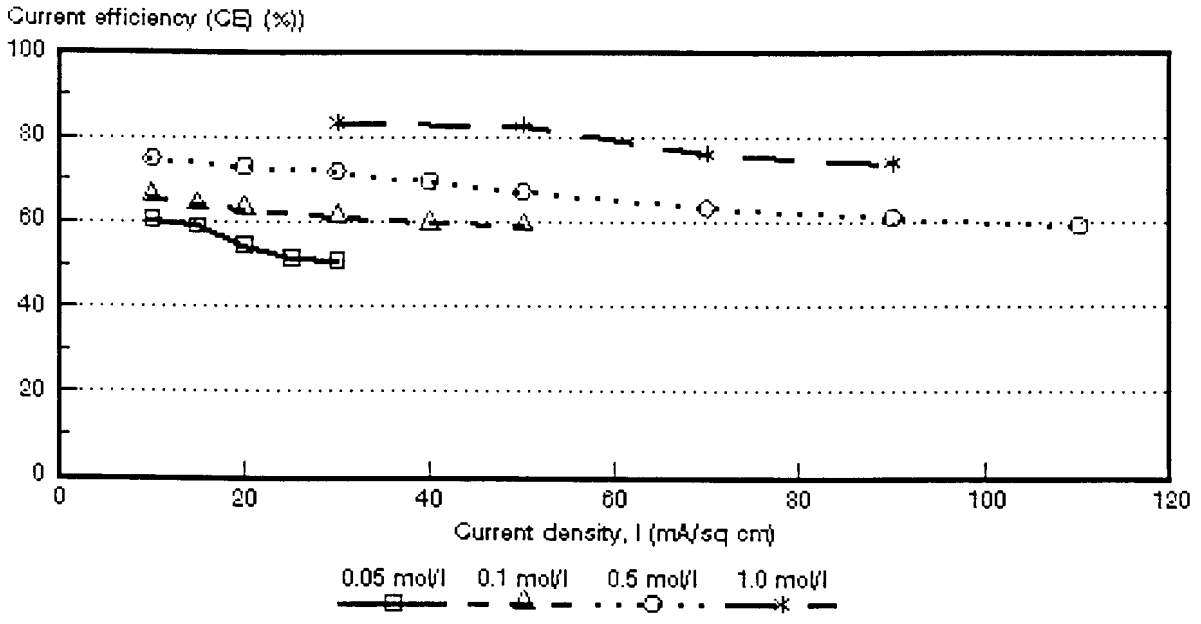

Figure 6.49: **Current efficiency (e_p) as a function of current density for 4 different NaCl feed concentrations. WTPSTA-3 and WTPSTC-3 membranes.**

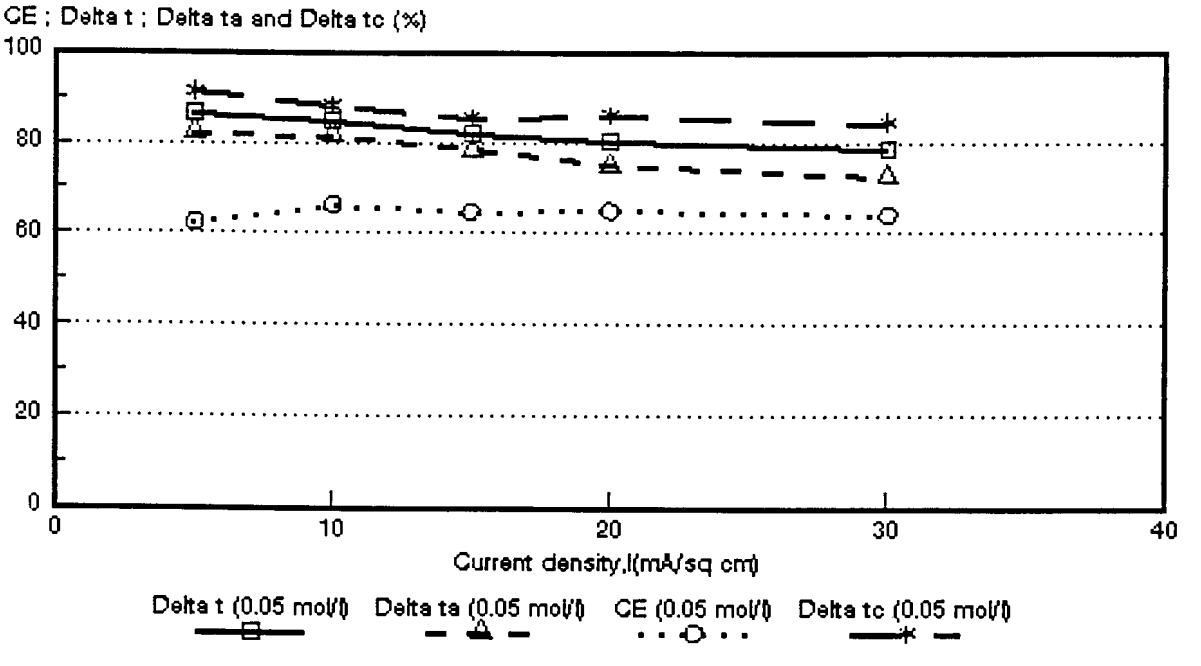

Figure 6.50: **Current efficiency (CE = e_p) and apparent transport numbers as a function of current density for 0,05 mol/ℓ NaCl feed. *Selemion* AMV and CMV membranes. Delta t = $\bar{\Delta}t$; Delta ta = Δt^a; Delta tc = Δt^c.**

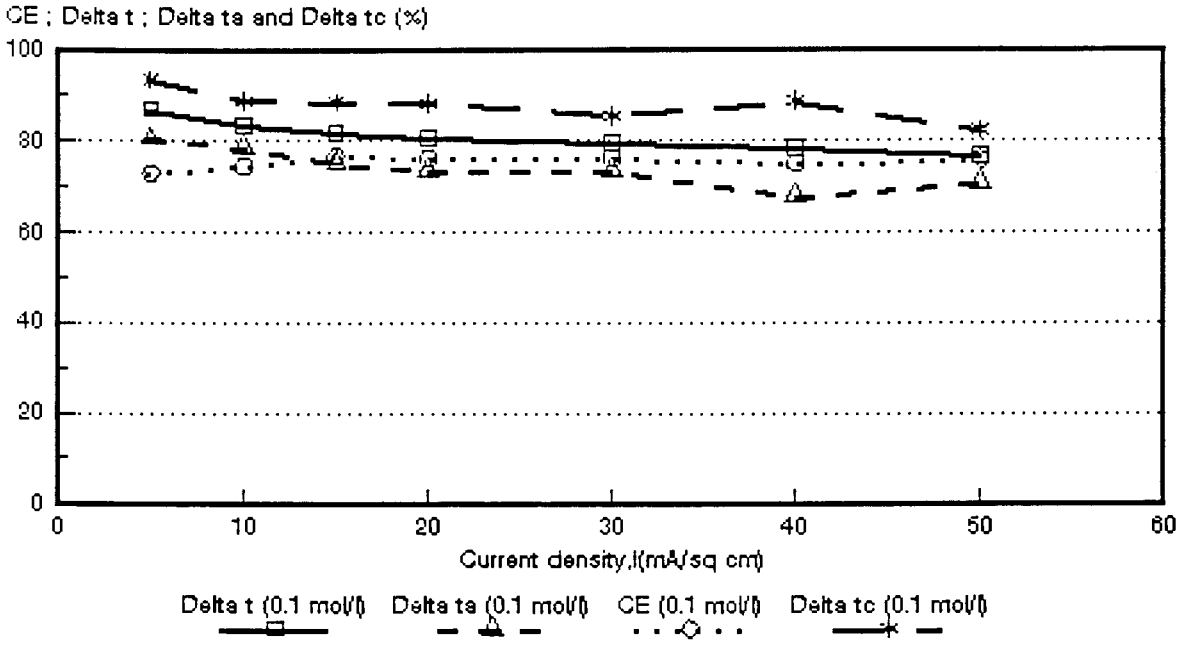

Figure 6.51: **Current efficiency (CE = ϵ_p) and apparent transport numbers as a function of current density for 0,1 mol/ℓ NaCl feed. *Selemion* AMV and CMV membranes. Delta t = $\bar{\Delta}t$; Delta ta = t^a; Delta tc = Δt^c.**

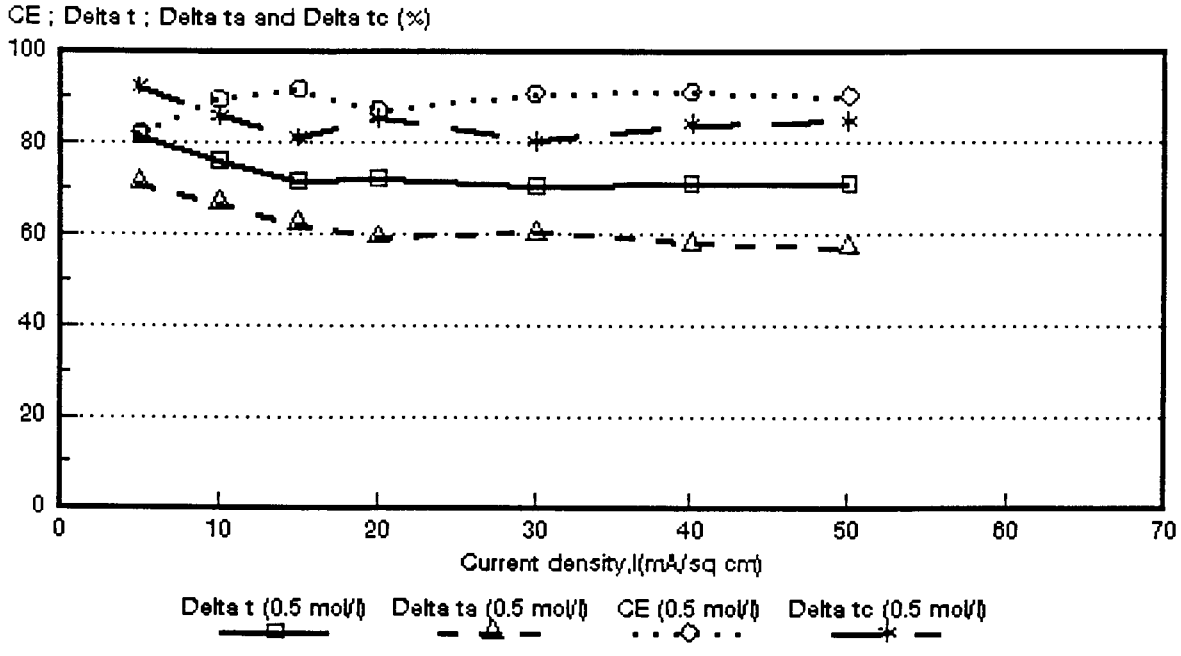

Figure 6.52: **Current efficiency (CE = ϵ_p) and apparent transport numbers as a function of current density for 0,5 mol/ℓ NaCl feed. *Selemion* AMV and CMV membranes. Delta t = $\bar{\Delta}t$; Delta ta = Δt^a; Delta tc = Δt^c.**

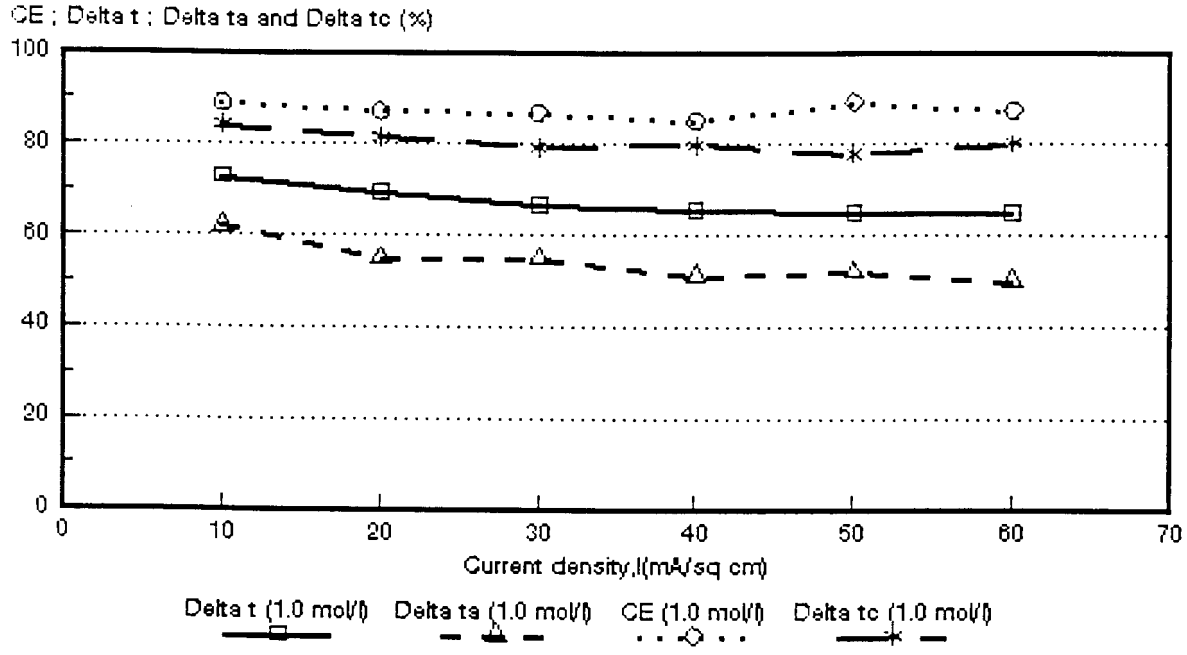

Figure 6.53: **Current efficiency (CE = ϵ_p) and apparent transport numbers as a function of current density for 1,0 mol/ℓ NaCl feed. *Selemion* AMV and CMV membranes. Delta t = $\bar{\Delta}t$; Delta ta = Δt^a; Delta tc = Δt^c.**

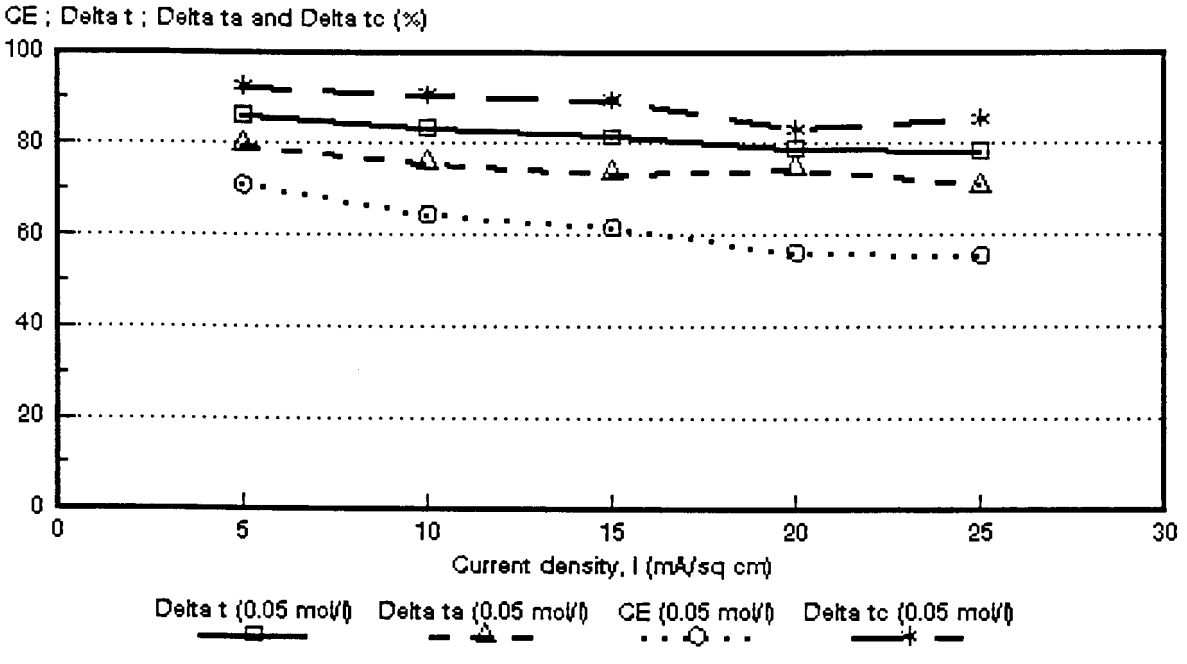

Figure 6.54: **Current efficiency (CE = ϵ_p) and apparent transport numbers as a function of current density for 0,05 mol/ℓ NaCl feed. *Ionac* MA-3475 and MC-3470 membranes. Delta t = $\bar{\Delta}t$; Delta ta = Δt^a; Delta tc = Δt^c.**

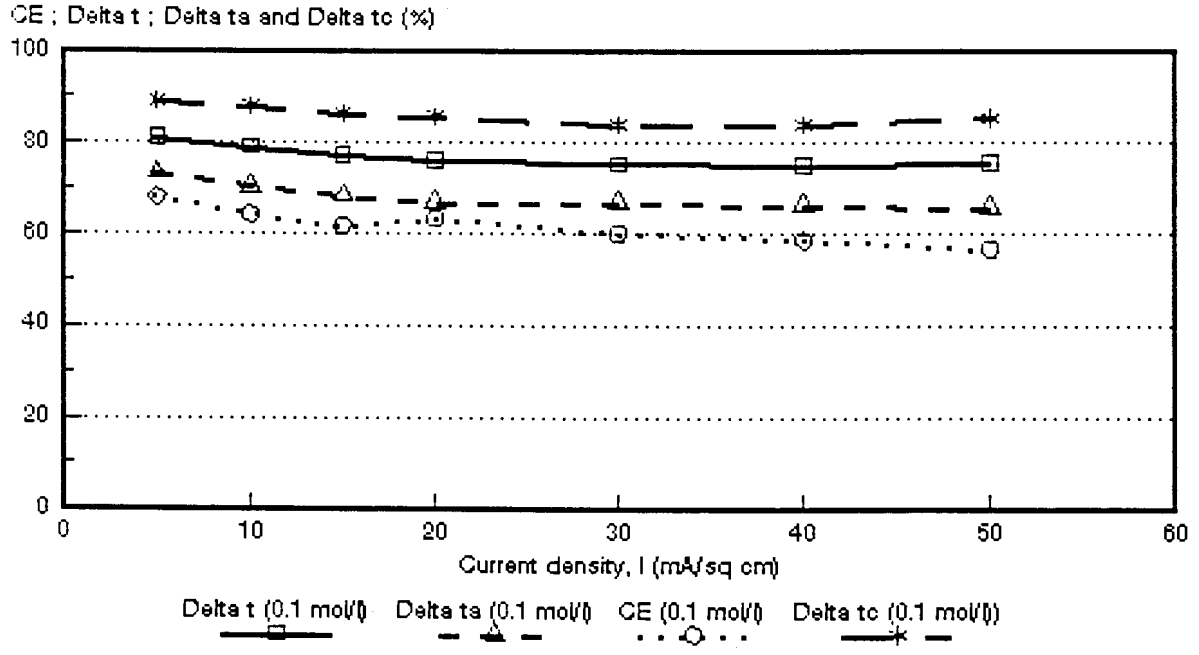

Figure 6.55: **Current efficiency (CE = ϵ_p) and apparent transport numbers as a function of current density for 0,1 mol/ℓ NaCl feed. *Ionac* MA-3475 and MC-3470 membranes. Delta t = $\bar{\Delta}t$; Delta ta = Δt^a; Delta tc = Δt^c.**

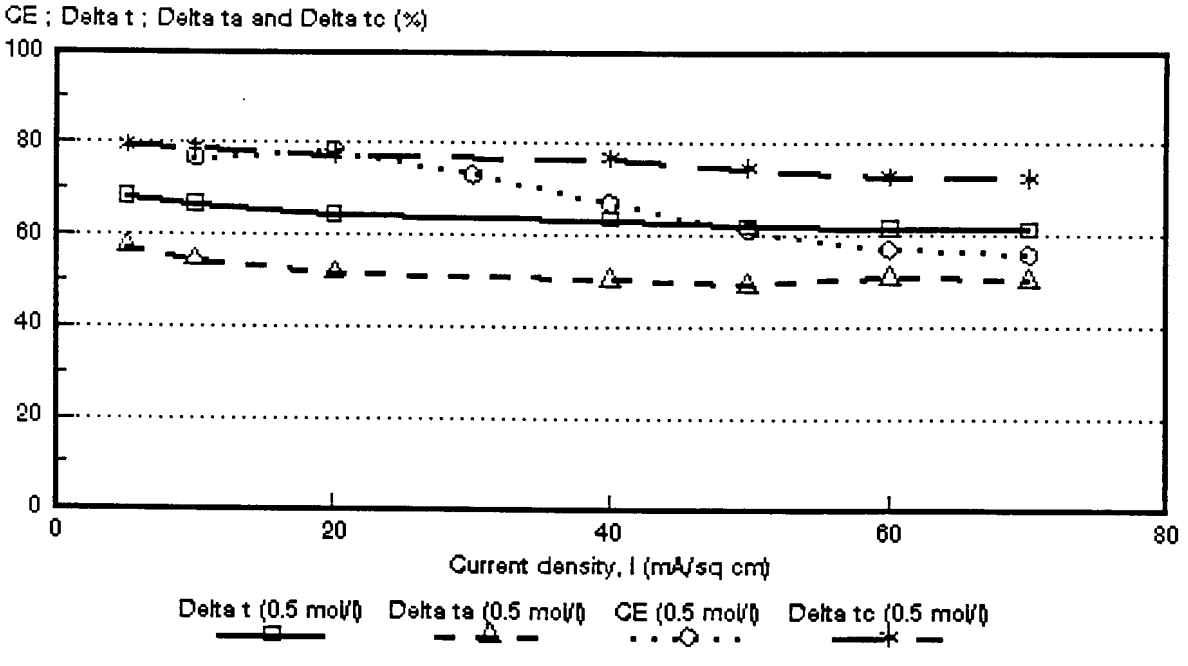

Figure 6.56: **Current efficiency (CE = ϵ_p) and apparent transport numbers as a function of current density for 0,5 mol/ℓ NaCl feed. *Ionac* MA-3475 and MC-3470 membranes. Delta t = $\bar{\Delta}t$; Delta ta = Δt^a; Delta tc = Δt^c.**

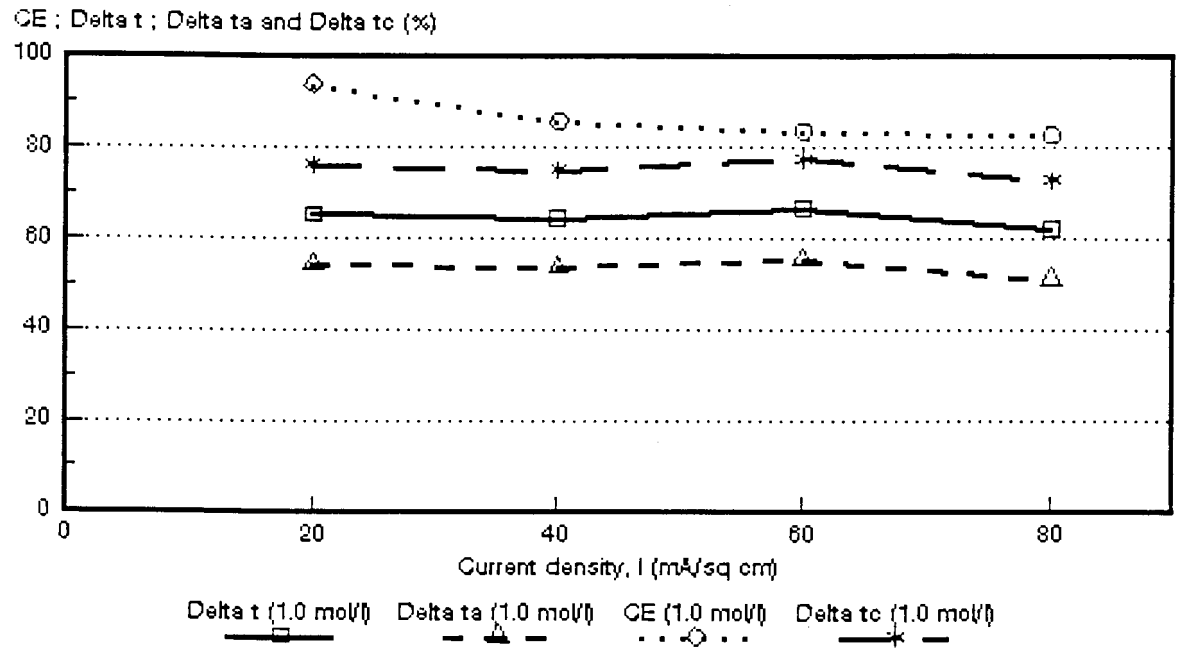

Figure 6.57: **Current efficiency (CE = ϵ_p) and apparent transport numbers as a function of current density for 1,0 mol/ℓ NaCl feed. *Ionac* MA-3475 and MC-3470 membranes. Delta t = $\bar{\Delta}t$; Delta ta = Δt^a; Delta tc = Δt^c.**

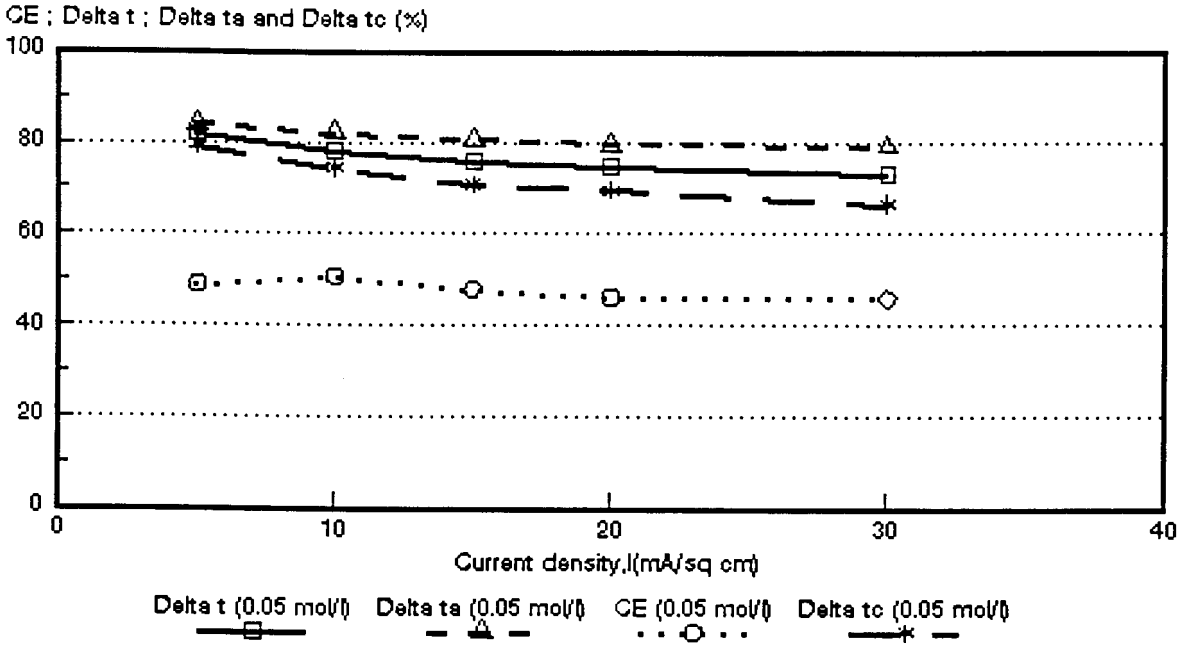

Figure 6.58: **Current efficiency (CE = ϵ_p) and apparent transport numbers as a function of current density for 0,05 mol/ℓ NaCl feed. *Raipore* R4030 and R4010 membranes. Delta t = $\bar{\Delta}t$; Delta ta = Δt^a; Delta tc = Δt^c.**

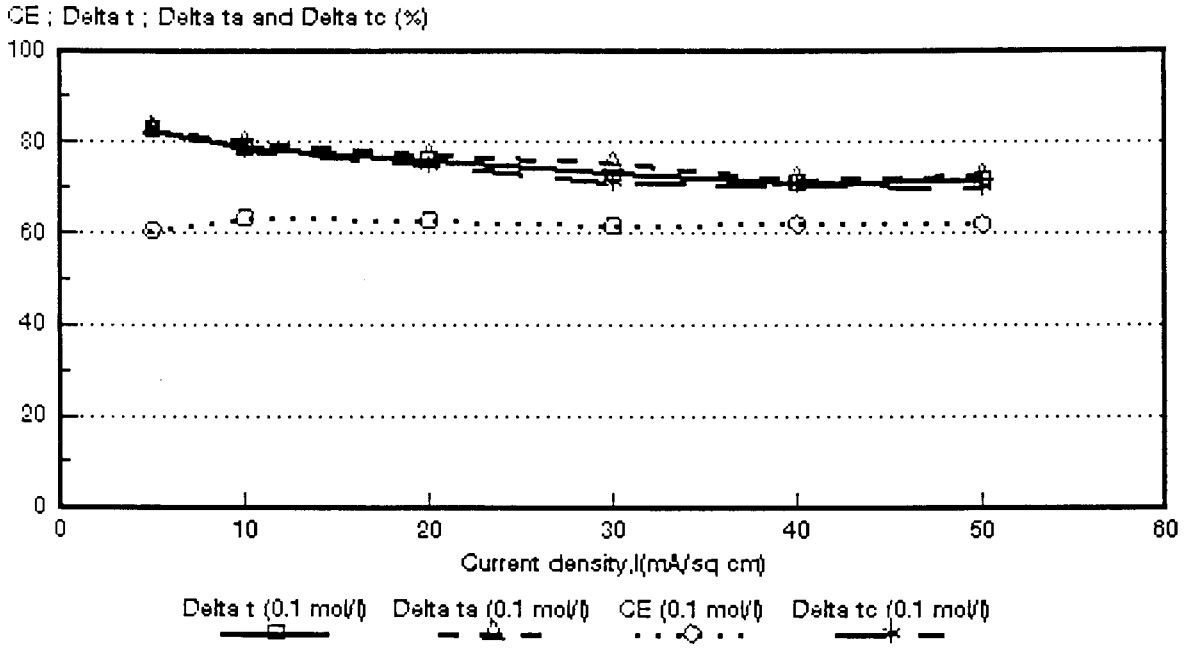

Figure 6.59: **Current efficiency (CE = e_p) and apparent transport numbers as a function of current density for 0,1 mol/ℓ NaCl feed. *Raipore* R4030 and R4010 membranes. Delta t = $\bar{\Delta}t$; Delta ta = Δt^a; Delta tc = Δt^c.**

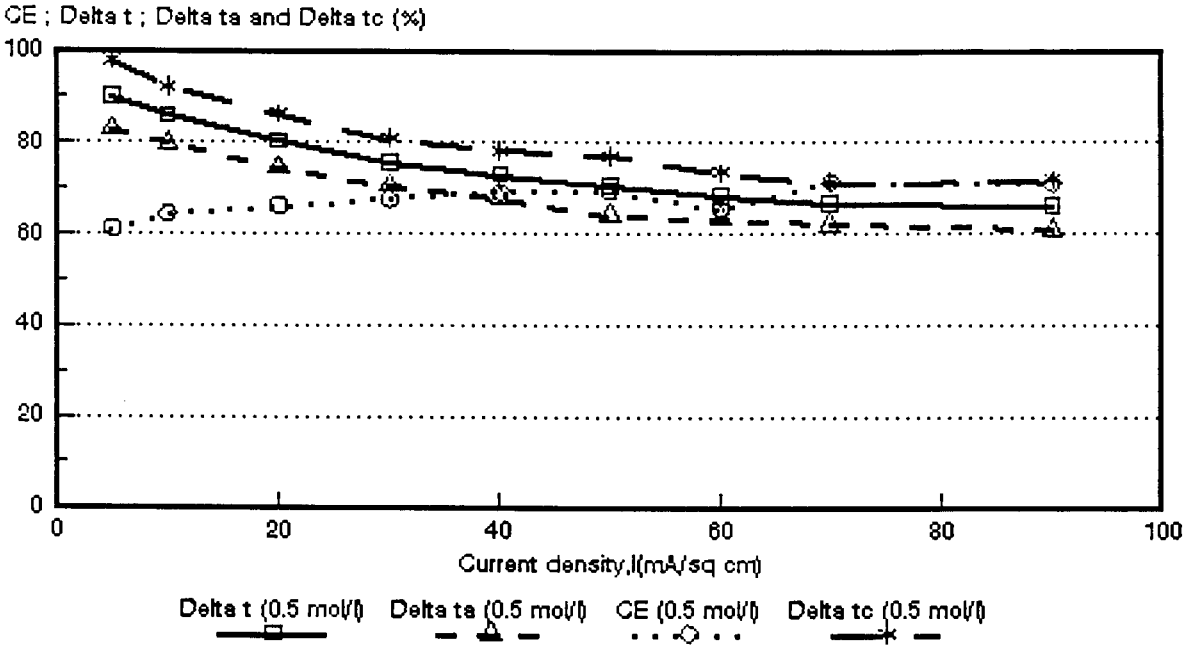

Figure 6.60: **Current efficiency (CE = e_p) and apparent transport numbers as a function of current density for 0,5 mol/ℓ NaCl feed. *Raipore* R4030 and R4010 membranes. Delta t = $\bar{\Delta}t$; Delta ta = Δt^a; Delta tc = Δt^c.**

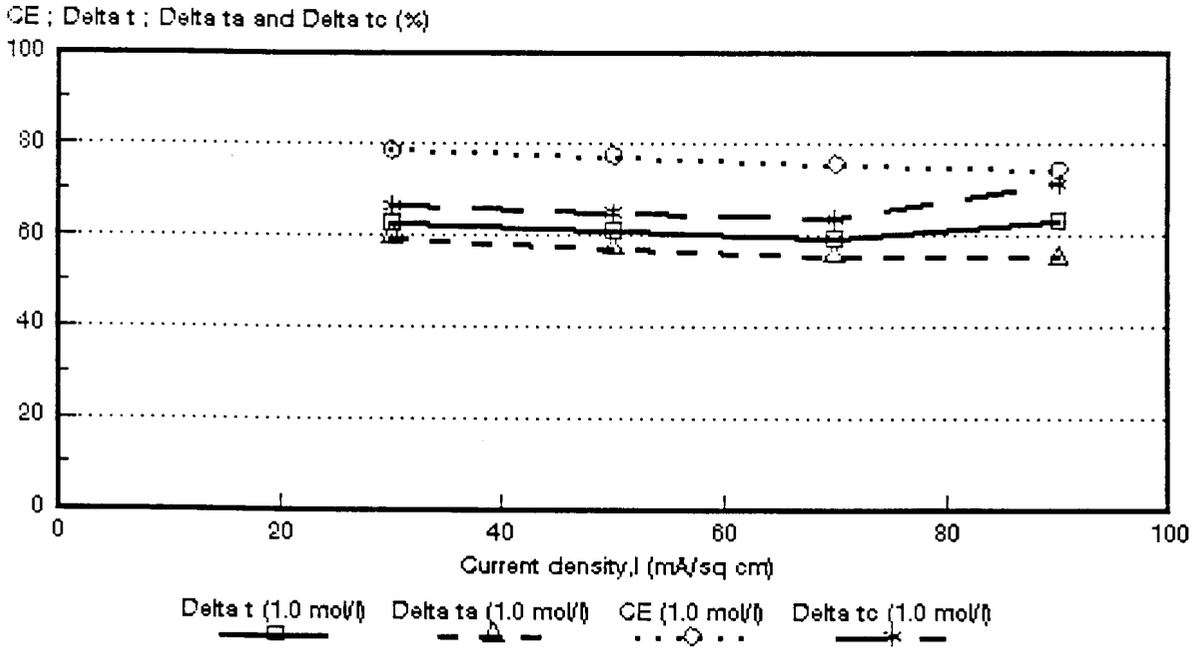

Figure 6.61: **Current efficiency (CE = ϵ_p) and apparent transport numbers as a function of current density for 1,0 mol/ℓ NaCl feed. *Raipore* R4030 and R4010 membranes. Delta t = $\bar{\Delta}t$; Delta ta = Δt^a; Delta tc = Δt^c.**

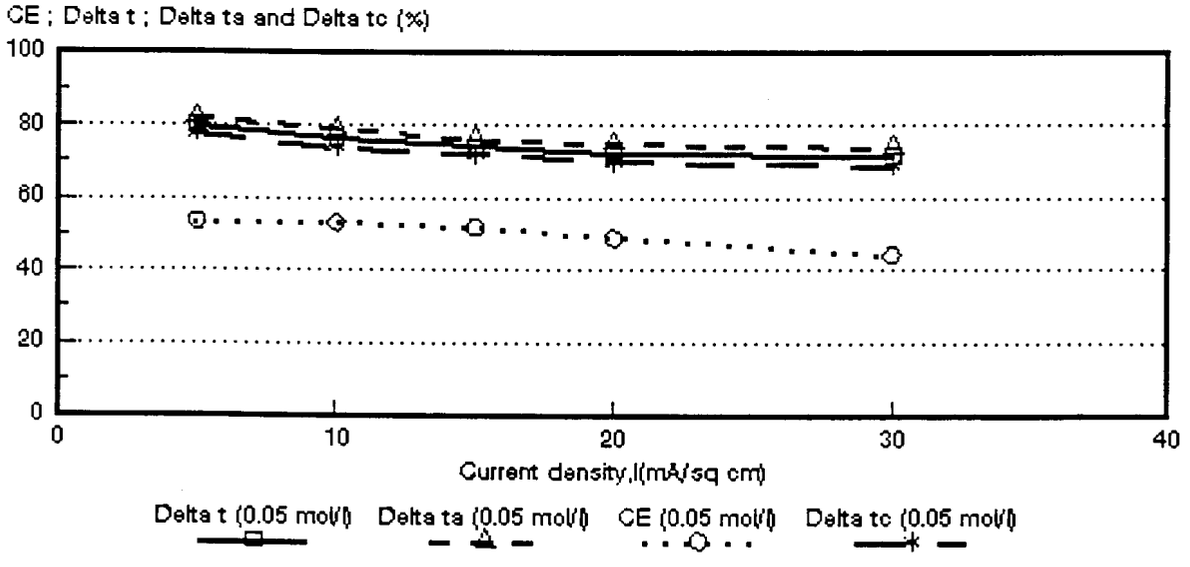

Figure 6.62: **Current efficiency (CE = ϵ_p) and apparent transport numbers as a function of current density for 0,05 mol/ℓ NaCl feed. *Ionics* A-204-UZL-386 and C-61-CZL-386 membranes. Delta t = $\bar{\Delta}t$; Delta ta = Δt^a; Delta tc = Δt^c.**

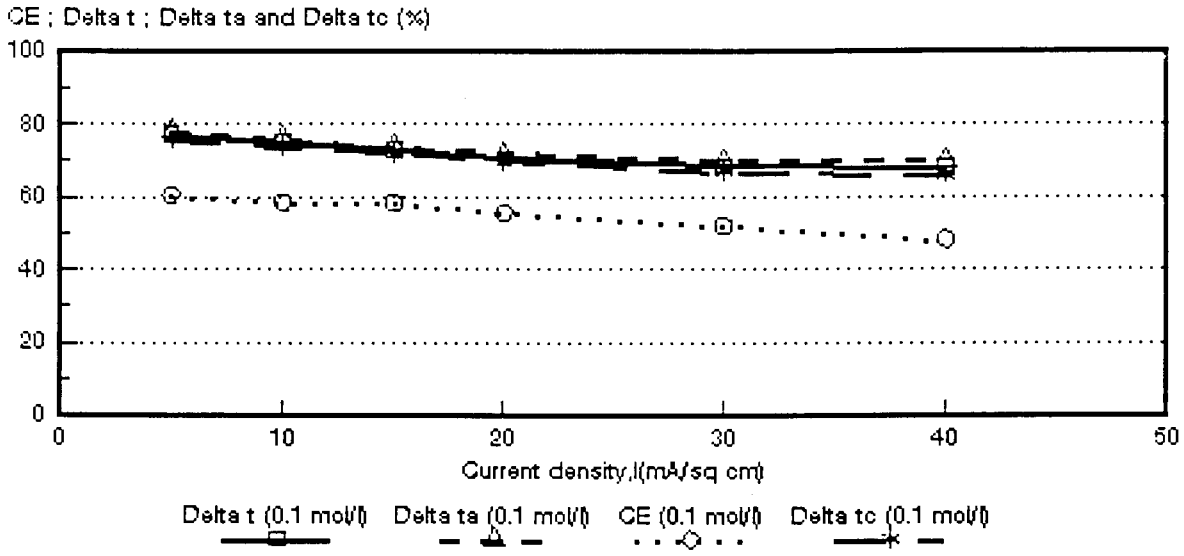

Figure 6.63: **Current efficiency (CE = e_p) and apparent transport numbers as a function of current density for 0,1 mol/ℓ NaCl feed. *Ionics* A-204-UZL-386 and C-61-CZL-386 membranes. Delta t = $\bar{\Delta}$t; Delta ta = Δt^a; Delta tc = Δt^c.**

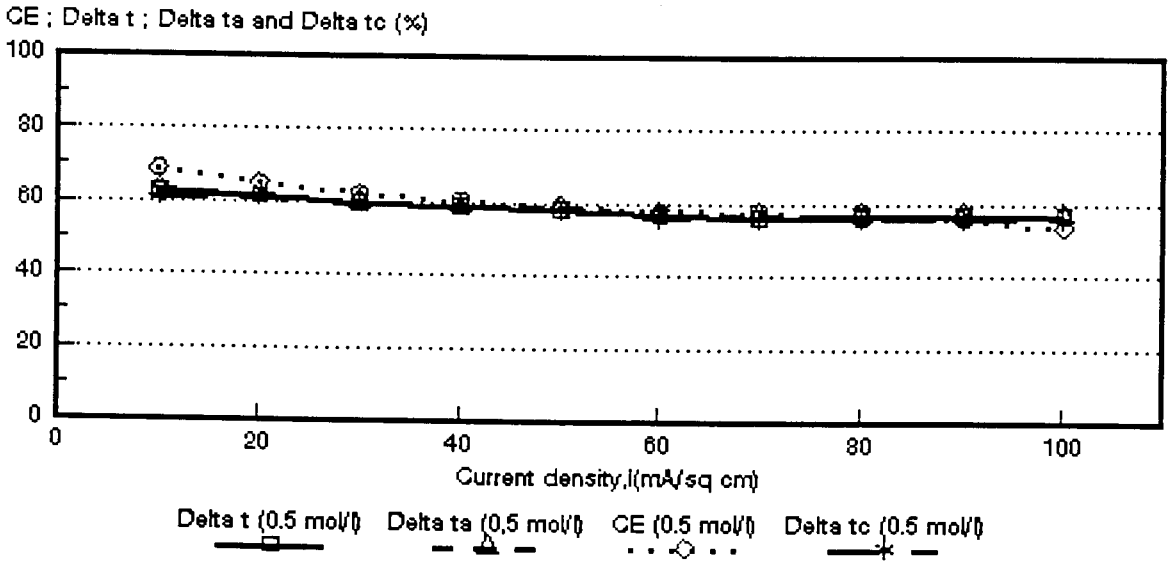

Figure 6.64: **Current efficiency (CE = e_p) and apparent transport numbers as a function of current density for 0,5 mol/ℓ NaCl feed. *Ionics* A-204-UZL-386 and C-61-CZL-386 membranes. Delta t = $\bar{\Delta}$t; Delta ta = Δt^a; Delta tc = Δt^c.**

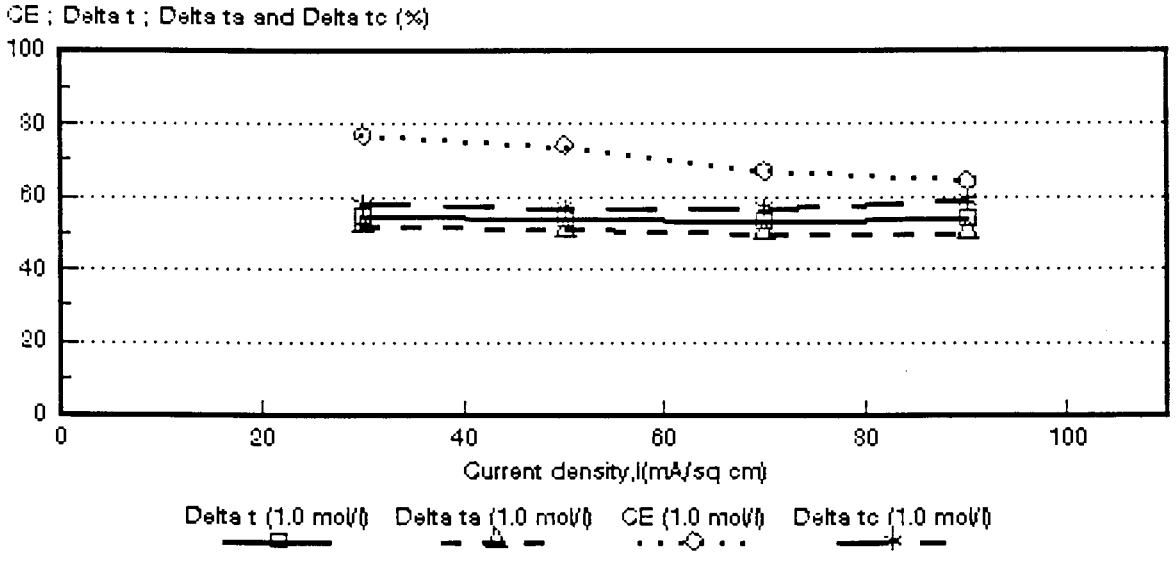

Figure 6.65: Current efficiency (CE = ϵ_p) and apparent transport numbers as a function of current density for 1,0 mol/ℓ NaCl feed. *Ionics* A-204-UZL-386 and C-61-CZL-386 membranes. Delta t = $\bar{\Delta}t$; Delta ta = Δt^a; Delta tc = Δt^c.

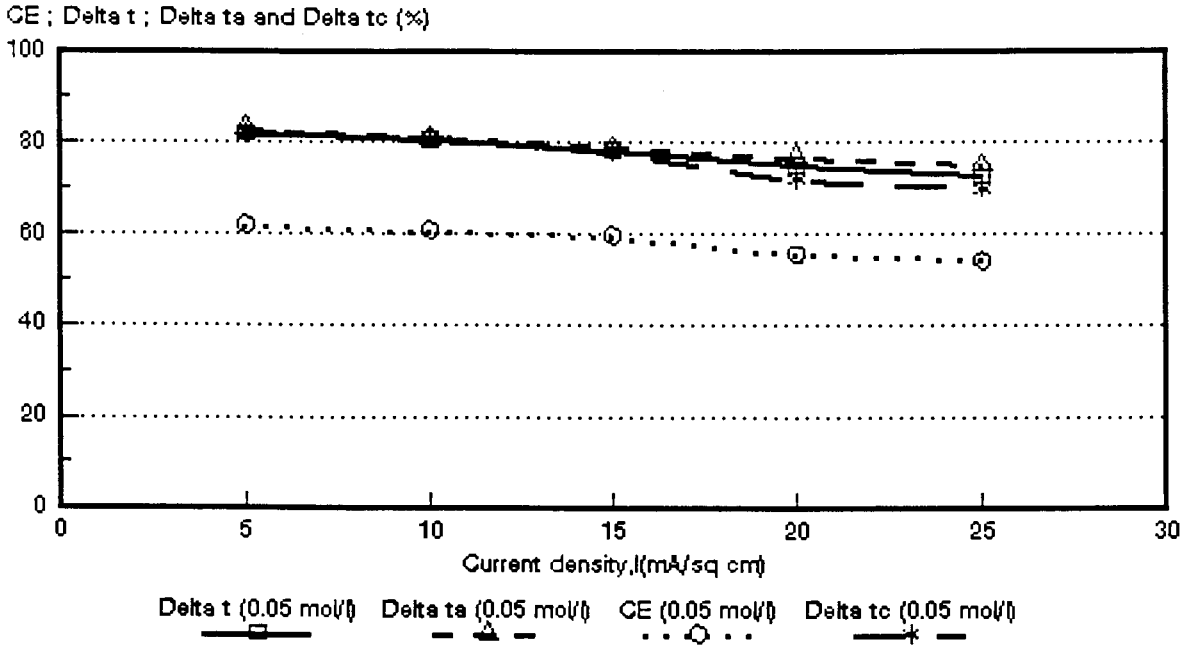

Figure 6.66: Current efficiency (CE = ϵ_p) and apparent transport numbers as a function of current density for 0,05 mol/ℓ NaCl feed. WTPSA-1 and WTPSC-1 membranes. Delta t = $\bar{\Delta}t$; Delta ta = Δt^a; Delta tc = Δt^c.

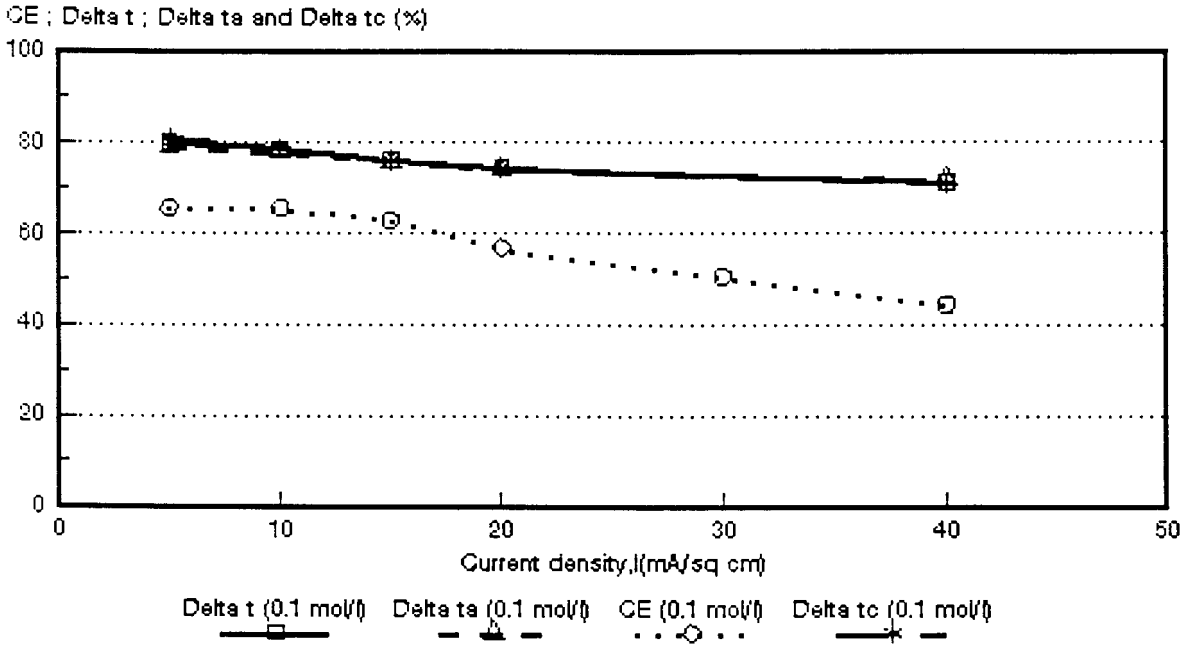

Figure 6.67: **Current efficiency (CE = ϵ_p) and apparent transport numbers as a function of current density for 0,1 mol/ℓ NaCl feed. WTPSA-1 and WTPSC-1 membranes. Delta t = $\bar{\Delta}t$; Delta ta = Δt^a; Delta tc = Δt^c.**

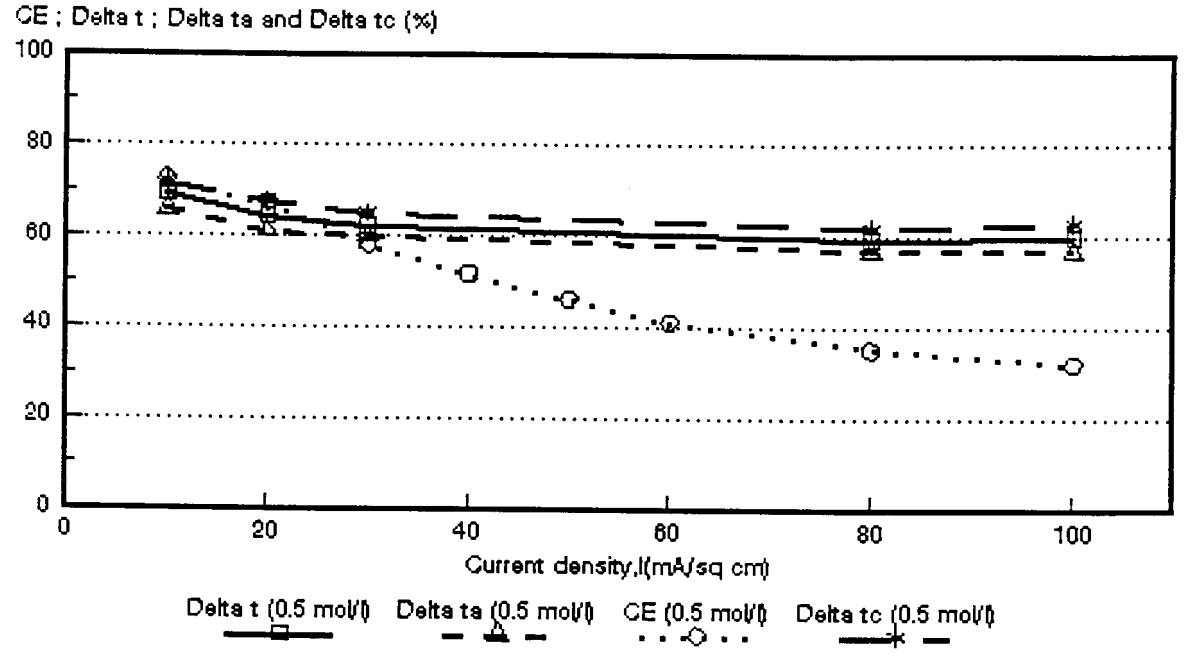

Figure 6.68: **Current efficiency (CE = ϵ_p) and apparent transport numbers as a function of current density for 0,5 mol/ℓ NaCl feed. WTPSA-1 and WTPSC-1 membranes. Delta t = $\bar{\Delta}t$; Delta ta = Δt^a; Delta tc = Δt^c.**

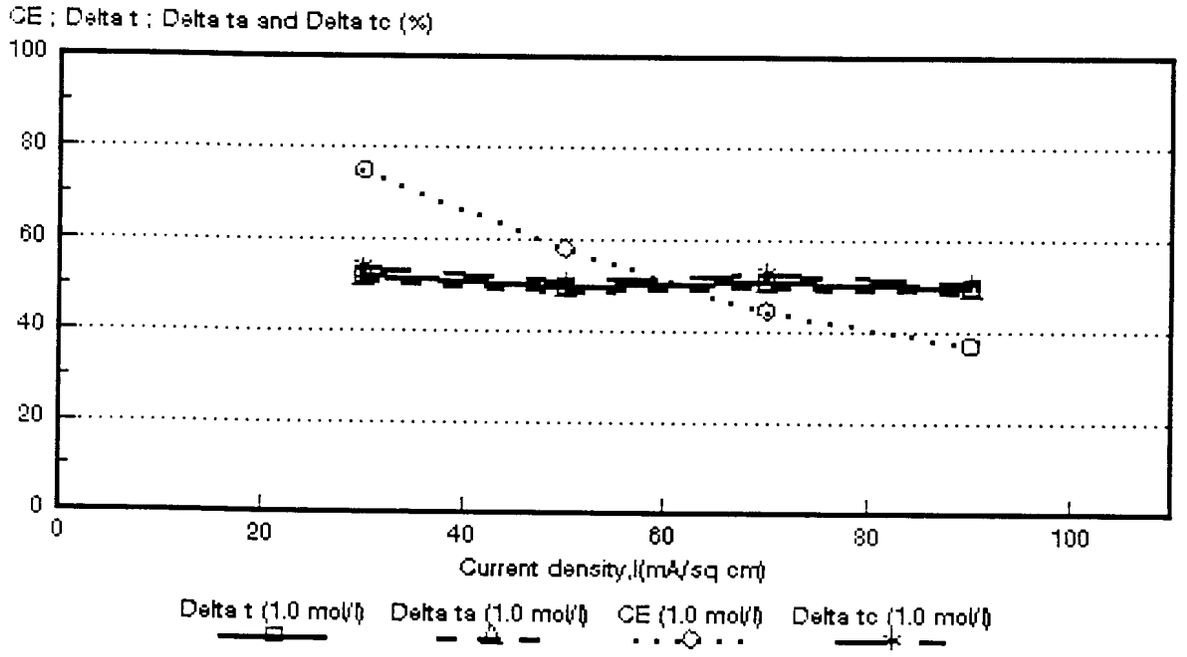

Figure 6.69: **Current efficiency (CE = ϵ_p) and apparent transport numbers as a function of current density for 1,0 mol/ℓ NaCl feed. WTPSA-1 and WTPSC-1 membranes. Delta t = $\bar{\Delta}t$; Delta ta = Δt^a; Delta tc = Δt^c.**

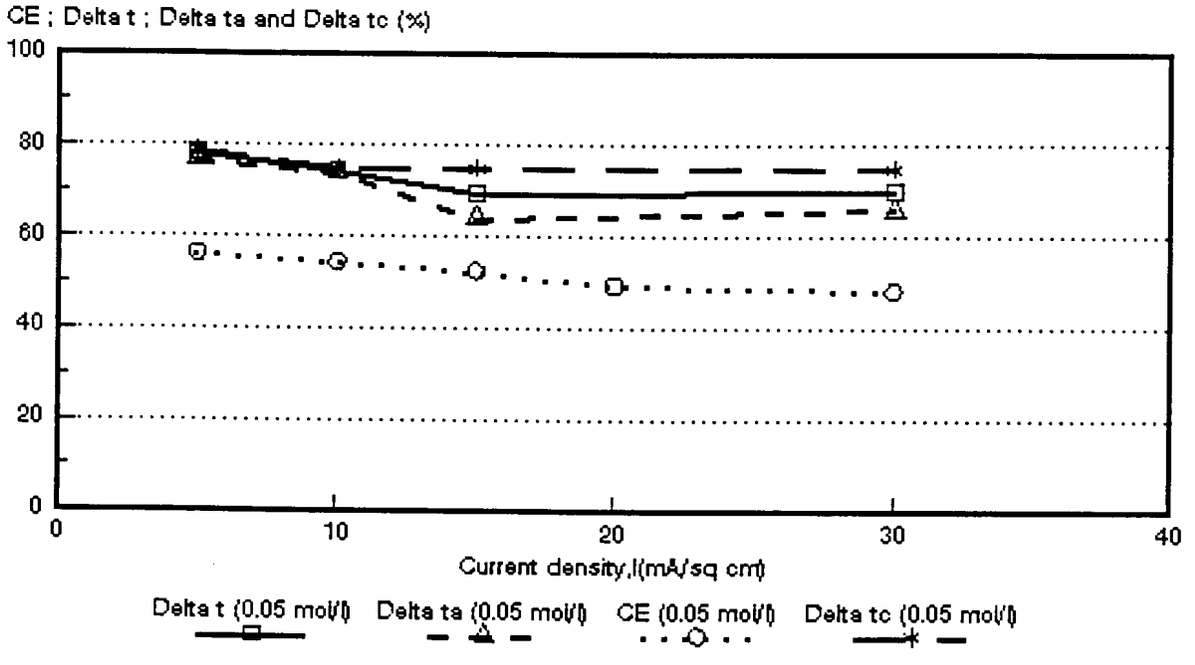

Figure 6.70: **Current efficiency (CE = ϵ_p) and apparent transport numbers as a function of current density for 0,05 mol/ℓ NaCl feed. WTPVCA-2 and WTPVCC-2 membranes. Delta t = $\bar{\Delta}t$; Delta ta = Δt^a; Delta tc = Δt^c.**

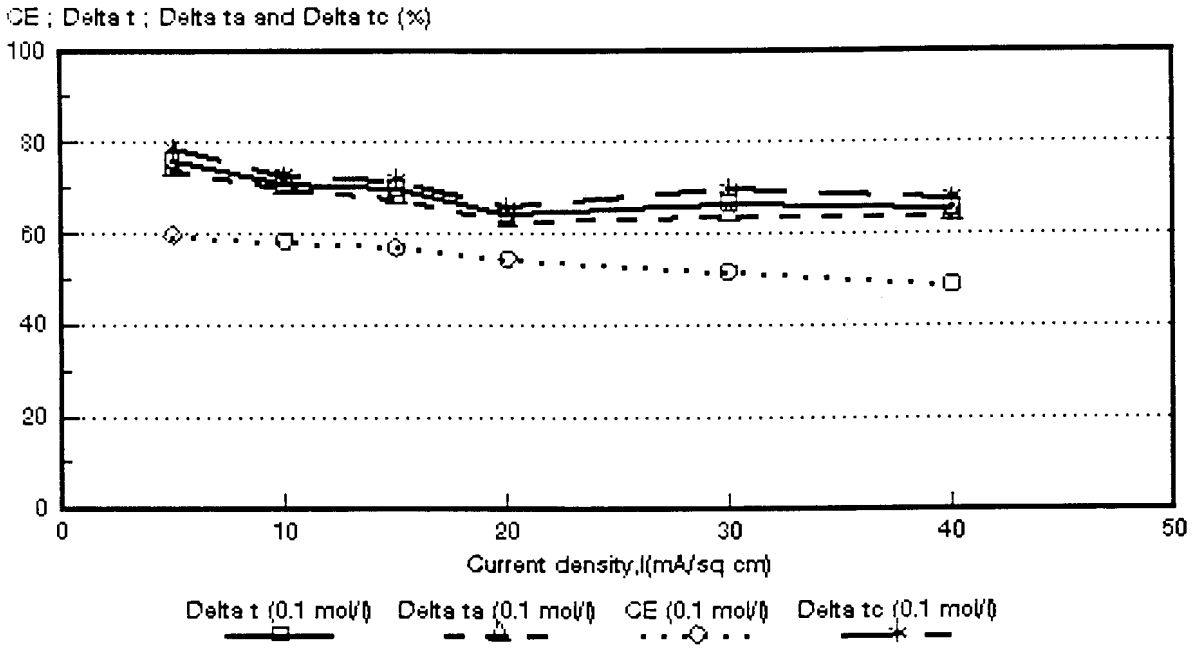

Figure 6.71: Current efficiency (CE = ϵ_p) and apparent transport numbers as a function of current density for 0,1 mol/ℓ NaCl feed. WTPVCA-2 and WTPVCC-2 membranes. Delta t = $\bar{\Delta}t$; Delta ta = Δt^a; Delta tc = Δt^c.

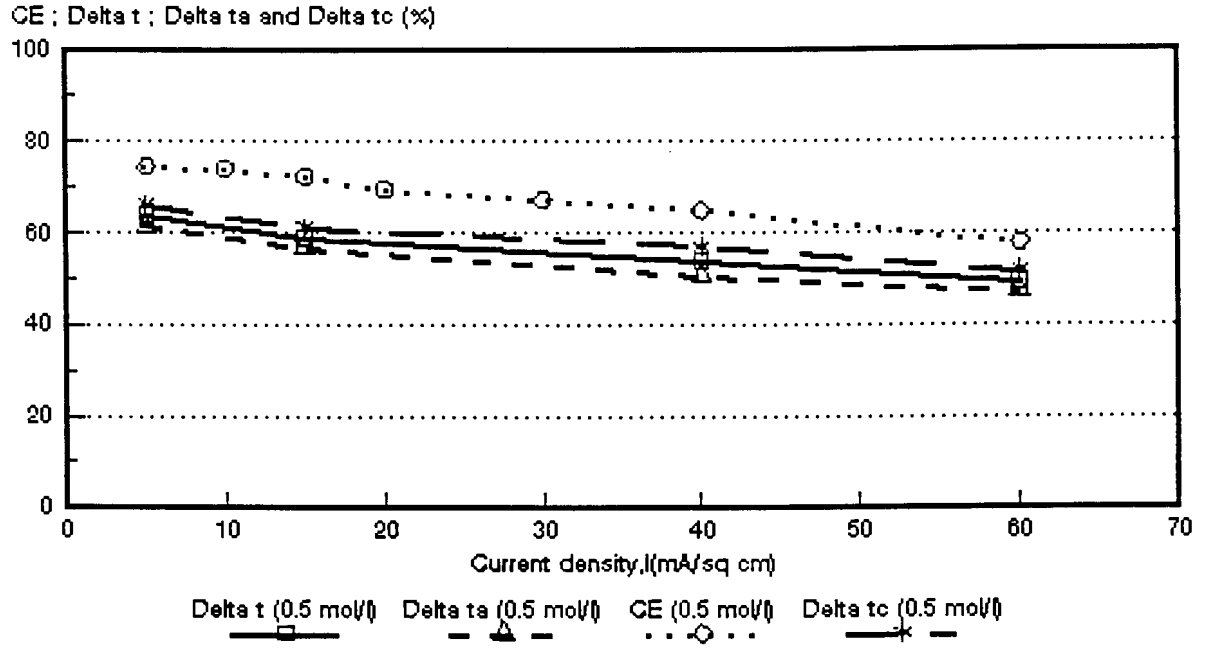

Figure 6.72: Current efficiency (CE = ϵ_p) and apparent transport numbers as a function of current density for 0,5 mol/ℓ NaCl feed. WTPVCA-2 and WTPVCC-2 membranes. Delta t = $\bar{\Delta}t$; Delta ta = Δt^a; Delta tc = Δt^c.

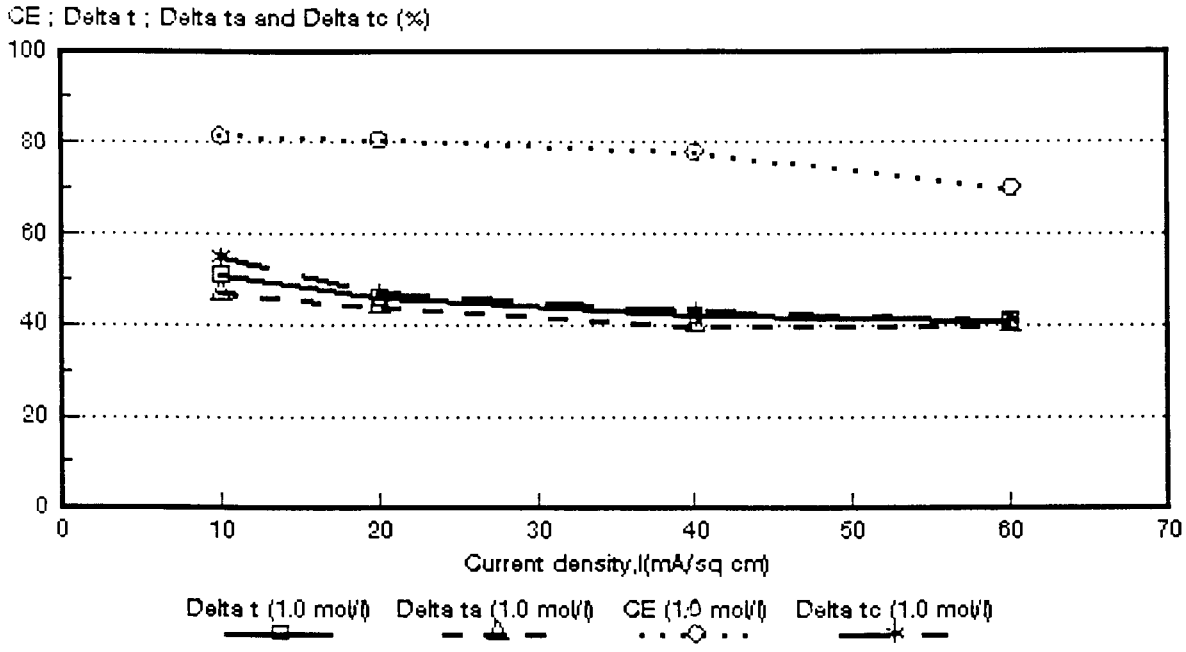

Figure 6.73: Current efficiency (CE = ϵ_p) and apparent transport numbers as a function of current density for 1,0 mol/ℓ NaCl feed. WTPVCA-2 and WTPVCC-2 membranes. Delta t = $\bar{\Delta}t$; Delta ta = Δt^a; Delta tc = Δt^c.

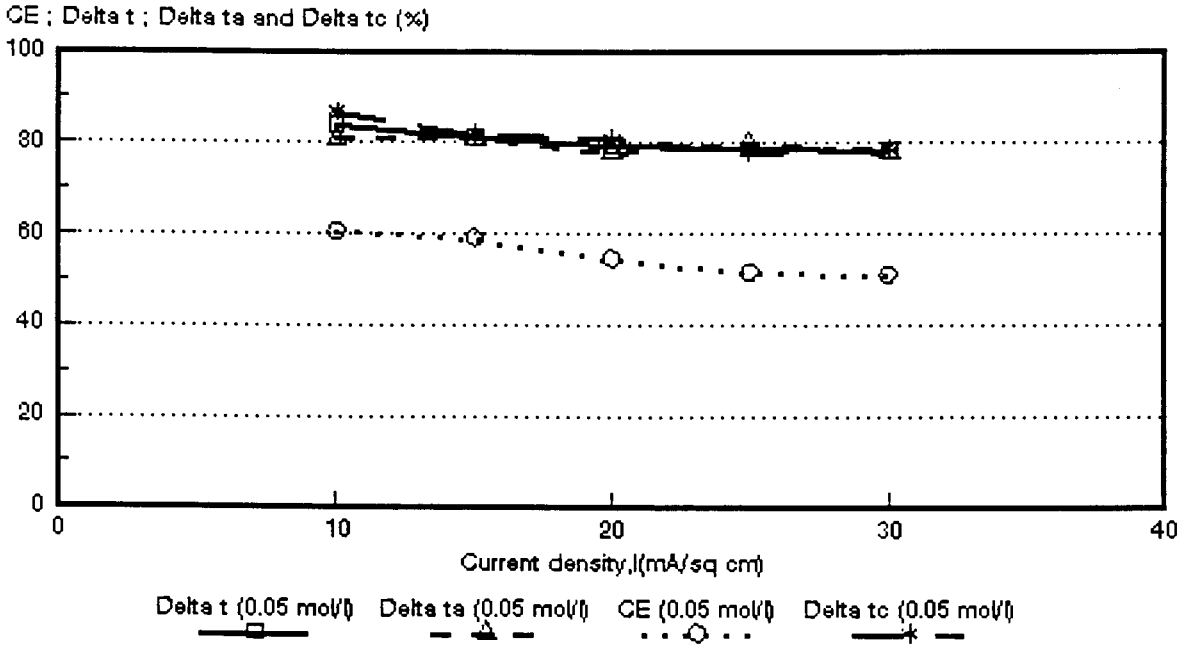

Figure 6.74: Current efficiency (CE = ϵ_p) and apparent transport numbers as a function of current density for 0,05 mol/ℓ NaCl feed. WTPSTA-3 and WTPSTC-3 membranes. Delta t = $\bar{\Delta}t$; Delta ta = Δt^a; Delta tc = Δt^c.

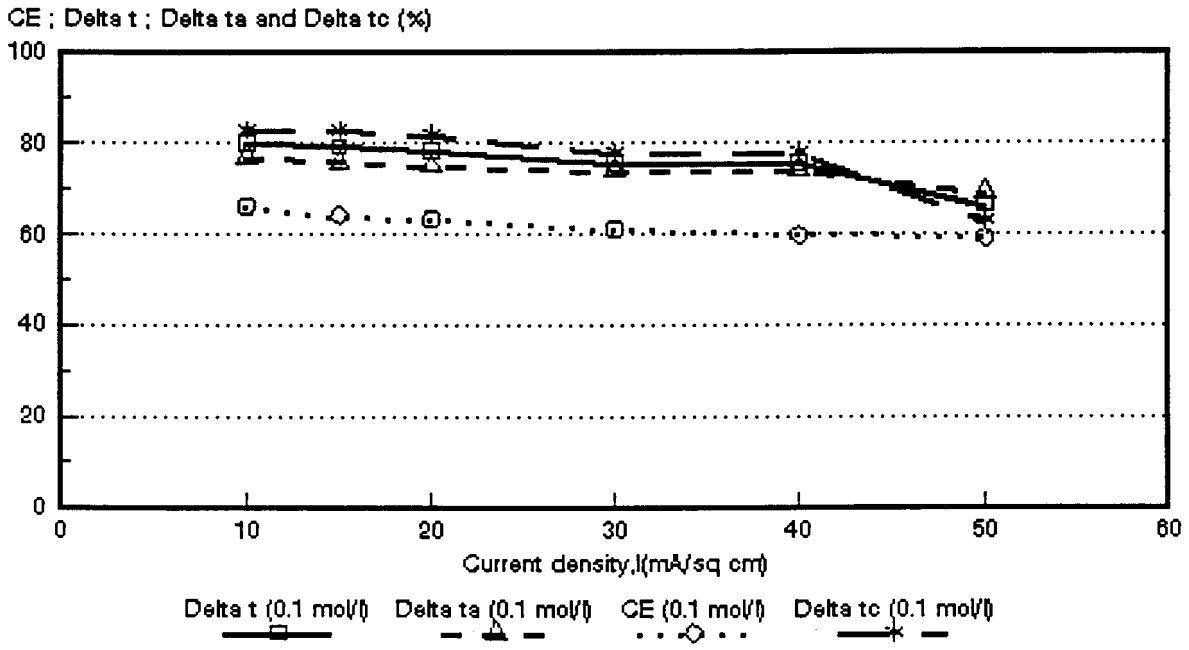

Figure 6.75: Current efficiency (CE = ϵ_p) and apparent transport numbers as a function of current density for 0,1 mol/ℓ NaCl feed. WTPSTA-3 and WTPSTC-3 membranes. Delta t = $\bar{\Delta}t$; Delta ta = Δt^a; Delta tc = Δt^c.

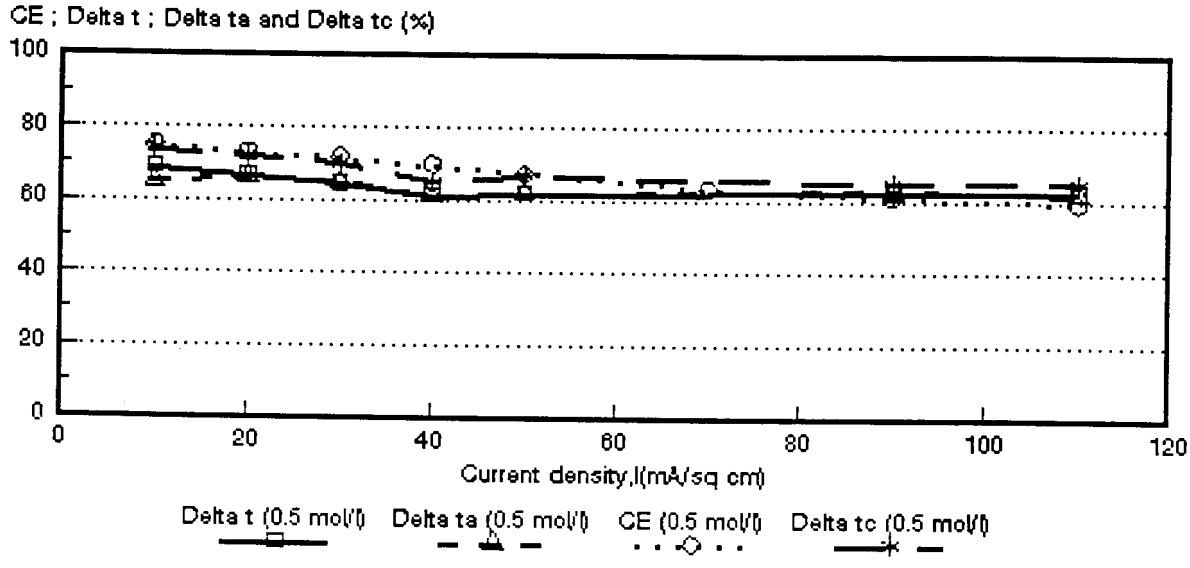

Figure 6.76: Current efficiency (CE = ϵ_p) and apparent transport numbers as a function of current density for 0,5 mol/ℓ NaCl feed. WTPSTA-3 and WTPSTC-3 membranes. Delta t = $\bar{\Delta}t$; Delta ta = Δt^a; Delta tc = Δt^c.

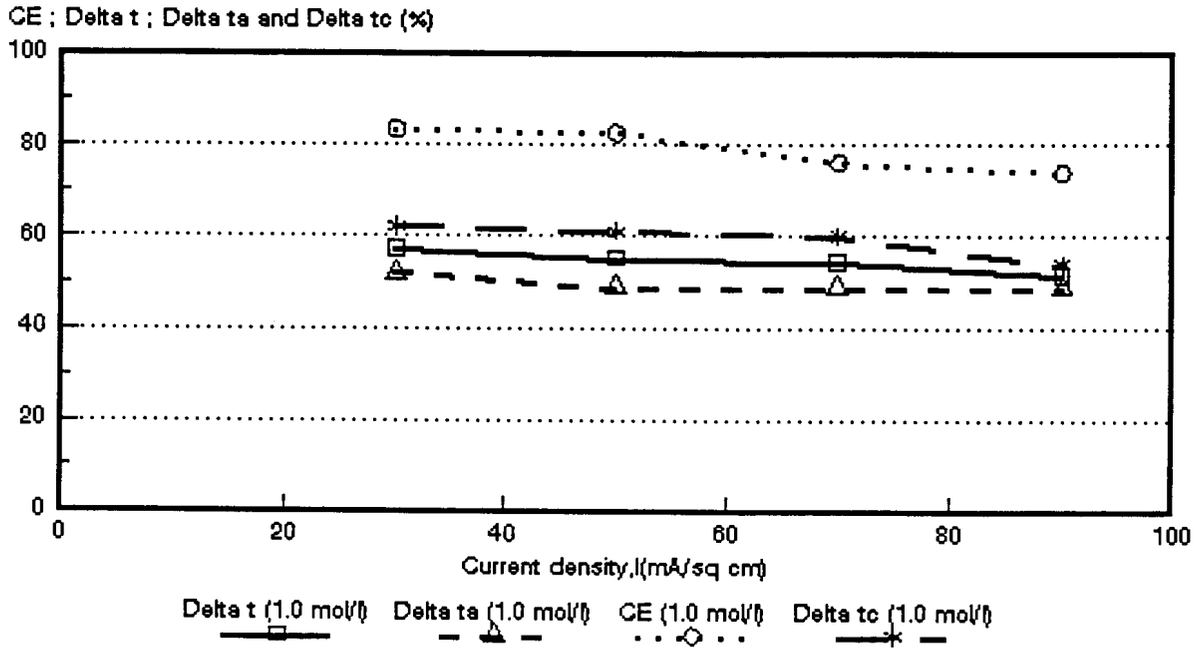

Figure 6.77: Current efficiency (CE = ϵ_p) and apparent transport numbers as a function of current density for 1,0 mol/ℓ NaCl feed. WTPSTA-3 and WTPSTC-3 membranes. Delta t = $\bar{\Delta}t$; Delta ta = Δt^a; Delta tc = Δt^c.

current efficiencies at the higher feed water concentrations (0,5 to 1,0 mol/ℓ). The only exception in this regard was obtained with the *Raipore* membranes where the apparent transport numbers became lower than the current efficiency at 1,0 mol/ℓ feed concentration.

Good correlations were obtained between the apparent transport number of a membrane pair ($\bar{\Delta}t$) and current efficiency (ϵ_p) for all the membranes investigated depending on the feed concentration and current density used (Table 6.32). The ratio between $\bar{\Delta}t/\epsilon_p$ for the *Selemion* membranes varied between 1,01 and 1,07 in the current density range from 15 to 50 mA/cm^2 (0,1 mol/ℓ feed). This ratio for the *Ionac* membranes varied between 0,95 to 1,09 in the current density range from 40 to 70 mA/cm^2 (0,5 mol/ℓ feed). For the *Raipore* membranes the ratio ($\bar{\Delta}t/\epsilon_p$) varied between 0,94 and 1,05 in the current density range from 40 to 90 mA/cm^2 (0,5 mol/ℓ feed). For the *Ionics* membranes the ratio varied between 0,95 and 1,02 in the current density range from 20 to 90 mA/cm^2 (0,5 mol/ℓ feed). A good correlation was obtained

between $\bar{\Delta}t$ and ϵ_p (0,95 to 1,07 at 0,5 mol/ℓ feed) for the WTPS membranes in the current density range from 10 to 30 mA/cm^2. The correlations, however, at high current densities (Table 6.32, 80 mA/cm^2) were not very good due to polarization that was taking place. Relatively good correlations were also obtained between $\bar{\Delta}t$ and ϵ_p for the WTPVC and WTPST membranes. The correlation varied between 0,82 to 0,86 (5 to 60 mA/cm^2, WTPVC) and between 0,88 and 1,04 (10 to 110 mA/cm^2, WTPST) at 0,5 mol/ℓ feed concentration. The ratio between $\bar{\Delta}t/\epsilon_p$ varied between approximately 0,82 and 1,09 in the feed concentration range from 0,1 to 0,5 mol/ℓ for the different membranes investigated. Therefore, it appears that apparent transport numbers determined from a simple membrane potential method should give a good approximate estimation of membrane performance for ED concentration/desalination applications. Membrane performance for concentration/desalination applications should be predicted with an accuracy of approximately 10% from membrane potential measurements depending on the feed concentration and current density used.

The apparent transport numbers of the anion- (Δt^a) and cation (Δt^c) membranes should also be used to predict membrane performance for concentration/desalination applications (Tables 6.33 and 6.34). However, the accuracy of the prediction will depend on the feed concentration and current density used.

Table 6.32: Correlation between apparent transport number for a membrane pair ($\bar{\Delta}t$) and current efficiency (e_p).

Current Density	$\bar{\Delta}t/e_p$																											
	Selemion AMV & CMV Concentration, mol/ℓ				Ionac MA-3475 & MC-3470 Concentration, mol/ℓ				Raipore R4030 & R4010 Concentration, mol/ℓ				Ionics A-204-UZL & C-61-CZL Concentration, mol/ℓ				WTPS WTPSA & WTPSC Concentration, mol/ℓ				WTPVC WTPVCA & WTPVCC Concentration, mol/ℓ				WTPST WTPSTA & WTPSTC Concentration, mol/ℓ			
mA/cm²	0,05	0,1	0,5	1,0	0,05	0,1	0,5	1,0	0,05	0,1	0,5	1,0	0,05	0,1	0,5	1,0	0,05	0,1	0,5	1,0	0,05	0,1	0,5	1,0	0,05	0,1	0,5	1,0
5	1,39	1,19	0,99		1,21	1,19	0,72		1,68	1,37	1,47		1,49	1,27			1,32	1,22			1,41	1,27	0,86					
10	1,28	1,13	0,85	0,82	1,29	1,23	0,87		1,54	1,25	1,34		1,43	1,28	0,90		1,33	1,21	0,95		1,36	1,21		0,62	1,39	1,21	0,92	
15	1,27	1,07			1,33	1,25			1,58				1,43	1,25			1,32	1,21			1,34	1,23	0,82		1,37	1,23		
20	1,25	1,06	0,79	0,78	1,41	1,20	0,83	0,69	1,62	1,21	1,21		1,49	1,28	0,95		1,35	1,30	0,95		1,19	1,19		0,57	1,46	1,23	0,90	
25					1,41												1,35								1,52			
30	1,23	1,05	0,82	0,77		1,25			1,59	1,19	1,12	0,80	1,61	1,32	0,96	0,72			1,07	0,69	1,45	1,30			1,55	1,24	0,90	0,68
40		1,04	0,78	0,77		1,28	0,95	0,75		1,15	1,05			1,41	0,99			1,60				1,35	0,83	0,54		1,27	0,88	
50		1,01	0,78	0,73		1,34	1,01			1,16	1,02	0,79			0,98	0,73				0,86						1,11	0,92	0,87
60			0,78	0,74			1,09	0,80			1,05				0,98								0,85	0,58				
70							1,09				0,94	0,79			0,97	0,79				1,14							0,84	0,72
80								0,75							1,01				1,70									
90											1,03	0,84			1,02	0,84				1,35							1,03	0,70
100															1,06				1,87									
110																											1,04	

Table 6.33: Correlation between apparent transport number of the anion membrane (Δt^a) and current efficiency (e_p).

Current Density	$\Delta t^a/e_p$																											
	Selemion AMV & CMV Concentration, mol/ℓ				Ionac MA-3475 & MC-3470 Concentration, mol/ℓ				Raipore R4030 & R4010 Concentration, mol/ℓ				Ionics A-204-UZL & C-61-CZL Concentration, mol/ℓ				WTPS WTPSA & WTPSC Concentration, mol/ℓ				WTPVC WTPVCA & WTPVCC Concentration, mol/ℓ				WTPST WTPSTA & WTPSTC Concentration, mol/ℓ			
mA/cm²	0,05	0,1	0,5	1,0	0,05	0,1	0,5	1,0	0,05	0,1	0,5	1,0	0,05	0,1	0,5	1,0	0,05	0,1	0,5	1,0	0,05	0,1	0,5	1,0	0,05	0,1	0,5	1,0
5	1,31	1,11	0,86		1,13	1,07	0,59		1,72	1,37	1,36		1,53	1,29			1,34	1,20			1,37	1,24	0,82					
10	1,24	1,04	0,75	0,70	1,18	1,09	0,70		1,62	1,27	1,24		1,49	1,30	0,92		1,33	1,19	0,91		1,36	1,20		0,58	1,34	1,16	0,87	
15	1,20	0,98			1,19	1,10			1,69				1,47	1,27			1,33	1,21			1,22	1,20	0,78		1,37	1,18		
20	1,16	0,96	0,69	0,63	1,32	1,06	0,66	0,58	1,73	1,23	1,13		1,53	1,29	0,95		1,38	1,30	0,90		0,99	1,18		0,55	1,43	1,19	0,83	
25					1,28												1,38								1,55			
30	1,14	0,97	0,68	0,61		1,11			1,72	1,22	1,05	0,75	1,67	1,34	0,96	0,68			1,03	0,68	1,37	1,24			1,53	1,21	0,82	0,62
40		0,91	0,66	0,60		1,13	0,75	0,63		1,16	0,98			1,46	0,97			1,62				1,31	0,77	0,51		1,24	0,83	
50		0,94	0,64	0,58		1,16	0,80			1,18	0,92	0,73			0,99	0,69				0,84						1,17	0,85	0,59
60			0,62	0,57			0,90	0,66			0,98				0,98								0,81	0,57				
70							0,89				0,87	0,74			0,99	0,74				1,12							0,84	0,64
80								0,62							1,01				1,62									
90											0,86	0,74			1,02	0,78				1,32							0,96	0,66
100															1,06				1,78									
110																											1,01	

Table 6.34: Correlation between apparent transport number of the cation membrane (Δt^c) and current efficiency (e_p).

Current Density	$\Delta t^c/e_p$																											
	Selemion AMV & CMV Concentration, mol/ℓ				Ionac MA-3475 & MC-3470 Concentration, mol/ℓ				Raipore R4030 & R4010 Concentration, mol/ℓ				Ionics A-204-UZL & C-61-CZL Concentration, mol/ℓ				WTPS WTPSA & WTPSC Concentration, mol/ℓ				WTPVC WTPVCA & WTPVCC Concentration, mol/ℓ				WTPST WTPSTA & WTPSTC Concentration, mol/ℓ			
mA/cm²	0,05	0,1	0,5	1,0	0,05	0,1	0,5	1,0	0,05	0,1	0,5	1,0	0,05	0,1	0,5	1,0	0,05	0,1	0,5	1,0	0,05	0,1	0,5	1,0	0,05	0,1	0,5	1,0
5	1,46	1,29	1,12		1,31	1,30	0,83		1,62	1,37	1,60		1,46	1,26			1,32	1,23			1,41	1,32	0,89					
10	1,33	1,20	0,96	0,94	1,41	1,37	1,04		1,46	1,23	1,43		1,40	1,27	0,89		1,33	1,21	0,99		1,38	1,25		0,67	1,44	1,26	0,99	
15	1,31	1,16			1,46	1,39			1,48				1,39	1,23			1,31	1,21			1,43	1,27	0,84		1,39	1,29		
20	1,33	1,16	0,88	0,94	1,48	1,36	0,99	0,81	1,52	1,20	1,30		1,43	1,26	0,94		1,29	1,30	1,01		1,38	1,21		0,58	1,48	1,30	0,98	
25	1,31				1,55												1,29								1,51			
30		1,12	0,98	0,91		1,40			1,46	1,15	1,20	0,85	1,56	1,29	0,96	0,75			1,17	0,72	1,56	1,35			1,55	1,27	0,97	0,74
40		1,19	0,89	0,94		1,43	1,15	0,88		1,15	1,13			1,37	0,97			1,60				1,39	0,86	0,55		1,30	0,93	
50		1,08	0,92	0,88		1,50	1,23			1,13	1,10	0,84			0,98	0,77				0,88						1,06	1,00	0,74
60			0,93	0,91			1,28	0,93			1,13				0,97								0,88	0,58				
70							1,31				0,99	0,84			0,97	0,85				1,19							0,84	0,79
80								0,88							1,00				1,76									
90											1,02	0,95			1,00	0,92				1,37							1,06	0,73
100															1,04				1,96									
110																											1,09	

6.3 Water Flow

Water flow (J) through the membranes as a function of current density and feed water concentration is shown in Figures 6.78 to 6.84. Water flow (J_l) through the membranes relative to the flow at $J_{0,5\ mol/\ell}$ and $J_{0,1\ mol/\ell}$ is shown in Table 6.35. Water or volume flow through the membranes increases as a function of both current density and feed water concentration. All the membranes showed an increase in water flow with increasing feed water concentration except the *Selemion* membranes at 1,0 mol/ℓ feed concentration (Table 6.35). It is further interesting to note that water flows are significantly higher at the highest feed concentration (1,0 mol/ℓ) in the case of the *Ionac*- (Fig 6.79), *Raipore*- (Fig. 6.80), *Ionics*- (Fig. 6.81), WTPS- (Fig. 6.82), WTPVC- (Fig. 6.83) and WTPST- (Fig. 6.84) membranes. Current efficiencies for these membranes were also the highest at the highest feed concentration when more water flowed through the membranes (see Figs. 6.43 to 6.49). Therefore, it appears that increasing current efficiency is caused by increasing water flow through the membranes. This effect was especially pronounced for the more porous heterogeneous *Ionac*-, WTPS-, WTPVC- and WTPST membranes.

Water flow (J) through the membranes as a function of effective current density, I_{eff}, (actual current density times Coulomb efficiency) and feed water concentration for the different membranes are shown in Figures 6.85 to 6.91. Straight lines were obtained at higher values of I_{eff}. The slope of these lines corresponds to the combined electro-osmotic coefficient (2β) of a membrane pair. The electro-osmotic coefficients decreases significantly with increasing feed concentration in the case of the *Selemion*- (Fig. 6.85), *Raipore*- (Fig. 6.87), WTPS- (Fig. 6.89), WTPVC- (Fig. 6.90) and WTPST- (Fig. 6.91) membranes as can be seen from the slopes of the lines.

The electro-osmotic coefficients as a function of feed concentration are shown in Figures 6.92 to 6.98. The reduction in the electro-osmotic coefficients with increasing feed concentration can be ascribed to deswelling of the membranes at high feed concentration[27, 28, 42 - 44] and/or a reduction in membrane permselectivity at high feed concentration[25]. This effect was far less for the *Ionac*- and *Ionics* membranes. The WTPS membranes, on the other hand, showed an increase in the electro-osmotic coefficient with increasing feed concentration (Fig. 6.96). Therefore, it appears that this hydrophobic membrane starts to swell with increasing feed concentration in the feed concentration range from 0,05 to 0,5 mol/ℓ[42].

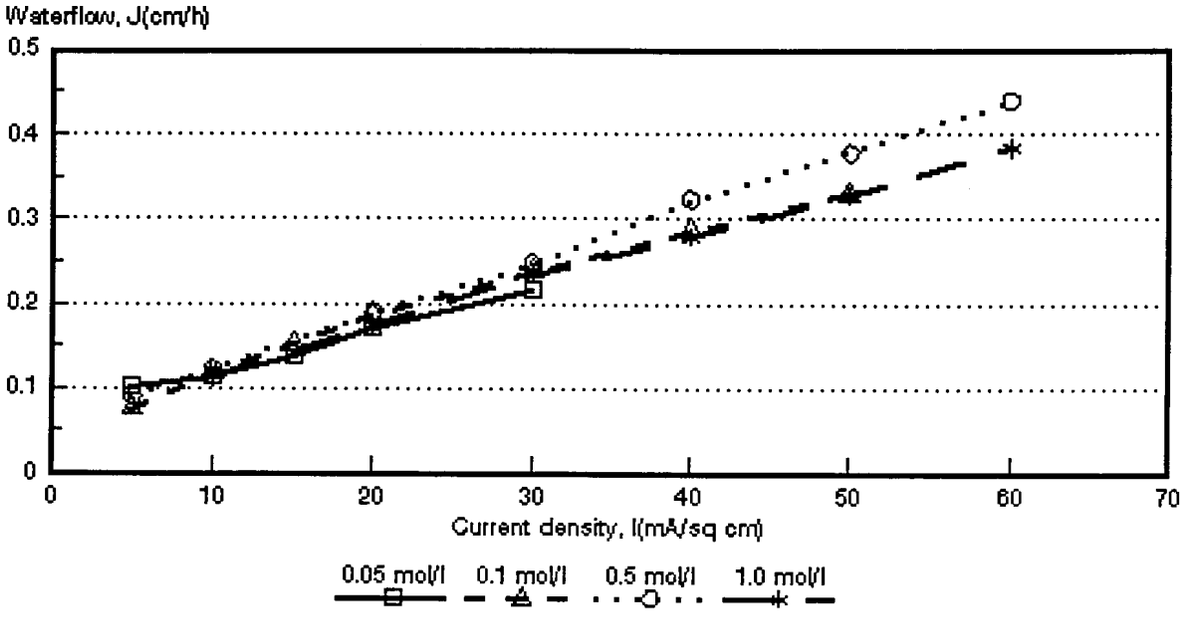

Figure 6.78: **Water flow through the Selemion AMV and CMV membranes as a function of current density and feed water concentration.**

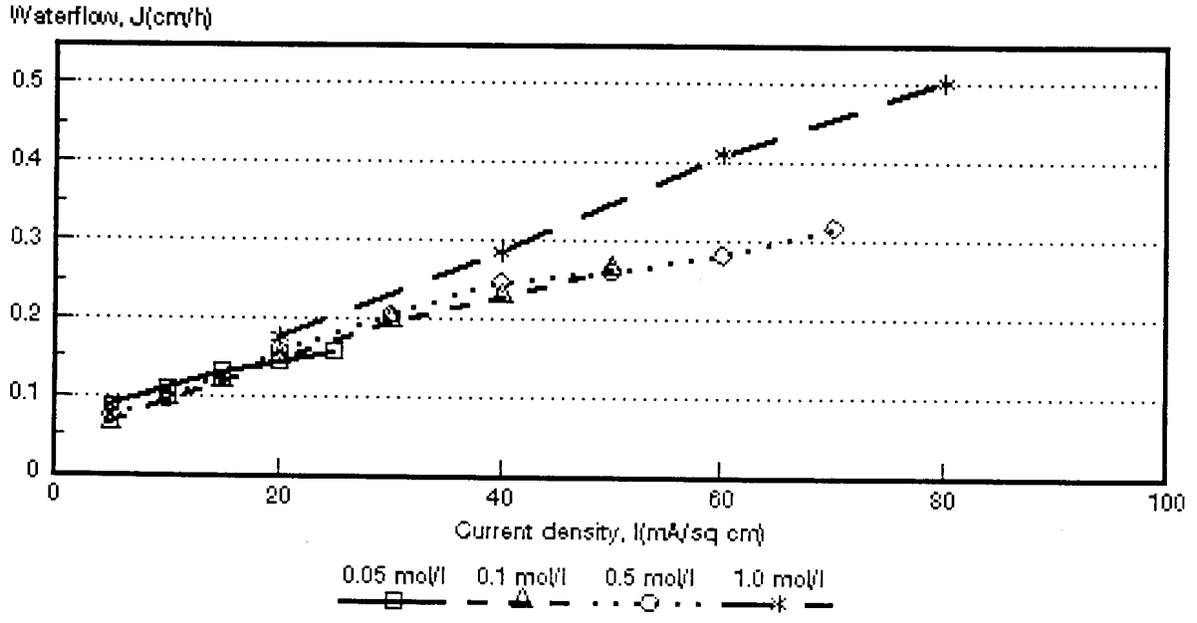

Figure 6.79: **Water flow through the Ionac MA-3475 and MC-3470 membranes as a function of current density and feed water concentration.**

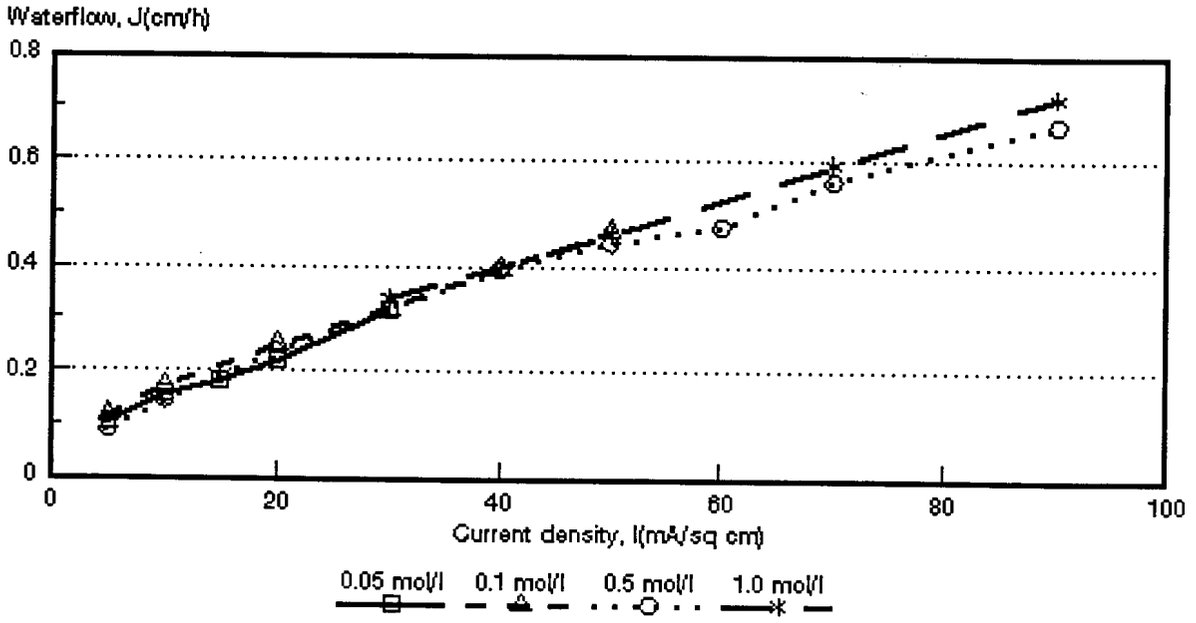

Figure 6.80: **Water flow through the Raipore R4030 and R4010 membranes as a function of current density and feed water concentration.**

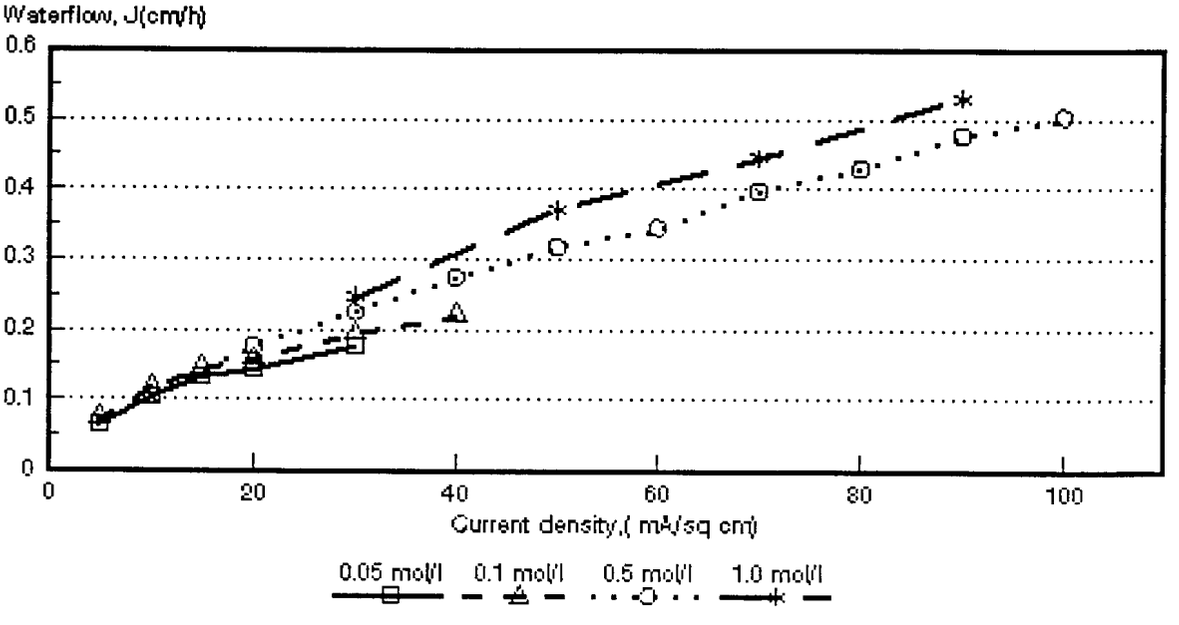

Figure 6.81: **Water flow through the Ionics A-204-UZL-386 and C-61-CZL-386 membranes as a function of current density and feed water concentration.**

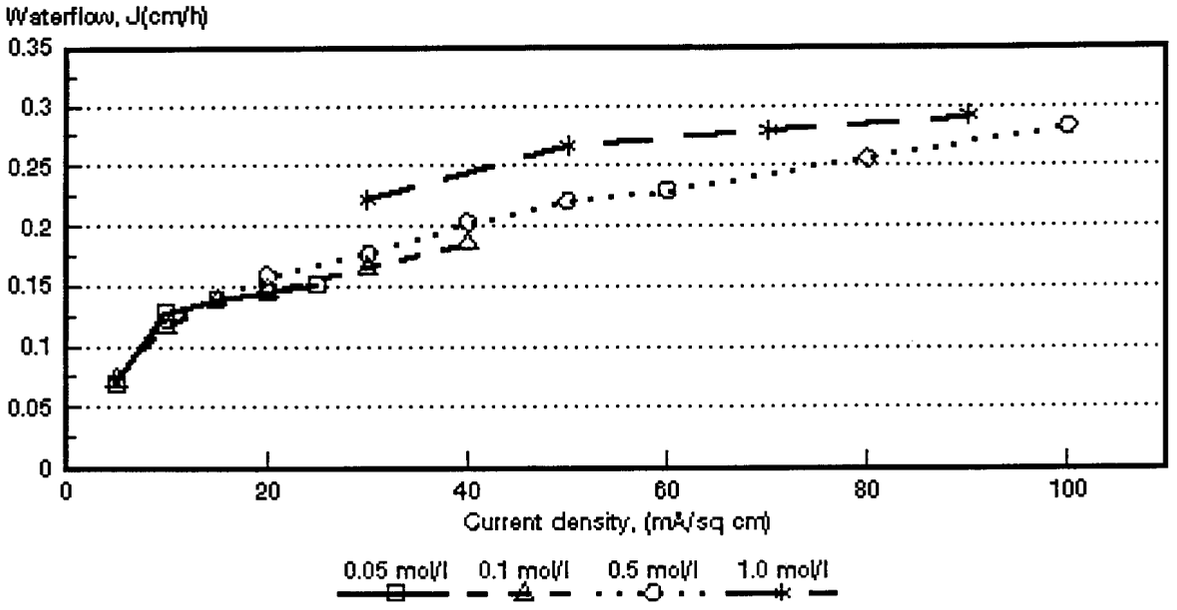

Figure 6.82: **Water flow through the WTPSA-1 and WTPSC-1 membranes as a function of current density and feed water concentration.**

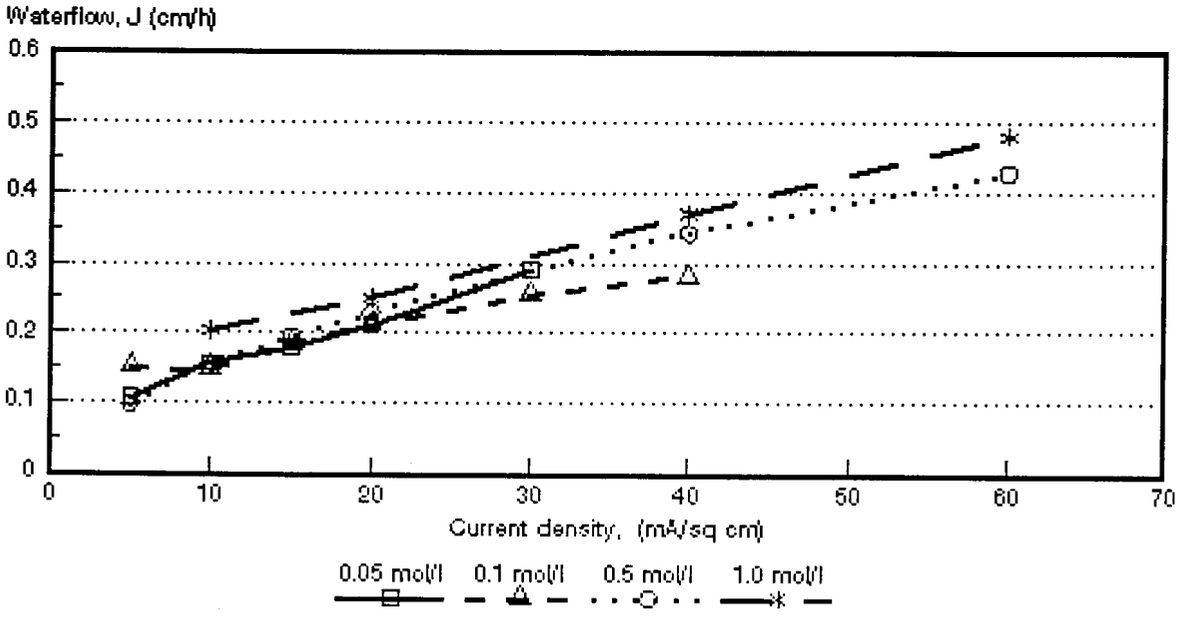

Figure 6.83: **Water flow through the WTPVCA-2 and WTPVCC-2 membranes as a function of current density and feed water concentration.**

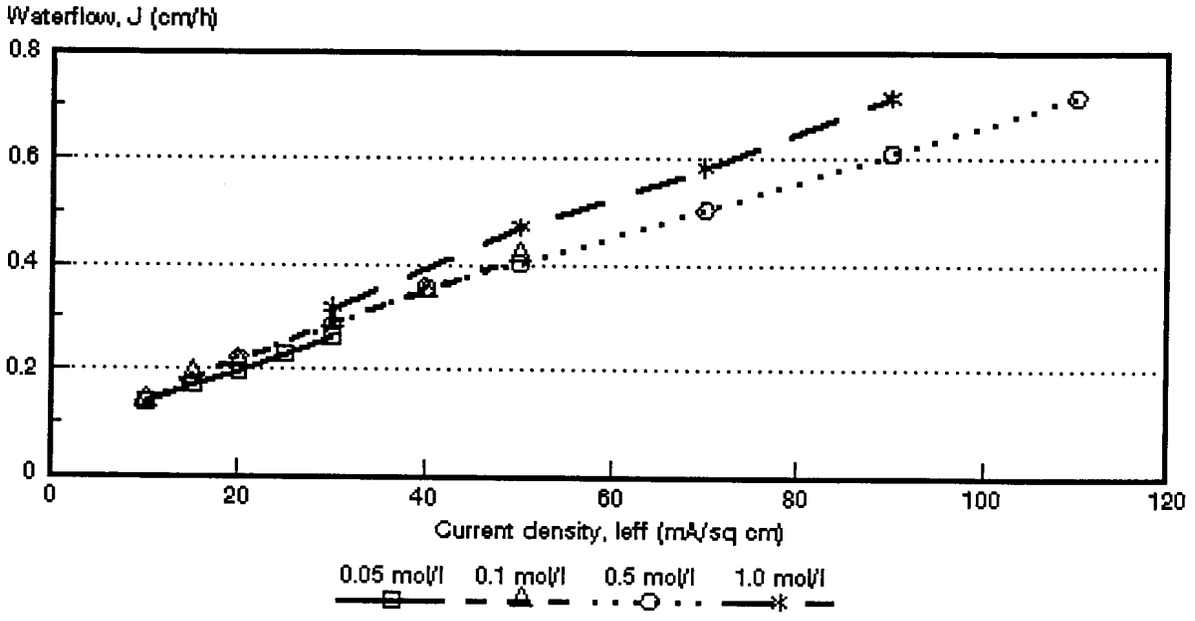

Figure 6.84: **Water flow through the WTPSTA-3 and WTPSTC-3 membranes as a function of current density and feed water concentration.**

Table 6.35: Water flow (J_i) through the membranes relative to the flow at $J_{0,5\ mol/\ell}$ or $J_{0,1\ mol/\ell}$

Current Density	$J_i/J_{0,5\ mol/\ell}$																											
	Selemion AMV & CMV Concentration, mol/ℓ				Ionac MA-3475 & MC-3470 Concentration, mol/ℓ				Raipore R4030 & R4010 Concentration, mol/ℓ				Ionics A-204-UZL & C-61-CZL Concentration, mol/ℓ				WTPS WTPSA & WTPSC Concentration, mol/ℓ				WTPVC WTPVCA & WTPVCC Concentration, mol/ℓ				WTPST WTPSTA & WTPSTC Concentration, mol/ℓ			
mA/cm²	0,05	0,1	0,5	1,0	0,05	0,1	0,5	1,0	0,05	0,1	0,5	1,0	0,05	0,1	0,5	1,0	0,05	0,1	0,5	1,0	0,05	0,1	0,5	1,0	0,05	0,1	0,5	1,0
5	1,14	0,85	1,0		1,17	0,87	1,0		1,18	1,28	1,0		1,0		1,0				1,0		1,11	1,55	1,0				1,0	
10	0,94	0,97	1,0	0,93	1,15	1,03	1,0		1,09	1,18	1,0		1,0	1,1	1,0		1,05	0,96	1,0		1,00	0,95	1,0	1,29	0,99	1,02	1,0	
15			1,0				1,0				1,0				1,0				1,0		0,92	0,95	1,0				1,0	
20	0,89	0,99	1,0	0,92	0,92	0,93	1,0	1,11	0,93	1,05	1,0		0,82	0,90	1,0		0,92	0,92	1,0		0,92	0,97	1,0	1,09	0,88	0,97	1,0	
25			1,0				1,0				1,0				1,0				1,0				1,0				1,0	
30	0,88	0,96	1,0	0,95		0,96	1,0		1,00	1,00	1,0	1,07	0,78	0,88	1,0	1,09		0,94	1,0	1,26	1,00	0,88	1,0		0,94	1,03	1,0	1,12
40		0,89	1,0	0,86		0,93	1,0	1,16		1,01	1,0			0,80	1,0			0,91	1,0			0,82	1,0	1,08		0,98	1,0	
50		0,87	1,0	0,87		1,01	1,0			1,05	1,0	1,04			1,0	1,17			1,0	1,21			1,0			1,04	1,0	1,17
60			1,0	0,87			1,0	1,45			1,0				1,0				1,0				1,0	1,12			1,0	
70 (5)*	(1,34)	(1,0)			(1,33)	(1,0)			(0,92)	(1,0)	1,0	1,06	(0,91)	(1,0)	1,0	1,12	(0,95)	(1,0)				1,0				1,0	1,0	1,16
80(10)*	(0,97)	(1,0)			(1,12)	(1,0)			(0,92)	(1,0)			(0,91)	(1,0)			(1,10)	(1,0)			(0,97)	(1,0)			(0,97)	(1,0)	1,0	
90(15)*	(0,90)	(1,0)			(1,11)	(1,0)			(0,89)	(1,0)	1,0	1,05	(0,91)	(1,0)	1,0	1,11	(1,00)	(1,0)			(0,90)	(1,0)			(0,90)	(1,0)	1,0	1,17
100(20)*	(0,90)	(1,0)			(0,98)	(1,0)			(0,89)	(1,0)			(0,91)	(1,0)			(1,00)	(1,0)			(0,91)	(1,0)			(0,91)	(1,0)	1,0	
110(30)*	(0,91)	(1,0)				(1,0)			(0,99)	(1,0)			(0,92)	(1,0)							(0,91)	(1,0)			(0,91)	(1,0)	1,0	

( )* : $J_{0,05} / J_{0,1}$

i = 0,05; 0,1; 0,5 and 1,0 mol/ℓ

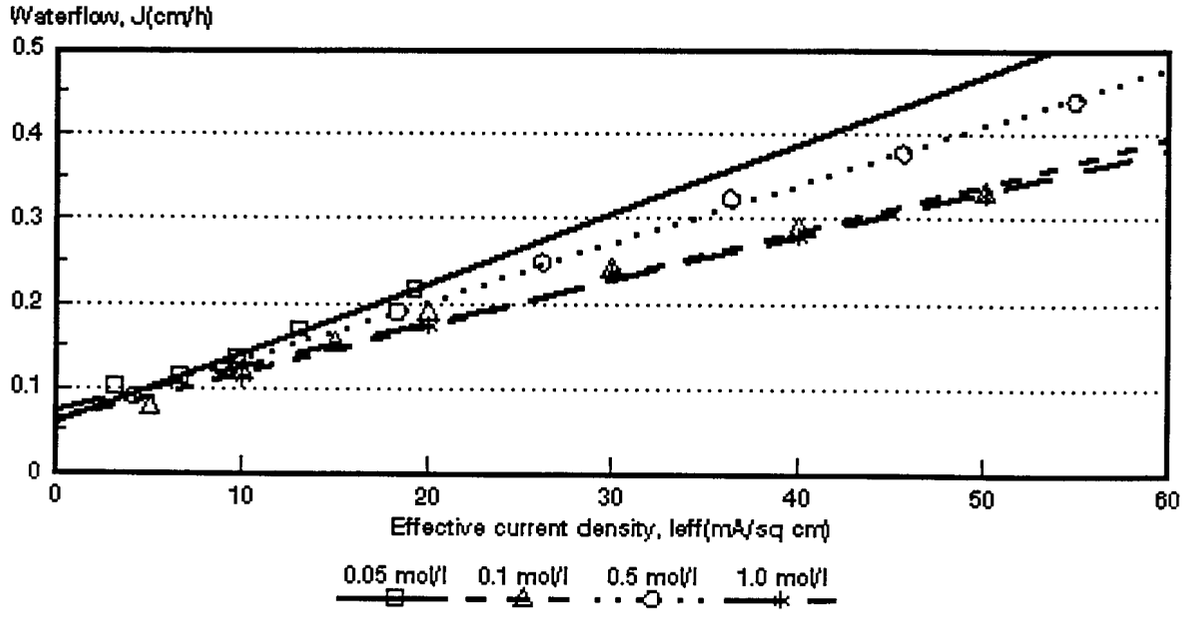

Figure 6.85: **Water flow through the *Selemion* AMV and CMV membranes as a function of effective current density and feed water concentration.**

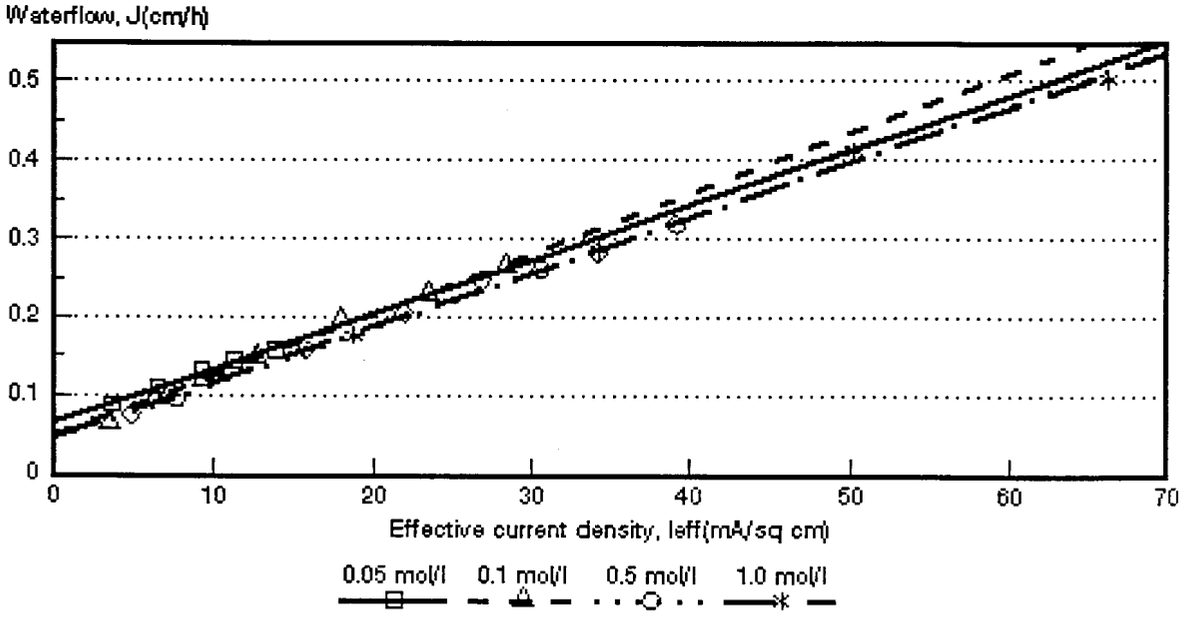

Figure 6.86: **Water flow through the *Ionac* MA-3475 and MC-3470 membranes as a function of effective current density and feed water concentration.**

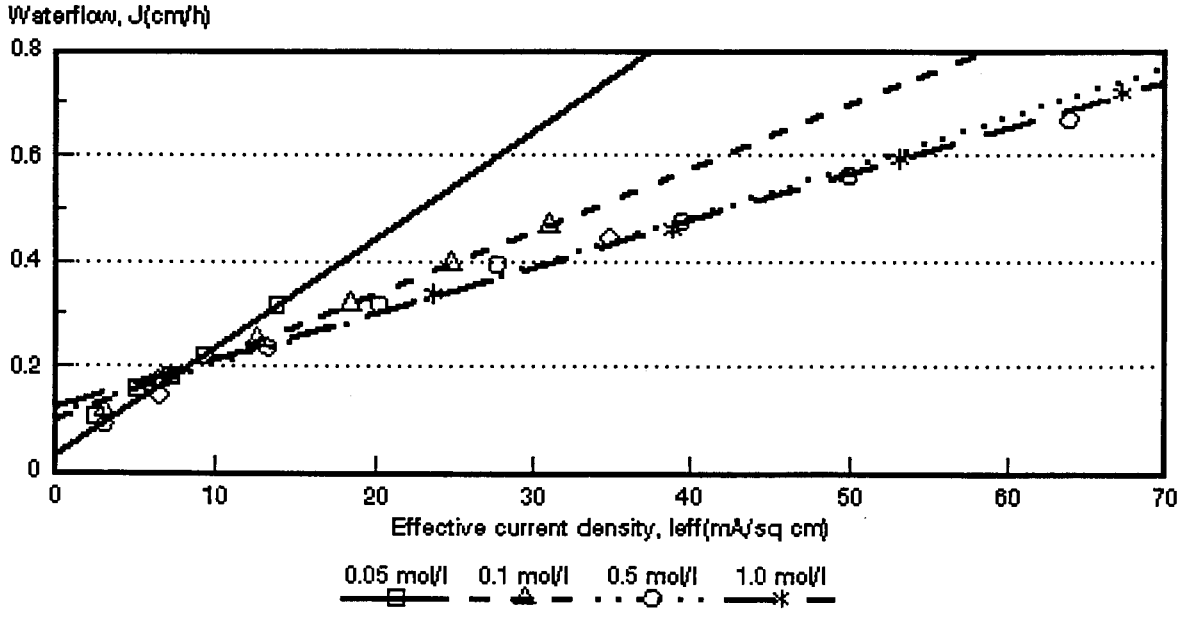

Figure 6.87: **Water flow through the *Raipore* R4030 and R4010 membranes as a function of effective current density and feed water concentration.**

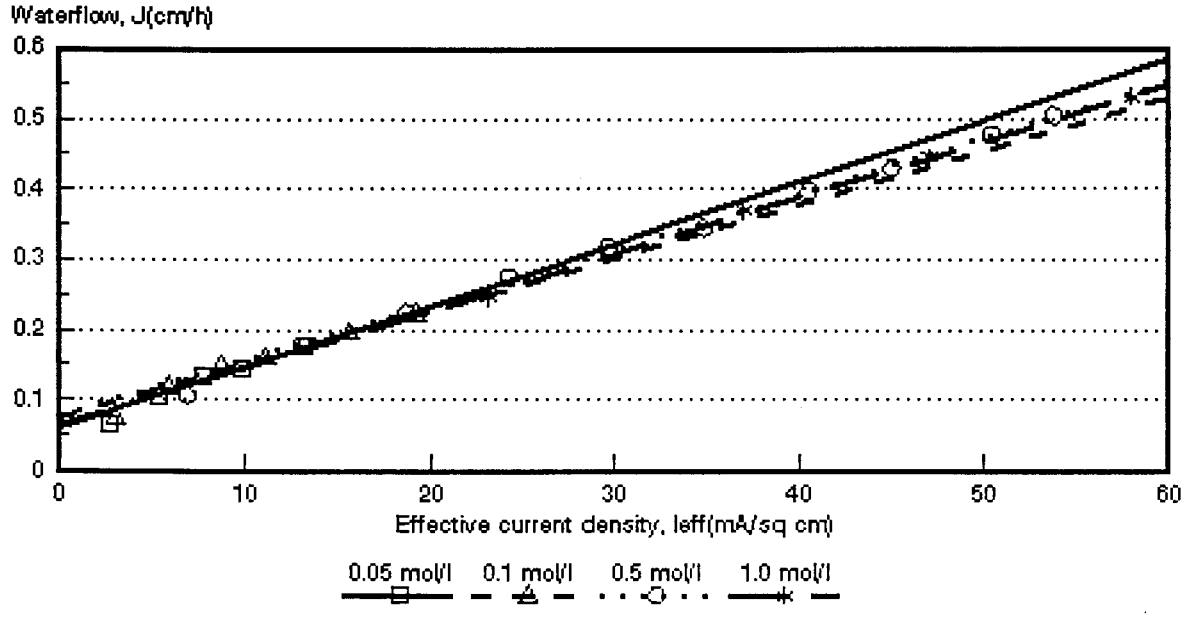

Figure 6.88: **Water flow through the *Ionics* A-204-UZL-386 and C-61-CZL-386 membranes as a function of effective current density and feed water concentration.**

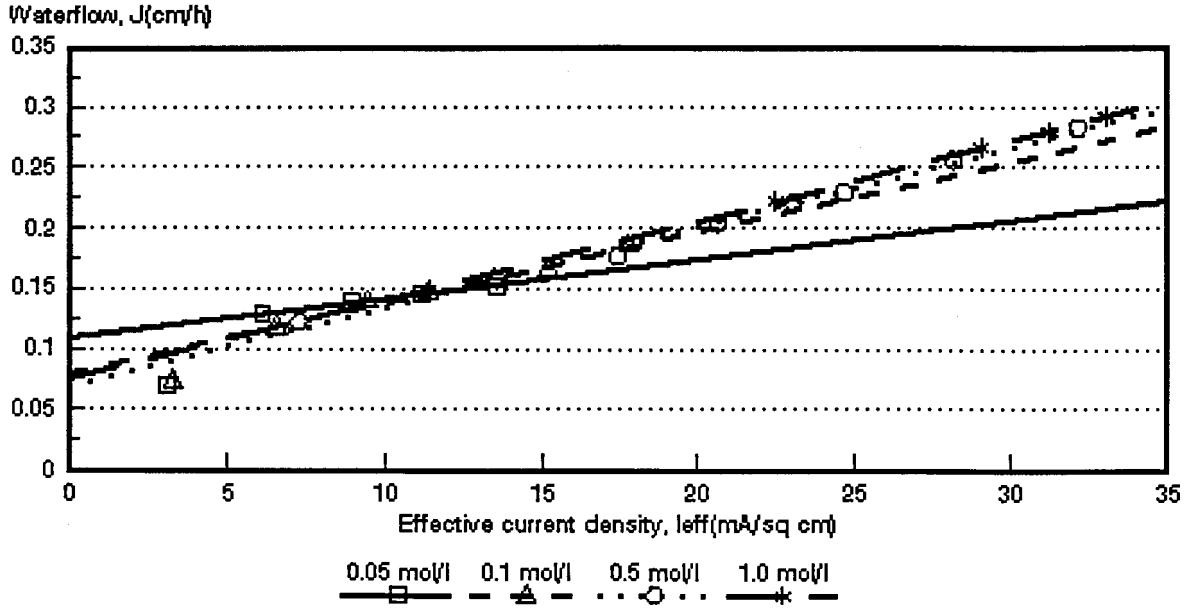

Figure 6.89: **Water flow through the WTPSA-1 and WTPSC-1 membranes as a function of effective current density and feed water concentration.**

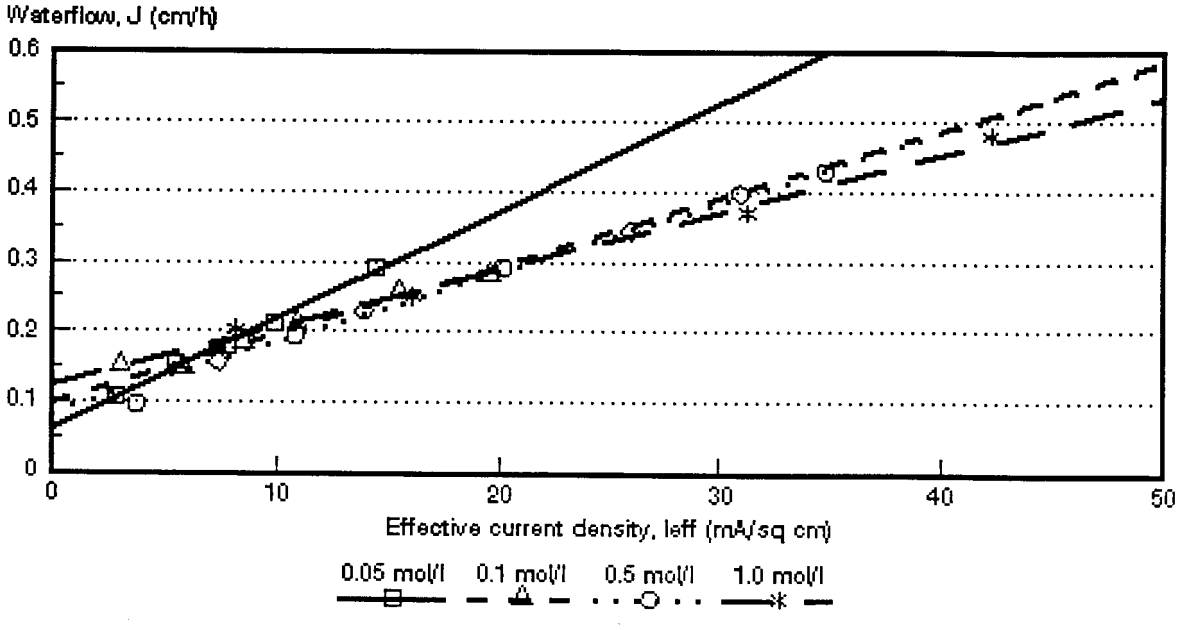

Figure 6.90: **Water flow through the WTPVCA-2 and WTPVCC-2 membranes as a function of effective current density and feed water concentration.**

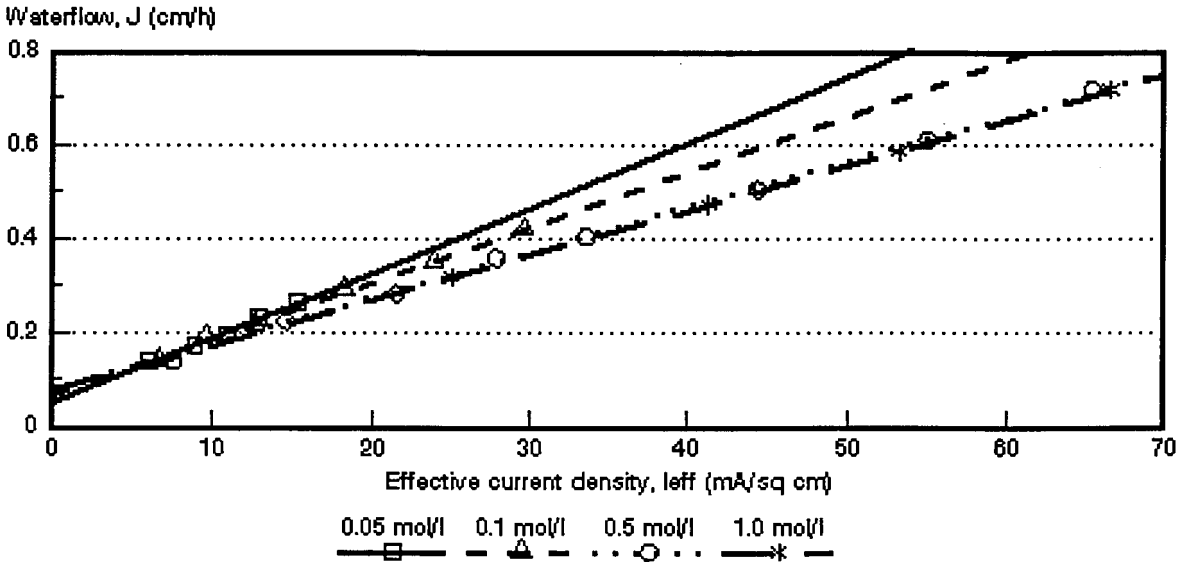

Figure 6.91: **Water flow through the WTPSTA-3 and WTPSTC-3 membranes as a function of effective current density and feed water concentration.**

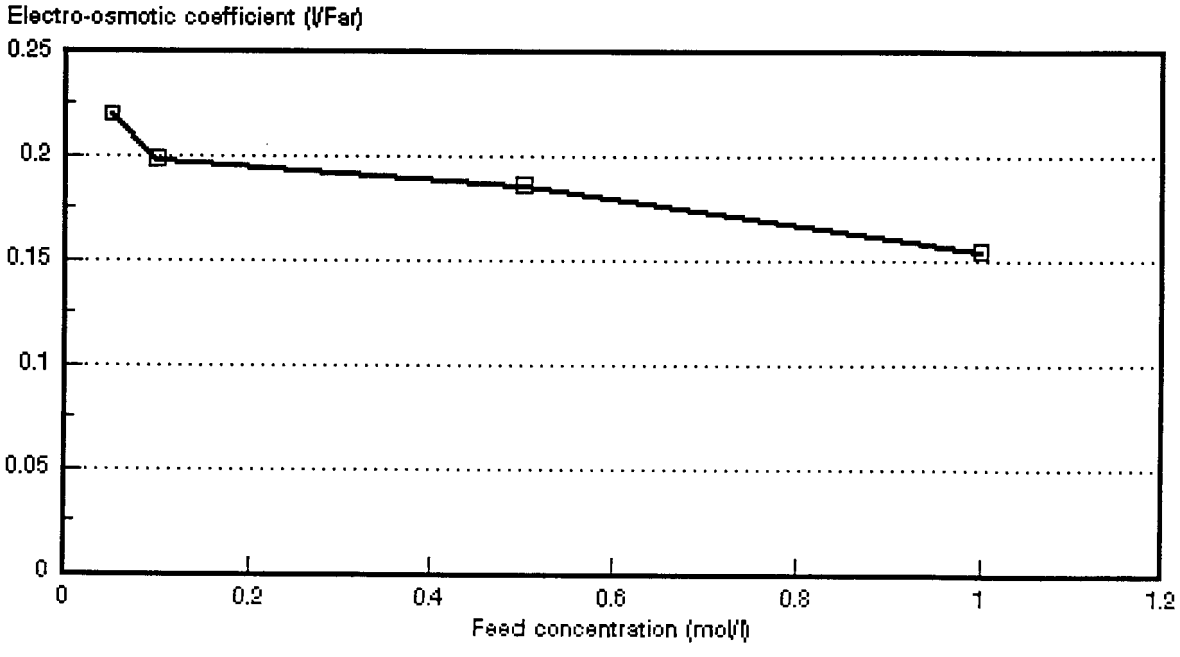

Figure 6.92: **Electro-osmotic coefficient as a function of NaCl feed concentration. *Selemion* AMV and CMV membranes.**

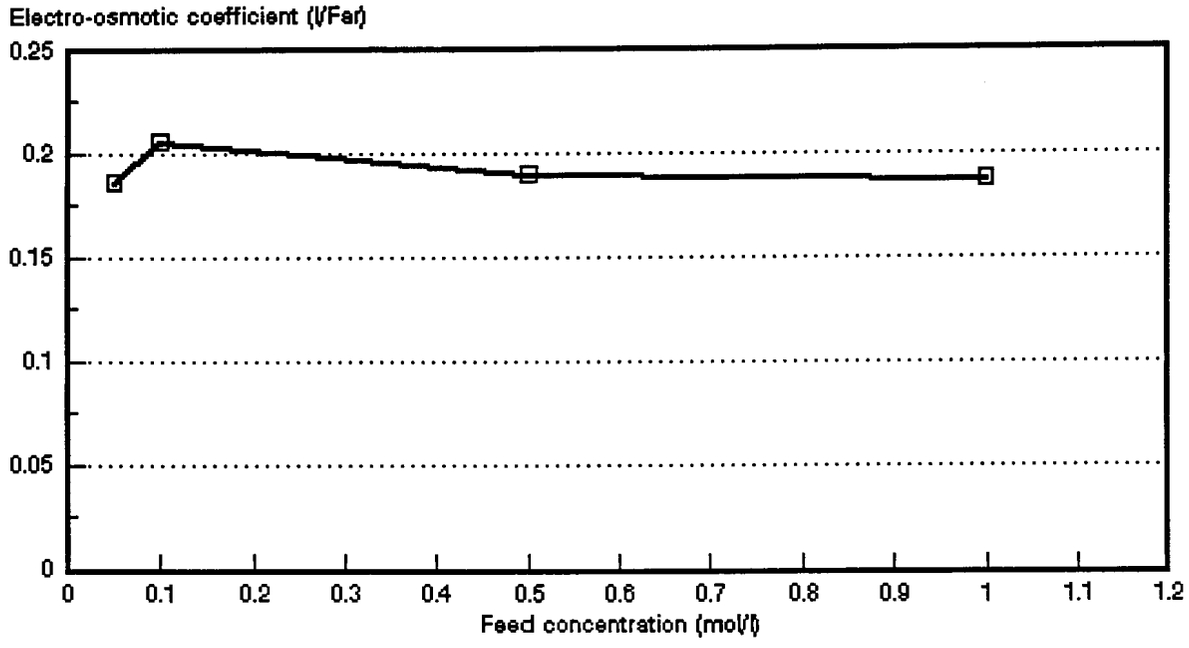

Figure 6.93: **Electro-osmotic coefficient as a function of NaCl feed concentrations. *Ionac* MA-3475 and MC-3470 membranes.**

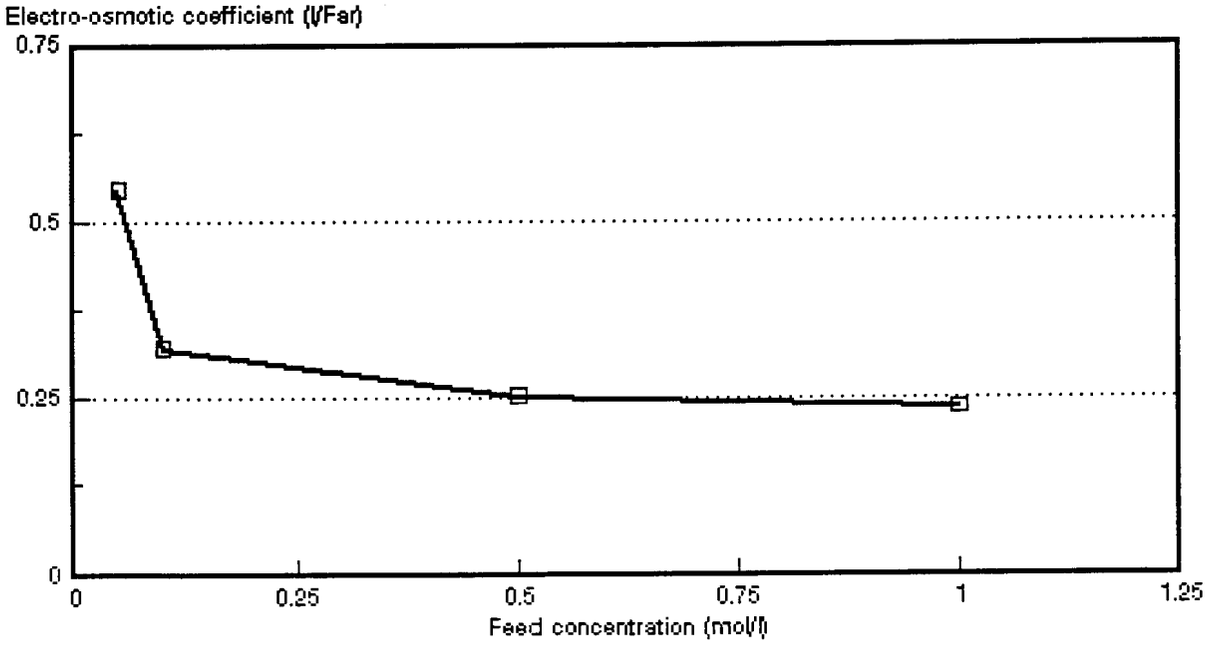

Figure 6.94 **Electro-osmotic coefficient as a function of NaCl feed concentrations. *Raipore* R4030 and R4010 membranes.**

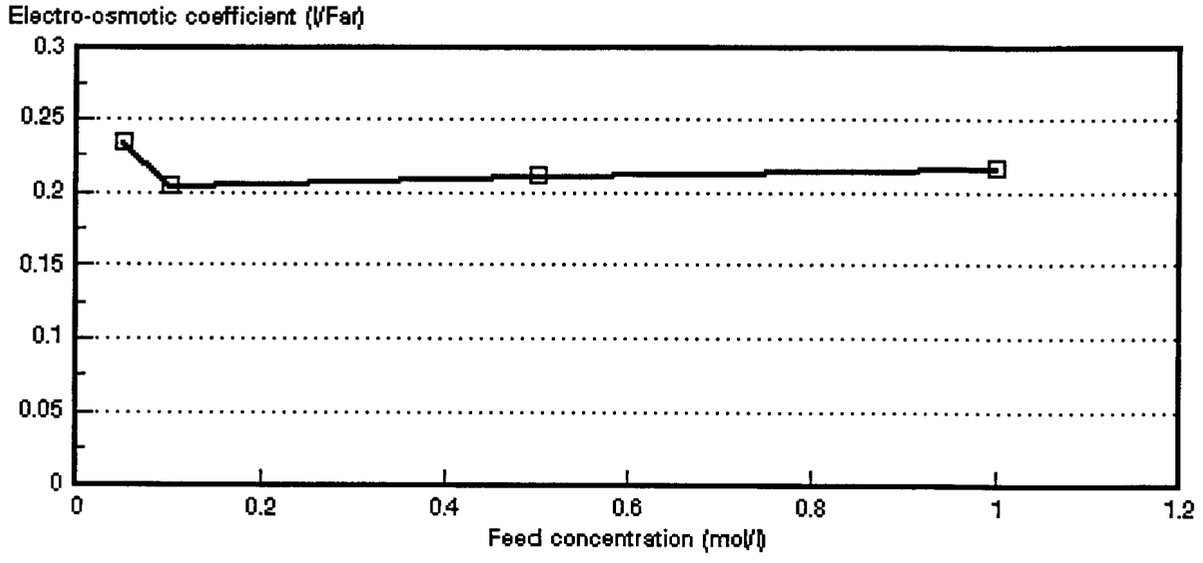

Figure 6.95: Electro-osmotic coefficient as a function of NaCl feed concentrations. *Ionics* A-204-UZL-386 and C-61-CZL-386 membranes.

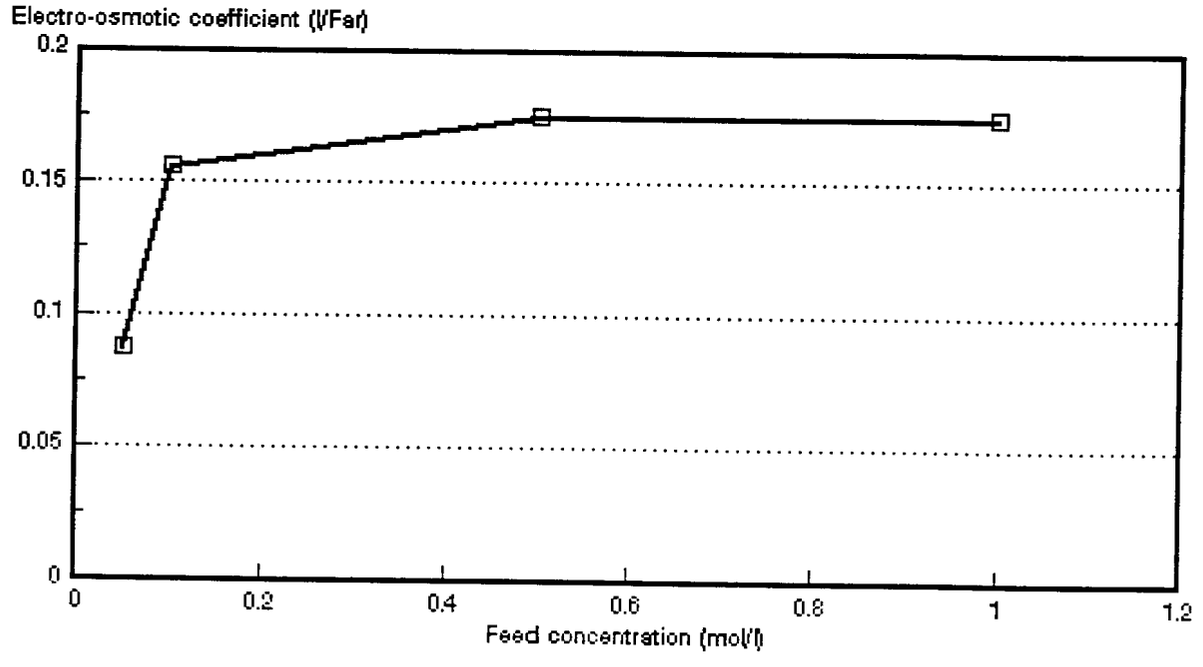

Figure 6.96: Electro-osmotic coefficient as a function of NaCl feed concentrations. WTPSA-1 and WTPSC-1 membranes.

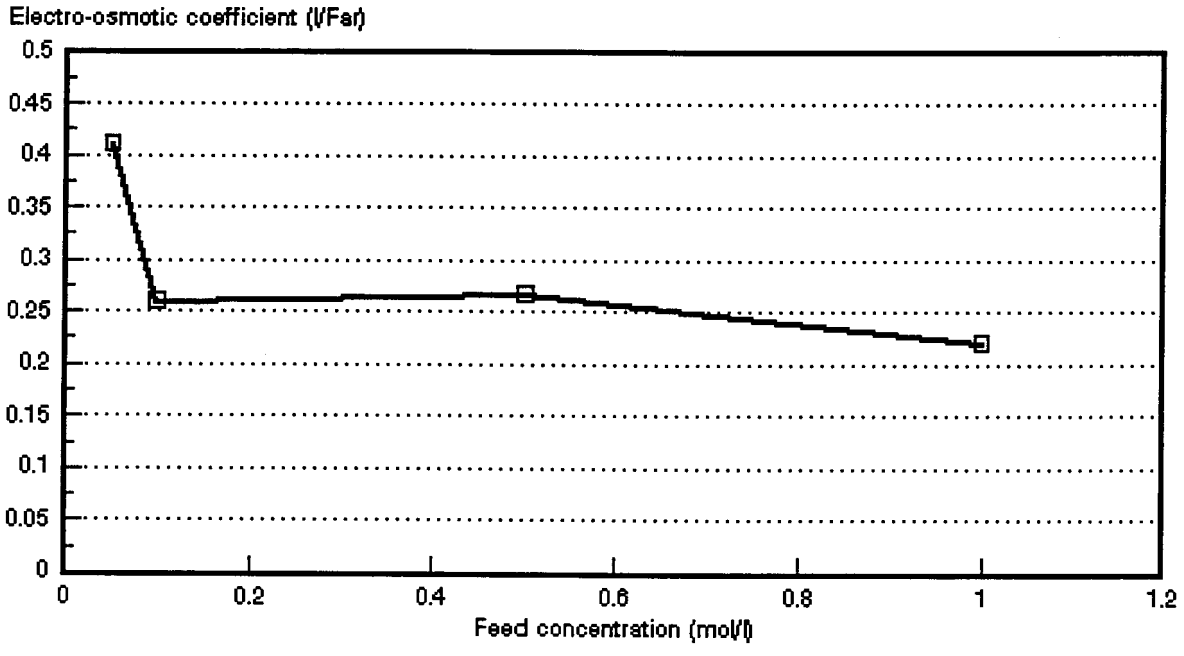

Figure 6.97: Electro-osmotic coefficient as a function of NaCl feed concentrations. WTPVCA-2 and WTPVCC-2 membranes.

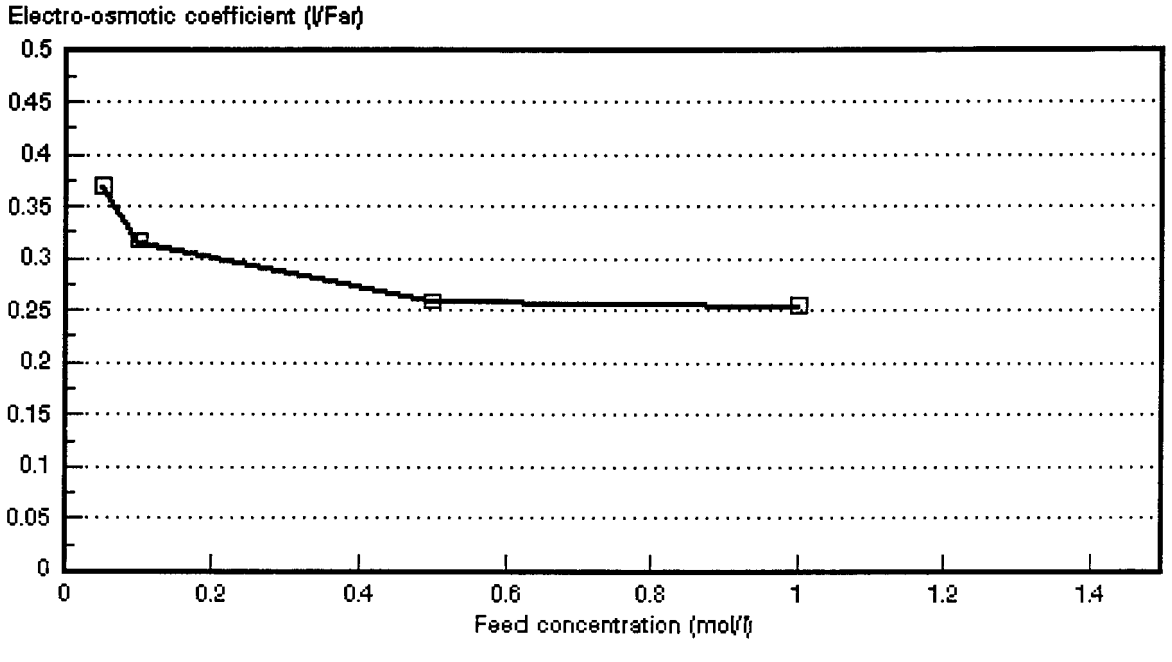

Figure 6.98: Electro-osmotic coefficient as a function of NaCl feed concentrations. WTPSTA-3 AND WTPSTC-3 membranes.

Table 6.36: Effect of the electro-osmotic coefficient (EOC)* on the maximum salt brine concentration, c_b^{max}.

Membranes	Feed Concentration (mol/ℓ)	EOC ℓ/Faraday	C_b^{max} mol/ℓ	mol H_2O/Faraday
Selemion AMV & CMV	0,05	0,219	4,55	12,2
	0,10	0,198	5,05	11,0
	0,5	0,187	5,36	10,4
	1,0	0,154	6,48	8,6
Ionac MA-3475 & MC-3470	0,05	0,186	5,37	10,3
	0,10	0,206	4,85	11,4
	0,5	0,190	5,26	10,6
	1,0	0,187	5,35	10,4
Raipore R4030 & R4010	0,05	0,547	1,83	30,4
	0,10	0,320	3,13	17,8
	0,50	0,251	3,98	13,9
	1,0	0,236	4,24	13,1
Ionics A-204-UZL & C-61-CZL-386	0,05	0,234	4,27	13,0
	0,10	0,204	4,89	11,3
	0,5	0,211	4,73	11,7
	1,0	0,216	4,63	12,0
WTPS WTPSCA-1 & WTPSA-1	0,05	0,087	11,5	4,8
	0,10	0,156	6,41	8,7
	0,5	0,175	5,71	9,7
	1,0	0,175	5,72	9,7
WTPVC WTPVCA-2 & WTPVCC-2	0,05	0,412	2,43	22,8
	0,10	0,261	3,84	14,5
	0,5	0,267	3,74	14,8
	1,0	0,221	4,54	12,3
WTPST WTPSTA-3 & WTPSTC-3	0,05	0,371	2,69	20,6
	0,1	0,317	3,15	17,6
	0,5	0,259	3,86	14,4
	1,0	0,257	3,90	14,3

* Data from Tables 6.1 to 6.28.

The effect of the electro-osmotic coefficient on the maximum brine concentration, c_b^{max}, is shown in Table 6.36. Maximum brine concentration increases with decreasing electro-osmotic coefficient. The electro-osmotic coefficients of the *Raipore* membranes were higher than the electro-osmotic coefficients of the other membranes. Consequently, lower brine concentrations were obtained with this membrane type. It is further interesting to note that the electro-osmotic coefficients of the WTPS membranes have been the lowest in the 0,05 to 0,5 mol/ℓ feed concentration range. Therefore, high brine concentrations could be obtained (Table 6.36).

Approximately 10 to 11 mol H_2O/Faraday passed through the *Selemion*-, *Ionac*- and *Ionics* membranes in the 0,1 to 0,5 mol/ℓ feed concentration range (Table 6.36).

Approximately 9 to 10 mol H_2O/Faraday passed through the WTPS membranes in this same feed concentration range. However, more water passed through the other membranes in this feed concentration range.

The osmotic flow (J_{osm}) relative to the total flow (J) through the membranes as a function of current density, is shown in Table 6.37. Osmotic flow decreases with increasing current density. The contribution of osmotic flow at a current density of 30 mA/cm^2 (0,1 mol/ℓ feed) in the case of the *Selemion*-, *Ionac*-, *Raipore*-, *Ionics*-, WTPS-, WTPVC- and WTPST membranes were 28,4%; 25,5%; 30,8%; 38,5%; 48,4%; 38,8% and 23,7% of the total flow through the membranes, respectively. Consequently, osmosis contributes significantly to water flow through the membranes especially at relatively low current density. The osmotic flow contribution to total water flow through the membranes was much less at high current density. Osmotic flow contribution to total flow through the membranes at a current density of 50 mA/cm^2 (0,1 mol/ℓ feed) was 20,5; 19,0; 21,1 and 16,5% for the *Selemion*-, *Ionac*-, *Raipore*- and WTPST membranes, respectively. Osmotic flow contribution was only 10,7% of total water flow in the case of the WTPST membranes at a current density of 110 mA/cm^2.

It is interesting to note that the water flow (J) versus the effective current density (I_{eff}) relationship becomes linear long before the maximum brine concentration, c_b^{max}, is reached.

Table 6.37: Osmotic flow* (J_{osm}) relative to the total flow (J) through the membranes as a function of current density.

Membranes	Current Density mA/cm²	J_{osm}/J (%) Feed Concentration (mol/ℓ)			
		0,05	**0,1**	**0,5**	**1,0**
Selemion AMV & CMV	10	52,3	57,4	51,2	69,9
	20	35,4	36,0	32,8	45,4
	30	27,7	28,4		33,5
	40			19,3	28,3
	50		20,5		
	60			14,1	20,6
Ionac MA-3475 & MC-3470	10	59,1	50,5	46,9	
	20	45,2	33,9	28,6	27,6
	30		25,5	22,2	17,0
	40		21,9	18,4	
	50		19,0		11,9
	60			16,1	9,7
	80				
Raipore R4030 & R4010	10	21,9	57,3	76,8	
	20	15,6	39,3	46,9	
	30	11,0	30,8	35,2	37,3
	40		24,8	28,3	
	50		21,1	25,1	27,4
	60		-	23,5	
	70			19,91	21,3
	90			16,2	17,6
Ionics A-204-UZL & C-61-CZL-386	10	57,8	64,2	73,7	
	20	42,1	47,1	44,2	
	30	34,7	38,5	34,5	26,5
	40		33,9	28,34	
	50			24,6	17,7
	60			22,7	
	80			18,2	
	90			16,4	12,3
	100			15,5	
WTPS	10	85,2	68,8	57,4	
WTPSA-1 &	20	74,9	55,1	44,0	
WTPSC-1	30		48,4	39,6	34,3
	40		43,2	34,4	
	50			31,7	28,5
	60			30,5	
	70				27,3
	80			27,3	
	90				26,2
	100			24,7	
WTPVC	10	41,6	67,1	55,6	62,8
WTPVCA-2 &	20	30,6	44,8	37,9	50,2
WTPVCC-2	30	22,2	38,8	29,8	
	40		35,2	25,2	34,0
	60			20,3	26,2
WTPST	10	36,7	49,2	57,7	
WTPSTA-3 &	20	25,6	32,1	35,7	
WTPSTC-3	30	19,0	23,7	27,7	24,1
	40		19,8	22,2	
	50		16,5	19,7	16,3
	70			15,8	
	90			13,0	13,2
	110			11,1	10,7

* Data from Tables 6.1 to 6.28.

6.4 Membrane Permselectivity

Membrane permselectivity ($\bar{\Delta}t$) as a function of brine concentration for various initial feed concentrations, is shown in Figures 6.99 to 6.105. Membrane permselectivity decreased with increasing brine concentration for all the membranes investigated. Permselectivity decreased with increasing feed concentration in the case of the *Selemion*-, *Ionac*-, WTPS-, WTPVC- and WTPST membranes. However, permselectivity was slightly higher at 1,0 mol/ℓ feed concentration than at 0,5 mol/ℓ feed concentration in the case of the Ionac membranes (Fig. 6.100). Permselectivity showed an increase with increasing feed concentration in the case of the *Raipore* membrane (Fig. 6.101).

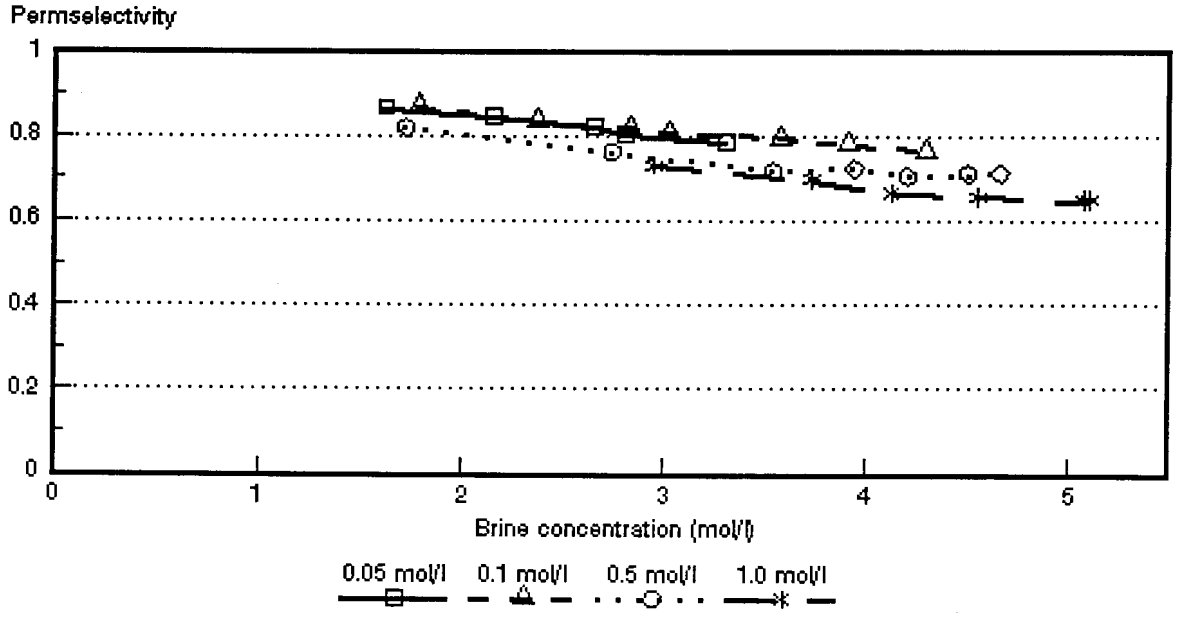

Figure 6.99: Membrane permselectivity ($\bar{\Delta}t$) as a function of brine concentration for different NaCl feed concentrations. *Selemion* AMV and CMV membranes.

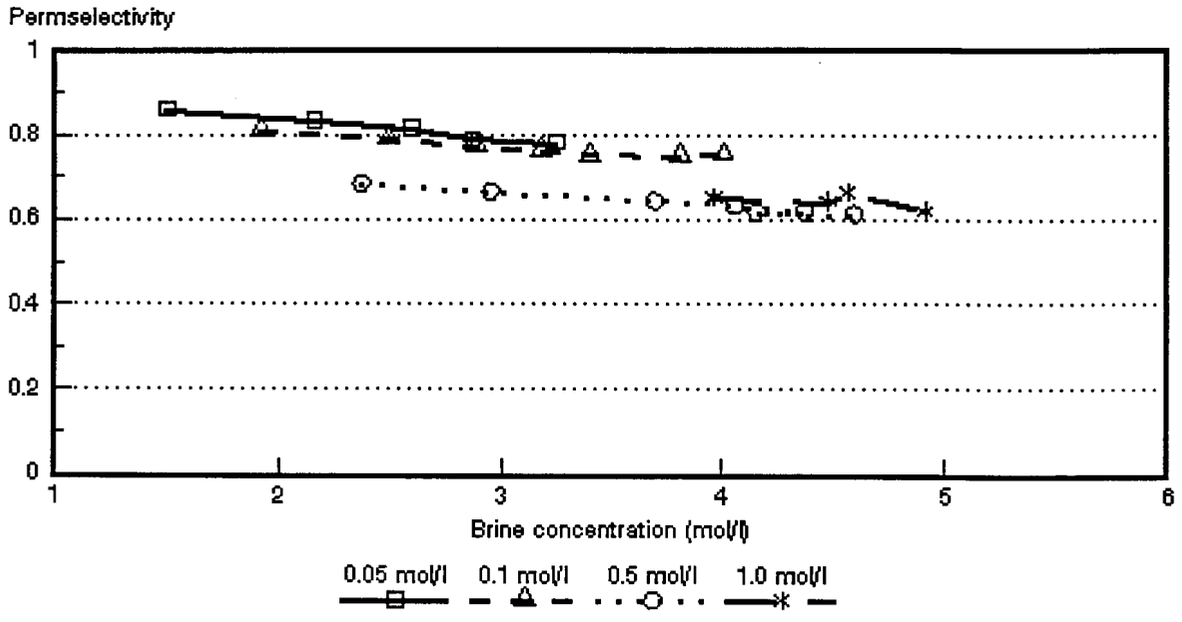

Figure 6.100: **Membrane permselectivity ($\bar{\Delta}t$) as a function of brine concentration for different NaCl feed concentrations. *Ionac* MA-3475 and MC-3470 membranes.**

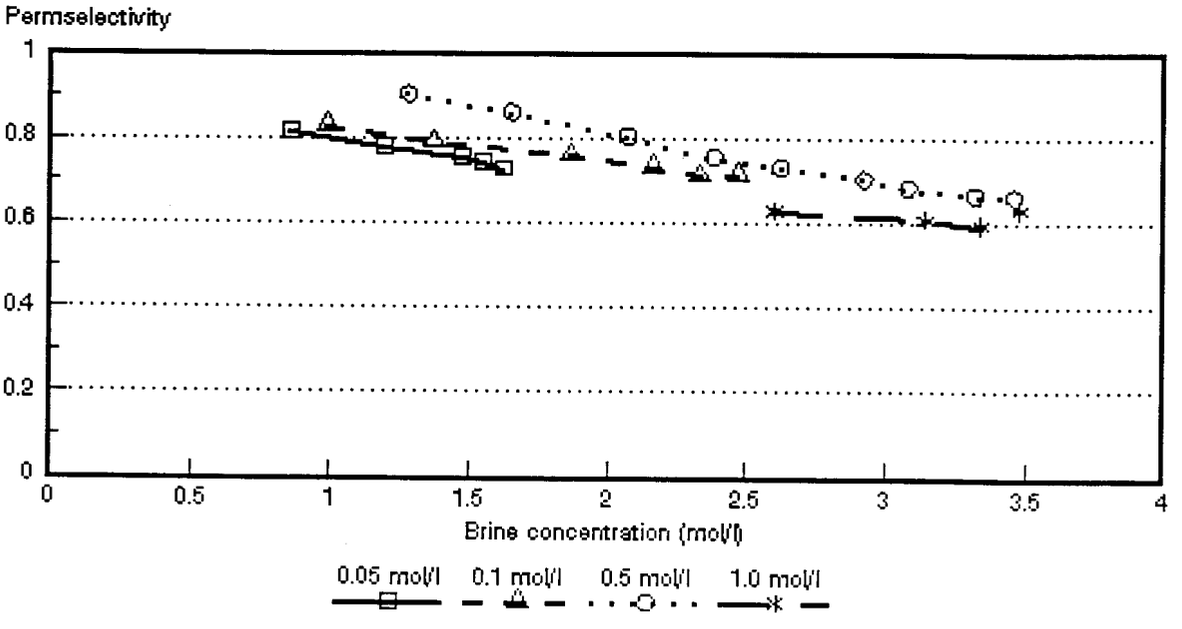

Figure 6.101: **Membrane permselectivity ($\bar{\Delta}t$) as a function of brine concentration for different NaCl feed concentrations. *Raipore* R4030 and R4010 membranes.**

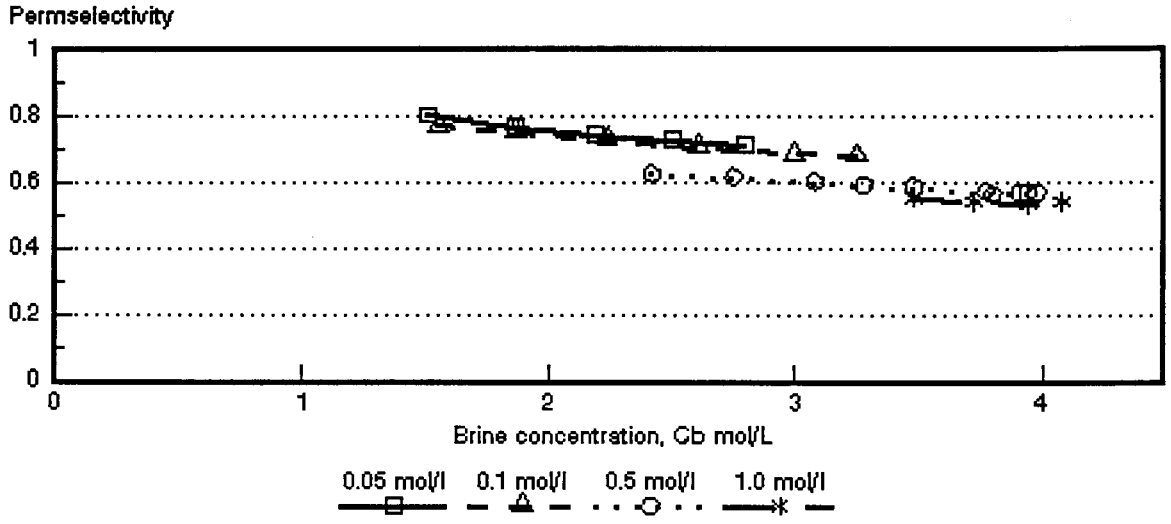

Figure 6.102: **Membrane permselectivity ($\bar{\Delta}t$) as a function of brine concentration for different NaCl feed concentrations. *Ionics* A-204-UZL-386 and C-61-CZL-386 membranes.**

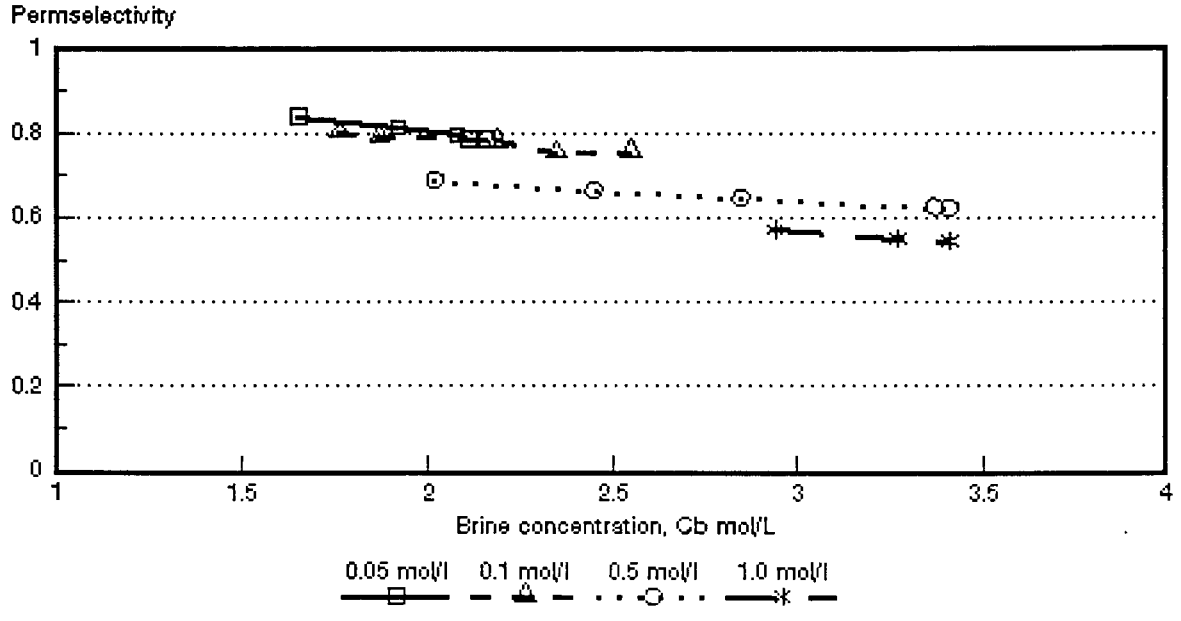

Figure 6.103: **Membrane permselectivity ($\bar{\Delta}t$) as a function of brine concentration for different NaCl feed concentrations. WTPSA-1 and WTPSC-1 membranes.**

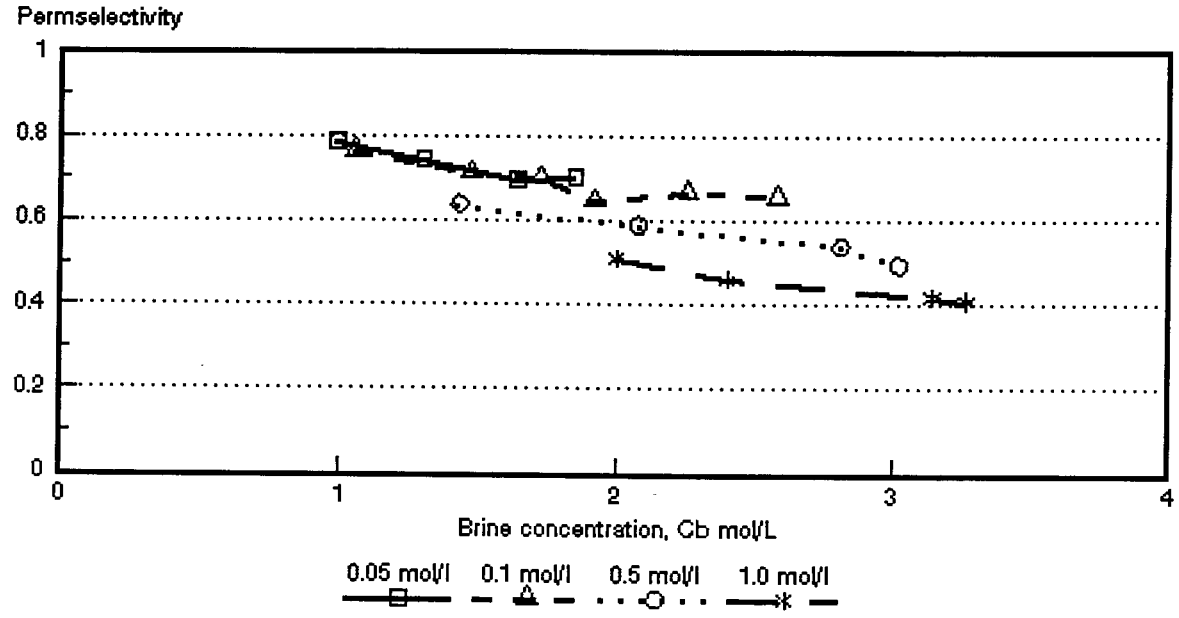

Figure 6.104: **Membrane permselectivity ($\bar{\Delta}t$) as a function of brine concentration for different NaCl feed concentrations. WTPVCA-2 and WTPVCC-2 membranes.**

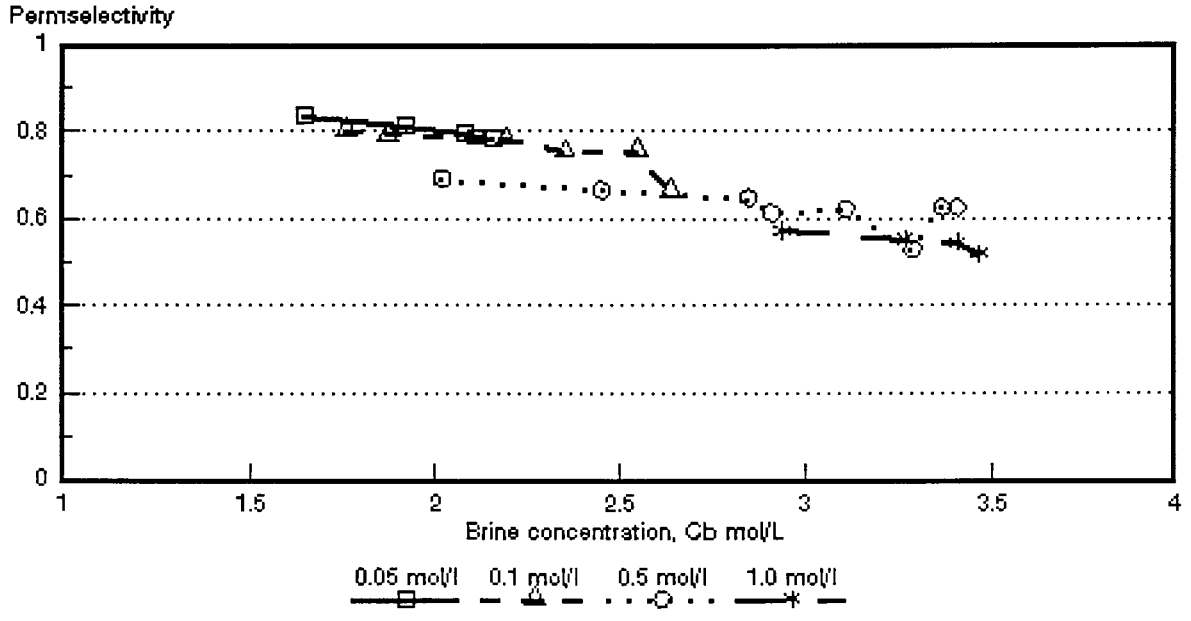

Figure 6.105: **Membrane permselectivity ($\bar{\Delta}t$) as a function of brine concentration for different NaCl feed concentrations. WTPSTA-3 and WTPSTC-3 membranes.**

6.5 Membrane Characteristics

6.5.1 Membrane resistance

Membrane resistances are summarized in Table 6.38.

Table 6.38: Membrane resistances of the membranes used for EOP of sodium chloride solutions

Membrane	Resistance - ohm·cm²	
	0,1 mol/ℓ NaCl	0,5 mol/ℓ NaCl
Selemion AMV	4,7	1,5
Selemion CMV	3,8	1,0
Ionac MA-3475	36,6	19,4
Ionac MC-3470	42,0	24,3
Raipore R4030	3,1	1,0
Raipore R4010	1,3	-
Ionics A-204-UZL-386	13,4	12,3
Ionics C-61-CZL-386	14,2	15,2
WTPSA-1	97,9	60,3
WTPSC-1	12,8	8,6
WTPVCA-2	21,1	11,1
WTPVCC-2	24,9	14,9
WTPSTA-3	83,3	49,3
WTPSTC-3	24,9	14,3

6.5.2 Gel water contents and ion-exchange capacities of the membranes used for EOP of sodium chloride solutions

The gel water contents and the ion-exchange capacities are summarized in Table 6.39.

Table 6.39: Gel water contents and ion-exchange capacities of the membranes used for the EOP of sodium chloride solutions.

Membrane	Gel Water Content (%)	Ion-exchange capacity me/dry g
Selemion AMV	18,4	1,26
Selemion CMV	22,7	2,4
Ionac MA-3475	17,8	1,06
Ionac MC-3470	18,5	1,82
Ionics A-204-UZL-386	22,9	1,49
Ionics C-61-CZL-386	23,7	1,51
WTPSA-1	26,4	0,54
WTPSC-1	43,4	1,75
WTPVCA-2	15,9	1,15
WTPVCC-2	29,8	0,76
WTPSTA-3	35,57	1,13
WTPSTC-3	31,44	0,61

6.5.3 Permselectivities of the membranes used for the EOP of sodium chloride solutions

The permselectivities of the membranes at different salt gradients are summarized in Table 6.40.

Table 6.40: Membrane perselectivities of the membranes used for EOP of sodium chloride solutions at different salt gradients

Membrane	Δt(1)*	Δt(2)**	Δt(3)***
Selemion AMV	0,86	0,75	0,71
Selemion CMV	1,00	0,99	0,88
Ionac MA-3475	0,83	0,66	0,64
Ionac MC-3470	1,00	0,91	0,78
Raipore R4030	0,85	0,72	0,66
Raipore R4010	0,96	0,85	0,63
Ionics A-204-UZL-386	0,92	0,75	0,67
Ionics C-61-CZL-386	0,94	0,82	0,70
WTPSA-1	0,92	0,75	0,68
WTPSC-1	0,90	0,77	0,58
WTPVCA-2	0,86	0,65	0,50
WTPVCC-2	0,90	0,71	0,54
WTPSTA-3	0,91	0,73	0,65
WTPSTC-3	0,89	0,72	0,69

(1)* : 0,1/0,2 mol/ℓ (2)** : 0,5/1,0 mol/ℓ
(3)*** : 0,1/4,0 mol/ℓ NaCl

7. ELECTRO-OSMOTIC PUMPING OF HYDROCHLORIC ACID SOLUTIONS WITH DIFFERENT ION-EXCHANGE MEMBRANES

Acid brine concentrations, water flows and current efficiencies were determined at different current densities for different hydrochloric acid feed water concentrations. Membrane permselectivities (apparent transport numbers) were measured at concentration differences similar to those obtained during EOP experiments. The results are summarized in Tables 7.1 to 7.17.

7.1 Brine Concentration

Acid brine concentration (c_b) as a function of current density is shown in Figures 7.1 to 7.5. Acid concentration increases more rapidly in the beginning as has been experienced with the salt solutions and then starts to level off. The levelling off in acid concentration is more pronounced at the lower acid feed concentrations (0,05 mol/ℓ, Figs. 7,3 and 7,5). The acid concentration curves were steeper than the curves obtained during sodium chloride concentration. Higher current densities could be obtained easier with the acid feed solutions.

Acid brine concentration increases with increasing current density and increasing acid feed water concentration as has been the case with sodium chloride solutions. The highest acid concentrations were obtained with the *Selemion* AAV and CHV membranes followed by the ABM-3 and CHV and ABM-2 and CHV membranes (Table 7.18). Acid brine concentrations of 25,0; 22,6 and 22,9% could be obtained from 0,5 mol/ℓ feed solutions with *Selemion* AAV and CHV, ABM-3 and CHV and ABM-2 and CHV membranes, respectively. The ABM-1 and CHV membranes did not perform as well as the other membranes for acid concentration while very low acid brine concentrations were obtained with the *Selemion* AMV and CMV membranes. The reason for the low acid concentrations obtained with the *Selemion* AMV and CMV membranes compared to the other anion membranes could be ascribed to the very low permselectivity of the *Selemion* AMV membrane for chloride ions (Tables 7.1 to 7.17). The permselectivity (Δt^a) of the *Selemion* AMV membrane was only 0,2 at 0,1 mol/ℓ hydrochloric acid feed (20 mA/cm^2) compared to 0,64 for the *Selemion* AAV; 0,62 for the ABM-3; approximately 0,5 for the ABM-2 and 0,57 for the ABM-1 membranes (Tables 7.1; 7.5; 7.9; 7.13; 7.16). The concentration gradients across the *Selemion* AAV, ABM-3, ABM-2 and ABM-1 membranes were also much higher than the concentration gradient across the *Selemion* AMV membrane during determination

Table 7.1 : Electro-osmotic pumping experimental conditions and results for 0,1 mol/ℓ hydrochloric acid (Selemion AMV and CMV)

Current Density	Brine concentration c_b, mol/l		Water flow	Current Efficiency	Effective Current Density	Transport Numbers				
I, mA/cm²	$c_{b\,exp.}$	$c_{b\,calc.}$	J, cm/h	e_p, %	I_{eff}, mA/cm²	Δt^c	Δt^a	$\bar{\Delta}t$	$\bar{t}_1^c$	$\bar{t}_2^a$
10	0,88	4,36	0,0555	13,15	1,32	1,00	0,30	0,65	1,00	0,65
20	1,17	4,67	0,093	14,57	2,91	0,96	0,20	0,58	0,98	0,60
30	1,45	5,14	0,121	15,63	4,69	0,97	0,13	0,55	0,99	0,57
40	1,62	5,49	0,140	15,20	6,08	0,95	0,08	0,52	0,98	0,54
50	1,78	5,43	0,170	16,21	8,11	0,95	0,04	0,50	0,97	0,52
60	1,95	5,58	0,189	16,46	9,88	0,92	0,02	0,47	0,96	0,51

Electro-osmotic coefficient (2ß) = 0,357 ℓ/F (slope = 0,013304 mℓ/mAh)
J_{osm} = y-intercept = 0,059376 cm/h
c_b^{max} = 2,80 mol/l
$\Delta t^c = t_1^c - t_2^c$

$\Delta t^a = t_2^a - t_1^a$
$\bar{\Delta}t$ = Average transport number of membrane pair
$\bar{t}_1^c$ = Transport number of cation through cation membrane
$\bar{t}_2^a$ = Transport number of anion through anion membrane.

Table 7.2: Electro-osmotic pumping experimental conditions and results for 0,54 mol/ℓ hydrochloric acid (Selemion AMV and CMV)

Current Density	Brine concentration c_b, mol/l		Water flow	Current Efficiency	Effective Current Density	Transport Numbers				
I, mA/cm²	$c_{b\,exp.}$	$c_{b\,calc.}$	J, cm/h	e_p, %	I_{eff}, mA/cm²	Δt^c	Δt^a	$\bar{\Delta}t$	$\bar{t}_1^c$	$\bar{t}_2^a$
10	1,07	4,42	0,047	13,40	1,34	0,96	0,15	0,56	0,98	0,58
20	1,37	4,99	0,074	13,60	2,72	0,95	0,04	0,50	0,97	0,52
30	1,58	5,17	0,103	15,58	4,37	0,92	0,02	0,47	0,96	0,51
40	1,75	5,33	0,126	14,73	5,89	0,90	0,02	0,46	0,95	0,51
50	1,91	5,96	0,155	15,85	7,93	0,90	0,06	0,48	0,95	0,53
60	2,05	6,16	0,176	16,10	9,66	0,90	0,08	0,49	0,95	0,54

Electro-osmotic coefficient (2ß) = 0,371 ℓ/F (slope = 0,0138374 mℓ/mAh)
J_{osm} = y-intercept = 0,0436566 cm/h
c_b^{max} = 2,70 mol/l
$\Delta t^c = t_1^c - t_2^c$

$\Delta t^a = t_2^a - t_1 a$
$\bar{\Delta}t$ = Average transport number of membrane pair
$\bar{t}_1^c$ = Transport number of cation through cation membrane
$\bar{t}_2^a$ = Transport number of anion through anion membrane.

Table 7.3: Electro-osmotic pumping experimental conditions and results for 1,0 mol/ℓ hydrochloric acid (Selemion AMV and CMV)

Current Density	Brine concentration c_b, mol/l		Water flow	Current Efficiency	Effective Current Density	Transport Numbers				
I, mA/cm²	$c_{b\,exp.}$	$c_{b\,calc.}$	J, cm/h	e_p, %	I_{eff}, mA/cm²	Δt^c	Δt^a	$\bar{\Delta}t$	$\bar{t}_1^c$	$\bar{t}_2^a$
10	1,36	5,39	0,0336	12,40	1,24	0,88	0,09	0,49	0,94	0,55
20	1,62	5,63	0,0608	13,17	2,63	0,81	0,11	0,46	0,91	0,55
30	1,79	5,51	0,0940	15,03	4,51	0,82	0,11	0,46	0,91	0,55
40	1,97	7,03	0,1095	14,45	5,78	0,87	0,17	0,52	0,93	0,58
50	2,15	6,82	0,1280	14,69	7,35	0,81	0,13	0,47	0,90	0,57
60	2,29	7,65	0,1480	15,20	9,12	0,82	0,19	0,51	0,91	0,60
70	2,42	8,04	0,1630	15,10	10,57	0,82	0,18	0,50	0,91	0,59

Electro-osmotic coefficient (2ß) = 0,306 ℓ/F (slope = 0,011409 mℓ/mAh)
J_{osm} = y-intercept = 0,043319 cm/h
c_b^{max} = 3,27 mol/l
$\Delta t^c = t_1^c - t_2^c$

$\Delta t^a = t_2^a - t_1^a$
$\bar{\Delta}t$ = Average transport number of membrane pair
$\bar{t}_1^c$ = Transport number of cation through cation membrane
$\bar{t}_2^a$ = Transport number of anion through anion membrane.

Table 7.4: Electro-osmotic pumping experimental conditions and results for 0,05 mol/ℓ hydrochloric acid (Selemion AAV and CHV)

Current Density	Brine concentration c_b, mol/l		Water flow	Current Efficiency	Effective Current Density	Transport Numbers				
I, mA/cm²	$c_{b\ exp.}$	$c_{b\ calc.}$	J, cm/h	ϵ_p, %	I_{eff}, mA/cm²	Δt^c	Δt^a	$\bar{\Delta t}$	$\bar{t}_1^c$	$\bar{t}_2^a$
10	2,59	4,88	0,062	42,91	4,29	0,95	0,67	0,81	0,98	0,83
20	3,25	6,13	0,093	40,38	8,08	0,91	0,61	0,76	0,96	0,81
30	3,69	6,83	0,123	40,66	12,20	0,91	0,59	0,75	0,95	0,80
40	4,12	7,66	0,141	39,01	15,60	0,90	0,55	0,72	0,95	0,77
50	4,45	8,27	0,160	38,16	19,08	0,89	0,53	0,71	0,94	0,76
60	4,70	9,64	0,178	37,41	22,45	0,88	0,49	0,69	0,94	0,75
70	5,01	9,04	0,196	37,52	26,26	0,87	0,49	0,68	0,93	0,74

Electro-osmotic coefficient (2ß) = 0,140 ℓ/F (slope = 0,00523 mℓ/mAh)
J_{osm} = y-intercept = 0,059609 cm/h
c_b^{max} = 7,14 mol/l
$\Delta t^c = t_1^c - t_2^c$

$\Delta t^a = t_2^a - t_1^a$
$\bar{\Delta t}$ = Average transport number of membrane pair
$\bar{t}_1^c$ = Transport number of cation through cation membrane
$\bar{t}_2^a$ = Transport number of anion through anion membrane.

Table 7.5 : Electro-osmotic pumping experimental conditions and results for 0,1 mol/ℓ hydrochloric acid (Selemion AAV and CHV)

Current Density	Brine concentration c_b, mol/l		Water flow	Current Efficiency	Effective Current Density	Transport Numbers				
I, mA/cm²	$c_{b\ exp.}$	$c_{b\ calc.}$	J, cm/h	ϵ_p, %	I_{eff}, mA/cm²	Δt^c	Δt^a	$\bar{\Delta t}$	$\bar{t}_1^c$	$\bar{t}_2^a$
10	2,68	5,12	0,060	43,4	4,34	0,94	0,71	0,83	0,97	0,85
20	3,36	6,76	0,086	38,88	7,78	0,91	0,64	0,78	0,96	0,82
30	3,84	7,17	0,117	40,05	12,02	0,90	0,59	0,75	0,95	0,80
40	4,41	7,86	0,140	41,36	16,54	0,89	0,59	0,74	0,94	0,79
50	4,63	8,47	0,157	38,95	19,48	0,88	0,54	0,71	0,94	0,77
60	4,87	8,67	0,180	39,05	23,43	0,88	0,51	0,70	0,94	0,76
70	5,12	8,64	0,211	41,29	28,90	0,88	0,51	0,70	0,94	0,76
80	5,33	9,03	0,225	40,18	32,14	0,87	0,51	0,69	0,94	0,76
100	5,73	9,62	0,264	40,48	40,48	0,88	0,48	0,68	0,94	0,74

Electro-osmotic coefficient (2ß) = 0,141 ℓ/F (slope = 0,005249 mℓ/mAh)
J_{osm} = y-intercept = 0,055129 cm/h
c_b^{max} = 7,09 mol/l
$\Delta t^c = t_1^c - t_2^c$

$\Delta t^a = t_2^a - t_1^a$
$\bar{\Delta t}$ = Average transport number of membrane pair
$\bar{t}_1^c$ = Transport number of cation through cation membrane
$\bar{t}_2^a$ = Transport number of anion through anion membrane.

Table 7.6: Electro-osmotic pumping experimental conditions and results for 0,5 mol/ℓ hydrochloric acid (Selemion AAV and CHV)

Current Density	Brine concentration c_b, mol/l		Water flow	Current Efficiency	Effective Current Density	Transport Numbers				
I, mA/cm²	$c_{b\ exp.}$	$c_{b\ calc.}$	J, cm/h	ϵ_p, %	I_{eff}, mA/cm²	Δt^c	Δt^a	$\bar{\Delta t}$	$\bar{t}_1^c$	$\bar{t}_2^a$
10	2,62	5,87	0,050	35,45	3,55	0,89	0,69	0,79	0,94	0,84
20	3,53		0,089	42,24	8,45	0,87	0,62	0,75	0,94	0,81
30	4,03	6,95	0,115	41,45	12,44	0,86	0,57	0,71	0,93	0,79
40	4,39		0,138	40,65	16,26	0,81	0,56	0,70	0,92	0,78
50	4,72	8,01	0,160	40,34	20,17	0,83	0,55	0,69	0,91	0,77
60	5,10		0,173	39,33	23,60	0,82	0,52	0,67	0,91	0,76
70	5,35	8,83	0,195	39,90	27,93	0,78	0,54	0,66	0,89	0,77
80	5,67		0,213	40,46	32,37	0,84	0,59	0,71	0,92	0,80
100	5,96	8,80	0,258	41,26	41,26	0,73	0,49	0,61	0,86	0,75
120	6,35		0,289	41,08	49,30	0,82	0,47	0,64	0,91	0,73
140	6,84	9,50	0,304	39,78	55,69	0,76	0,54	0,65	0,88	0,77

Electro-osmotic coefficient (2ß) = 0,126 ℓ/F (slope = 0,004688 mℓ/mAh)
J_{osm} = y-intercept = 0,061762 cm/h
c_b^{max} = 7,93 mol/l
$\Delta t^c = t_1^c - t_2^c$

$\Delta t^a = t_2^a - t_1^a$
$\bar{\Delta t}$ = Average transport number of membrane pair
$\bar{t}_1^c$ = Transport number of cation through cation membrane
$\bar{t}_2^a$ = Transport number of anion through anion membrane.

Table 7.7: Electro-osmotic pumping experimental conditions and results for 1,0 mol/ℓ hydrochloric acid (Selemion AAV and CHV)

Current Density	Brine concentration c_b, mol/l		Water flow	Current Efficiency	Effective Current Density	Transport Numbers				
I, mA/cm²	$c_{b\,exp.}$	$c_{b\,calc.}$	J, cm/h	e_p, %	I_{eff}, mA/cm²	Δt^c	Δt^a	$\bar{\Delta}t$	$\bar{t}_1^c$	$\bar{t}_2^a$
10	2,87	5,47	0,051	39,30	3,93	0,91	0,59	0,75	0,96	0,79
20	3,58		0,085	40,89	8,18	0,82	0,56	0,69	0,91	0,78
30	4,10	6,69	0,111	40,60	12,18	0,82	0,50	0,66	0,91	0,75
40	4,63		0,135	42,00	16,80	0,80	0,50	0,65	0,90	0,75
50	5,01	7,95	0,149	40,13	20,07	0,80	0,47	0,64	0,90	0,73
60	5,31	8,08	0,172	40,85	24,51	0,81	0,44	0,62	0,90	0,72
80	5,86	8,69	0,209	40,96	32,77	0,76	0,46	0,61	0,88	0,73
100	6,19	9,50	0,245	40,73	40,73	0,75	0,50	0,62	0,88	0,75
140	7,00	10,40	0,299	40,08	56,11	0,71	0,48	0,60	0,86	0,74
180	7,44	11,42	0,351	38,94	70,09	0,70	0,49	0,60	0,85	0,75

Electro-osmotic coefficient (2ß) = 0,125 ℓ/F (slope = 0,004674 mℓ/mAh)
J_{osm} = y-intercept = 0,055604 cm/h
c_b^{max} = 8,00 mol/l
$\Delta t^c = t_1^c - t_2^c$

$\Delta t^a = t_2^a - t_1^a$
$\bar{\Delta}t$ = Average transport number of membrane pair
$\bar{t}_1^c$ = Transport number of cation through cation membrane
$\bar{t}_2^a$ = Transport number of anion through anion membrane.

Table 7.8: Electro-osmotic pumping experimental conditions and results for 0,05 mol/ℓ hydrochloric acid (ABM-3 and Selemion CHV)

Current Density	Brine concentration c_b, mol/l		Water flow	Current Efficiency	Effective Current Density	Transport Numbers				
I, mA/cm²	$c_{b\,exp.}$	$c_{b\,calc.}$	J, cm/h	e_p, %	I_{eff}, mA/cm²	Δt^c	Δt^a	$\bar{\Delta}t$	$\Delta\bar{t}_1^c$	$\Delta\bar{t}_2^a$
10	2,47	4,55	0,064	42,53	4,25	0,90	0,66	0,78	0,95	0,83
20	2,91	5,79	0,098	38,42	7,68	0,93	0,60	0,77	0,97	0,80
30	3,33	7,13	0,117	34,81	10,44	0,90	0,59	0,74	0,95	0,79
40	3,78	7,69	0,138	34,89	13,96	0,90	0,53	0,71	0,95	0,76
50	4,00	8,44	0,154	33,06	16,53	0,89	0,50	0,70	0,95	0,75
60	4,16	8,68	0,176	32.70	19,62	0,88	0,48	0,68	0,94	0,74

Electro-osmotic coefficient (2ß) = 0,171 ℓ/F (slope = 0,0063924 mℓ/mAh)
J_{osm} = y-intercept = 0,0495041 cm/h
c_b^{max} = 5,85 mol/l
$t^c = t_1^c - t_2^c$

$t^a = t_2^a - t_1^a$
$\bar{\Delta}t$ = Average transport number of membrane pair
$\bar{t}_1^c$ = Transport number of cation through cation membrane
$\bar{t}_2^a$ = Transport number of anion through anion membrane.

Table 7.9: Electro-osmotic pumping experimental conditions and results for 0,1 mol/ℓ hydrochloric acid (ABM-3 and Selemion CHV)

Current Density	Brine concentration c_b, mol/l		Water flow	Current Efficiency	Effective Current Density	Transport Numbers				
I, mA/cm²	$c_{b\,exp.}$	$c_{b\,calc.}$	J, cm/h	e_p, %	I_{eff}, mA/cm²	Δt^c	Δt^a	$\bar{\Delta}t$	$\bar{t}_1^c$	$\bar{t}_2^a$
10	2,27	4,76	0,0675	41,01	4,1	0,97	0,75	0,86	0,99	0,88
20	2,90	5,95	0,0976	37,80	7,56	0,94	0,62	0,78	0,97	0,81
30	3,41	6,80	0,119	36,32	10,90	0,92	0,52	0,72	0,96	0,76
40	3,78	7,09	0,147	37,31	14,92	0,92	0,48	0,70	0,96	0,74
50	3,99	7,46	0,166	35,42	17,71	0,90	0,43	0,66	0,95	0,71
60	4,38	9,00	0,178	34,99	20,99	0,89	0,55	0,72	0,94	0,77

Electro-osmotic coefficient (2ß) = 0,166 ℓ/F (slope = 0,0061880 mℓ/mAh)
J_{osm} = y-intercept = 0,0523128 cm/h
c_b^{max} = 6,02 mol/l
$t^c = t_1^c - t_2^c$

$t^a = t_2^a - t_1^a$
$\bar{\Delta}t$ = Average transport number of membrane pair
$\bar{t}_1^c$ = Transport number of cation through cation membrane
$\bar{t}_2^a$ = Transport number of anion through anion membrane.

Table 7.10 : Electro-osmotic pumping experimental conditions and results for 0,5 mol/ℓ hydrochloric acid (ABM-3 and Selemion CHV)

Current Density, I, mA/cm²	Brine concentration, c_b, mol/l		Water flow, J, cm/h	Current Efficiency, Ep, %	Effective Current Density, I_{eff}, mA/cm²	Transport Numbers				
	$C_{b\ exp.}$	$C_{b\ calc.}$				Δt^c	Δt^a	$\bar{\Delta}t$	$\bar{t}_1^c$	$\bar{t}_2^a$
10	2,41	4,64	0,062	40,42	4,04	0,92	0,64	0,78	0,96	0,82
20	3,04	5,70	0,093	38,05	7,61	0,90	0,53	0,71	0,95	0,76
30	3,61	6,48	0,114	36,88	11,06	0,86	0,46	0,66	0,93	0,73
40	3,97		0,138	36,65	14,64	0,85	0,40	0,62	0,92	0,70
50	4,35	7,36	0,152	35,52	17,76	0,84	0,36	0,60	0,92	0,68
70	5,30	8,52	0,172	34,95	24,47	0,82	0,30	0,56	0,91	0,65
90	5,50	8,81	0,212	34,72	31,25	0,83	0,29	0,56	0,91	0,64
110	5,95	8,76	0,252	36,09	40,14	0,82	0,26	0,54	0,91	0,63
120	6,18	8,34	0,284	37,13	48,27	0,82	0,24	0,53	0,91	0,62

Electro-osmotic coefficient (2ß) = 0,124 ℓ/F (slope = 0,0046224 mℓ/mAh)
J_{osm} = y-intercept = 0,0643752 cm/h
c_b^{max} = 8,06 mol/l
$t^c = t_1^c - t_2^c$

$t^a = t_2^a - t_1^a$
$\bar{\Delta}t$ = Average transport number of membrane pair
$\bar{t}_1^c$ = Transport number of cation through cation membrane
$\bar{t}_2^a$ = Transport number of anion through anion membrane.

Table 7.11: Electro-osmotic pumping experimental conditions and results for 1,0 mol/ℓ hydrochloric acid (ABM-3 and Selemion CHV)

Current Density I, mA/cm²	Brine concentration c_b, mol/l		Water flow J, cm/h	Current Efficiency e_p, %	Effective Current Density I_{eff}, mA/cm²	Transport Numbers				
	$c_{b\ exp.}$	$c_{b\ calc.}$				Δt^c	Δt^a	$\bar{\Delta}t$	$\bar{t}_1^c$	$\bar{t}_2^a$
20	3.05	4.07	0.145	59.558	11.911	1.00	0.57	0.79	1,00	0,78
40	4.19	5.81	0.184	51.694	20.678	0.93	0.50	0.72	0,97	0,75
60	4.66	6.41	0.238	49.634	29.780	0.93	0.44	0.68	0,96	0,71
80	5.4	7.87	0.261	47.291	37.833	0.91	0.47	0.69	0,95	0,73

Electro-osmotic coefficient (2ß) = 0,125 ℓ/F (slope = 0,0046471 mℓ/mAh)
J_{osm} = y-intercept = cm/h
c_b^{max} = 8.03 mol/l
$\Delta t^c = t_1^c - t_2^c$

$\Delta t^a = t_2^a - t_1^a$
$\bar{\Delta}t$ = Average transport number of membrane pair
$\bar{t}_1^c$ = Transport number of cation through cation membrane
$\bar{t}_2^a$ = Transport number of anion through anion membrane.

Table 7.12 : Electro-osmotic pumping experimental conditions and results for 0,05 mol/ℓ hydrochloric acid (ABM-2 and Selemion CHV)

Current Density, I, mA/cm²	Brine concentration, c_b, mol/l		Water flow, J, cm/h	Current Efficiency, E_p, %	Effective Current Density, I_{eff}, mA/cm²	Transport Numbers				
	$C_{b\ exp.}$	$C_{b\ calc}$				Δt^c	Δt^a	$\bar{\Delta}t$	$\bar{t}_1^c$	$\bar{t}_2^a$
10	3,15	5,2	0,050	42,87	4,29	0,90	0,51	0,71	0,95	0,76
20	3,92		0,076	40,01	8,00					
30	4,40	7,6	0,095	37,49	11,24	0,88	0,40	0,64	0,94	0,70
40	4,72		0,117	36,86	14,74					
50	4,80		0,143	36,81	18,40					
60	4,90	9,1	0,145	31,89	19,14	0,87	0,32	0,59	0,93	0,66

Electro-osmotic coefficient (2ß) = 0,170 ℓ/F (slope = 0,0063345 mℓ/mAh)
J_{osm} = y-intercept = 0,0245486 cm/h
c_b^{max} = 5,88 mol/l
$t^c = t_1^c - t_2^c$

$t^a = t_2^a - t_1^a$
$\bar{\Delta}t$ = Average transport number of membrane pair
$\bar{t}_1^c$ = Transport number of cation through cation membrane
$\bar{t}_2^a$ = Transport number of anion through anion membrane.

Table 7.13 : Electro-osmotic pumping experimental conditions and results for 0,1 mol/ℓ hydrochloric acid (ABM-2 and Selemion CHV)

Current Density	Brine concentration c_b, mol/l		Water flow	Current Efficiency	Effective Current Density	Transport Numbers				
I, mA/cm²	$c_{b\ exp.}$	$c_{b\ calc.}$	J, cm/h	ϵ_p, %	I_{eff}, mA/cm²	Δt^c	Δt^a	$\bar{\Delta}t$	$\bar{t}_1^c$	$\bar{t}_2^a$
10	2,1	3,3	0,091	51,13	5,11	0,96	0,65	0,81	0,97	0,82
20	2,95		0,117	46,08	9,21					
30	3,40		0,132	40,24	12,07					
40	3,82	6,8	0,146	37,29	14,91	0,88	0,45	0,66	0,94	0,55
50	4,28		0,152	34,95	17,48					
60	4,42		0,172	34,00	20,40					
80	4,82		0,198	32,08	25,6					
100	5,18	10,02	0,230	31,87	31,87	0,87	0,36	0,62	0,93	0,68

Electro-osmotic coefficient (2ß) = 0,133 ℓ/F (slope = 0,0049643 mℓ/mAh)
J_{osm} = y-intercept = 0,0704871 cm/h
c_b^{max} = 7,51 mol/l
$t^c = t_1^c - t_2^c$

$t^a = t_2^a - t_1^a$
$\bar{\Delta}t$ = Average transport number of membrane pair
$\bar{t}_1^c$ = Transport number of cation through cation membrane
$\bar{t}_2^a$ = Transport number of anion through anion membrane.

Table 7.14: Electro-osmotic pumping experimental conditions and results for 0,5 mol/ℓ hydrochloric acid (ABM-2 and Selemion CHV)

Current Density	Brine concentration c_b, mol/l		Water flow,	Current Efficiency,	Effective Current	Transport Numbers,				
I, mA/cm²	$c_{b\ exp.}$	$c_{b\ calc.}$	J, cm/h	E_p, %	Density, I_{eff}, mA/cm²	Δt^c	Δt^a	$\bar{\Delta}t$	t_1^c	t_2^a
10	2,88	4,3	0,0625	48,26	4,83	0,90	0,55	0,73	0,95	0,77
20	4,06		0,086	46,85	9,37					
30	4,44		0,1130	44,43	13,33					
40	5,02	6,3	0,127	42,81	17,12	0,82	0,25	0,53	0,90	0,62
60	5,30		0,1576	37,32	22,39					
80	5,70		0.194	37,1	29,68					
100	5,95	7,5	0,229	36,61	36,61	0,75	0,17	0,46	0,87	0,58
120	6,30		0,256	36,03	43,24					

Electro-osmotic coefficient (2ß) = 0,131 ℓ/F (slope = 0,0049116 mℓ/mAh)
J_{osm} = y-intercept = 0,0465110 cm/h
c_b^{max} = 7,6 mol/l
$\Delta t^c = t_1^c - t_2^c$

$\Delta t^a = t_2^a - t_1^a$
$\bar{\Delta}t$ = Average transport number of membrane pair
$\bar{t}_1^c$ = Transport number of cation through cation membrane
$\bar{t}_2^a$ = Transport number of anion through anion membrane.

Table 7.15 Electro-osmotic pumping experimental conditions and results for 0,05 mol/ℓ hydrochloric acid (ABM-1 and Selemion CHV)

Current Density	Brine concentration c_b, mol/l		Water flow	Current Efficiency	Effective Current Density	Transport Numbers				
I, mA/cm²	$c_{b\ exp.}$	$cC_{b\ calc.}$	J, cm/h	ϵ_p, %	I_{eff}, mA/cm²	Δt^c	Δt^a	$\bar{\Delta}t$	$\bar{t}_1^c$	$\bar{t}_2^a$
10	2,00	4,24	0,0675	36,24	3,621	0,98	0,55	0.77	0,99	0,76
20	2,65	5,86	0,0927	32,93	6,586	0,96	0,50	0.73	0,98	0.75
30	3,1		0,1336	29,35	8,805					
40	3,1		0,1456	30.267	12.106					
50	3,7		0,1483	29,425	14.712					
60	3,95	10,15	0,1509	26.645	15,987	0,92	0,45	0.68	0.96	0.72
80	4,00		0,1854	24,852	19,882					

Electro-osmotic coefficient (2ß) = 0,188 ℓ/F (slope = 0,0070105 mℓ/mAh)
J_{osm} = y-intercept = 0,0465611 cm/h
c_b^{max} = 5,32 mol/l
$\Delta t^c = t_1^c - t_2^c$

$\Delta t^a = t_2^a - t_1^a$
$\bar{\Delta}t$ = Average transport number of membrane pair
$\bar{t}_1^c$ = Transport number of cation through cation membrane
$\bar{t}_2^a$ = Transport number of anion through anion membrane.

Table 7.16 : Electro-osmotic pumping experimental conditions and results for 0,1 mol/ℓ hydrochloric acid (ABM-1 and Selemion CHV)

Current Density	Brine concentration c_b, mol/l		Water flow	Current Efficiency	Effective Current Density	Transport Numbers				
I, mA/cm²	$c_{b\ exp.}$	$c_{b\ calc.}$	J, cm/h	e_p, %	I_{eff}, mA/cm²	Δt^c	Δt^a	$\bar{\Delta t}$	$\bar{t}_1^c$	$\bar{t}_2^a$
10	2,2	3,00	0,0675	39,84	3,98	0,92	0,16	0,54	0,96	0,58
20	2,85	6,0	0,0927	35,42	7,08	0,91	0,57	0,74	0,95	0,79
30	3,3		0,1324	35,05	11,72					
40	3,5	6,6	0,1483	34,79	13,91	0,87	0,45	0,66	0,93	0,73
50	3,9		0,1655	34,62	17,31					
60	4,15	7,03	0,1942	36,02	21,6	0,86	0,35	0,61	0,93	0,68
80	4,5		0,211	31,95	25,56					
100	4,9	8,76	0,247	32,47	32,47	0,85	0,30	0,58	0,93	0,65

Electro-osmotic coefficient (2ß) = 0,152 ℓ/F (slope = 0,0056523 mℓ/mAh)
J_{osm} = y-intercept = 0,0692712 cm/h
c_b^{max} = 6,58 mol/l
$\Delta t^c = t_1^c - t_2^c$

$\Delta t^a = t_2^a - t_1^a$
$\bar{\Delta t}$ = Average transport number of membrane pair
$\bar{t}_1^c$ = Transport number of cation through cation membrane
$\bar{t}_2^a$ = Transport number of anion through anion membrane.

Table 7.17 : Electro-osmotic pumping experimental conditions and results for 0,5 mol/ℓ hydrochloric acid (ABM-1 and Selemion CHV)

Current Density	Brine concentration c_b, mol/l		Water flow	Current Efficiency	Effective Current Density	Transport Numbers				
I, mA/cm²	$c_{b\ exp.}$	$c_{b\ calc.}$	J, cm/h	e_p, %	I_{eff}, mA/cm²	Δt^c	Δt^a	Δt	$\bar{t}_1^c$	$\bar{t}_2^a$
10	2,35		0,0635	40,05	4,00					
20	2,80	5,2	0,0971	36,45	7,29	0,87	0,46	0,67	0,94	0,73
30	3,3		0,1165	34,36	10,31					
40	3,62	6,2	0,1456	35,34	14,14	0,84	0,35	0,60	0,92	0,68
60	4,2	6,2	0,1854	34,79	20,88	0,83	0,18	0,51	0,92	0,59
80	4,65		0,2119	33,02	26,42					
100	5,1	7,8	0,2613	35,73	35,73	0,79	0,12	0,46	0,90	0,56
120	5,25		0,291	34,17	41,00					

Electro-osmotic coefficient (2ß) = 0,149 ℓ/F (slope = 0,0055429 mℓ/mAh)
J_{osm} = y-intercept = 0,0647860 cm/h
c_b^{max} = 6,71 mol/l
$\Delta t^c = t_1^c - t_2^c$

$\Delta t^a = t_2^a - t_1^a$
Δt = Average transport number of membrane pair
$\bar{t}_1^c$ = Transport number of cation through cation membrane
$\bar{t}_2^a$ = Transport number of anion through anion membrane.

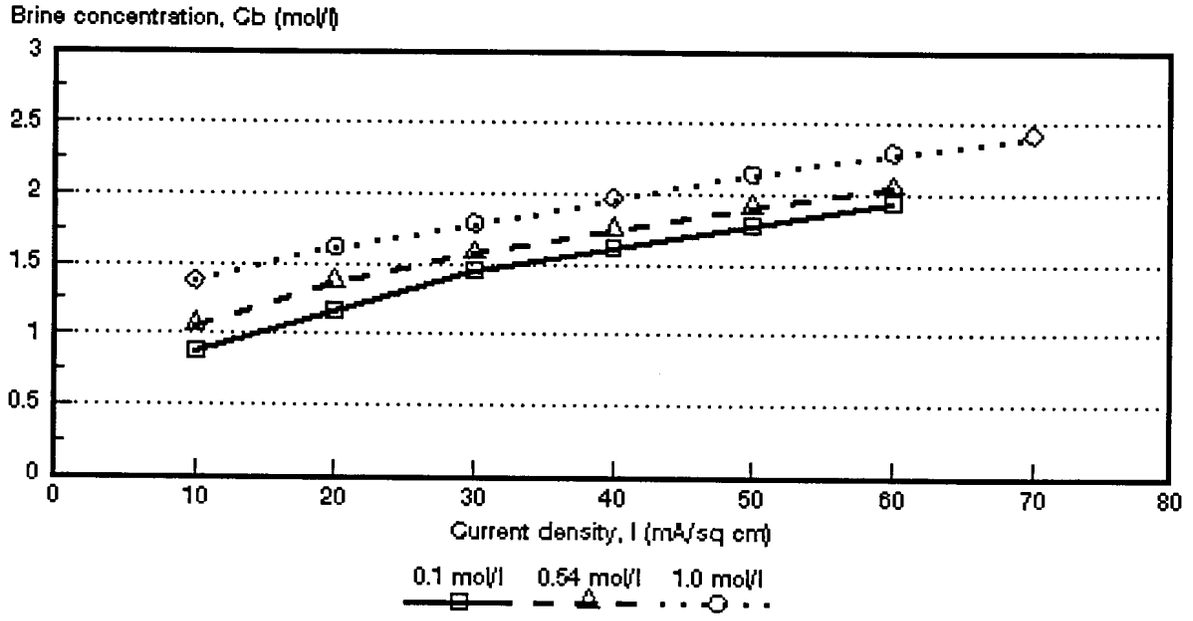

Figure 7.1: **Acid concentration as a function of current density for 3 different HCl feed concentrations. *Selemion* AMV and CMV membranes.**

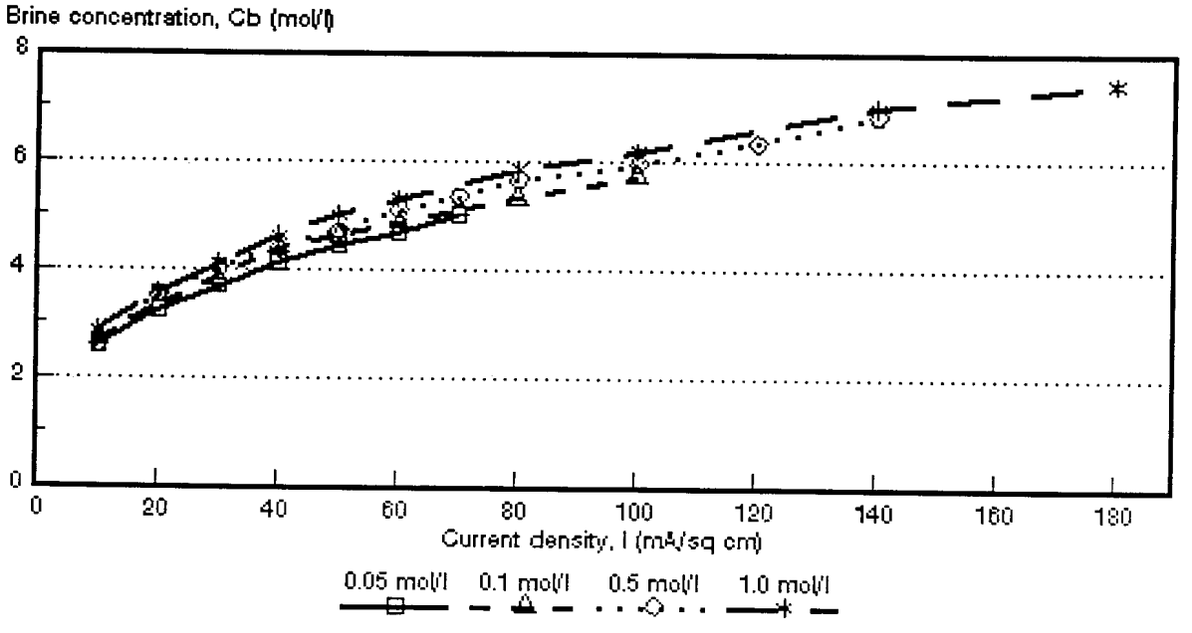

Figure 7.2: **Acid concentration as a function of current density for 4 different HCl feed concentrations. *Selemion* AAV and CHV membranes.**

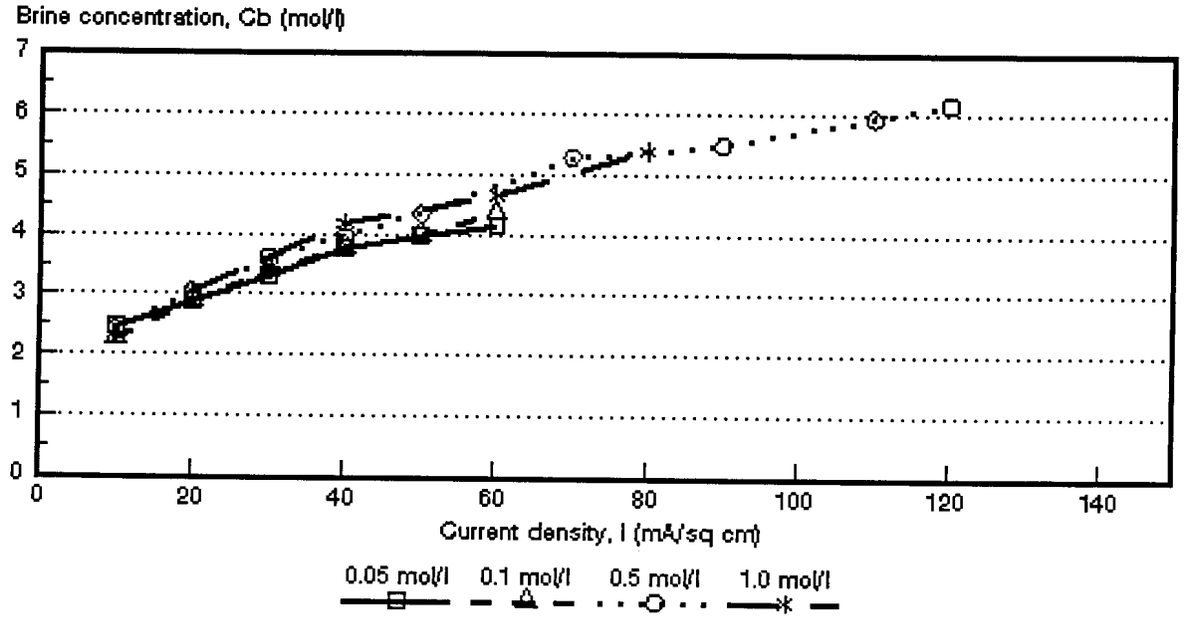

Figure 7.3: **Acid concentration as a function of current density for 3 different HCl feed concentrations. ABM-3 and *Selemion* CHV membranes.**

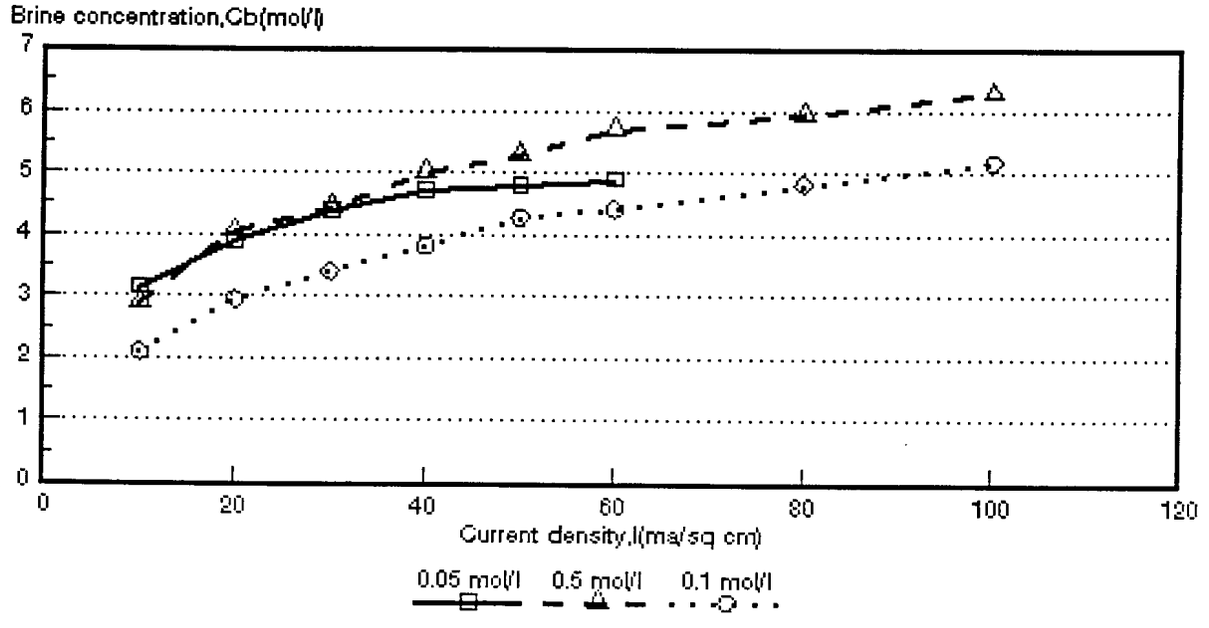

Figure 7.4 **Acid concentration as a function of current density for 3 different HCl feed concentrations. ABM-2 and *Selemion* CHV membranes.**

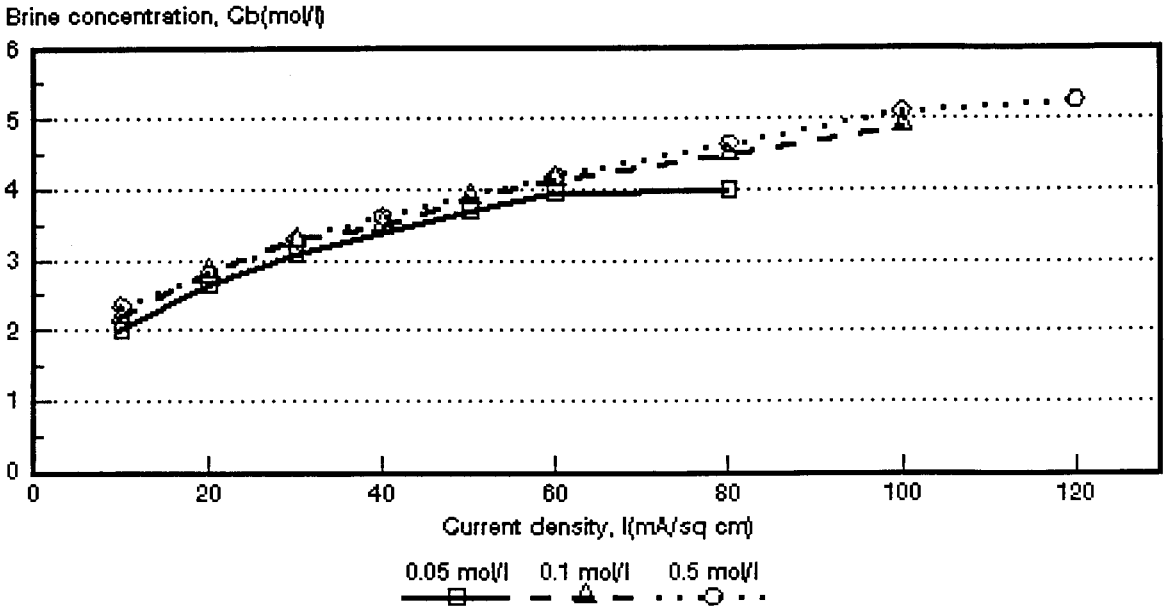

Figure 7.5: **Acid concentration as a function of current density for 3 different HCl feed concentrations. ABM-1 and *Selemion* CHV membranes.**

Table 7.18 **Acid brine concentrations obtained at the highest current densities investigated for different hydrochloric acid feed concentrations.**

Feed Concentration	Brine Concentration* (%)				
	Selemion	Selemion	Israeli & Selemion	Israeli & Selemion	Israeli & Selemion
mol/ℓ	AMV & CMV	AAV & CHV	ABM-3 & CHV	ABM-2 & CHV	ABM-1 & CHV
0,05	-	18,3	15,2	17,9	14,6
0,10	7,1	20,9	16,0	18,9	17,9
0,50**	7,5	25,0	22,6	22,9	19,2
1,0	8,8	27,2	19,7***		

* Brine concentrations obtained from the data in Tables 7.1 to 7.17.

** 0,54 mol/ℓ for AMV and CMV.

*** Lower current density.

of membrane permselectivity. Adsorbed hydrochloric acid and ion association are factors which decrease the proton leakage of anion exchange membranes[48].

It also appears as has been experienced with sodium chloride solutions that acid brine concentration will approach a maximum value, c_b^{max}. The maximum brine concentration, c_b^{max}, will be reached faster for the lower acid feed concentrations than for the higher acid feed concentrations (Figs. 7.3, 7.4 and 7.5). However, it appears that the maximum brine concentration for acid, especially at the higher acid feed concentrations, will be reached at much higher current densities than has been the case with the sodium chloride solutions. Maximum acid brine concentrations were calculated from the same relationships as used in 6.1. The results are shown in Table 7.19 and Figures 7.6 to 7.10. Very good correlations were obtained by the two methods.

The maximum acid brine concentration that can be obtained depends on the acid feed concentration. This was evident for all the membranes investigated. However, the maximum acid brine concentration remained almost constant in the case of the *Selemion* AAV and CHV membranes at 0,5 and 1,0 mol/ℓ feed concentration (Table 7.19, Fig. 7.7). The same behaviour was observed for the ABM-3 and CHV membranes (Fig. 7.8). Maximum acid brine concentration for the ABM-2-, ABM-1- and CHV membranes remained constant at 0,1 and 0,5 mol/ℓ feed concentration (Figs. 7.9 and 7.10).

Acid brine concentration at different current densities was predicted from measured transport numbers (Δt's) and volume flows with the same relationship as used in 6.1. The experimental and calculated acid brine concentrations are shown in Tables 7.1 to 7.17 and Figures 7.11 to 7.27.

The calculated acid brine concentrations were determined from the average apparent transport number of a membrane pair ($\overline{\Delta t}$). The correlations between the calculated and the experimentally determined acid brine concentrations were not satisfactory as could be seen from Figures 7.11 to 7.27 and Table 7.20. The calculated acid brine concentrations were much higher than the experimentally determined concentrations. The calculated acid brine concentrations were approximately 3 to 4 times higher for the *Selemion* AMV and CMV membranes than the experimentally determined concentrations (Table 7.20). The calculated acid brine concentrations were approximately 1,5 to 2 times higher for the *Selemion* AAV and CHV membranes than

the experimentally determined values in the feed concentration and current density ranges studied. Approximately the same results were obtained for the ABM-3, ABM-2 and ABM-1 membranes. Therefore, it appears that simple membrane potential measurements for a membrane pair ($\bar{\Delta}t$) cannot be applied effectively to predict acid brine concentration accurately. The reason for this may be ascribed to backdiffusion of acid during EOP experiments which reduces current efficiency and therefore acid brine concentration.

Table 7.19: Maximum acid brine concentration calculated from $c_b^{max} = 1/2\ F\beta^*$ and $c_b^{max} = c_b\ (1 + J_{osm}/J_{elosm})^{**}$

Feed Concentration	Maximum Acid Brine Concentration, c_b^{max} (mol/ℓ)									
	Selemion		Selemion		Israeli & Selemion		Israeli & Selemion		Israeli & Selemion	
mol/ℓ	AMV & CMV		AAV & CHV		ABM-3 & CHV		ABM-2 & CHV		ABM-1 & CHV	
	1	2	1	2	1	2	1	2	1	2
0,05			7,1	7,1	5,9	5,8	5,9	5,9	5,3	5,2
0,10	2,8	2,8	7,1	7,4	6,0	5,8	7,5	7,5	6,6	6,7
0,50	2,7	2,7	7,9	8,1	8,1	8,0	7,6	7,6	6,7	6,6
1,00	3,3	3,3	8,0	8,2	8,0	8,0				

1 : $c_b^{max} = 1/2\ F\beta$
2 : $c_b^{max} = c_b\ (1 + J_{osm}/J_{elosm})$
* : calculated from electro-osmotic coefficients (Tables 7.1 to 7.17)
** : Calculated from $J_{elosm} = J - J_{osm}$ (y-intercept and the corresponding c_b values) (Tables 7.1 to 7.17)

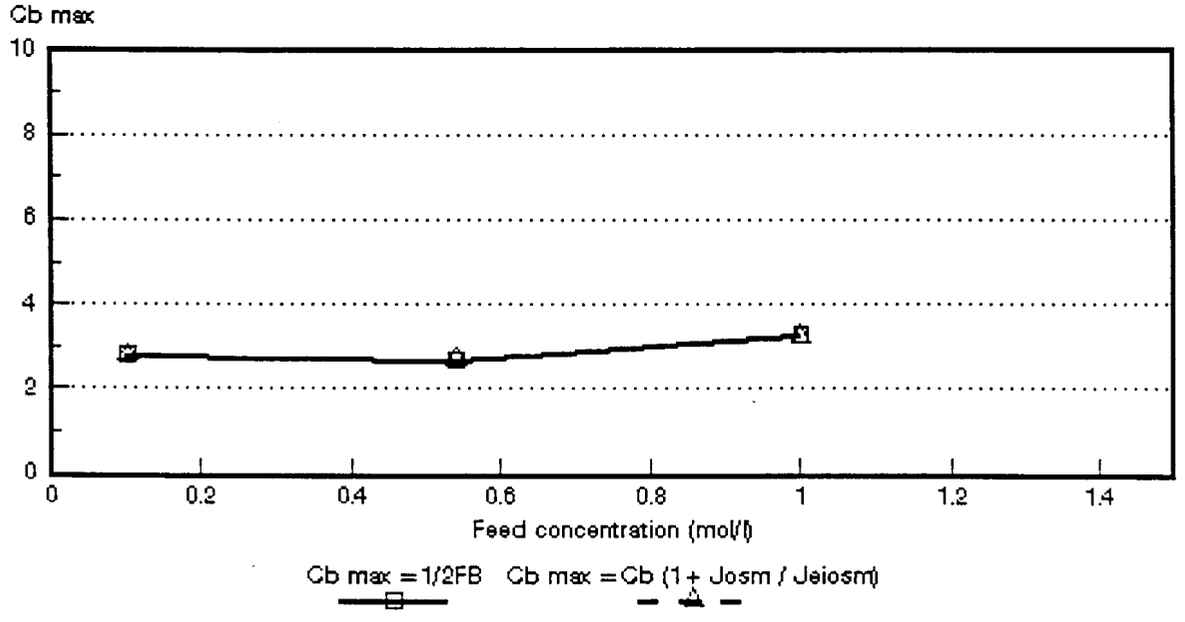

Figure 7.6: Maximum acid brine concentration as a function of feed concentration for different HCl feed concentrations. *Selemion* AMV and CMV membranes.

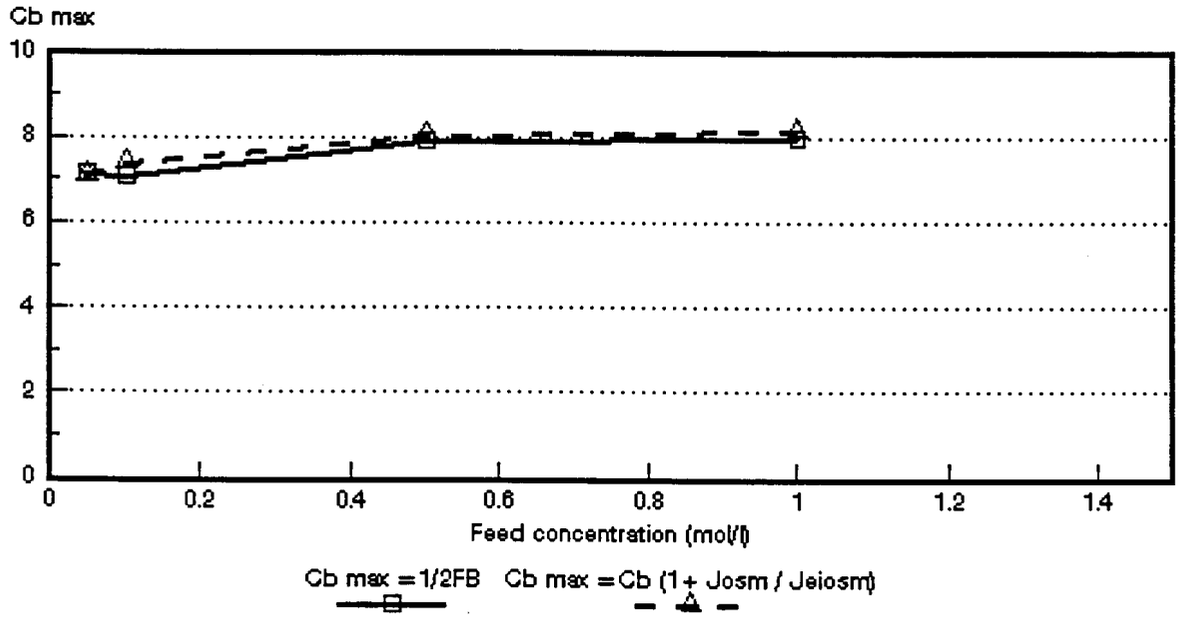

Figure 7.7: **Maximum acid brine concentration as a function of feed concentration for different HCl feed concentrations. *Selemion* AAV and CHV membranes.**

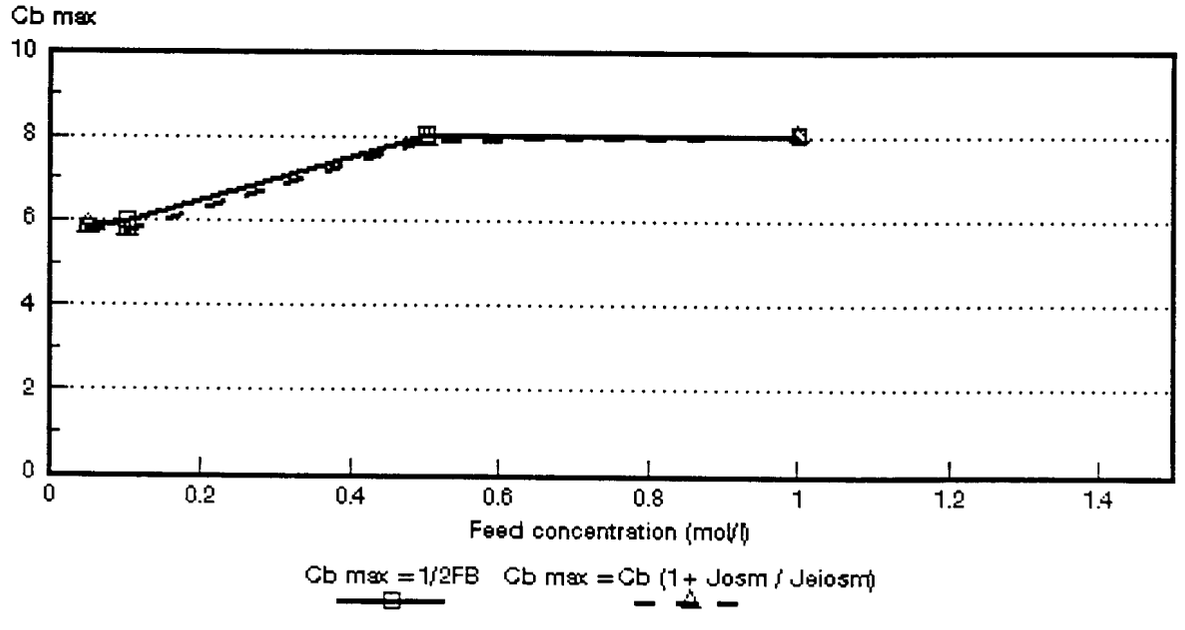

Figure 7.8: **Maximum acid brine concentration as a function of feed concentration for different HCl feed concentrations. ABM-3 and *Selemion* CHV membranes.**

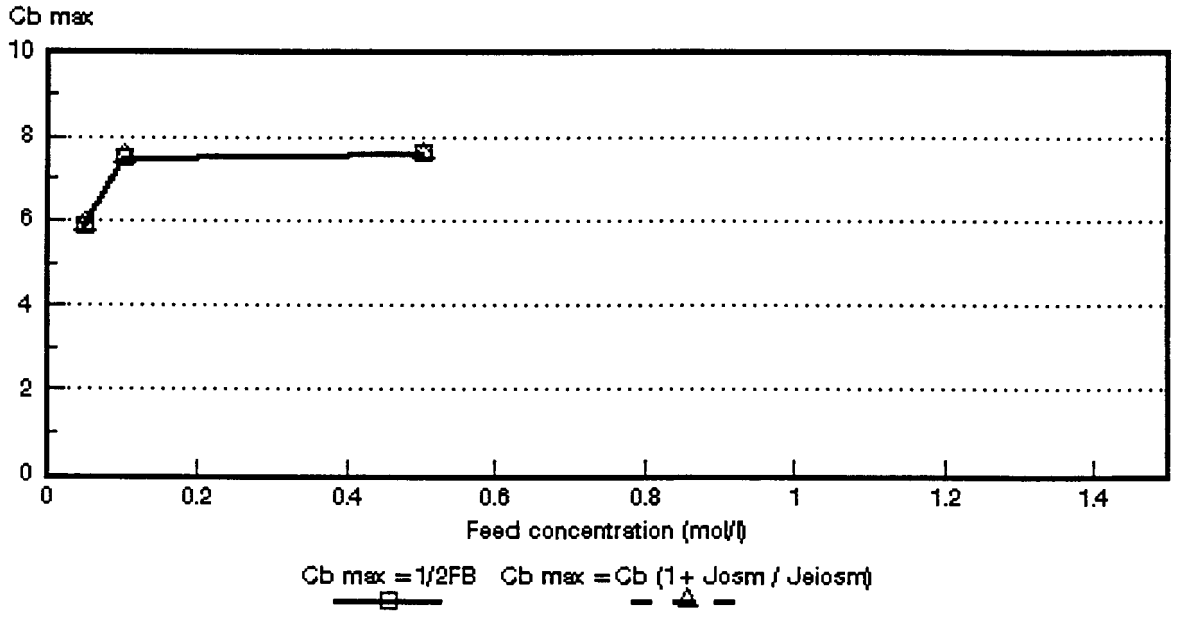

Figure 7.9: **Maximum acid brine concentration as a function of feed concentration for different HCl feed concentrations. ABM-2 and *Selemion* CHV membranes.**

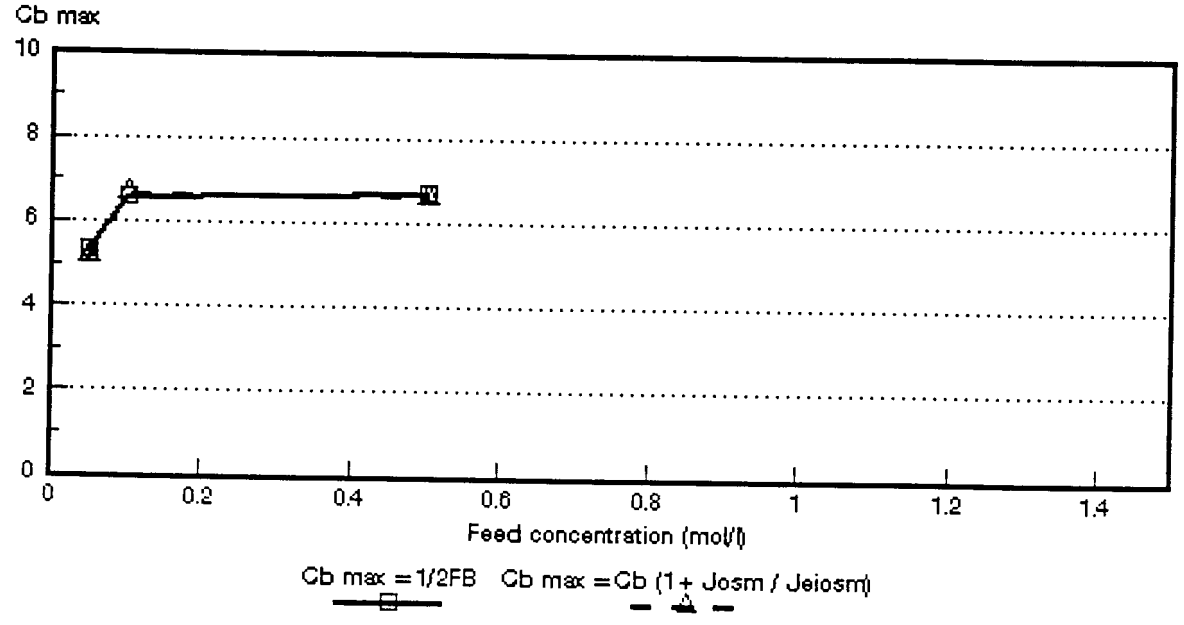

Figure 7.10: **Maximum acid brine concentration as a function of feed concentration for different HCl feed concentrations. ABM-1 and *Selemion* CHV membranes.**

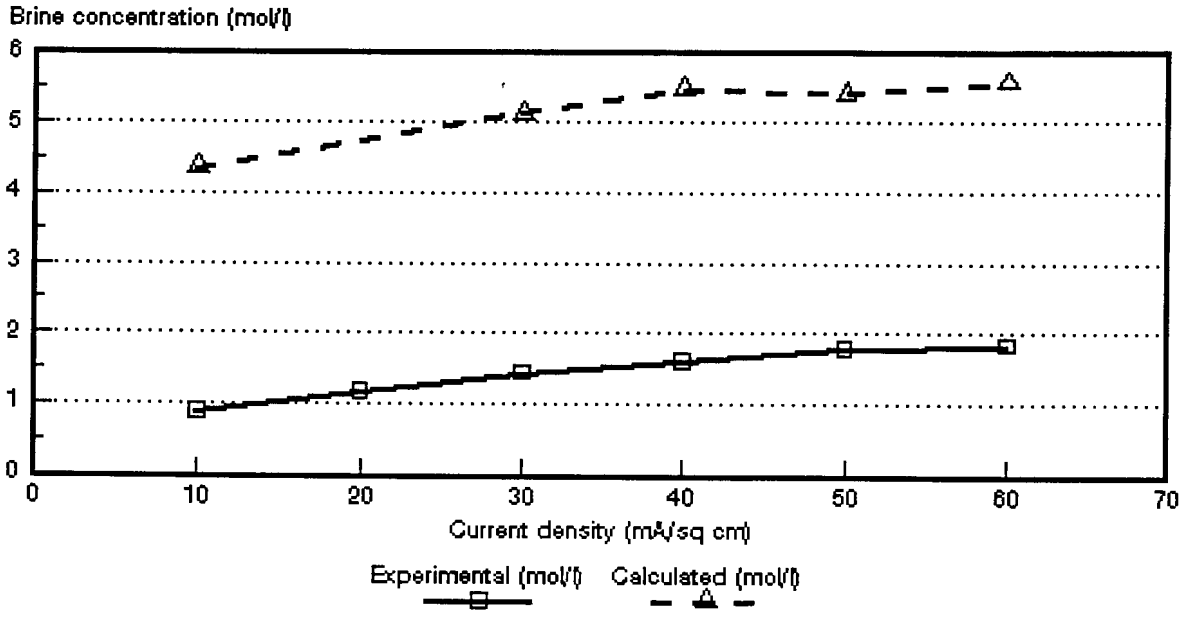

Figure 7.11: **Experimental and calculated acid brine concentrations as a function of current density for 0,1 mol/ℓ HCl feed solution. *Selemion* AMV and CMV membranes.**

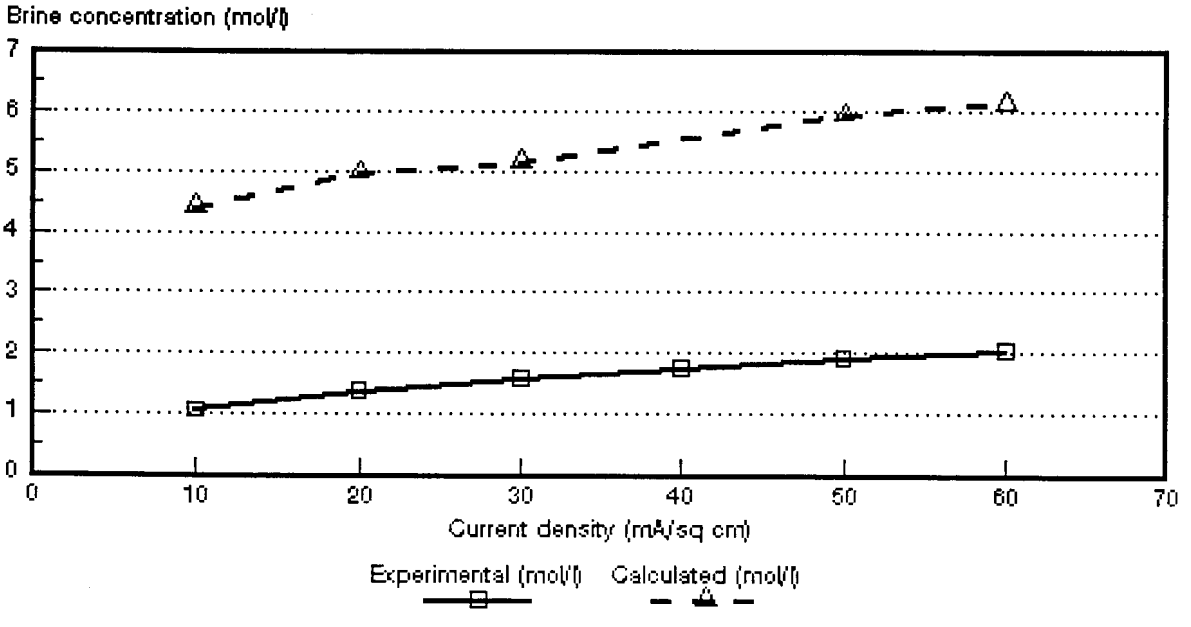

Figure 7.12: **Experimental and calculated acid brine concentrations as a function of current density for 0,54 mol/ℓ HCl feed solution. *Selemion* AMV and CMV membranes.**

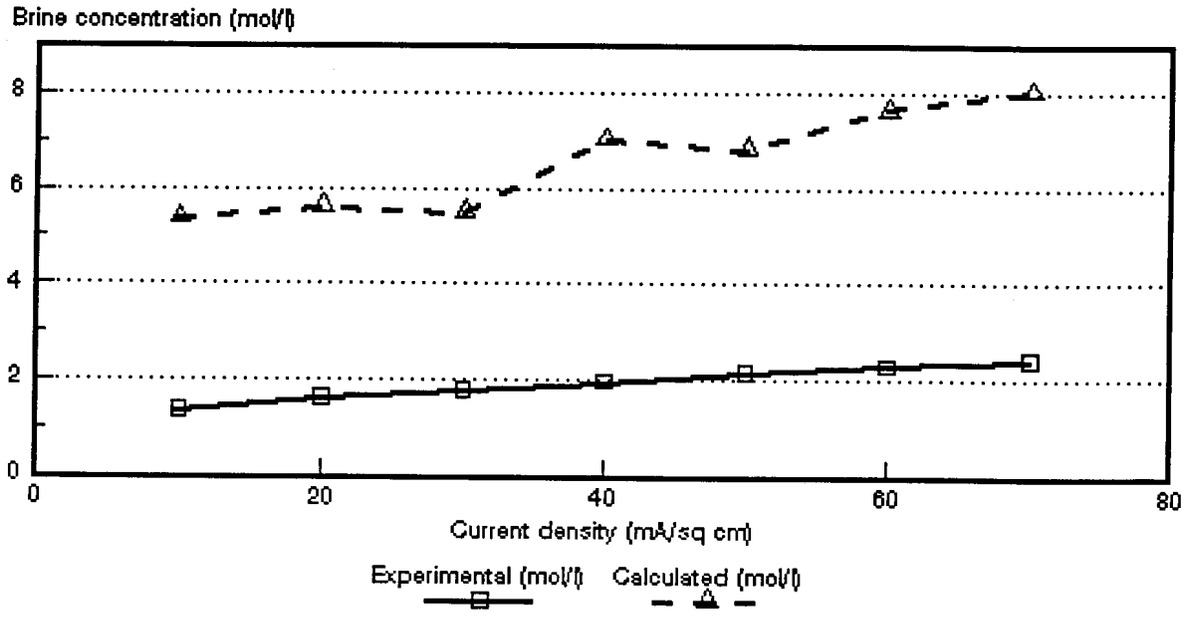

Figure 7.13: **Experimental and calculated acid brine concentrations as a function of current density for 1,0 mol/ℓ HCl feed solution. *Selemion* AMV and CMV membranes.**

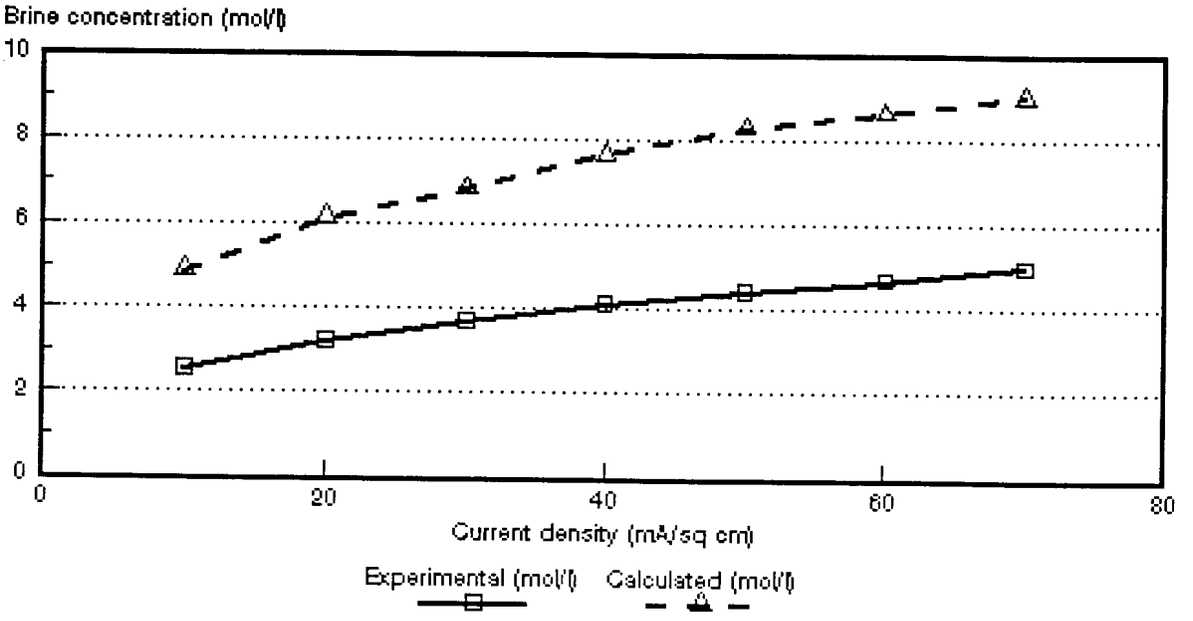

Figure 7.14: **Experimental and calculated acid brine concentrations as a function of current density for 0,05 mol/ℓ HCl feed solution. *Selemion* AAV and CHV membranes.**

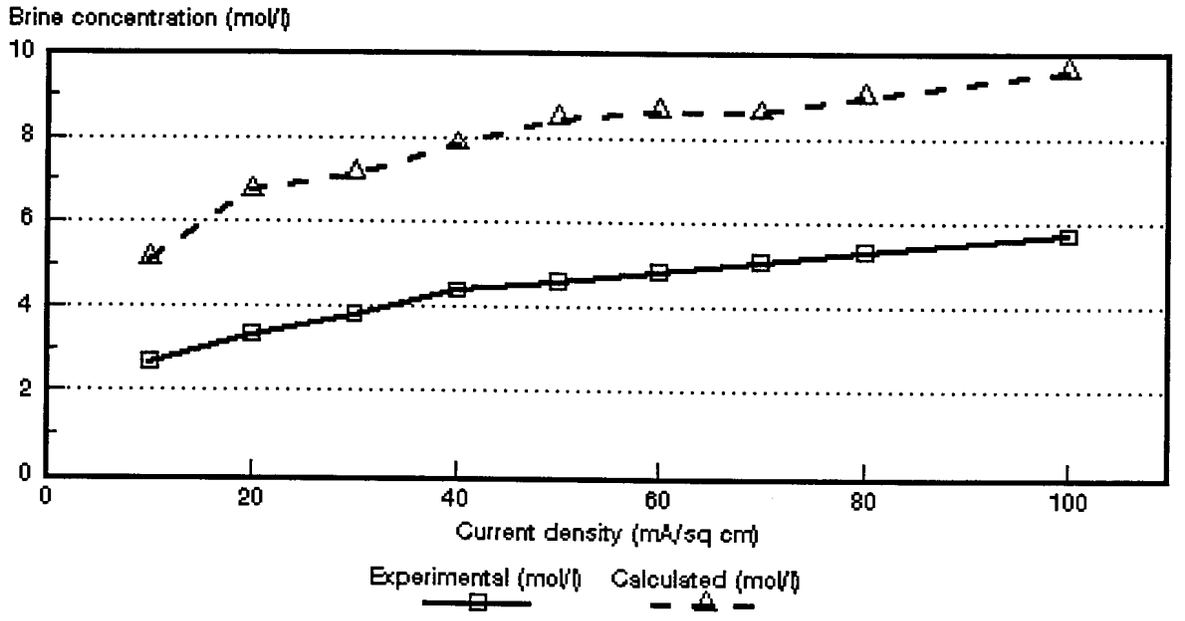

Figure 7.15: **Experimental and calculated acid brine concentrations as a function of current density for 0,1 mol/ℓ HCl feed solution. *Selemion* AAV and CHV membranes.**

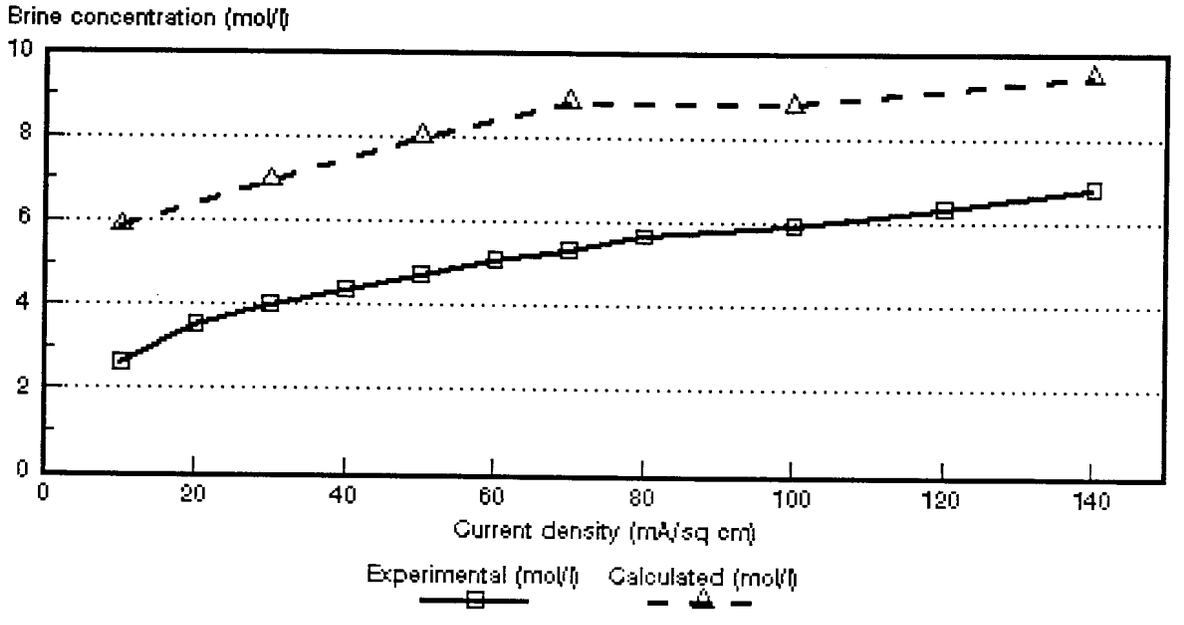

Figure 7.16: **Experimental and calculated acid brine concentrations as a function of current density for 0,5 mol/ℓ HCl feed solution. *Selemion* AAV and CHV membranes.**

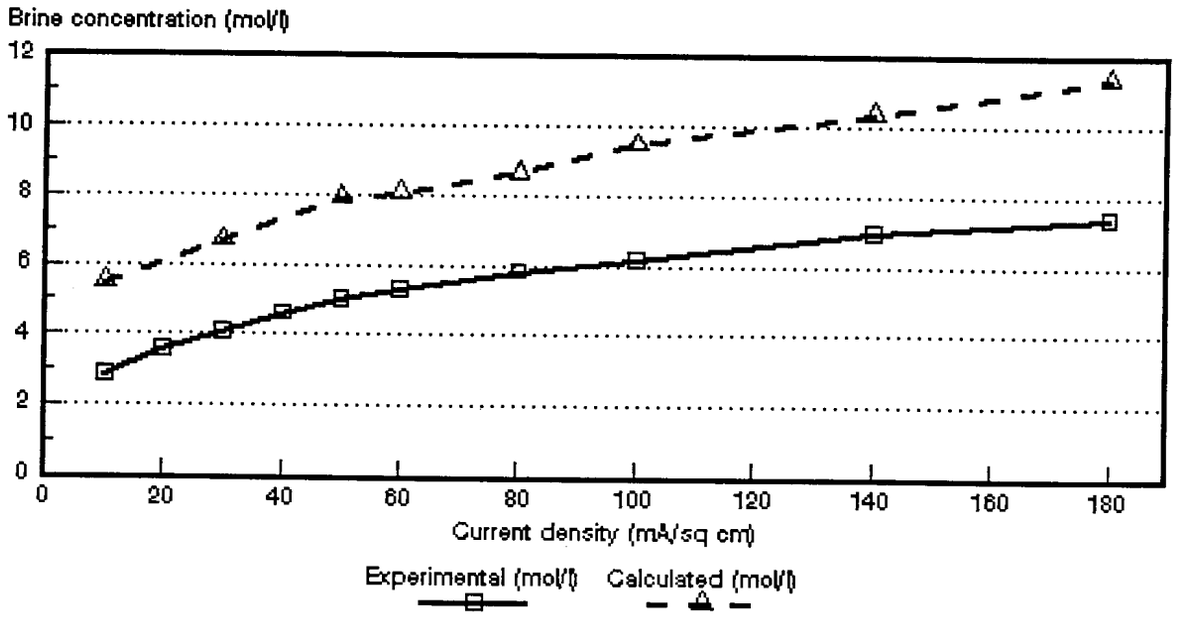

Figure 7.17: **Experimental and calculated acid brine concentrations as a function of current density for 1,0 mol/ℓ HCl feed solution. *Selemion* AAV and CHV membranes.**

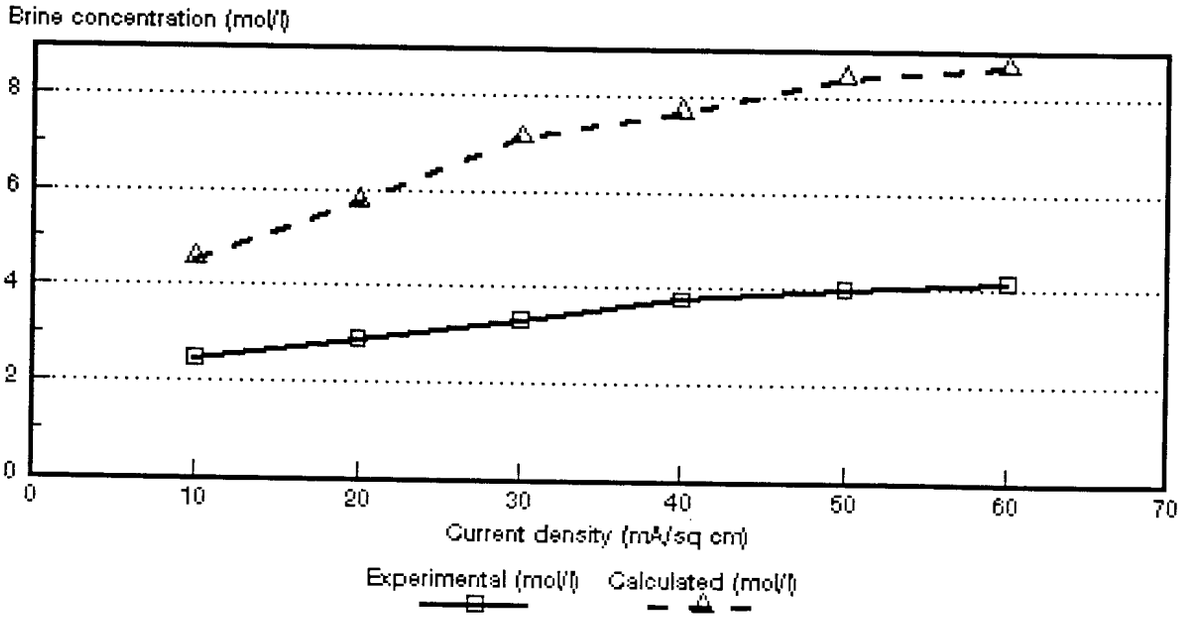

Figure 7.18: **Experimental and calculated acid brine concentrations as a function of current density for 0,05 mol/ℓ HCl feed solution. ABM-3 and CHV membranes.**

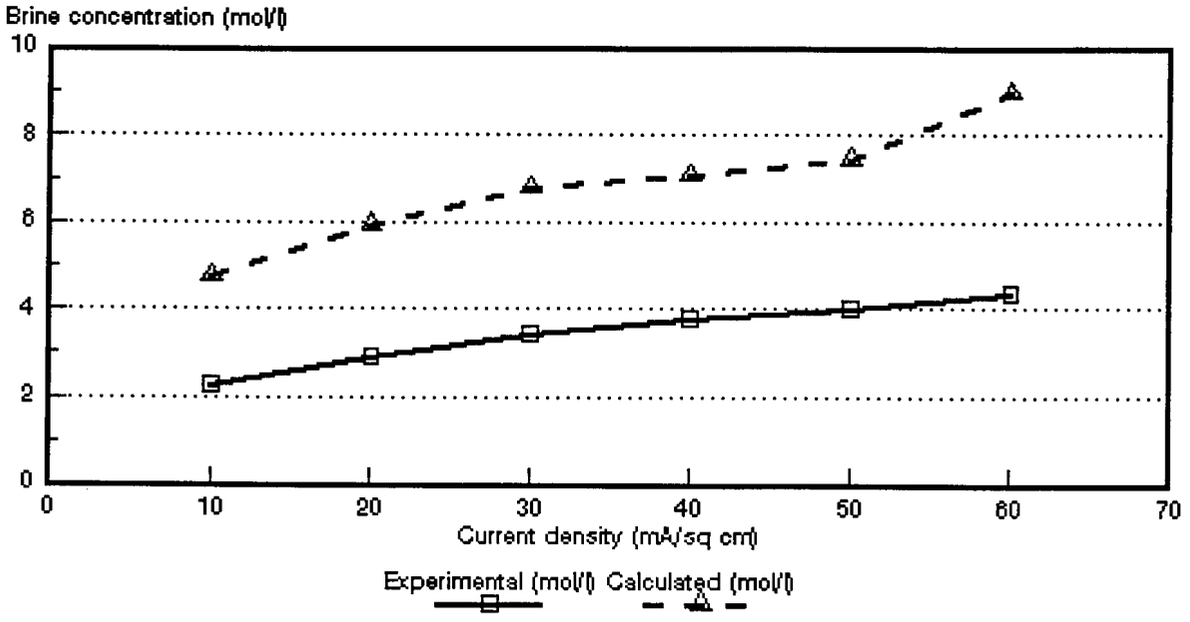

Figure 7.19: **Experimental and calculated acid brine concentrations as a function of current density for 0,1 mol/ℓ HCl feed solution. ABM-3 and CHV membranes.**

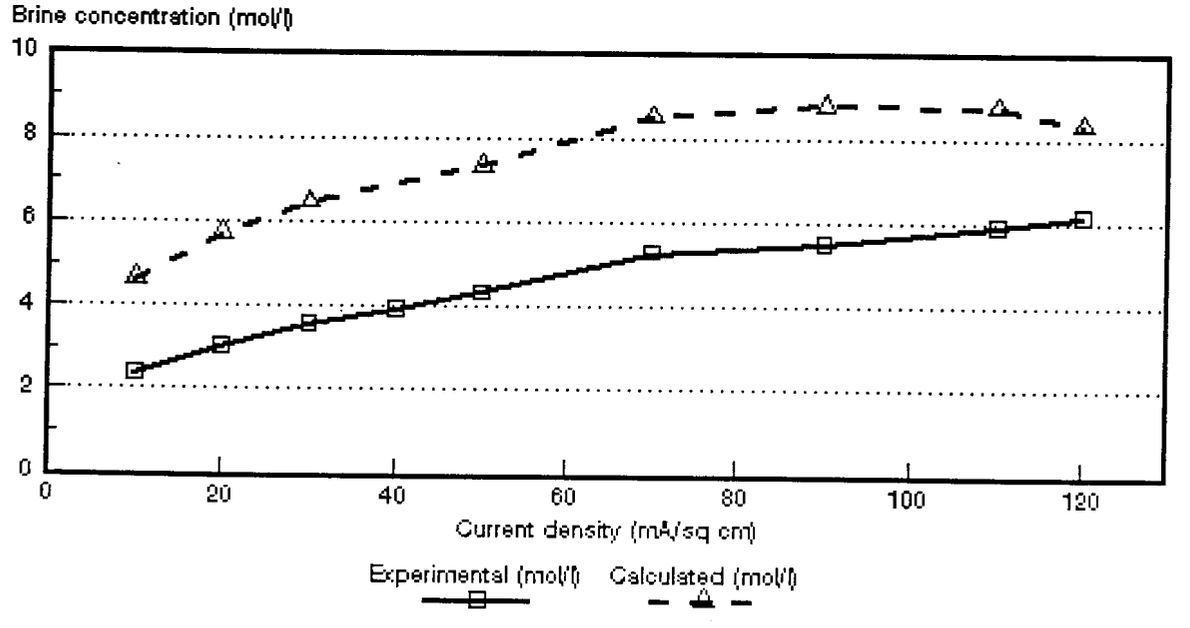

Figure 7.20: **Experimental and calculated acid brine concentrations as a function of current density for 0,5 mol/ℓ HCl feed solution. ABM-3 and CHV membranes.**

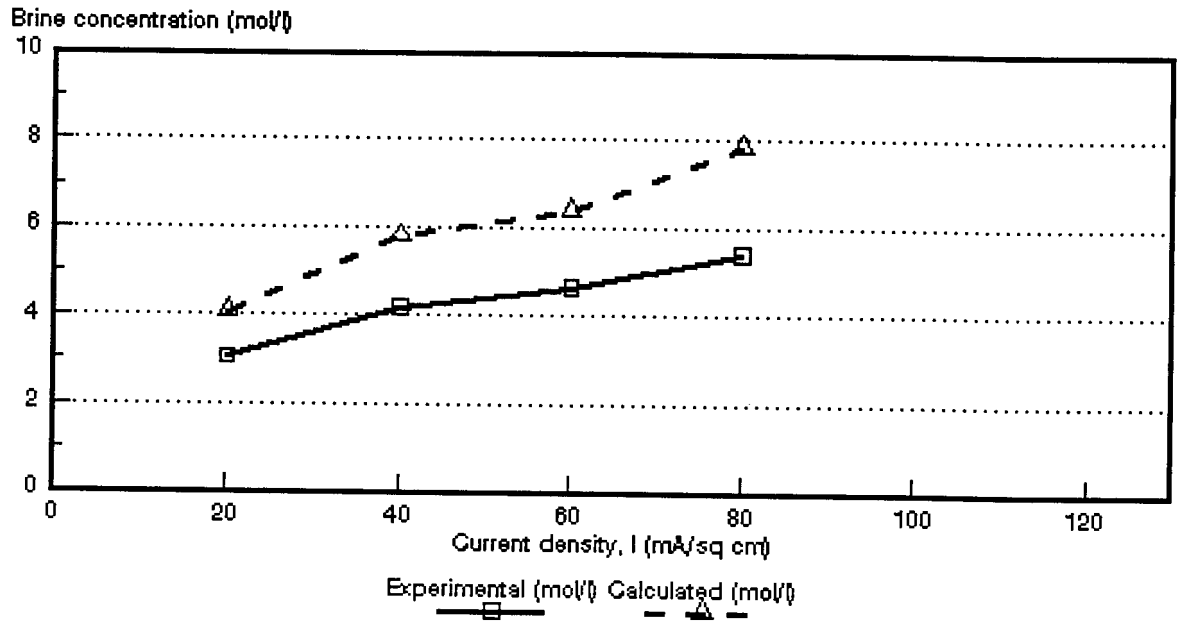

Figure 7.21: **Experimental and calculated acid brine concentrations as a function of current density for 1,0 mol/ℓ HCl feed solution. ABM-3 and CHV membranes.**

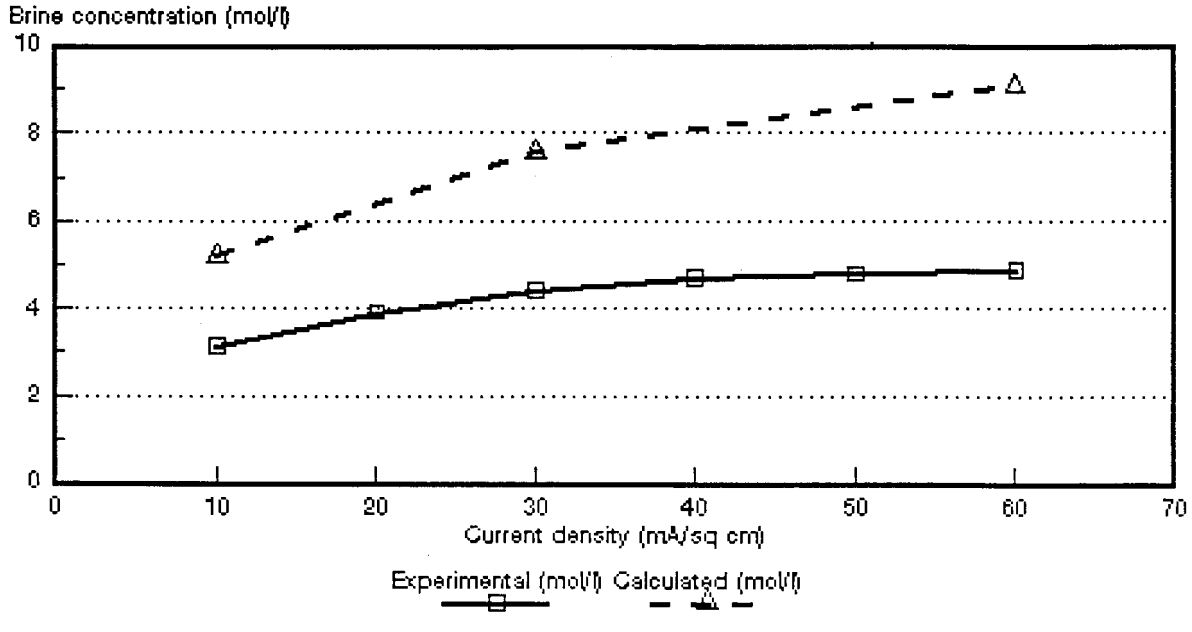

Figure 7.22: **Experimental and calculated acid brine concentrations as a function of current density for 0,05 mol/ℓ HCl feed solution. ABM-2 and CHV membranes.**

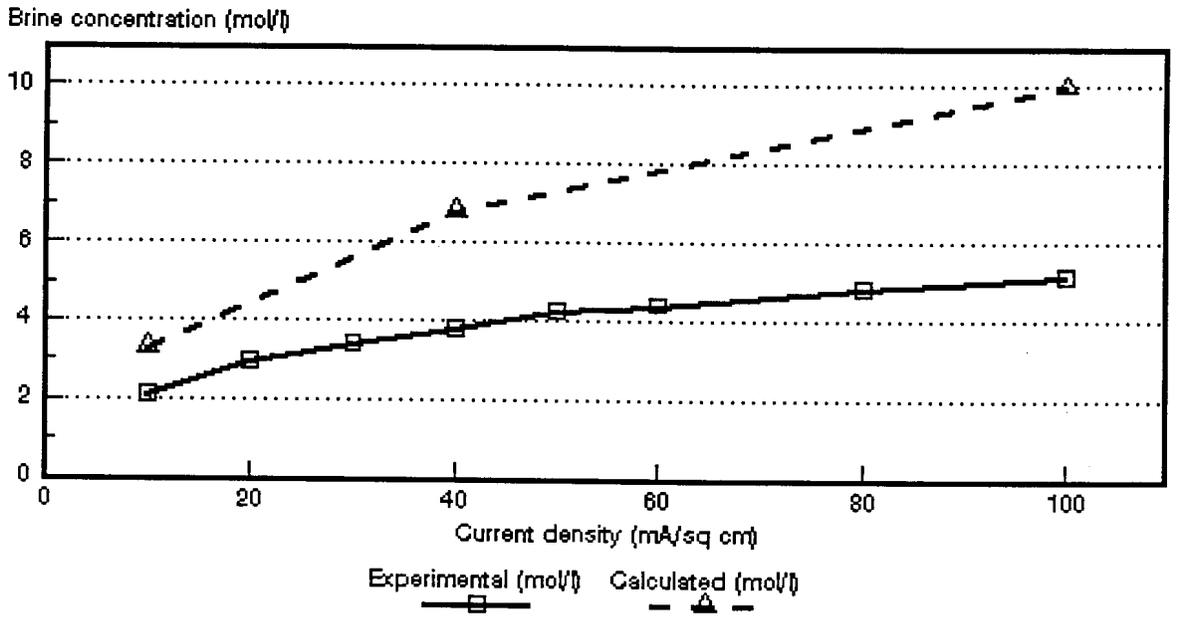

Figure 7.23: **Experimental and calculated acid brine concentrations as a function of current density for 0,1 mol/ℓ HCl feed solution. ABM-2 and CHV membranes.**

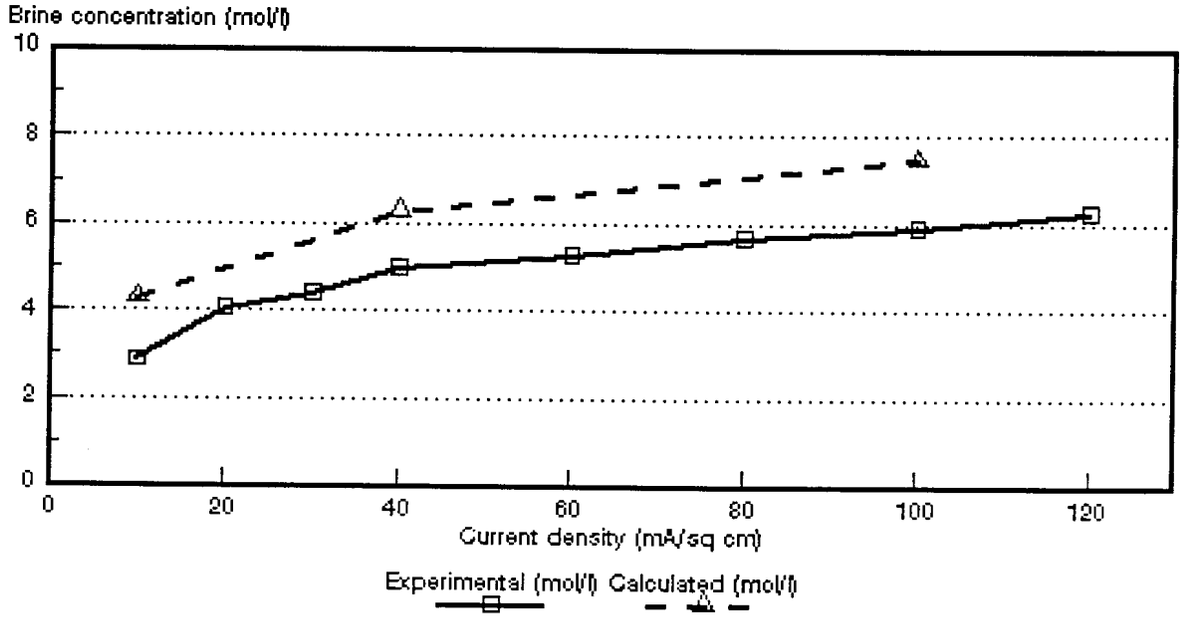

Figure 7.24: **Experimental and calculated acid brine concentrations as a function of current density for 0,5 mol/ℓ HCl feed solution. ABM-2 and CHV membranes.**

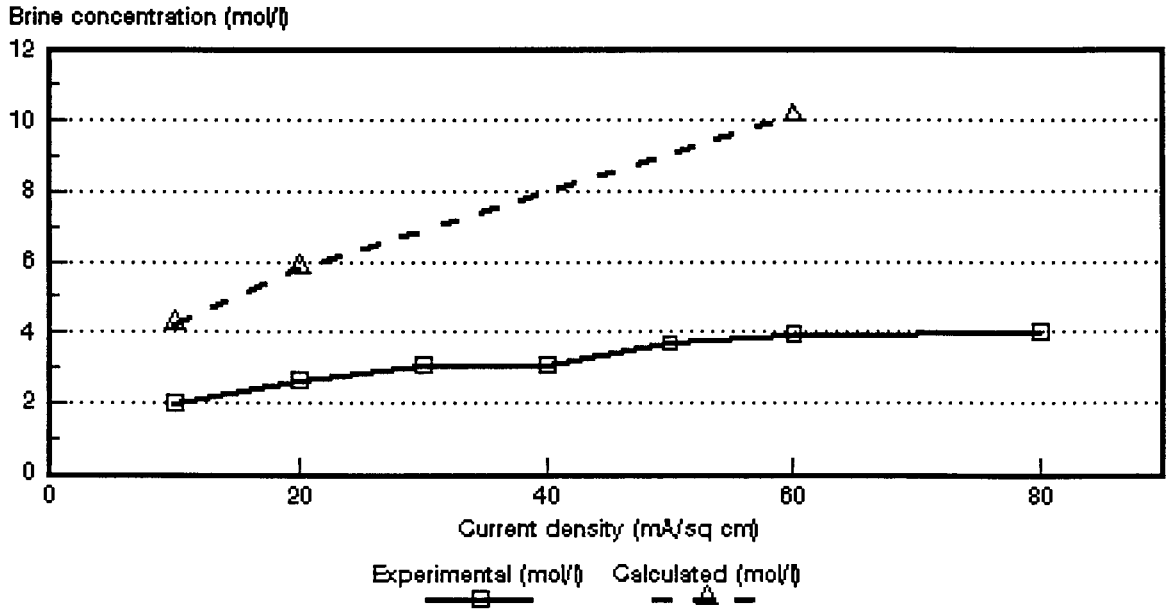

Figure 7.25: **Experimental and calculated acid brine concentrations as a function of current density for 0,05 mol/ℓ HCl feed solution. ABM-1 and CHV membranes.**

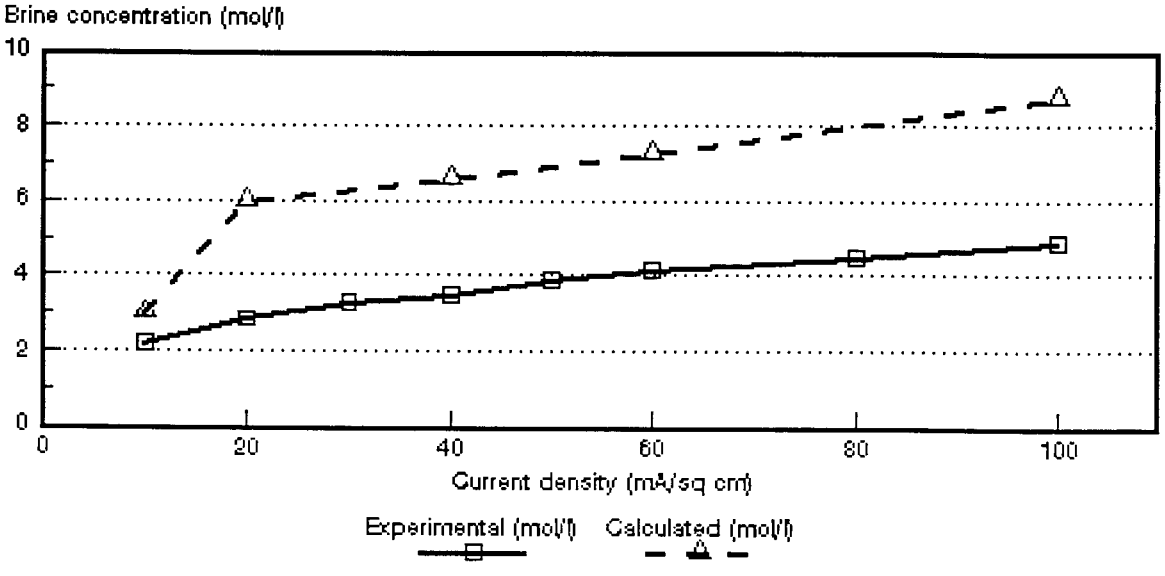

Figure 7.26: **Experimental and calculated acid brine concentrations as a function of current density for 0,1 mol/ℓ HCl feed solution. ABM-1 and CHV membranes.**

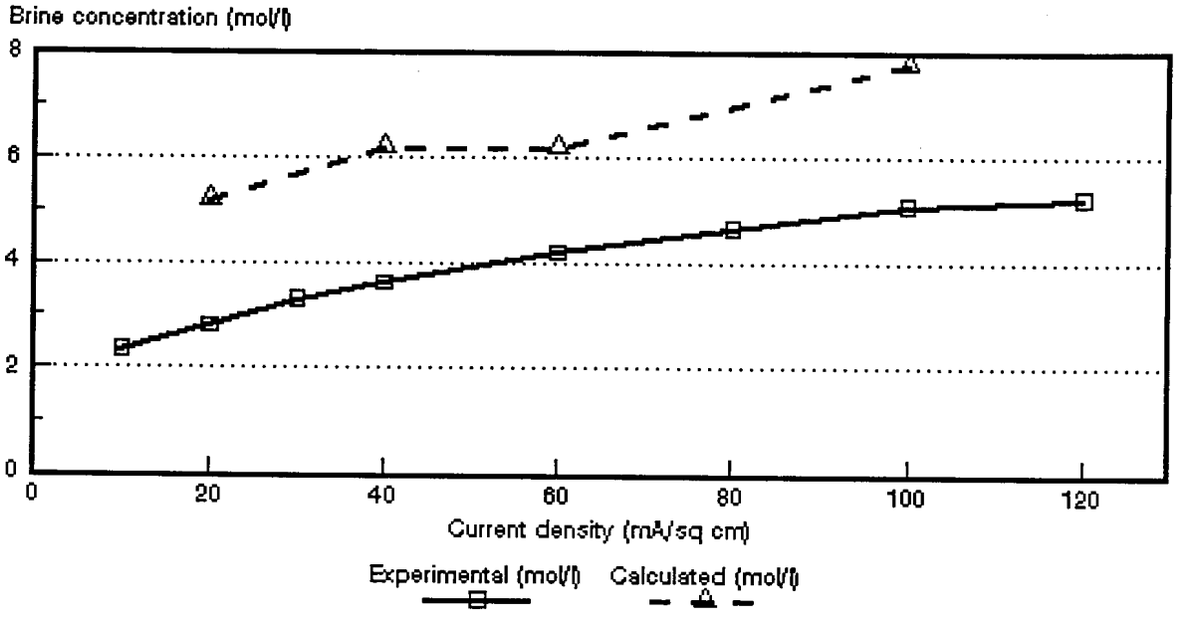

Figure 7.27: **Experimental and calculated acid brine concentrations as a function of current density for 0,5 mol/ℓ HCl feed solution. ABM-1 and CHV membranes.**

Tabel 7.20: Correlation between calculated (c_{bcalc}) and experimentally (c_{bexp}) determined acid brine concentrations.

Current Density	c_{bcalc}/c_{bexp}																			
	Selemion AMV & CMV Concentration, mol/ℓ				Selemion AAV & CHV Concentration, mol/ℓ				Israeli & Selemion ABM-3 & CHV Concentration, mol/ℓ				Israeli & Selemion ABM-2 & CHV Concentration, mol/ℓ				Israeli & Selemion ABM-1 & CHV Concentration, mol/ℓ			
mA/cm²	0,05	0,1	0,5	1,0	0,05	0,1	0,5	1,0	0,05	0,1	0,5	1,0	0,05	0,1	0,5	1,0	0,05	0,1	0,5	1,0
10		4,95	4,13	3,96	1,88	1,91	2,24	1,91	1,84	2,10	1,93		1,65	1,57	1,49		2,12	1,36		
20		3,99	3,64	3,48	1,89	2,01			2,00	2,05	1,88	1,33					2,21	2,11	1,86	
30		3,54	3,27	3,08	1,85	1,87	1,72	1,63	2,14	1,99	1,80		1,73							
40		3,39	3,05	3,57	1,86	1,78			2,03	1,88		1,39		1,78				1,89	1,71	
50		3,05	3,12	3,17	1,86	1,83	1,70	1,59	2,11	1,87	1,69				1,25					
60		2,86	3,00	3,34	2,05	1,78		1,52	2,09	2,05		1,38	1,86				2,57	1,69	1,48	
70				3,32	1,80	1,69	1,65				1,61									
80						1,69		1,48				1,46								
90											1,60									
100						1,68	1,48	1,53							1,26			1,79	1,53	
110											1,47			1,93						
120											1,35									
130																				
140							1,40	1,49												
150																				
160																				
170																				
180								1,53												

7.2 Current Efficiency

Current efficiency (ϵ_p) determined during EOP experiments as a function of current density is shown in Figures 7.28 to 7.32. Current efficiency was determined to be very low (approximately 13 to 16%) for the *Selemion* AMV and CMV membranes (Fig. 7.28). This low current efficiency can be ascribed to the low permselectivity of the *Selemion* AMV membranes for chloride ions (proton leakage) (Tables 7.1 to 7.3). The permselectivity (Δt^a) of the *Selemion* AMV membrane was shown to vary between 0,3 and 0,02 at 0,1 mol/ℓ acid feed concentration at different concentration gradients in the current density range from 10 to 60 mA/cm^2. Permselectivities varied from 0,15 to 0,08 and from 0,09 to 0,18 at 0,54 and 1,0 mol/ℓ acid feed concentration, respectively. Therefore, the *Selemion* AMV membrane has a very low permselectivity for chloride ions.

Current efficiencies obtained with the *Selemion* AAV and CHV membranes were much higher than current efficiencies obtained with the *Selemion* AMV and CMV membranes (Fig. 7.29). Current efficiency of the *Selemion* AAV and CHV membranes was determined at approximately 40%. The apparent transport numbers of the anion-exchange membrane were much higher in this case (Table 7.4 to 7.7) than in the case of the Selemion AMV membrane. The apparent transport numbers for the AAV anion-exchange membrane (Δt^a) varied between 0,67 and 0,49 at 0,05 mol/ℓ feed concentration (Table 7.4). Approximately the same values were obtained for the apparent transport number of the *Selemion* AAV membrane in the 0,1 to 1,0 mol/ℓ feed concentration range. Current efficiencies obtained for the ABM-3 and CHV membranes were slightly lower than that obtained for the *Selemion* AAV and CHV membranes in the 0,05 to 0,5 mol/ℓ feed concentration range (Fig. 7.30). Current efficiency was determined at approximately 37%. However, current efficiency for the ABM-3 and CHV membranes was much higher at 1,0 mol/ℓ feed concentration. Current efficiency varied between 60 and 47%. Current efficiency for the ABM-2 and CHV membranes was initially higher than 40% (Fig. 7.31) but then decreased to between 30 and 40%. Current efficiency for the ABM-1 and CHV membranes was determined at between 25 and 40%. It is interesting to note that current efficiency has increased with increasing acid feed concentration in the case of the ABM and CHV membranes.

Current efficiency remained almost constant with increasing current density and increasing acid feed concentration in the case of the *Selemion* AMV and CMV and

Selemion AAV and CHV membranes (Figs. 7.28 and 7.29). However, current efficiency decreased somewhat with increasing current density in the case of the ABM-3, ABM-2 and ABM-1 membranes (Fig's. 7.30 to 7.32). This was more pronounced at the lower acid feed concentrations. Therefore, it appeared that the limiting current density was exceeded. However, current efficiency remained approximately constant at the higher acid feed concentrations (0,5 mol/ℓ) at high current densities showing that polarization was absent.

The apparent transport numbers ($\bar{\Delta}t$, Δt^a and Δt^c) for a concentration difference similar to that obtained in the EOP experiments are shown in Figures 7.33 to 7.49. The current efficiencies (ϵ_p) as determined by the EOP method and shown in Figures 7.28 to 7.32 are also shown in Figures 7.33 to 7.49. The correlation between the apparent transport numbers ($\bar{\Delta}t$, Δt^a, Δt^c) and current efficiency is shown in Tables 7.21 to 7.23.

The apparent transport numbers ($\bar{\Delta}t$'s) were much higher than the current efficiencies (ϵ_p's) as determined by the EOP method (Tables 7.21 to 7.23 and Figs. 7.33 to 7.49). The apparent transport numbers were from 3 to 5 times higher than the current efficiencies in the case of the *Selemion* AMV and CMV membranes in the acid feed concentration and current density ranges investigated (Table 7.21). In the case of the Selemion AAV and CHV membranes the apparent transport numbers were 1,5 to 2 times higher than the current efficiencies. Much the same results were found for the ABM and CHV membranes. Therefore, it appears that a simple membrane potential measurement cannot be used effectively in the case of acids to predict membrane performance accurately. The reason for the big difference between the apparent transport number and the current efficiency may be ascribed to backdiffusion of acid during EOP of acids.

It is interesting to note that much better correlations have been obtained between the apparent transport numbers of the anion membranes (Δt^a) and current efficiencies (Table 7.22). The apparent transport numbers were approximately 1,3 to 1,4 times higher than the current efficiencies in the case of the *Selemion* AAV and CHV membranes in the current density range from 30 to 70 mA/cm^2 (0,5 mol/ℓ feed). An even better correlation was obtained at 1,0 mol/ℓ feed concentration in the current density range from 40 to 140 mA/cm^2. The apparent transport numbers were from 1,05 to 1,19 times higher than current efficiencies in this range. The ratio between apparent transport number and current efficiency ($\Delta t^a/\epsilon_p$) varied between 1,22 and 0,86 for the ABM-3 and CHV membranes in the current density range from 30 to 70

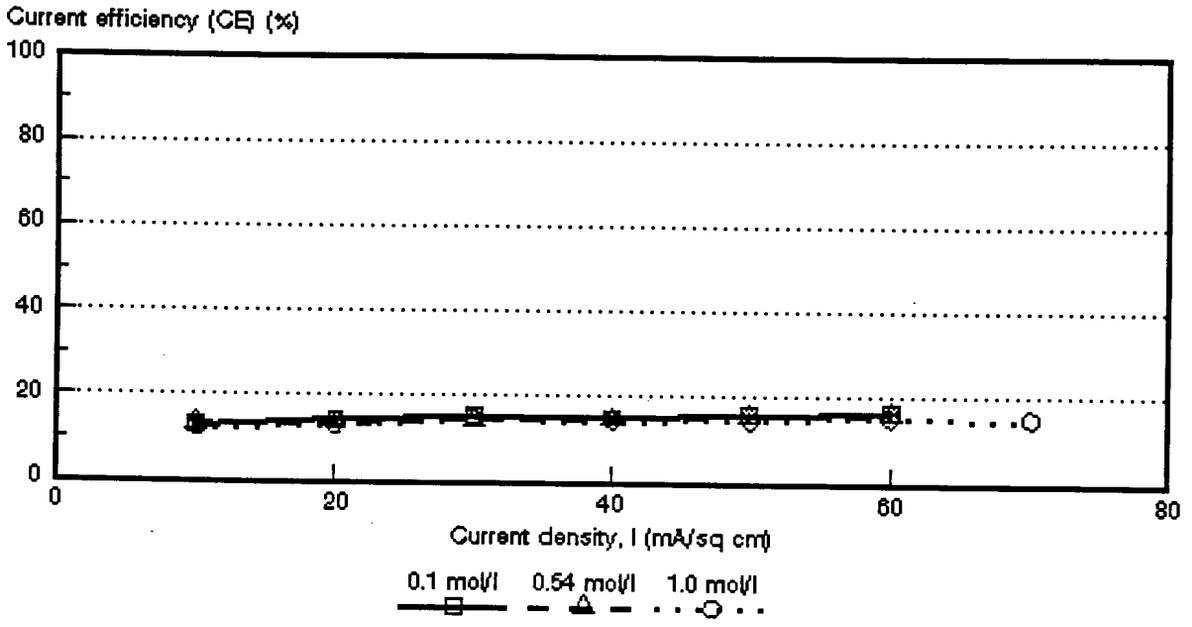

Figure 7.28: **Current efficiency (ϵ_p) as a function of current density for 3 different HCl feed concentrations. *Selemion* AMV and CMV membranes.**

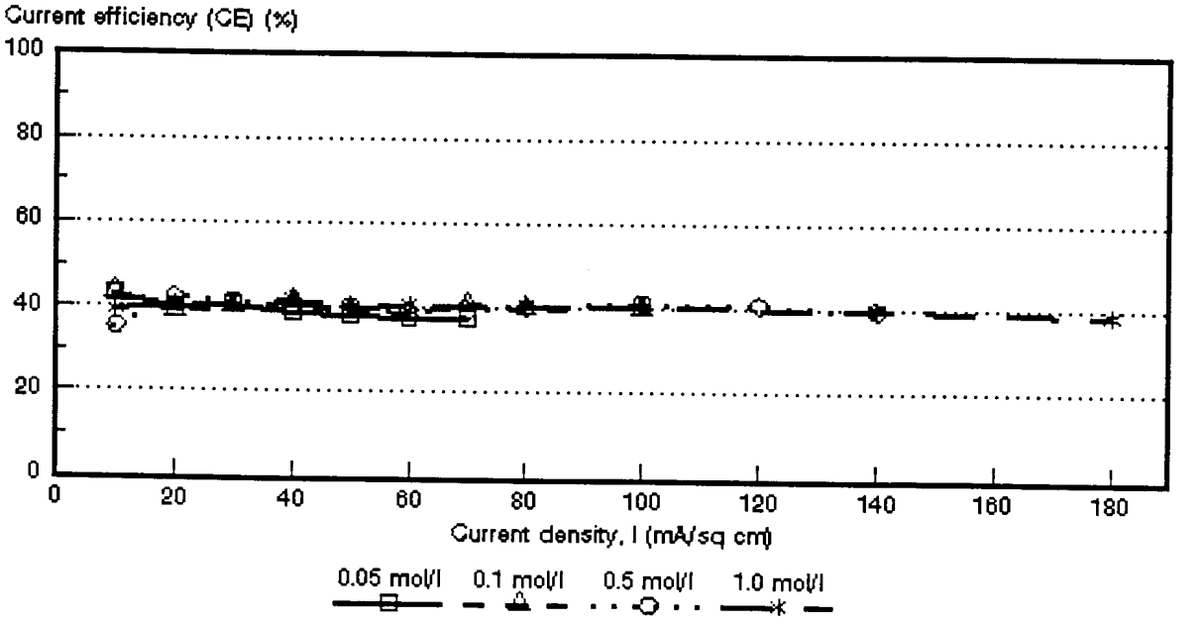

Figure 7.29: **Current efficiency (ϵ_p) as a function of current density for 4 different HCl feed concentrations. *Selemion* AAV and CHV membranes.**

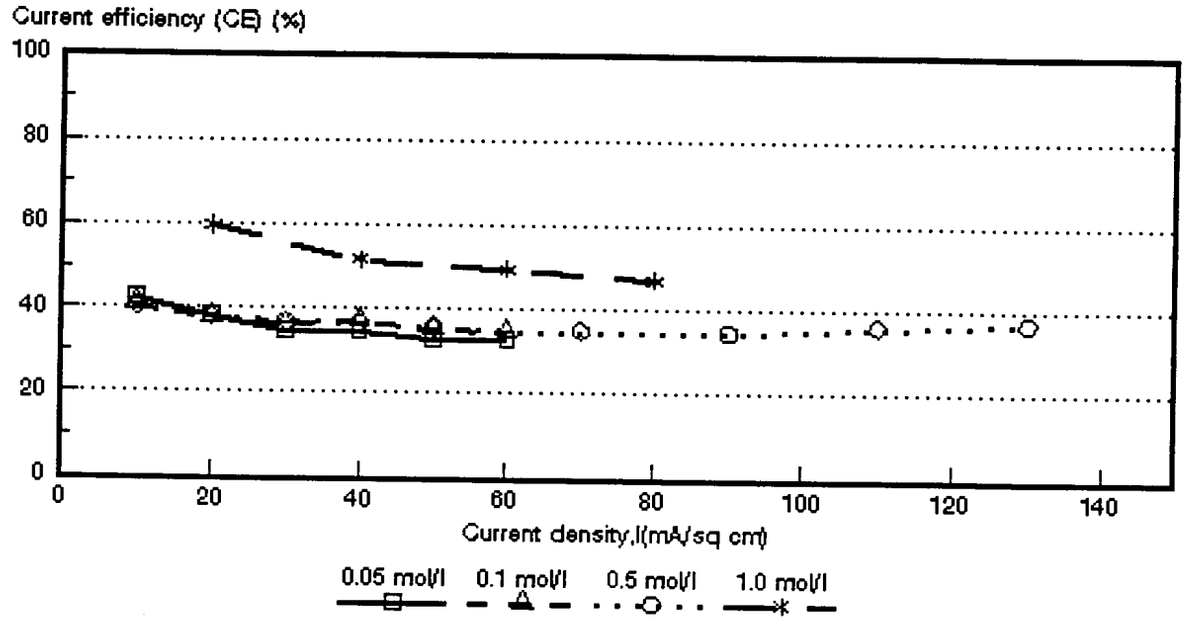

Figure 7.30: **Current efficiency (ϵ_p) as a function of current density for 4 different HCl feed concentrations. ABM-3 and *Selemion* CHV membranes.**

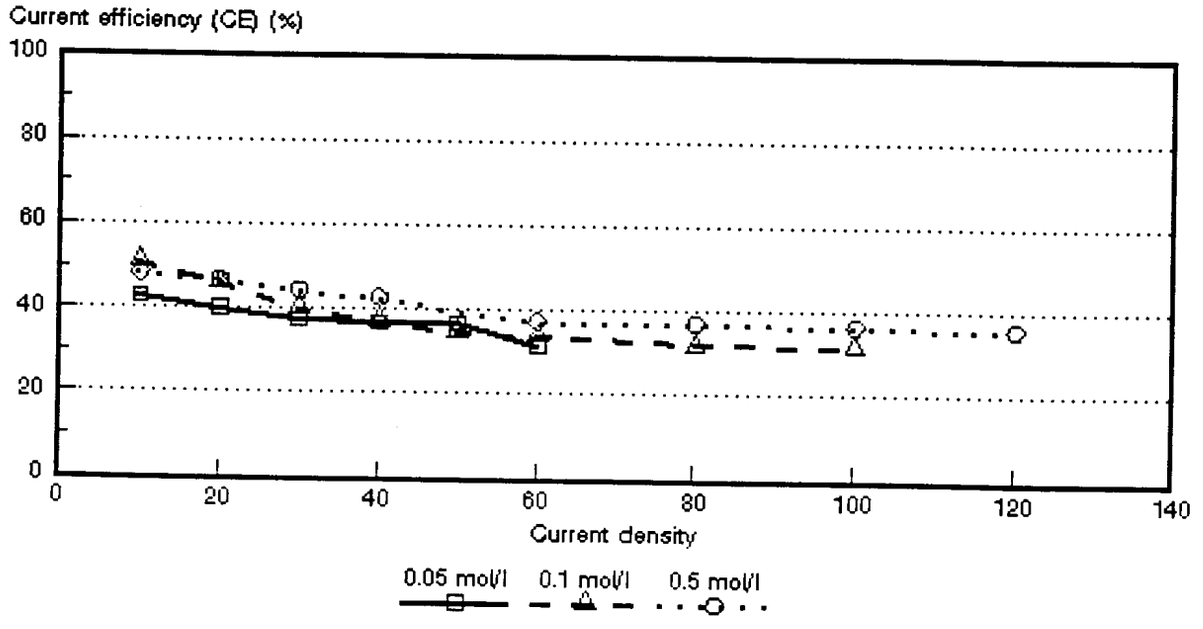

Figure 7.31: **Current efficiency (ϵ_p) as a function of current density for 3 different HCl feed concentrations. ABM-2 and *Selemion* CHV membranes.**

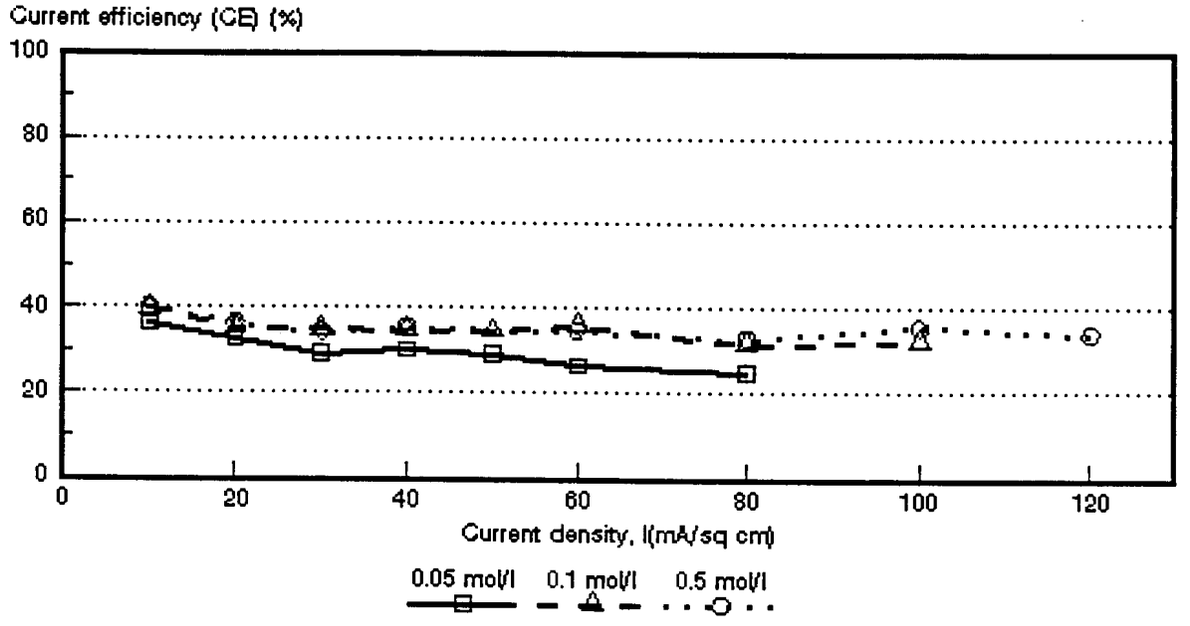

Figure 7.32: **Current efficiency (e_p) as a function of current density for 3 different HCl feed concentrations. ABM-1 and *Selemion* CHV membranes.**

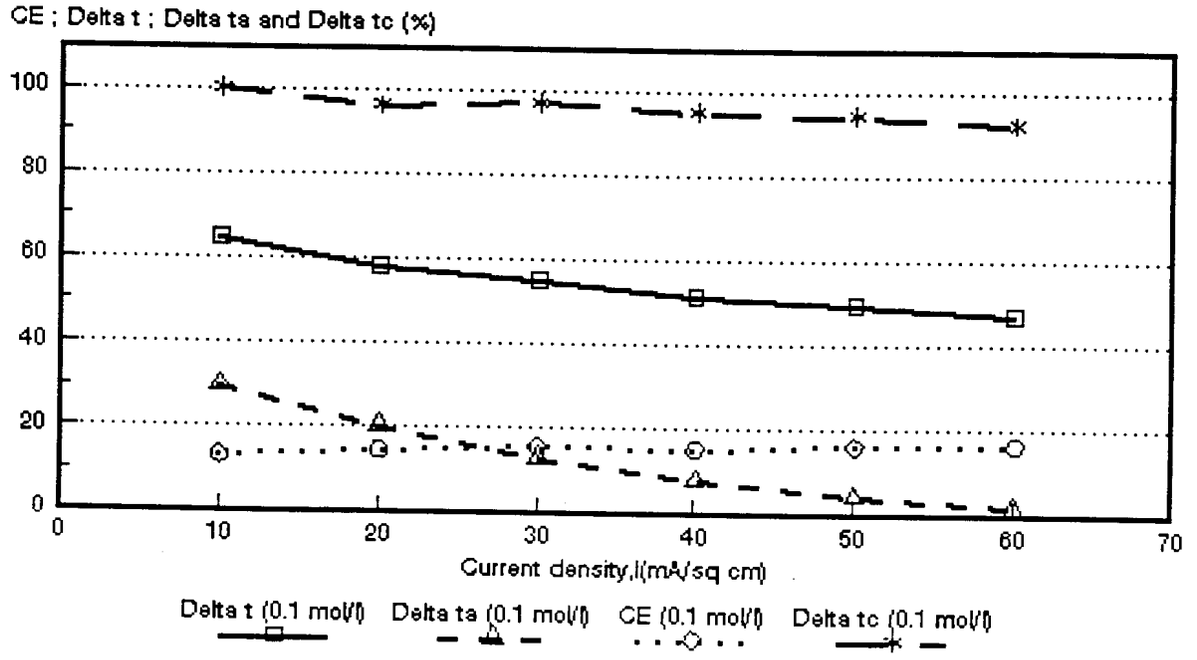

Figure 7.33: **Current efficiency (CE = e_p) as a function of current density for 0,1 mol/ℓ HCl feed. *Selemion* AMV and CMV membranes. Delta t = $\bar{\Delta}t$; Delta ta = Δt^a; Delta tc = Δt^c**

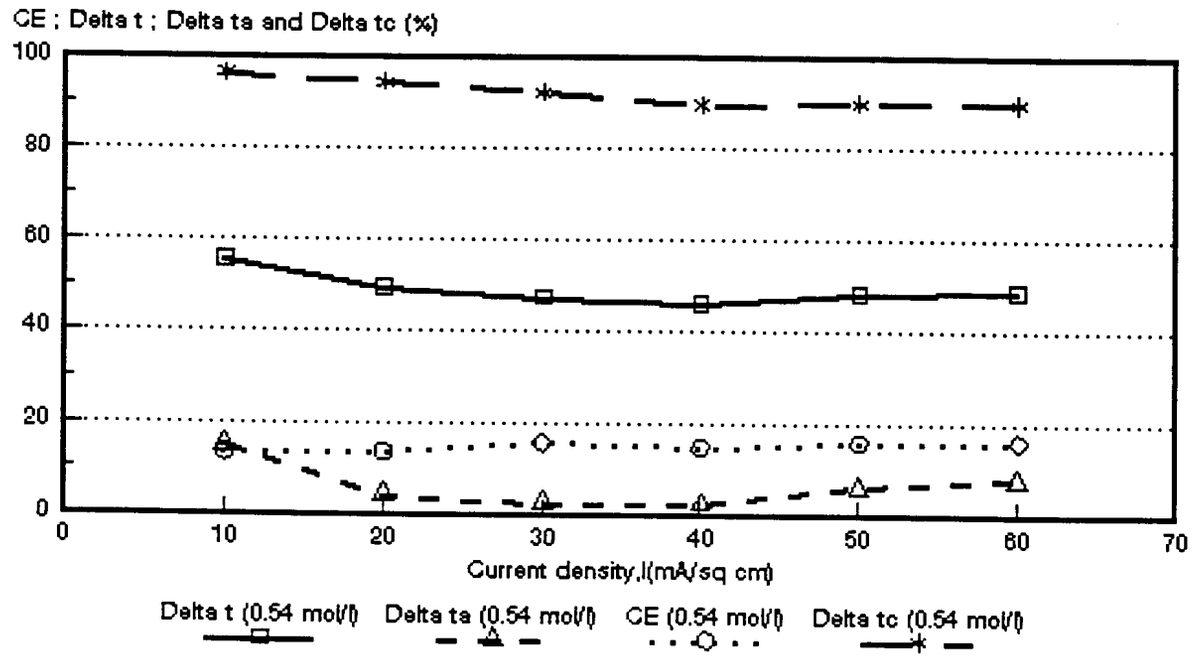

Figure 7.34: **Current efficiency (CE = ϵ_p) as a function of current density for 0,54 mol/ℓ HCl feed. *Selemion* AMV and CMV membranes. Delta t = $\bar{\Delta}t$; Delta ta = Δt^a; Delta tc = Δt^c**

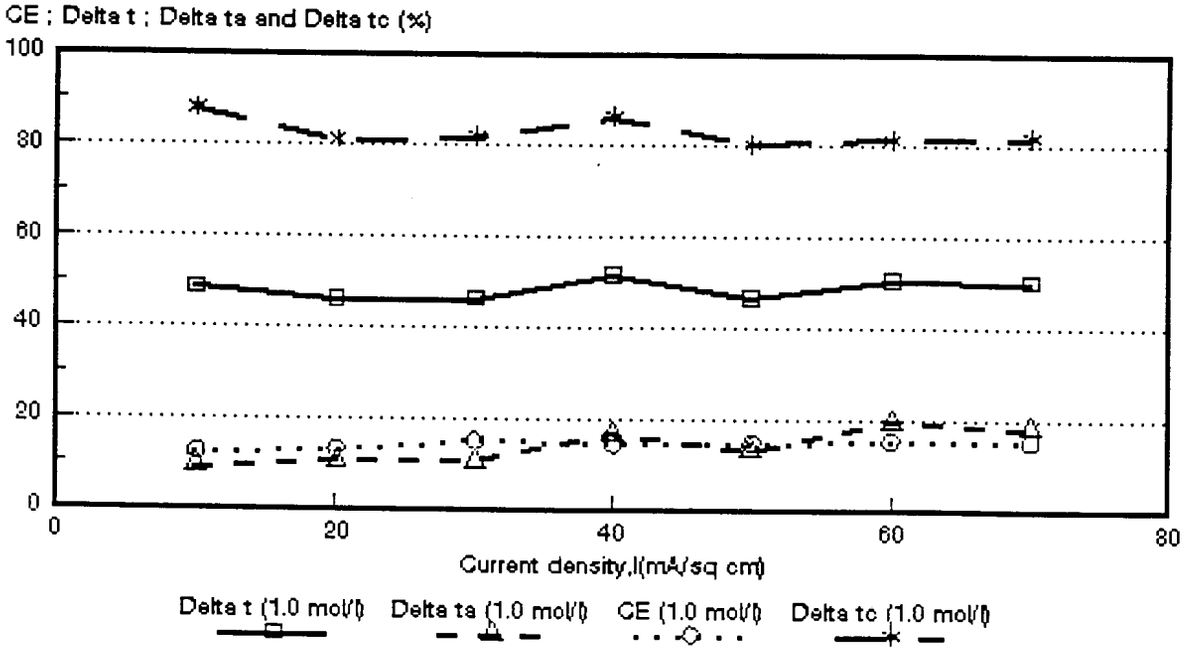

Figure 7.35: **Current efficiency (CE = ϵ_p) as a function of current density for 1,0 mol/ℓ HCl feed. *Selemion* AMV and CMV membranes. Delta t = $\bar{\Delta}t$; Delta ta = Δt^a; Delta tc = Δt^c**

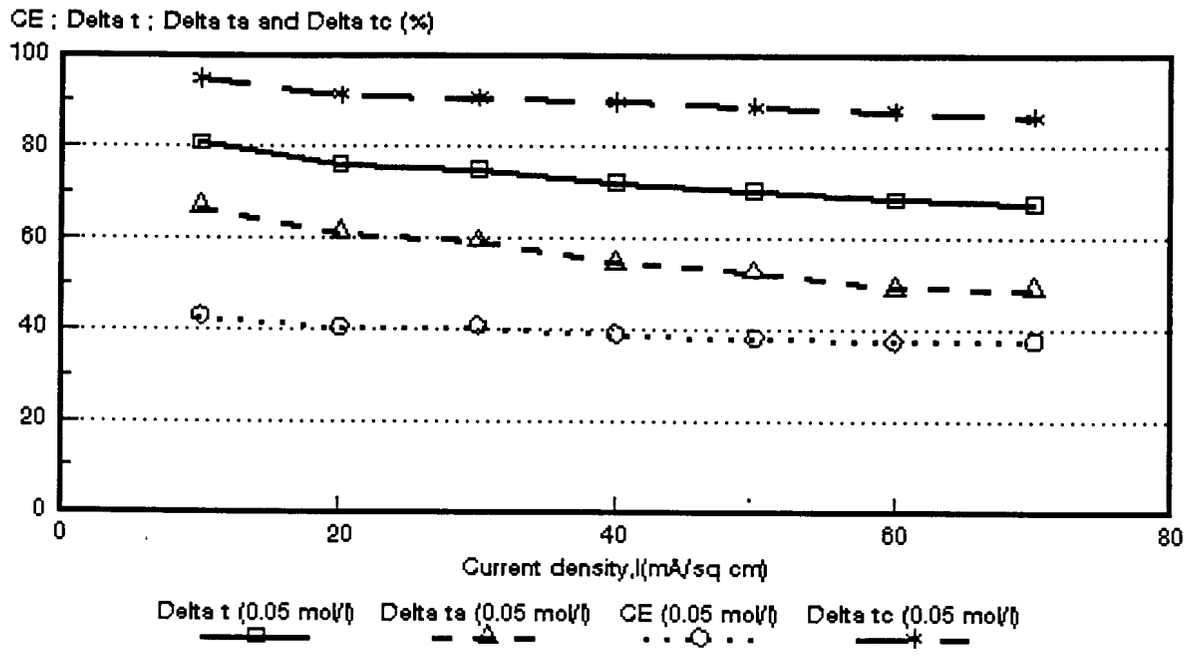

Figure 7.36: Current efficiency (CE = ϵ_p) as a function of current density for 0,05 mol/ℓ HCl feed. *Selemion* AMV and CMV membranes. Delta t = $\bar{\Delta}t$; Delta ta = Δt^a; Delta tc = Δt^c

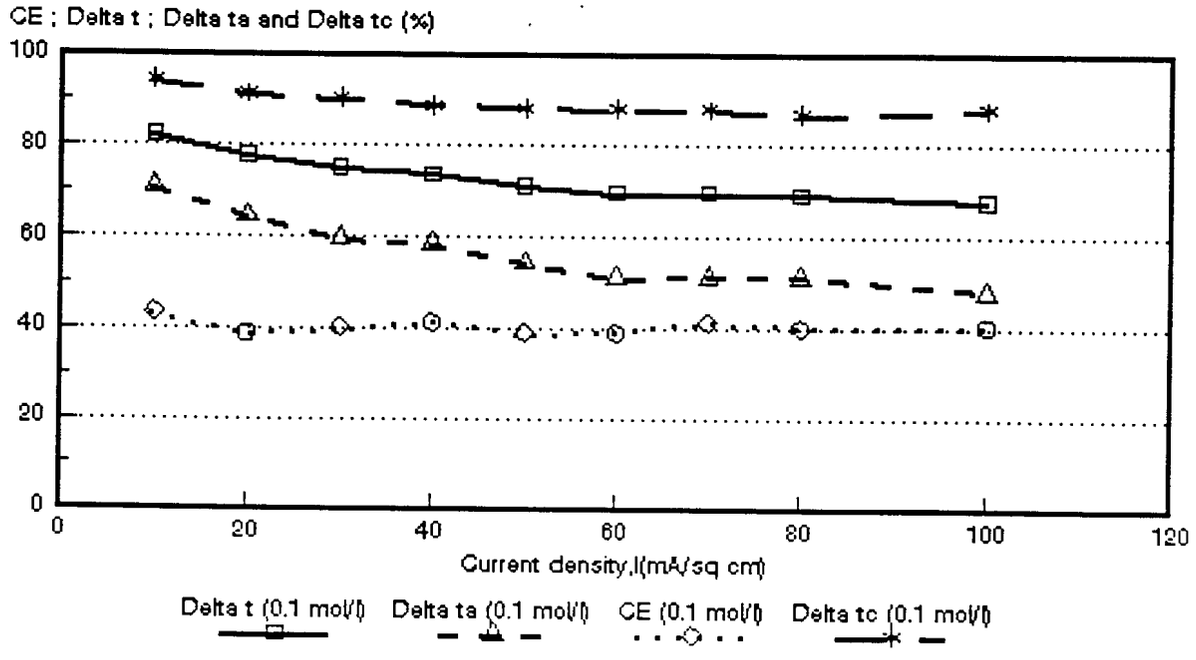

Figure 7.37: Current efficiency (CE = ϵ_p) as a function of current density for 0,1 mol/ℓ HCl feed. *Selemion* AAV and CHV membranes. Delta t = $\bar{\Delta}t$; Delta ta = Δt^a; Delta tc = Δt^c

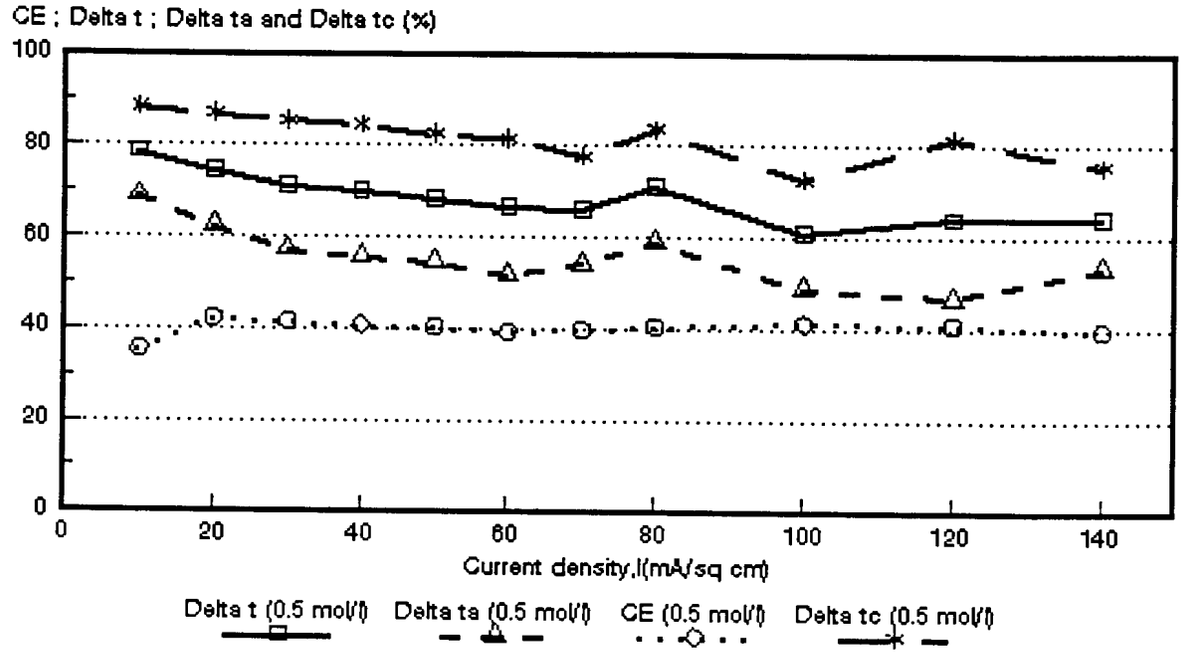

Figure 7.38: **Current efficiency (CE = ϵ_p) as a function of current density for 0,5 mol/ℓ HCl feed. *Selemion* AAV and CHV membranes. Delta t = $\bar{\Delta}t$; Delta ta = Δt^a; Delta tc = Δt^c**

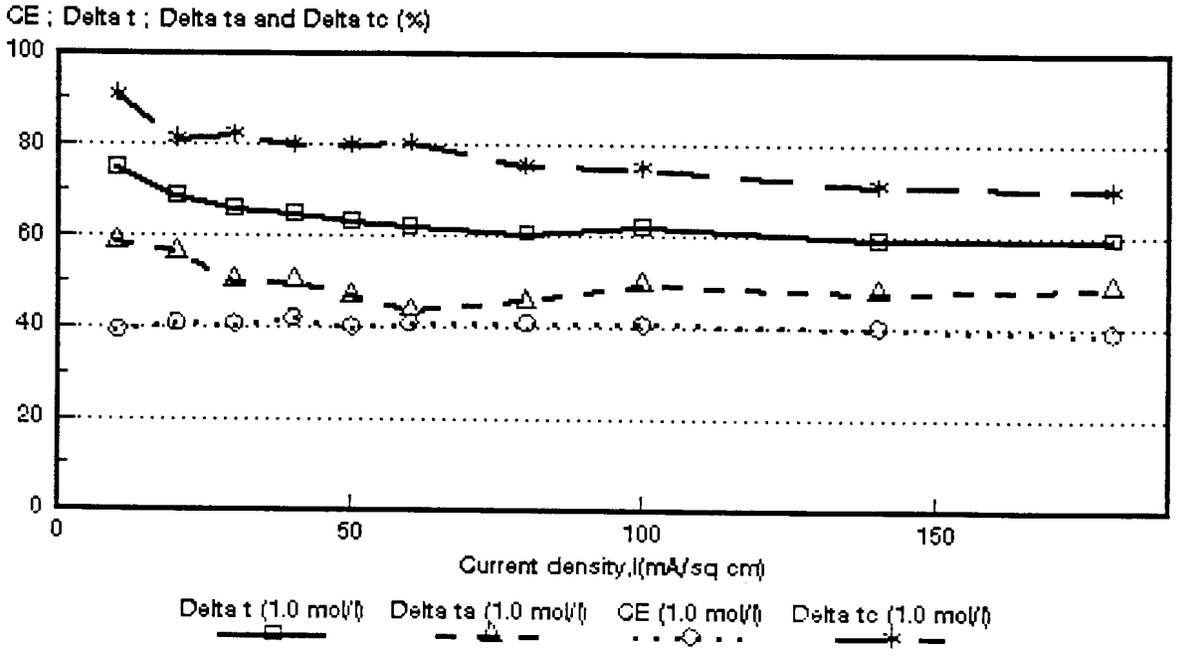

Figure 7.39: **Current efficiency (CE = ϵ_p) as a function of current density for 1,0 mol/ℓ HCl feed. *Selemion* AAV and CHV membranes. Delta t = $\bar{\Delta}t$; Delta ta = Δt^a; Delta tc = Δt^c**

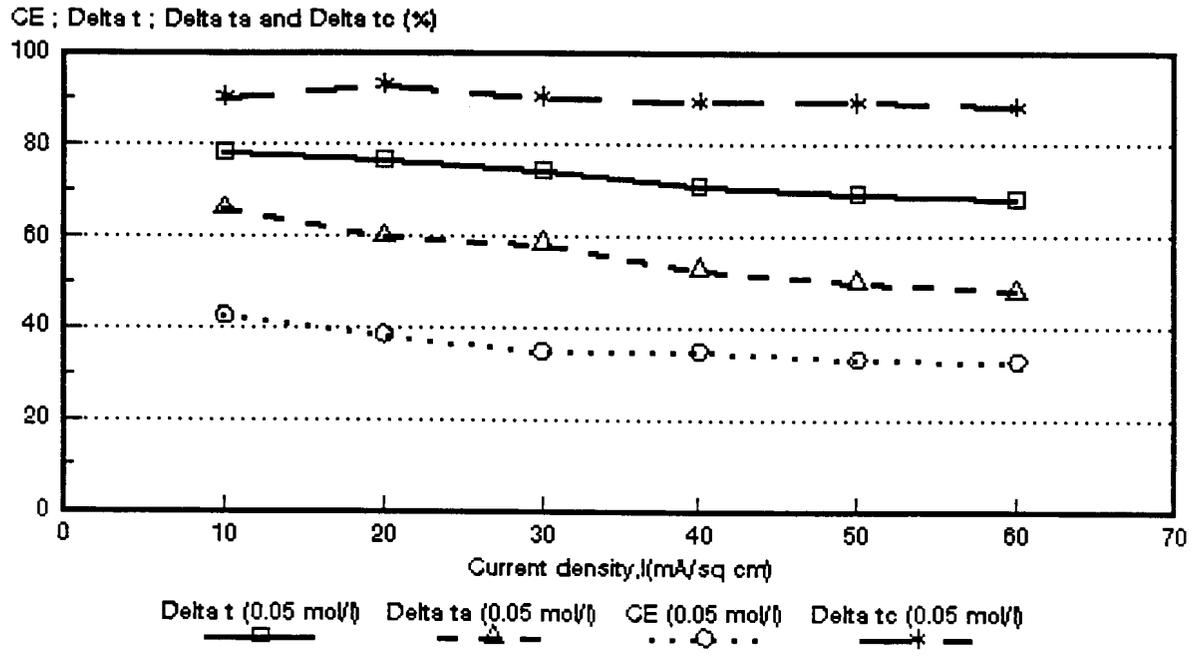

Figure 7.40: Current efficiency (CE = ϵ_p) as a function of current density for 0,05 mol/ℓ HCl feed. *Selemion* ABM-3 and CHV membranes. Delta t = $\bar{\Delta}t$; Delta ta = Δt^a; Delta tc = Δt^c

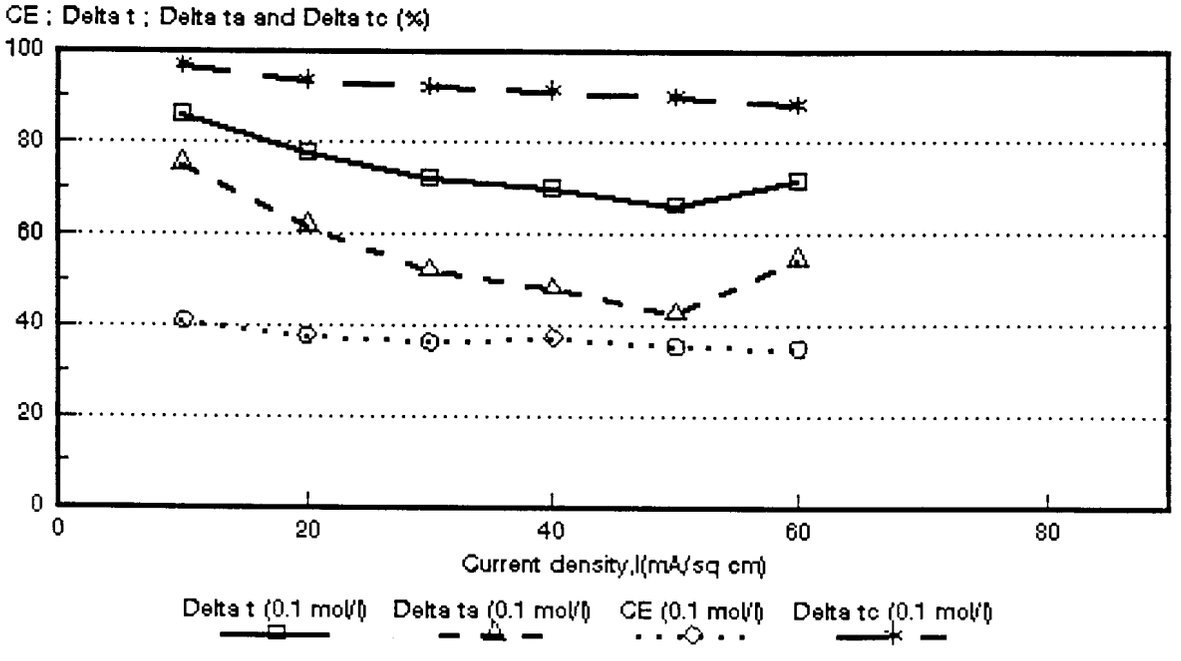

Figure 7.41: Current efficiency (CE = ϵ_p) as a function of current density for 0,1 mol/ℓ HCl feed. ABM-3 and *Selemion* CHV membranes. Delta t = $\bar{\Delta}t$; Delta ta = Δt^a; Delta tc = Δt^c

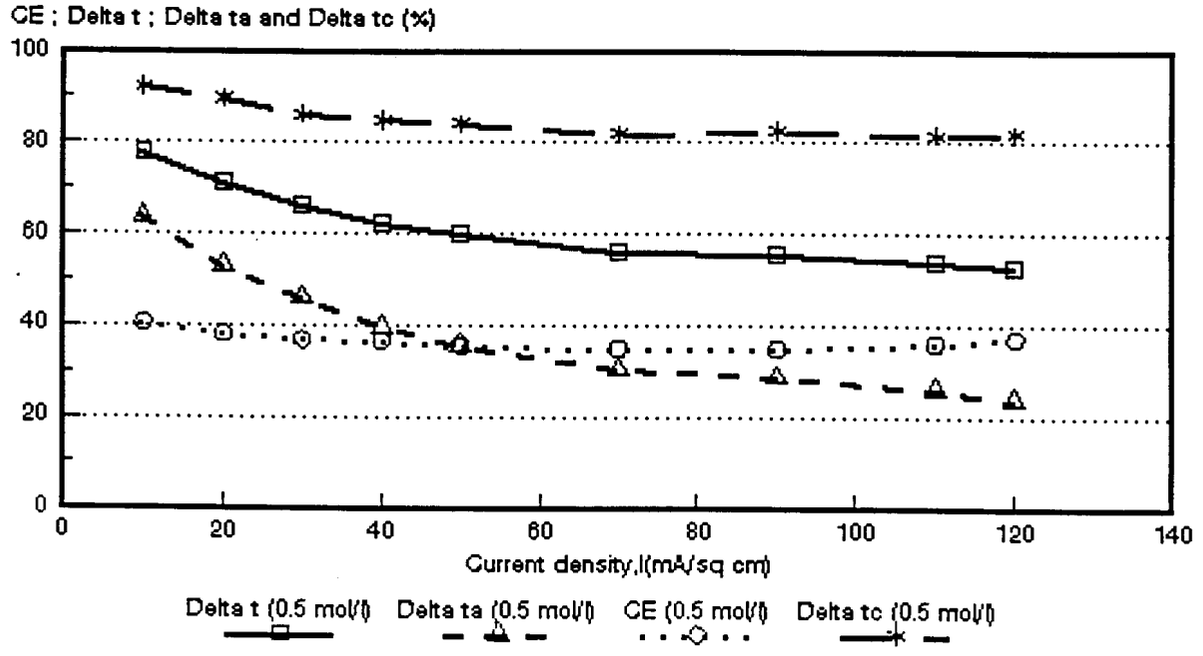

Figure 7.42: **Current efficiency (CE = ϵ_p) as a function of current density for 0,5 mol/ℓ HCl feed. *Selemion* ABM-3 and CHV membranes. Delta t = $\bar{\Delta}t$; Delta ta = Δt^a; Delta tc = Δt^c**

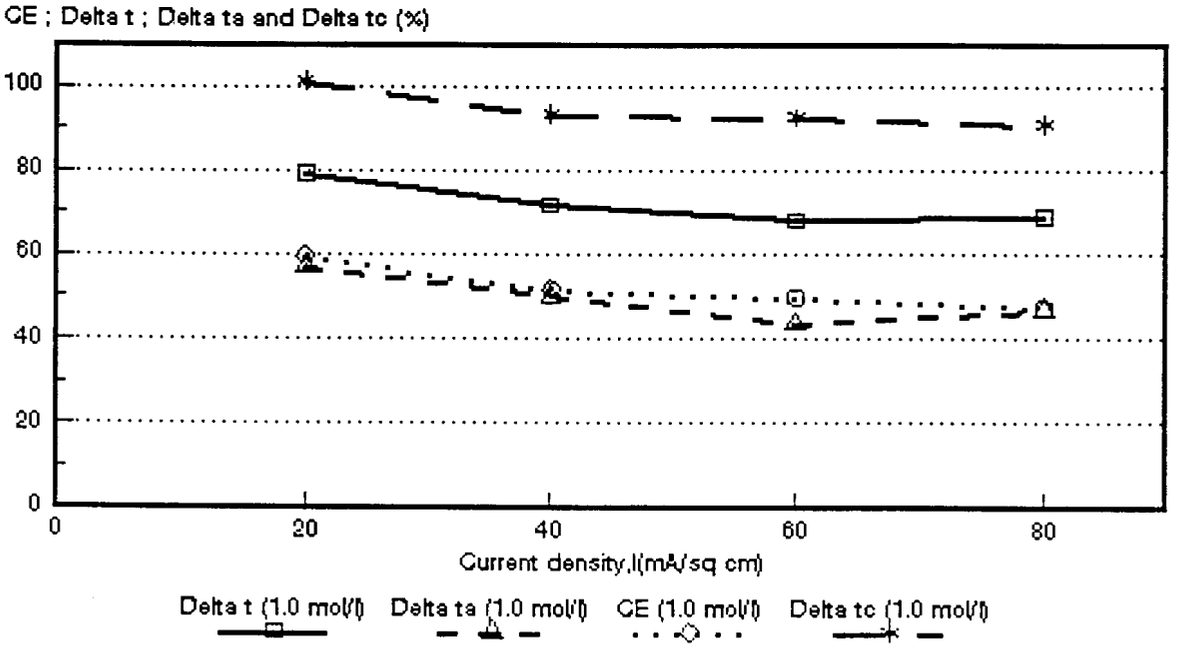

Figure 7.43: **Current efficiency (CE = ϵ_p) as a function of current density for 1,0 mol/ℓ HCl feed. ABM-3 and *Selemion* CHV membranes. Delta t = $\bar{\Delta}t$; Delta ta = Δt^a; Delta tc = Δt^c**

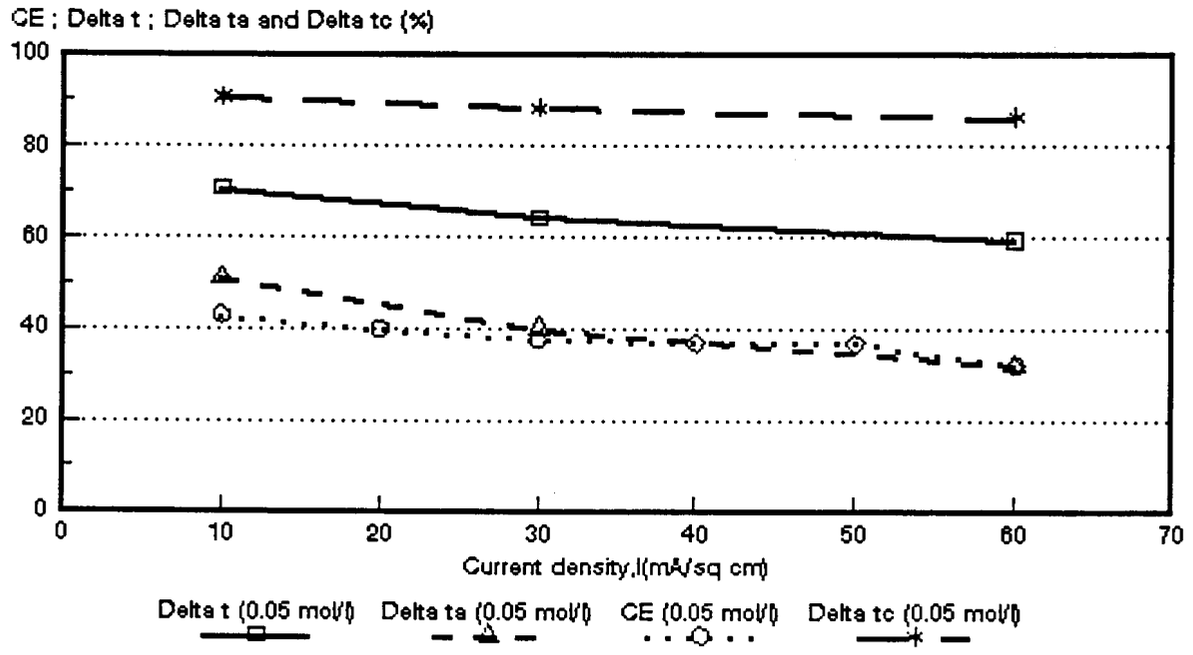

Figure 7.44: **Current efficiency (CE = ϵ_p) as a function of current density for 0,05 mol/ℓ HCl feed. ABM-2 and *Selemion* CHV membranes. Delta t = $\bar{\Delta}t$; Delta ta = Δt^a; Delta tc = Δt^c**

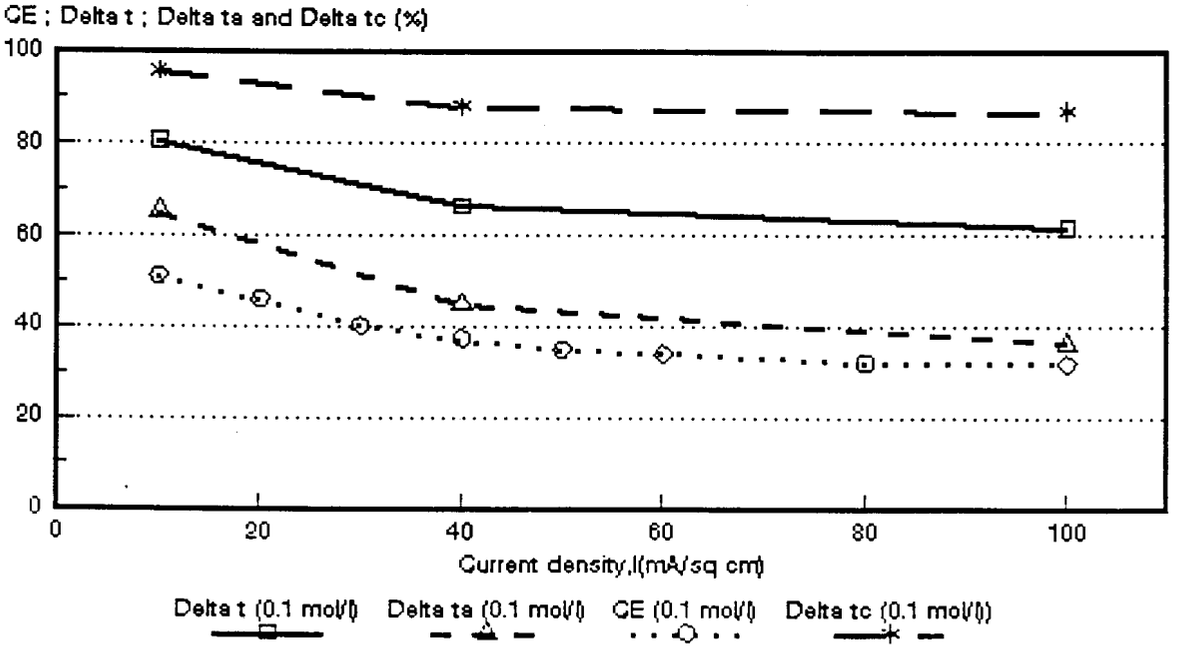

Figure 7.45: **Current efficiency (CE = ϵ_p) as a function of current density for 0,1 mol/ℓ HCl feed. ABM-2 and Selemion CHV membranes. Delta t = $\bar{\Delta}t$; Delta ta = Δt^a; Delta tc = Δt^c**

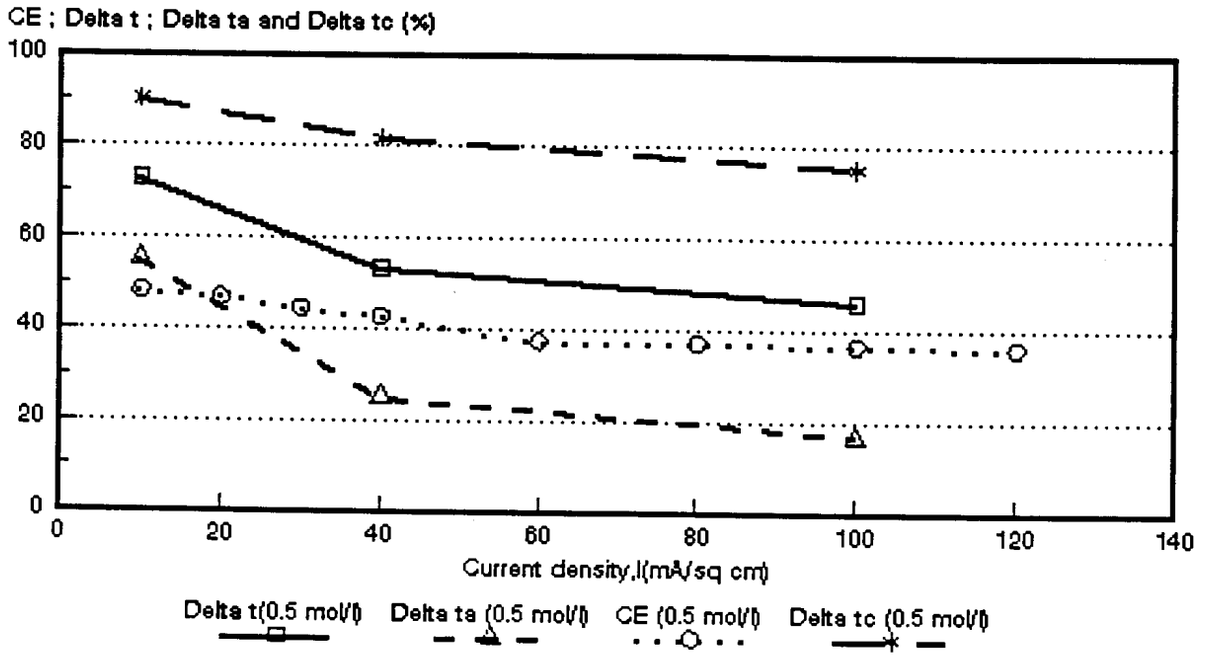

Figure 7.46: **Current efficiency (CE = ϵ_p) as a function of current density for 0,5 mol/ℓ HCl feed. ABM-2 and *Selemion* CHV membranes. Delta t = $\bar{\Delta}t$; Delta ta = Δt^a; Delta tc = Δt^c.**

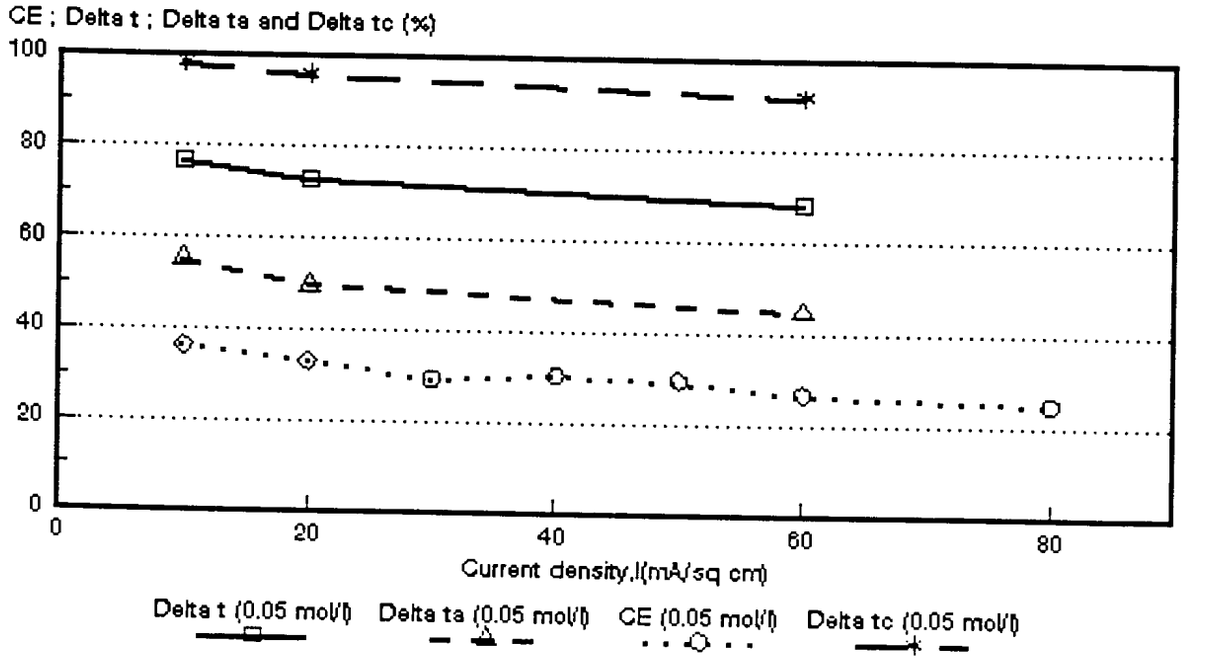

Figure 7.47: **Current efficiency (CE = ϵ_p) as a function of current density for 0,05 mol/ℓ HCl feed. ABM-1 and *Selemion* CHV membranes. Delta t = $\bar{\Delta}t$; Delta ta = Δt^a; Delta tc = Δt^c.**

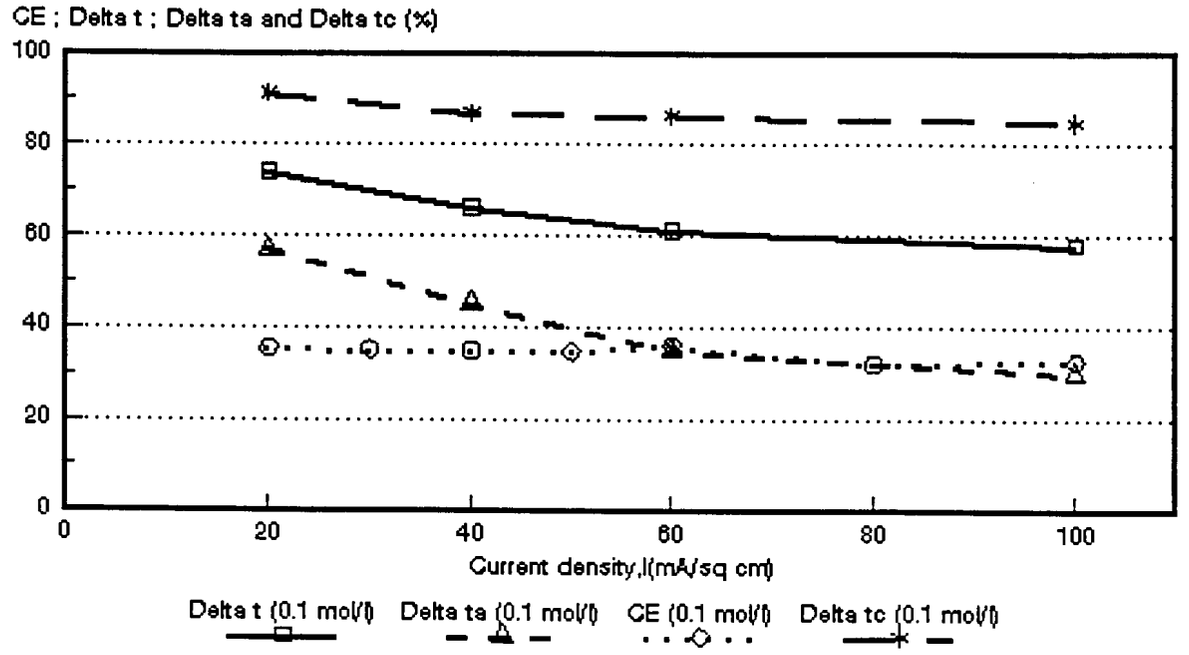

Figure 7.48: **Current efficiency (CE = ϵ_p) as a function of current density for 0,1 mol/ℓ HCl feed. ABM-1 and *Selemion* CHV membranes. Delta t = $\bar{\Delta}t$; Delta ta = Δt^a; Delta tc = Δt^c.**

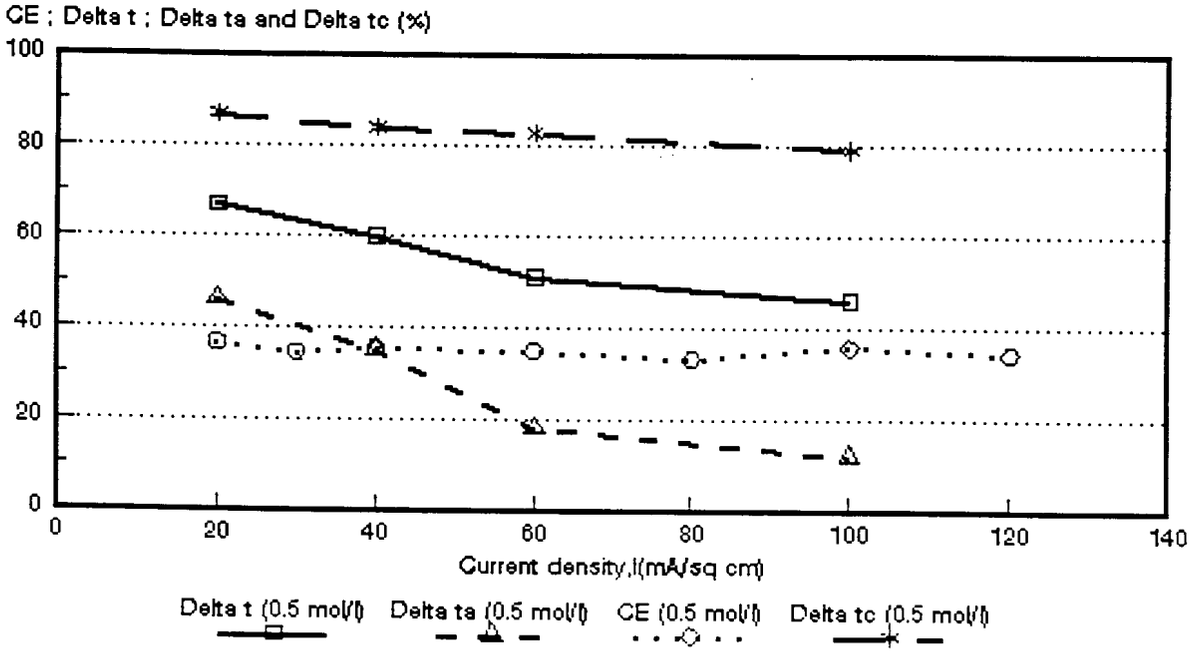

Figure 7.49: **Current efficiency (CE = ϵ_p) as a function of current density for 0,5 mol/ℓ HCl feed. ABM-1 and *Selemion* CHV membranes. Delta t = $\bar{\Delta}t$; Delta ta = Δt^a; Delta tc = Δt^c.**

Tabel 7.21: Correlation between apparent transport number of the membrane pair ($\bar{\Delta}t$) and current efficiency (ϵ_p).

Current Density	$\bar{\Delta}t/\epsilon_p$																			
	Selemion AMV & CMV Concentration, mol/ℓ				Selemion AAV & CHV Concentration, mol/				Israeli & Selemion ABM-3 & CHV Concentration, mol/ℓ				Israeli & Selemion ABM-2 & CHV Concentration, mol/ℓ				Israeli & Selemion ABM-1 & CHV Concentration, mol/ℓ			
mA/cm²	0,05	0,1	0,5	1,0	0,05	0,1	0,5	1,0	0,05	0,1	0,5	1,0	0,05	0,1	0,5	1,0	0,05	0,1	0,5	1,0
10		4,92	4,18	3,87	1,89	1,89	2,20	1,88	1,84	2,10	1,91		1,66	1,57	1,49		2,10	1,36		
20		3,97	3,68	3,41	1,88	1,98	1,75	1,69	1,98	2,04	1,86	1,33					2,19	2,11	1,84	
30		3,53	3,01	3,07	1,84	1,85	1,71	1,63	2,13	1,98	1,79		1,71							
40		3,42	3,13	3,52	1,85	1,76	1,72	1,55	2,03	1,85	1,69	1,37		1,77	1,24			1,90	1,70	
50		3,09	3,02	3,13	1,83	1,83	1,69	1,57	2,08	1,86	1,66						2,28			
60		2,85	3,04	3,36	1,82	1,76	1,68	1,52	2,08	2,03		1,37	1,85				2,56	1,69	1,47	
70				3,31	1,79	1,67	1,63				1,60									
80						1,72	1,75	1,47				1,44								
90											1,59									
100						1,68	1,45	1,52						1,91	1,26			1,78	1,29	
110											1,47									
120							1,56				1,40									
130																				
140							1,61	1,47												
150																				
160																				
170																				
180								1,52												

Tabel 7.22: Correlation between apparent transport number of the anion membrane (Δt^a) and current efficiency (e_p).

Current Density	Δt^a / e_p																			
	Selemion AMV & CMV Concentration, mol/ℓ				Selemion AAV & CHV Concentration, mol/ℓ				Israeli & Selemion ABM-3 & CHV Concentration, mol/ℓ				Israeli & Selemion ABM-2 & CHV Concentration, mol/ℓ				Israeli & Selemion ABM-1 & CHV Concentration, mol/ℓ			
mA/cm²	0,05	0,1	0,5	1,0	0,05	0,1	0,5	1,0	0,05	0,1	0,5	1,0	0,05	0,1	0,5	1,0	0,05	0,1	0,5	1,0
10		2,27	1,12	0,73	1,54	1,61	1,92	1,48	1,55	1,83	1,56		1,19	1,27	1,14		1,52			
20		1,37	0,29	0,83	1,51	1,65	1,47	1,37	1,56	1,61	1,36	0,94					1,49	1,61	1,26	
30		0,83	0,13	0,73	1,45	1,47	1,37	1,23	1,67	1,43	1,22		1,07							
40		0,53	0,14	1,17	1,38	1,40	1,35	1,19	1,49	1,29	1,06	0,97		1,18	0,56			1,30	0,99	
50		0,25	0,38	0,88	1,36	1,39	1,34	1,15	1,51	1,19	0,99									
60		0,12	0,50	1,25	1,31	1,30	1,30	1,05	1,47	1,55		0,87	1,00				1,65	0,97	0,52	
70				1,19	1,28	1,23	1,35				0,86									
80						1,27	1,46	1,10				0,97								
90											0,81									
100						1,19	1,19	1,20						1,23	0,44			0,92	0,34	
110											0,69									
120							1,12				0,62									
130																				
140							1,33	1,17												
150																				
160																				
170																				
180								1,26												

Tabel 7.23: **Correlation between apparent transport number of the cation membrane (Δt^c) and current efficiency (ϵ_p).**

Current Density	$\Delta t^c/\epsilon_p$																			
	Selemion AMV & CMV Concentration, mol/ℓ				Selemion AAV & CHV Concentration, mol/ℓ				Israeli & Selemion ABM-3 & CHV Concentration, mol/ℓ				Israeli & Selemion ABM-2 & CHV Concentration, mol/ℓ				Israeli & Selemion ABM-1 & CHV Concentration, mol/ℓ			
mA/cm²	0,05	0,1	0,5	1,0	0,05	0,1	0,5	1,0	0,05	0,1	0,5	1,0	0,05	0,1	0,5	1,0	0,05	0,1	0,5	1,0
10		7,58	7,16	7,10	2,21	2,17	2,48	2,32	2,12	2,37	2,28		2,10	1,86	1,86		2,71	2,31		
20		6,58	6,99	6,14	2,25	2,34	2,06	1,98	2,42	2,46	2,34	1,68					2,92	2,57	2,38	
30		6,22	5,90	5,47	2,21	2,24	2,05	2,02	2,59	2,53	2,33		2,35							
40		6,25	6,12	6,00	2,31	2,13	2,06	1,90	2,55	2,44	2,29	1,80		2,36	1,89			2,50	2,38	
50		5,86	5,66	5,51	2,30	2,26	2,03	2,00	2,69	2,54	2,37									
60		5,58	5,59	5,39	2,35	2,25	2,06	1,96	2,69	2,52		1,85	2,73				3,46	2,39	2,39	
70				5,43	2,29	2,13	1,93				2,32									
80						2,16	2,05	1,83				1,90								
90											2,36									
100						2,17	1,74	1,84						2,73	2,05			2,62	2,21	
110											2,24									
120							1,97				2,18									
130																				
140							1,88	1,77												
150																				
160								1,80												
170																				
180																				

mA/cm^2 (0,1 mol/ℓ feed). The correlation was even better at 1,0 mol/ℓ feed concentration and varied between 0,97 and 0,84 in the 20 to 80 mA/cm^2 current density range.

A satisfactory correlation was obtained between the apparent transport number (Δt^a) and current efficiency at 0,05 mol/ℓ feed concentration in the case of the ABM-2 and CHV membranes (30 to 60 mA/cm^2). The ratio of $\Delta t^a/e_p$ varied between 1,07 and 1,0. The ratio was approximately 1,18 at 0,1 mol/ℓ feed concentration in the same current density range. A very poor correlation, however, was obtained at 0,5 mol/ℓ feed concentration for the same membranes.

The ABM-1 and CHV membranes showed the best correlation (0,92 to 0,97) at 0,1 mol/ℓ feed concentration in the current density range from 60 to 100 mA/cm^2. A poor correlation, however, was obtained with the Selemion AMV and CMV membranes.

The correlations between the apparent transport numbers of the cation membrane (Δt^c) and current efficiencies (Table 7.23) were not as good as the correlations obtained between the apparent transport numbers of the membrane pair ($\bar{\Delta}t$) (Table 7.21) and that of the anion membrane (Δt^a) and current efficiency (Fig. 7.22). It therefore seems that the best correlation between transport numbers and current efficiency for acid can be obtained from the apparent transport number of the anion membrane. It also seems that the apparent transport number of the anion membrane gives the best approximate estimation of the performance of membranes for acid concentration/desalination. However, accuracy of performance depends on the acid feed concentration used. The performance of a membrane for acid concentration should be estimated with an accuracy of approximately 20% from the apparent transport number of the anion membrane, depending on the acid feed concentration used.

7.3 Water Flow

Water flow (J) through the membranes as a function of current density and acid feed water concentration is shown in Figures 7.50 to 7.54. Water flow (J_i) through the membranes relative to the flow at $J_{0,5\ mol/\ell}$ is shown in Table 7.24. Water flow through the membranes decreased significantly with increasing acid feed concentration in the case of the *Selemion* AMV and CMV membranes. A slight decrease in water flow was also experienced in the case of the *Selemion* AAV and CHV membranes. Therefore, there appeared to be no support (water flow) to improve current efficiency as had been experienced with the sodium chloride solutions (see Figs. 7.28 and 7.29 and Figs. 6.43 to 6.49). However, a definite increase in water flow was observed for the ABM-3 and CHV membranes, especially at the highest feed concentration (Table 7.24) and an increase in current efficiency was experienced for this membrane type at 1,0 mol/ℓ feed concentration (see Fig. 7.30). Increase in water flows were also experienced for the ABM-2, ABM-1 and CHV membranes with increasing acid feed concentration. Current efficiency also increased slightly in these cases (see Figs. 7.31 and 7.32). The high water flow that was experienced with the ABM-2 membranes at 0,1 mol/ℓ feed concentration may be ascribed to membrane leakage due to a partially torn membrane.

Water flow (J) through the membranes as a function of effective current density, I_{eff}, and feed water concentration are shown in Figures 7.55 to 7.59. Straight lines were obtained at higher values of I_{eff} as were experienced with the sodium chloride solutions. The slope of these lines corresponds to the combined electro-osmotic coefficient (2β) of a membrane pair. The electro-osmotic coefficients decreased as a function of increasing acid feed concentration in the feed concentration range from 0,05 to 1,0 mol/ℓ (Figs. 7.60 to 7.64). The electro-osmotic coefficient of the *Selemion* AMV and CMV membranes remained almost constant in the 0,1 to 0,5 mol/ℓ feed concentration range and then decreased more significantly to a lower value at 1,0 mol/ℓ feed concentration (Fig. 7.60). The electro-osmotic coefficient of the *Selemion* AAV and CHV membranes remained constant in the 0,05 to 0,1 mol/ℓ feed range (Fig. 7.61) and then decreased somewhat to remain almost constant in the 0,5 to 1,0 mol/ℓ feed concentration range. The electro-osmotic coefficients of the ABM-3 and CHV membranes decreased significantly in the 0,05 to 0,5 mol/ℓ feed concentration range and then remained constant (Fig. 7.62). Both the ABM-2 and ABM-1 membranes showed a reduction in the electro-osmotic coefficient in the 0,05 to 0,1 mol/ℓ feed concentration ranges and then remained constant in the 0,1 to 0,5 mol/ℓ feed

concentration range (Figs. 7.62 to 7.63). It, therefore, appears that the membranes deswell somewhat with increasing acid feed concentration.

The effect of the electro-osmotic coefficient on the maximum acid brine concentration c_b^{max}, is shown in Table 7.25. Maximum acid brine concentration increases with decreasing electro-osmotic coefficient. The electro-osmotic coefficients of the *Selemion* AMV and CMV membranes were much higher than that of the other membranes. The electro-osmotic coefficients of the *Selemion* AMV and CMV membranes were determined at 0,357 and 0,371 ℓ/Faraday at 0,1 and 0,54 mol/ℓ feed concentration, respectively. The electro-osmotic coefficients of the *Selemion* AAV and CHV; ABM-3 and CHV; ABM-2 and CHV and ABM-1 and CHV were determined at 0,141 and 0,126 ℓ/Faraday; 0,166 and 0,124 ℓ/Faraday; 0,133 and 0,131 ℓ/Faraday and 0,152 and 0,149 ℓ/Faraday under the same feed water conditions as above, respectively. Consequently, much higher acid brine concentrations could be obtained with these membranes.

Approximately 7 to 8 mol H_2O per Faraday passed through the *Selemion* AAV and CHV membranes in the acid feed concentration range from 0,1 to 0,5 mol/ℓ (Table 7.25). Approximately 7 to 9; 7 and 8 mol H_2O/Faraday passed through the ABM-3 and CHV; ABM-2 and CHV and ABM-1 and CHV membranes under the same feed conditions as above, respectively. Therefore, the newly developed Israeli ABM membranes compare favourably with the commercially available *Selemion* AAV and CHV membranes for acid concentration.

The osmotic water flow (J_{osm}) relative to the total water flow (J) through the membranes as a function of current density, is shown in Table 7.26. The osmotic flow (J_{osm}) relative to the total flow (J) decreases with increasing current density. Osmotic water flow contributes to approximately 50% of the total water flow through the membranes at a current density of 30 mA/cm^2 at 0,1 mol/ℓ feed concentration. However, the osmotic water flow contribution relative to the total water flow was much less at high current densities. Approximately 21% of the total water flow through the membranes was caused by osmosis in the case of the *Selemion* AAV and CHV membranes at a current density of 100 mA/cm^2 (0,1 mol/ℓ feed). The osmotic water flow contribution in the case of the ABM-3 and *Selemion* CHV membranes comprised 29,4% of the total water flow at a current density of 60 mA/cm^2 (0,1 mol/ℓ feed).

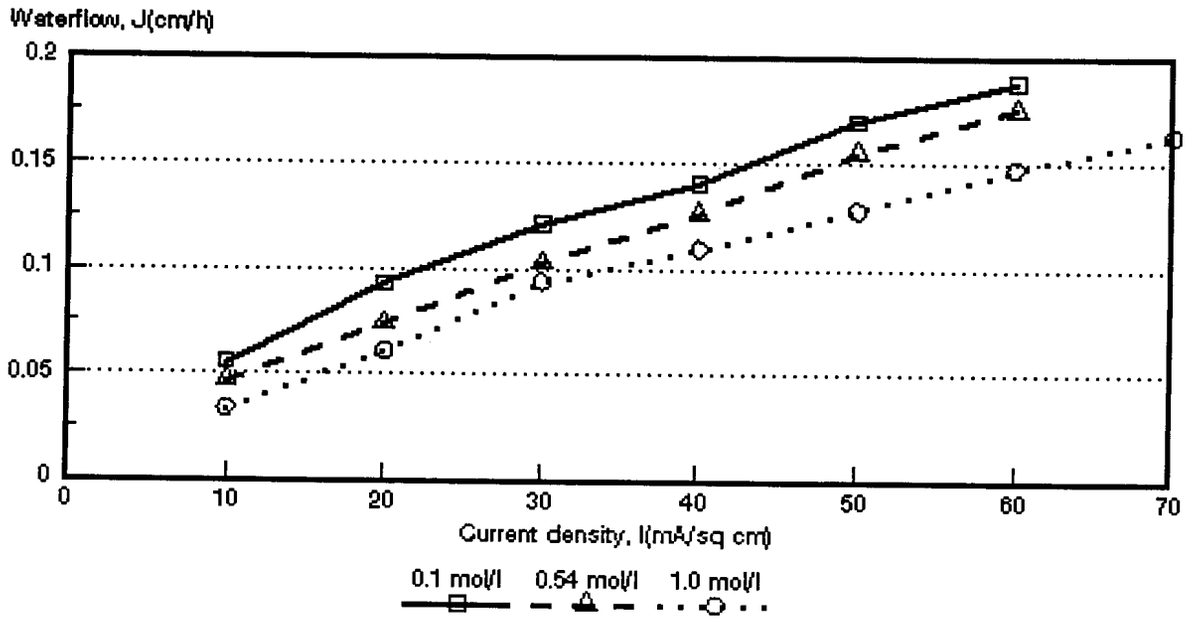

Figure 7.50: **Water flow through the membranes as a function of current density and feed water concentration. *Selemion* AMV and CMV membranes.**

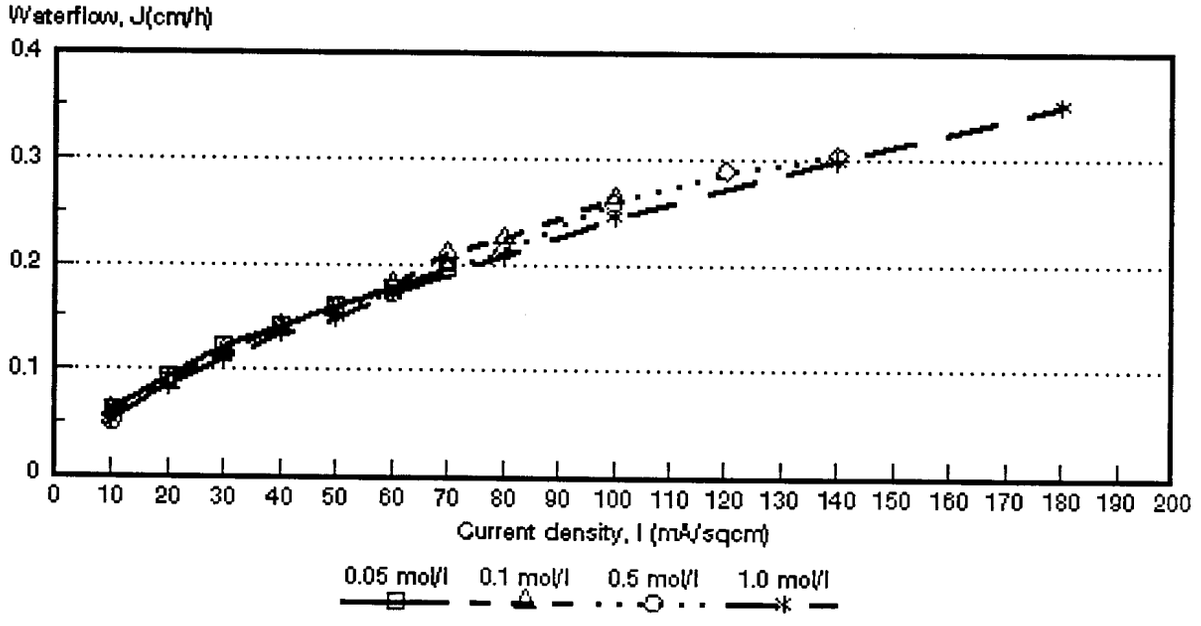

Figure 7.51: **Water flow through the membranes as a function of current denisty and feed water concentration. *Selemion* AAV and CHV membranes.**

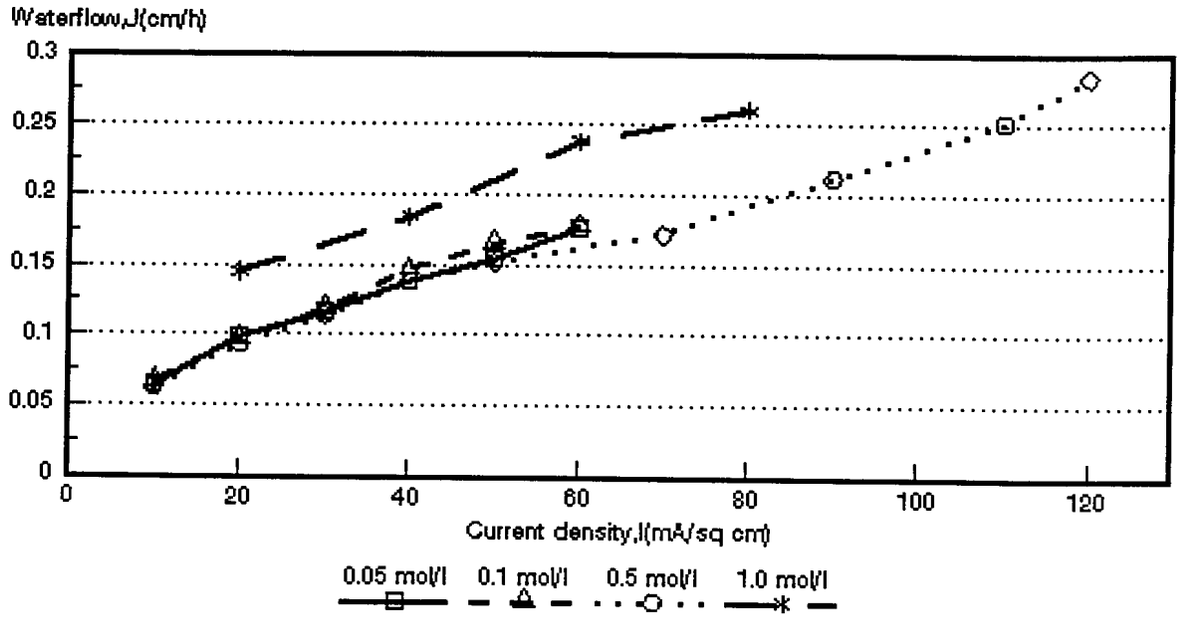

Figure 7.52: **Water flow through the membranes as a function of current density and feed water concentration. ABM-3 and *Selemion* CHV membranes.**

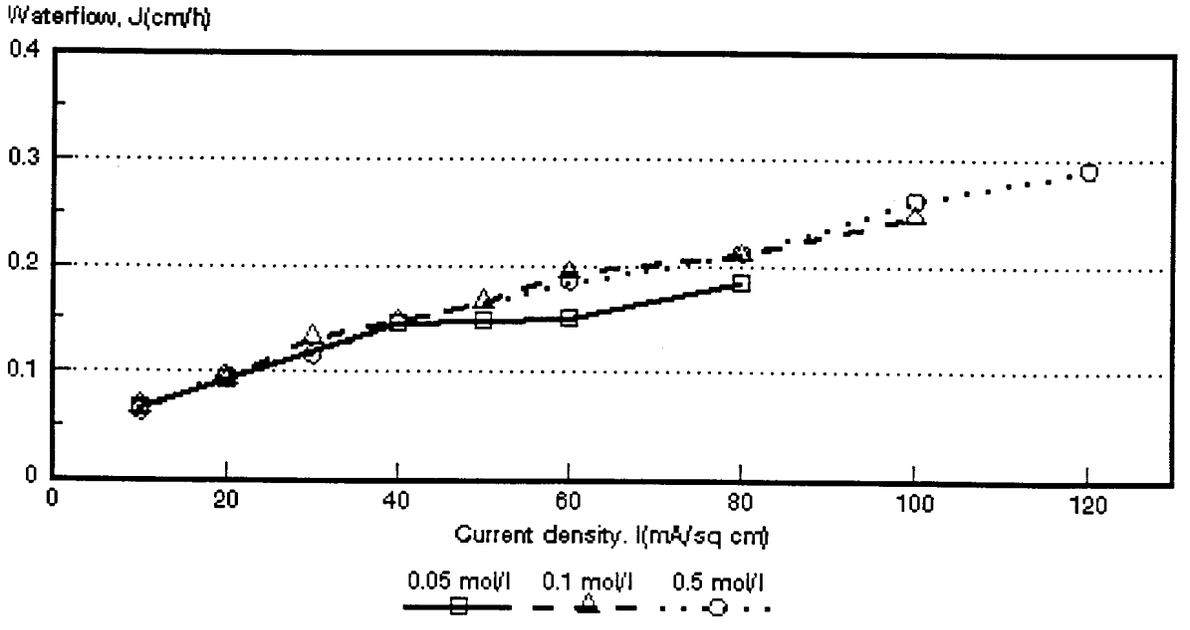

Figure 7.53: **Water flow through the membranes as a function of current denisty and feed water concentration. ABM-2 and *Selemion* CHV membranes.**

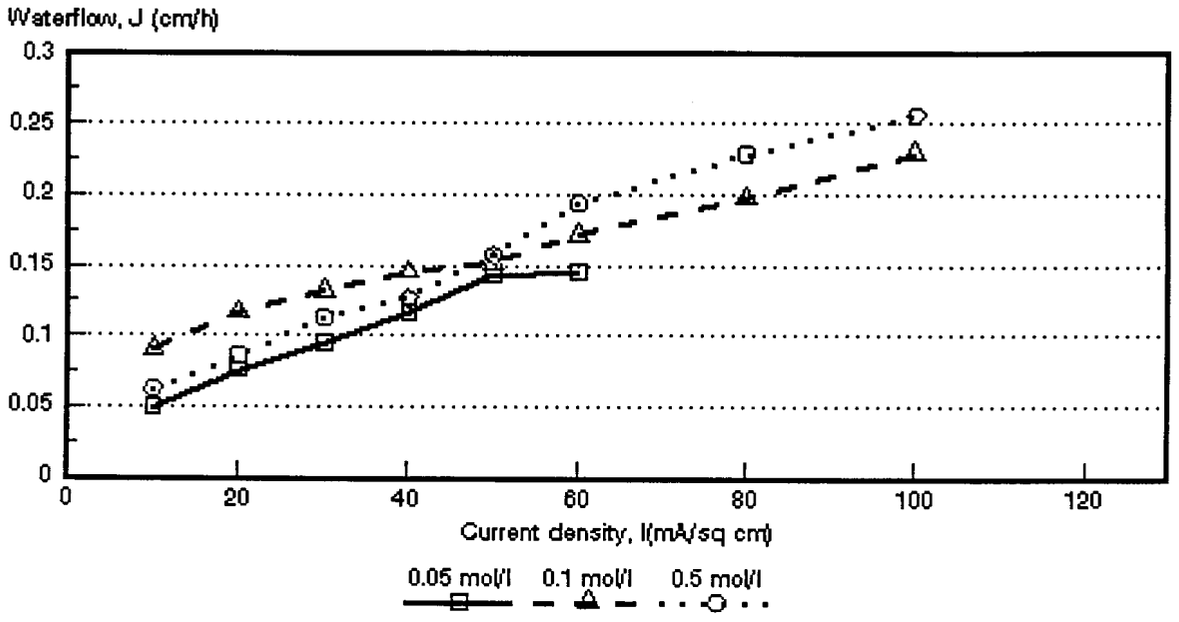

Figure 7.54: **Water flow through the membranes as a function of current density and feed water concentration. ABM-1 and *Selemion* CHV membranes.**

Tabel 7.24: Water flow (J_i) through the membranes relative to the flow at $J_{0,5\ mol/\ell}$

Current Density	$J_i/J_{0,5\ mol/\ell}$																			
	Selemion AMV & CMV Concentration, mol/ℓ				Selemion AAV & CHV Concentration, mol/ℓ				Israeli & Selemion ABM-3 & CHV Concentration, mol/ℓ				Israeli & Selemion ABM-2 & CHV Concentration, mol/ℓ				Israeli & Selemion ABM-1 & CHV Concentration, mol/ℓ			
mA/cm²	0,05	0,1	0,5	1,0	0,05	0,1	0,5	1,0	0,05	0,1	0,5	1,0	0,05	0,1	0,5	1,0	0,05	0,1	0,5	1,0
10		1,18	1,0	0,71	1,24	1,20	1,0	1,02	1,03	1,09	1,0		0,79	1,45	1,0		1,06	1,06	1,0	
20		1,26	1,0	0,82	1,05	0,97	1,0	0,96	1,05	1,05	1,0	1,56	0,88	1,35	1,0		0,95	0,95	1,0	
30		1,17	1,0	0,91	1,07	1,02	1,0	0,97	1,03	1,04	1,0		0,84	1,17	1,0					
40		1,11	1,0	0,87	1,02	1,01	1,0	0,98	1,00	1,07	1,0	1,33	0,91	1,14	1,0		1,00	1,02	1,0	
50		1,09	1,0	0,83	1,00	0,98	1,0	0,93	1,01	1,09	1,0				1,0				1,0	
60		1,07	1,0	0,84	1,03	1,04	1,0	0,99					0,92	1,09	1,0		0,81	1,05	1,0	
70					1,01	1,08	1,0								1,0				1,0	
80						1,06	1,0	0,98						1,02	1,0		0,87	0,99	1,0	
90							1,0								1,0				1,0	
100						1,02	1,0	0,95						1,00	1,0			0,95	1,0	
110																				
120																				
130																				
140								0,98												
150																				
160																				
170																				
180																				

i = 0,05; 0,1 and 1,0 mol/ℓ

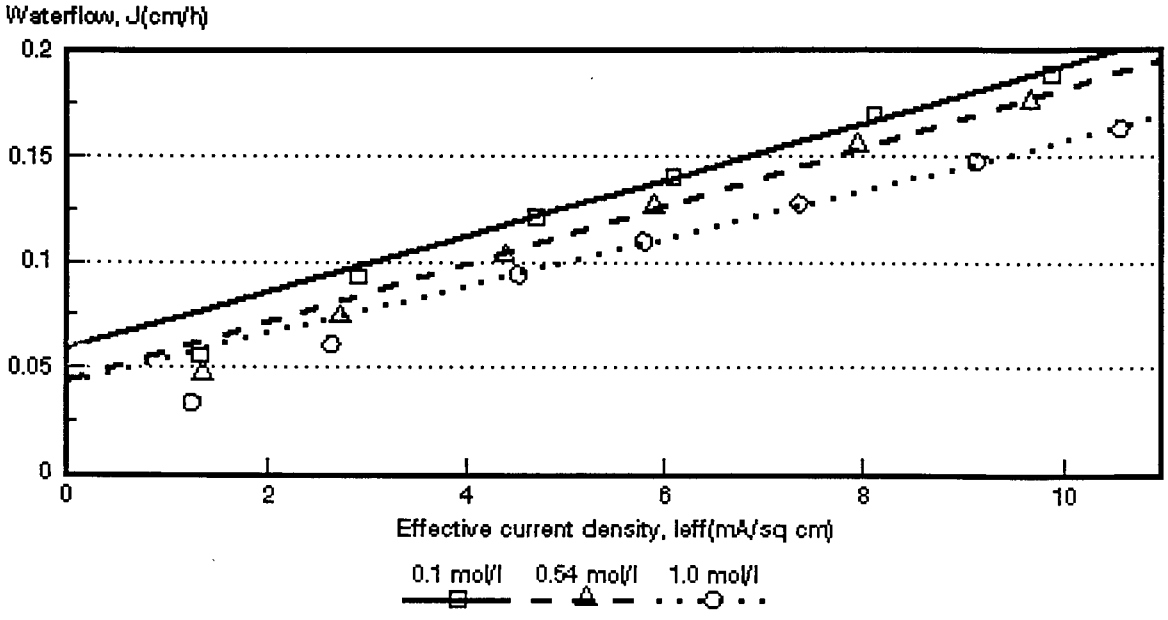

Figure 7.55: **Water flow through the membranes as a function of effective current density and HCl feed water concentration. *Selemion* AMV and CMV membranes.**

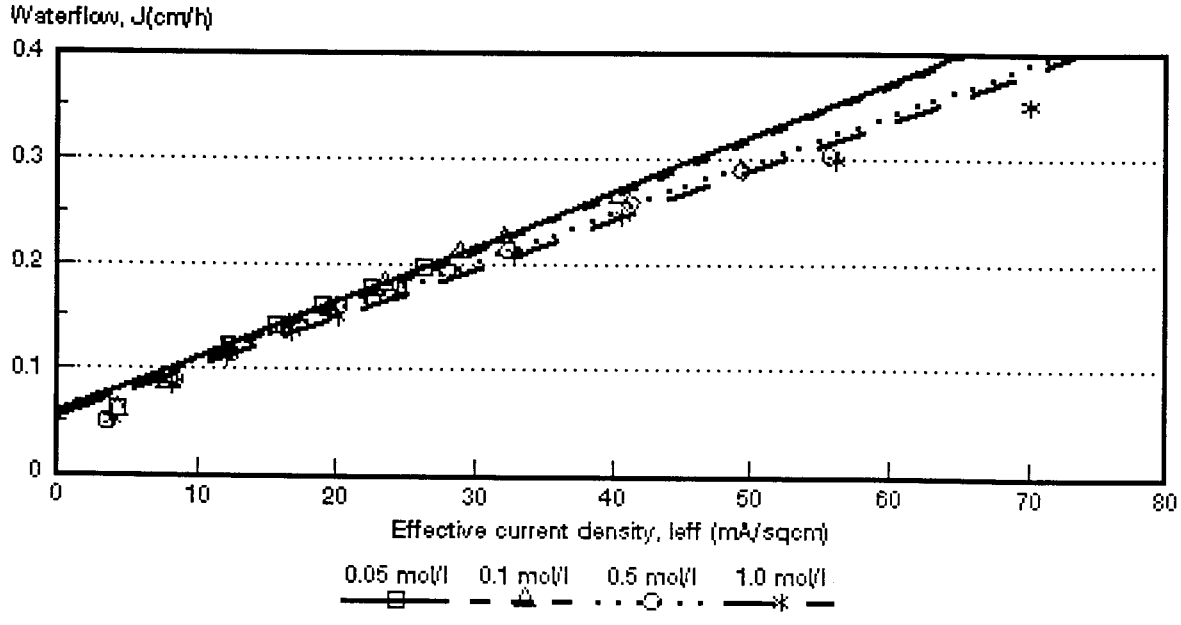

Figure 7.56: **Water flow through the membranes as a function of effective current density and HCl feed water concentration. *Selemion* AAV and CHV membranes.**

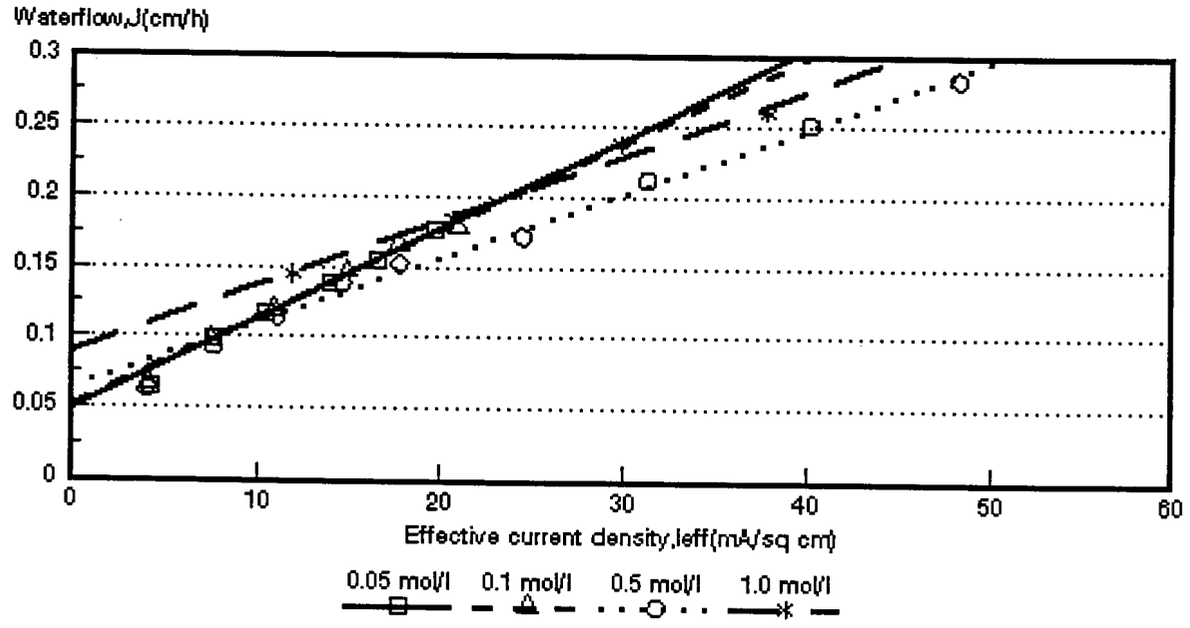

Figure 7.57: **Water flow through the membranes as a function of effective current density and HCl feed water concentration. ABM-3 and *Selemion* CHV membranes.**

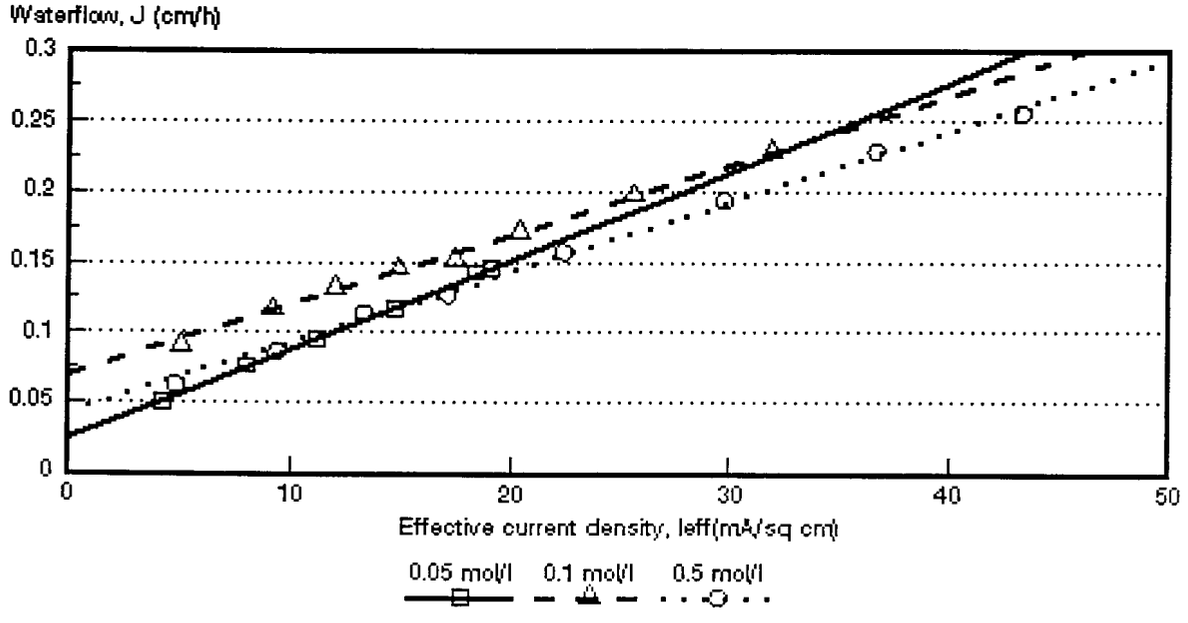

Figure 7.58: **Water flow through the membranes as a function of effective current density and HCl feed water concentration. ABM-2 and *Selemion* CHV membranes.**

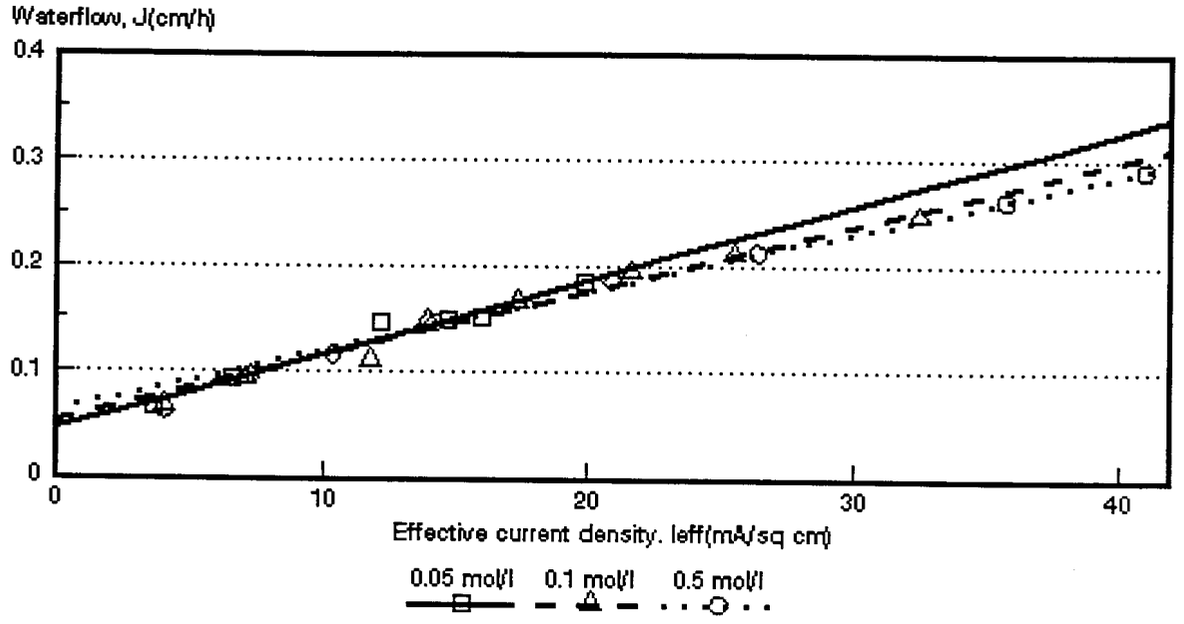

Figure 7.59: **Water flow through the membranes as a function of effective current density and HCl feed water concentration. ABM-1 and *Selemion* CHV membranes.**

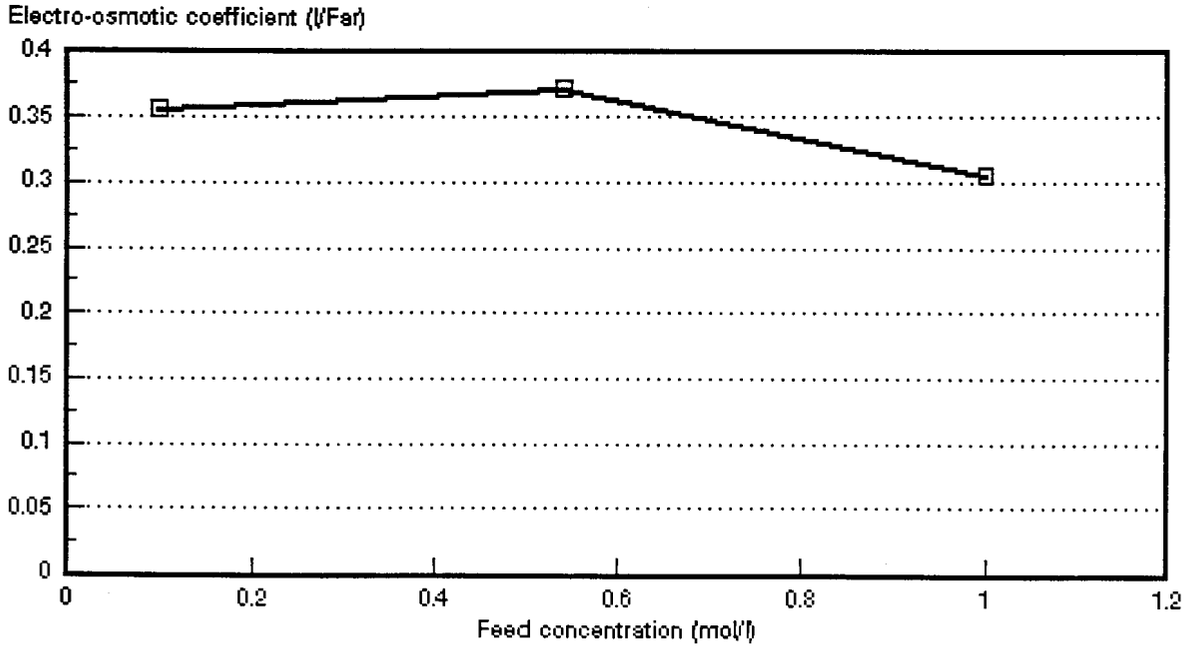

Figure 7.60: **Electro-osmotic coefficient as a function of HCl feed water concentration. *Selemion* AMV and CMV membranes.**

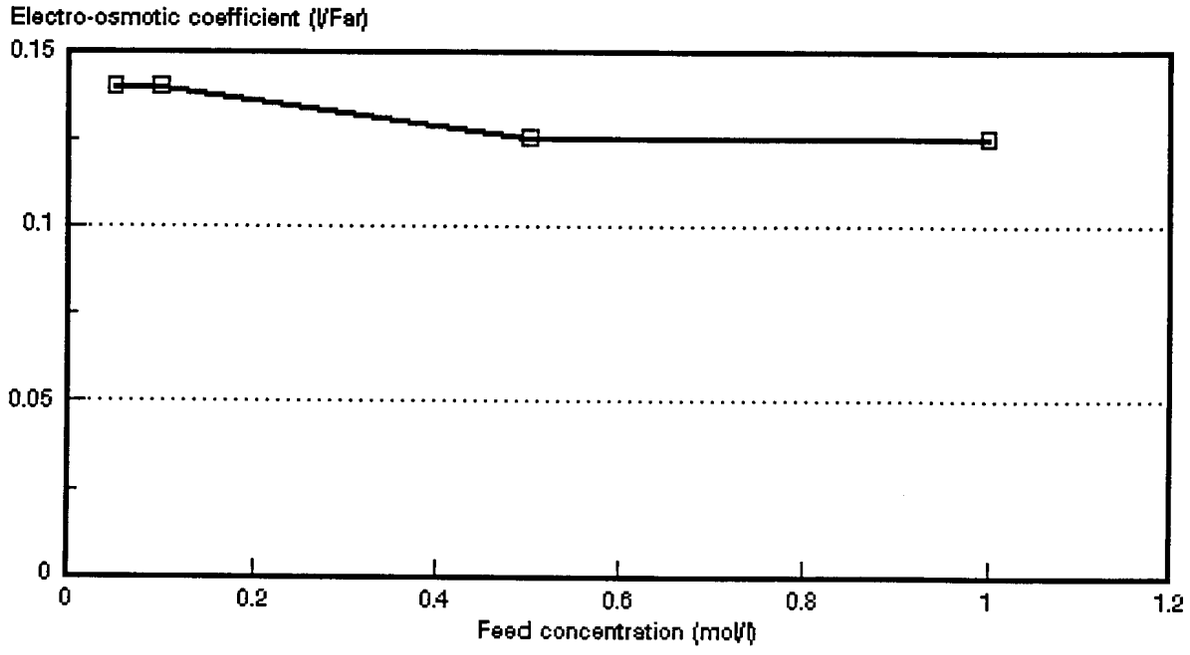

Figure 7.61: **Electro-osmotic coefficient as a function of HCl feed water concentration. *Selemion* AAV and CHV membranes.**

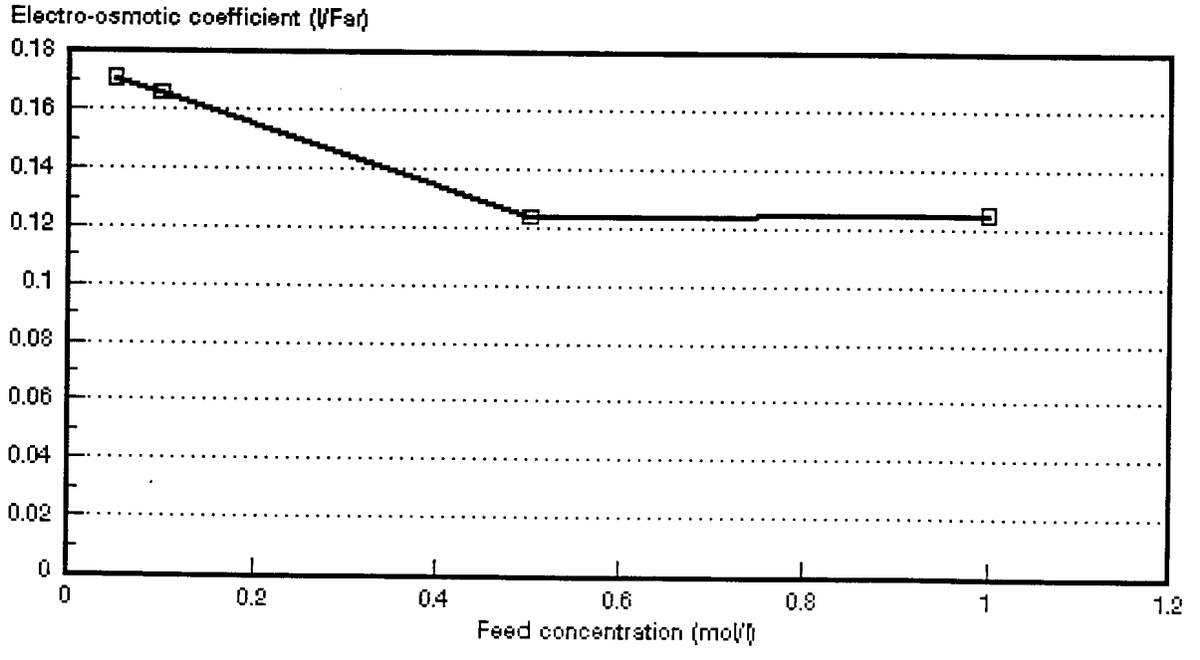

Figure 7.62: **Electro-osmotic coefficient as a function of HCl feed water concentration. ABM-3 and *Selemion* CHV membranes.**

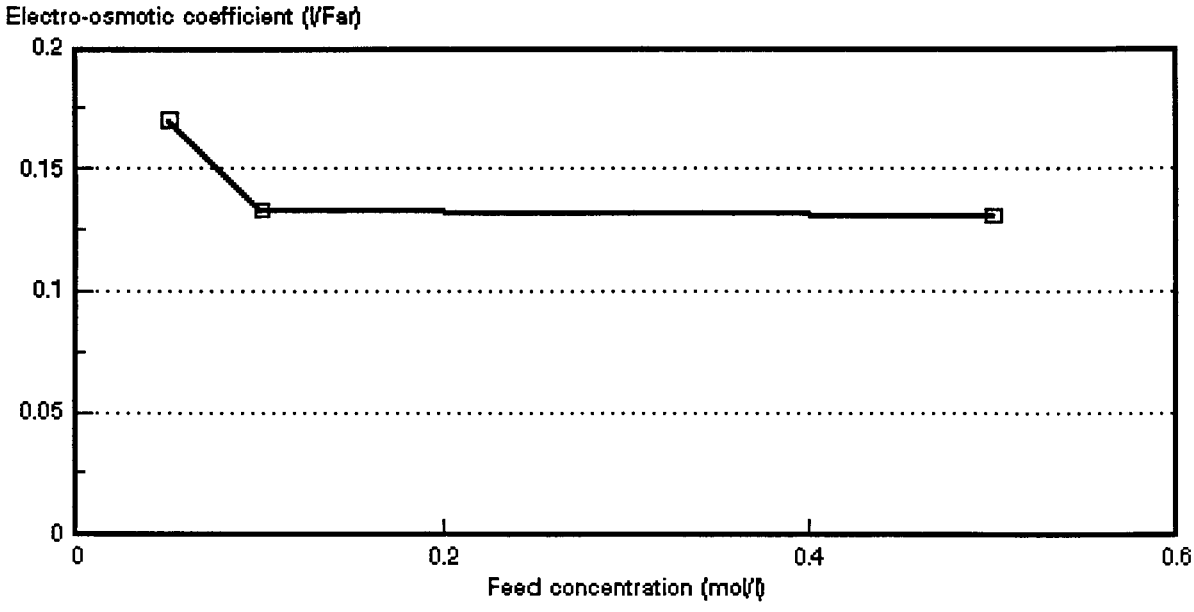

Figure 7.63: **Electro-osmotic coefficient as a function of HCl feed water concentration. ABM-2 and *Selemion* CHV membranes.**

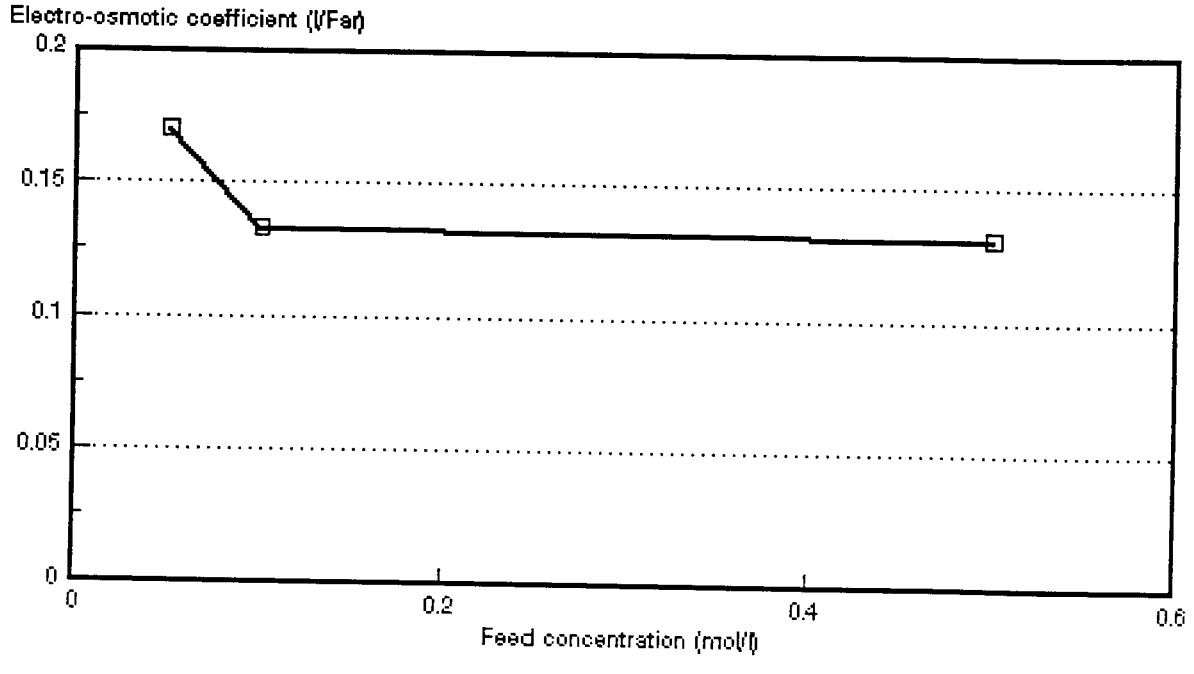

Figure 7.64: **Electro-osmotic coefficient as a function of HCl feed water concentration. ABM-1 and *Selemion* CHV membranes.**

Table 7.25: Effect of the electro-osmotic coefficient (EOC)* on the maximum acid brine concentration, c_b^{max}.

Membranes	Feed Concentration mol/ℓ	EOC ℓ/Faraday	c_b^{max} mol/ℓ	mol H_2O/Faraday
Selemion	0,1	0,357	2,80	19,8
AMV & CMV	0,54	0,371	2,70	20,6
	1,0	0,306	3,27	17,0
Selemion	0,05	0,140	7,14	7,8
AAV & CHV	0,10	0,141	7,09	7,8
	0,50	0,126	7,93	7,0
	1,0	0,125	8,00	7,9
Israeli	0,05	0,171	5,85	9,5
ABM-3 &	0,10	0,166	6,02	9,2
Selemion CHV	0,50	0,124	8,06	6,9
	1,0	0,125	8,03	6,9
Israeli	0,05	0,170	5,88	9,4
ABM-2 &	0,10	0,133	7,51	7,4
Selemion CHV	0,50	0,131	7,6	7,3
Israeli	0,05	0,188	5,32	10,4
ABM-1 &	0,10	0,152	6,58	8,4
Selemion CHV	0,50	0,149	6,71	8,3

* Data from Tables 7.1 to 7.17.

Table 7.26: Osmotic flow* (J_{osm}) relative to the total flow (J) through the membranes as a function of current density.

Membranes	Current Density mA/cm²	J_{osm}/J (%) Feed Concentration (mol/ℓ)			
		0,05	0,10	0,5	1,0
Selemion AMV & CMV	10		107,6	92,9	128,9
	20		63,8	58,9	71,2
	30		49,1	42,4	46,1
	40		42,4	34,6	39,6
	50		34,9	28,1	33,8
	60		31,4	24,8	26,6
Selemion AAV & CHV	10	96,1	91,9	123,5	109,0
	20	64,1	64,1	69,4	65,4
	30	48,5	47,1	53,7	50,1
	40	42,3	39,4	44,8	41,1
	50	37,3	35,1	38,6	37,3
	60	33,5	30,6	35,7	32,3
	70	30,4	26,1	31,7	
	80		24,5	29,0	26,6
	100		20,9	23,9	22,7
	120			21,4	
	140			20,3	18,6
	180				15,8
Israeli ABM-3 & Selemion CHV	10	77,4	77,5	103,8	
	20	50,5	53,6	69,2	
	30	42,3	44,0	56,4	
	40	35,9	35,6	46,6	
	50	31,1	31,5	42,4	
	60	28,1	29,4		
	70			37,4	
	90			30,4	
	110			25,5	
	120			22,7	
Israeli ABM-2 & Selemion CHV	10	49,1	77,5	74,4	
	20	32,3	60,2	54,1	
	30	25,8	53,4	41,2	
	40	21,0	48,3	36,6	
	50	17,2	46,4		
	60	16,9	41,0	29,5	
	80		35,6	24,0	
	100		30,6	20,3	
	120			18,1	
Israeli ABM-1 & Selemion CHV	10	69,0	102,6	102,0	
	20	50,2	74,7	66,7	
	30	34,9	52,3	55,6	
	40	32,0	46,7	44,5	
	50	31,4	41,9		
	60	30,9	35,7	34,9	
	80	25,1	32,8	30,6	
	100		28,0	24,8	
	120			22,3	

* Data from Tables 7.1 to 7.17.

7.4 Membrane Permselectivity

Membrane permselectivities (from potential measurements) as a function of acid brine concentration for different acid feed concentrations are shown in Figures 7.65 to 7.69. Membrane permselectivity decreased with increasing acid brine concentration and increasing acid feed concentration in the case of *Selemion* AMV and CMV; *Selemion* AAV and CHV; ABM-2 and CHV and ABM-1 and CHV membranes. However, a higher permselectivity was obtained at the highest feed concentration (1,0 mol/ℓ feed) in the case of the ABM-3 and CHV membranes.

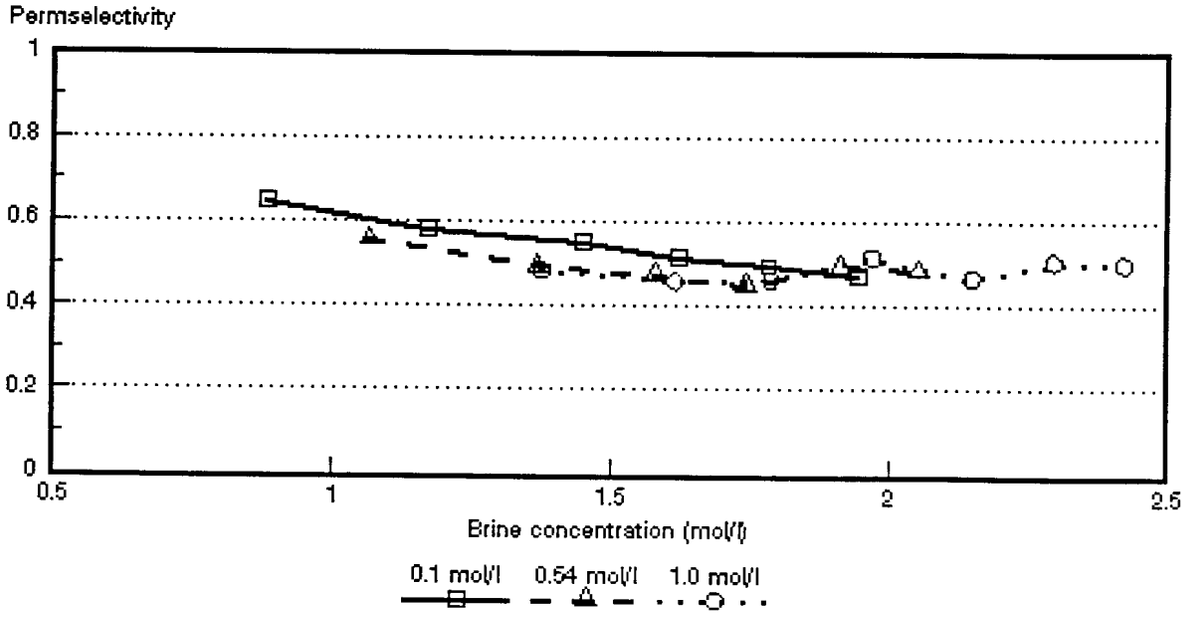

Figure 7.65: **Membrane permselectivity ($\bar{\Delta}t$) as a function of acid brine concentration for different HCl feed concentrations. *Selemion* AMV and CMV membranes.**

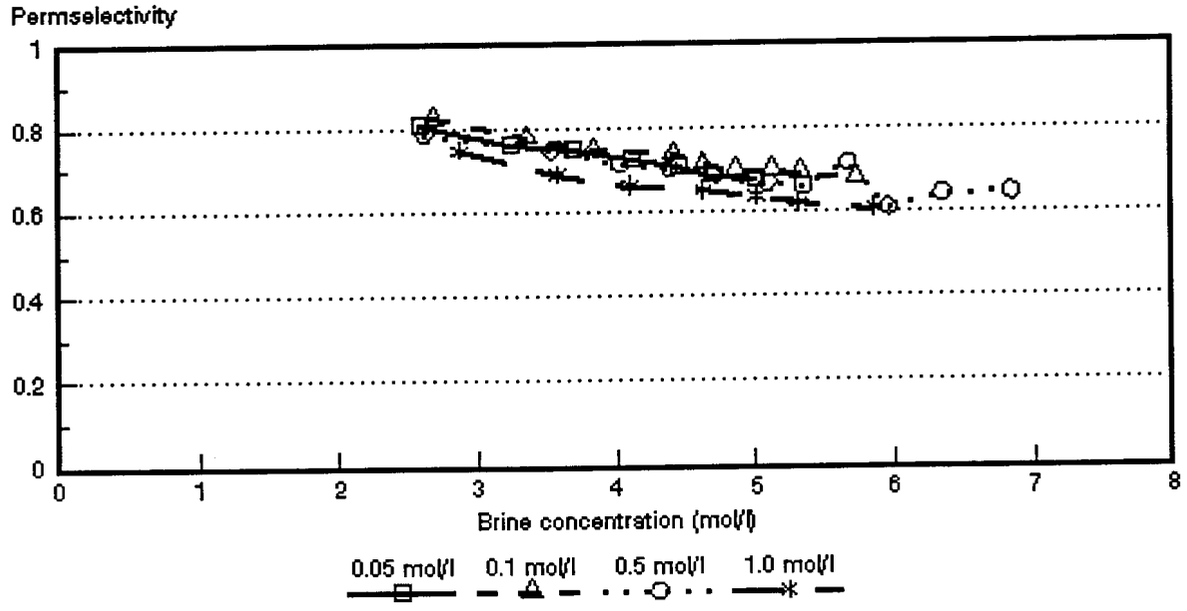

Figure 7.66: **Membrane permselectivity ($\bar{\Delta}t$) as a function of acid brine concentration for different HCl feed concentrations. *Selemion* AAV and CHV membranes.**

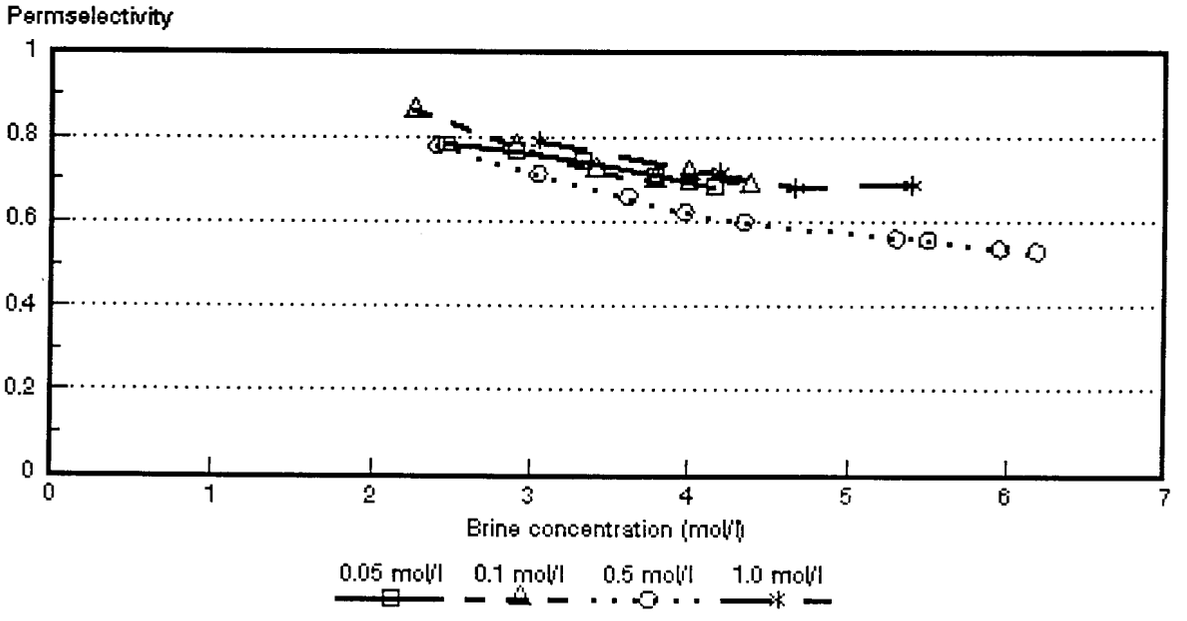

Figure 7.67: **Membrane permselectivity ($\bar{\Delta}t$) as a function of acid brine concentration for different HCl feed concentrations. ABM-3 and *Selemion* CHV membranes.**

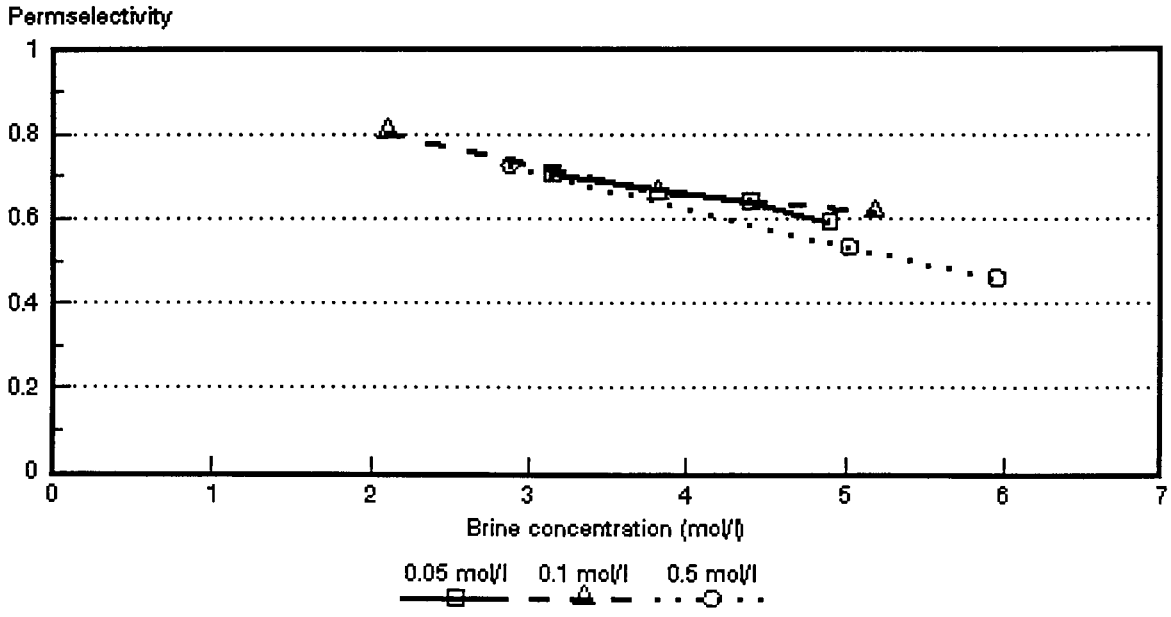

Figure 7.68: **Membrane permselectivity ($\bar{\Delta}t$) as a function of acid brine concentration for different HCl feed concentrations. ABM-2 and *Selemion* CHV membranes.**

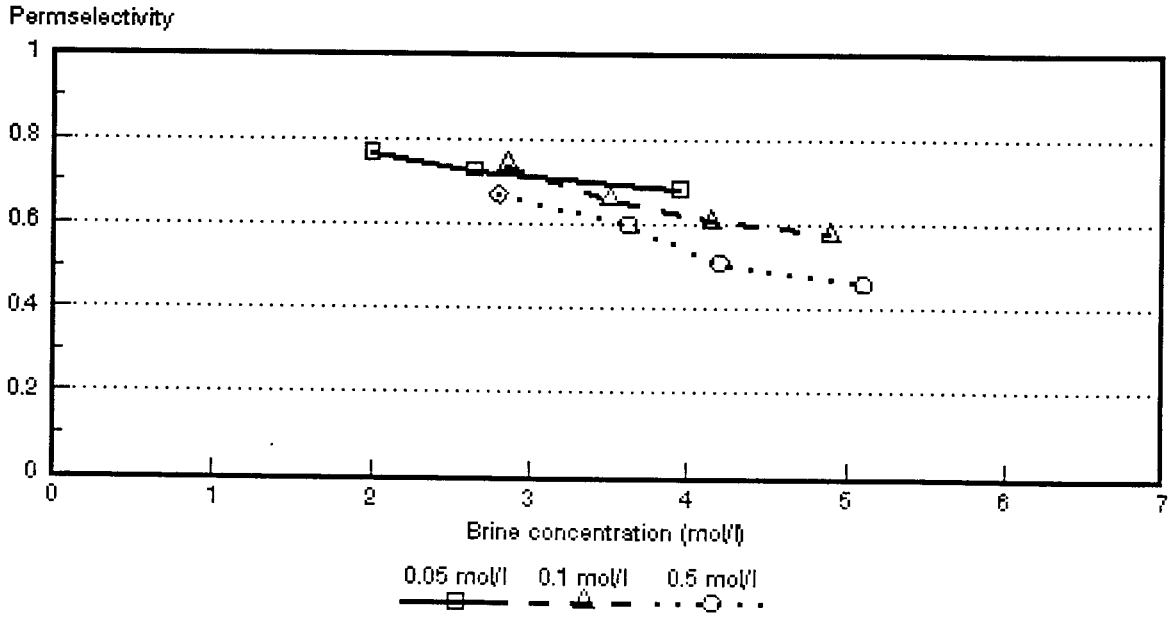

Figure 7.69: **Membrane permselectivity ($\bar{\Delta}t$) as a function of acid brine concentration for different HCl feed concentrations. ABM-1 and *Selemion* CHV membranes.**

7.5 Acid and Salt Diffusion through Membranes

The diffusion rate of sodium chloride and hydrochloric acid solutions through *Selemion* AMV and AAV membranes was determined in an attempt to explain the difference that was obtained between the apparent transport numbers as determined by the potential method and the current efficiencies as determined by the EOP method. Salt and acid solutions of different concentrations were separated by the membranes and the change in diluate concentration as a function of time was determined. The rate of concentration change per unit time was determined from the results. The results are shown in Table 7.27.

Table 7.27: Change of concentration rate of sodium chloride and hydrochloric acid solutions through Selemion AMV and AAV membranes.

Initial Feed Concentration mol/ℓ	Initial Brine Concentration mol/ℓ	Rate of Concentration Change (ge/h)*			
		Selemion AMV		Selemion AAV	
		Salt Diluate	Acid Diluate	Salt Diluate	Acid Diluate
0,05	2	0,000568	0,005872	0,000165	0,000494
0,05	4	0,000390	0,002800	0,000145	0,002805

* gram equivalents per hour.

The rate of concentration increase in the more dilute compartment was much higher for the acid than for the salt solutions for both membrane types. Consequently, backdiffusion of acid from the brine into the diluate compartment will cause the current efficiency to decrease much more in the case of acids than in the case of salt solutions.

7.6 Membrane Characteristics

7.6.1 Membrane resistance

Membrane resistances are summarized in Table 7.28.

Table 7.28: Membrane resistances of the membranes used for EOP of hydrochloric acid solution.

Membrane	Resistance - ohm·cm²	
	0,1 mol/ℓ	0,5 mol/ℓ HCl
Selemion AMV	7,4	2,0
Selemion CMV	0,8	0,8
Selemion AAV	8,7	5,2
Selemion CHV	0,6	1,5
ABM-3	48,3	34,7
ABM-2	75,7	47,0
ABM-1	30,6	12,4

7.6.2 Gel water contents and ion-exchange capacities of membranes used for EOP of hydrochloric acid solutions.

The gel water contents and ion-exchange capacities of the membranes used for EOP of hydrochloric acid solutions are shown in Table 7.29.

Table 7.29: Gel water contents and ion exchange capacities of the membranes used for EOP of hydrochloric acid solutions.

Membrane	Gel Water Content %	Ion-Exchange Capacity me/dry g
Selemion AMV	18,4	1.26
Selemion CMV	22,7	2,4
Selemion AAV	9,1	0,48
Selemion CHV	13,4	1,98

7.6.3 Permselectivities of the membranes used for EOP of hydrochloric acid solutions

The permselectivities of the membranes at different hydrochloric acid concentration gradients are summarized in Table 7.30.

Table 7.30: Membrane permselectivities of the membranes used for EOP of hydrochloric acid solutions at different acid concentration gradients

Membrane	Δt(1)*	Δt(2)**	Δt(3)***
Selemion AMV	0,74	0,46	0,13
Selemion CMV	1,00	0,88	0,88
Selemion AAV	0,97	0,83	0,54
Selemion CHV	0,99	0,87	0,87
ABM-3	0,88	0,63	0,44
ABM-2	0,92	0,77	0,49
ABM-1	0,84	0,60	0,40

(1)* : 0,1 / 0,2 mol/ℓ HCl
(2)** : 0,5 / 1,0 mol/ℓ HCl
(3)*** : 0,1 / 4,0 mol/ℓ HCl